

EXPLORING FUNCTIONALIZED SUGAR NUCLEOTIDES FOR CELL SURFACE  
ENGINEERING AND CONSTRUCTION OF ANTIBODY-DRUG CONJUGATES (ADCs)

by

TIANTIAN SUN

(Under the Direction of Geert-Jan Boons)

ABSTRACT

Glycans mediate a wide range of cellular functions, such as cell-cell interactions, adhesion and differentiation, by mediating intracellular signaling events. In addition, glycosylation plays an important role inside cells by regulating protein trafficking, turnover and signal transduction. Specifically, sialic acids are essential in mediating a variety of physiological and pathological processes, whose generation is governed by the sialic acid biosynthetic machinery. This dissertation has taken advantage of different functionalized CMP-sialic acids, combined with various click reactions, to achieve efficient cell surface glycoprotein labeling and construction of Antibody-Drug Conjugates (ADCs).

We have developed SEEL (selective exoenzymatic labeling) methodology to install chemical reporters on cell surface acceptor glycans using azide modified CMP-sialic acid, which only labels a specific class of cell surface molecules (e.g., *N*- vs *O*-glycans). In light of the direct nature of this method, we further developed a more efficient strategy, termed one-step SEEL, by employing a biotin modified CMP-sialic acid derivative. We found that this approach has

exceptional efficiency compared to two-step SEEL or metabolic labeling, which greatly improved the ability to enrich and identify large numbers of tagged glycoproteins by LC-MS/MS. The one-step approach offers exciting possibilities to study the trafficking and identification of subsets of cell surface glycoconjugates with unprecedented sensitivity in whole cells. Furthermore, we explored a new two-step SEEL, which takes advantage of a sugar nucleotide functionalized by tetrazine, and fast bioorthogonal reaction-DARinv (Inverse electron demand Diels-Alder reaction). This approach will first remodel the cell surface with high reactive tetrazines, followed by click reaction with trans-cyclooctenes (TCO) modified functionalities. This new approach has comparable efficiency with one-step SEEL benefit by the fast click reaction, but has broader applications.

We prepared well-defined anti-CD22 ADCs through DARinv and SPANC (Strained promoted alkyne-nitrone cycloaddition) by using tetrazine and nitrone modified CMP-sialic acid derivatives, and the formed ADCs showed dose-dependent cytotoxicity. Furthermore, DARinv and SPANC are orthogonal, which can be used together on the same mAb to deliver two different drugs to increase ADC efficacy and reduce toxicity at the same time.

INDEX WORDS: CMP-sialic acid, Click chemistry, cell surface labeling, SEEL, Antibody-Drug Conjugates, CuAAC, SPAAC, SPANC, DARinv.

EXPLORING FUNCTIONALIZED SUGAR NUCLEOTIDES FOR CELL SURFACE  
ENGINEERING AND CONSTRUCTION OF ANTIBODY-DRUG CONJUGATES (ADCs)

by

TIANTIAN SUN

B.S., Pharm., Ocean University of China, 2007

M.S., Pharm., Ocean University of China, 2010

A Dissertation Submitted to the Graduate Faculty of the University of Georgia in Partial  
Fulfillment of the Requirements for the Degree

DOCTOR OF PHILOSOPHY

ATHENS, GEORGIA

2017

© 2017

Tiantian Sun

All Rights Reserved



EXPLORING FUNCTIONALIZED SUGAR NUCLEOTIDES FOR CELL SURFACE  
ENGINEERING AND CONSTRUCTION OF ANTIBODY-DRUG CONJUGATES (ADCS)

by

TIANTIAN SUN

Major Professor: Geert-Jan Boons

Committee: Vladimir Popik  
Robert Phillips

Electronic Version Approved:

Suzanne Barbour  
Dean of the Graduate School  
The University of Georgia  
December 2017

## DEDICATION

I would like to dedicate my thesis to my parents Meihua Sun and Hongju Yang, and my husband Chengli Zong, for their undying support, love and encouragement. Your confidence and belief in me and my abilities has given me immense motivation to succeed.

## ACKNOWLEDGEMENTS

I would like to thank my advisor Prof. Dr. Geert-Jan Boons for giving me the opportunity to pursue PhD degree in his group. His constant support and guidance were irreplaceable throughout my PhD research, which make me a better researcher and will benefit my future life.

I would like to thank my committee members Dr. Vladimir Popik and Dr. Robert Phillips for their encouraging advice and guidance throughout my Ph.D. Special thanks to Dr. Frédéric Friscourt for his guidance, sharing his experience, and being good friend. Many thanks to Dr. Margreet Wolfert for help with manuscript submission. I would also like to thank Dr. Andre Venot and Dr. Xiuru Li for keeping the lab safe, organized, and clean. I would like to thank Dr. John Glushka for helping me with the NMR instruments and clarifying doubts about the spectrum.

I would like to thank Dr. Xiuru Li, Dr. Lin Liu, Dr. Chengli Zong for their help in my projects. I also want to express my appreciation toward all my lab mates and friends Manish Satish Hudlikar, Weigang Lu, Tiehai Li, Chantelle Jae Capicciotti, Anthony Robert Prudden, Robert Chapman, Apoorva Joshi, Pradeep Chopra, Maria Jesus Moure Garcia, Na Wei, Wei Huang, Nintin Supekar, Tao Fang, Rachel Bainum and other past and current Boons group members who have been very friendly, helpful, resourceful, and supportive.

I would like to thank my entire family and all my friends for their support and unconditional love.

## TABLE OF CONTENTS

	Page
ACKNOWLEDGEMENTS .....	v
LIST OF TABLES .....	ix
LIST OF FIGURES .....	x
LIST OF SCHEMES.....	xv
LIST OF ABBREVIATIONS .....	xvi
CHAPTER	
1 INTRODUCTION AND LITERATURE OVERVIEW.....	1
Bioorthogonal Reactions and Click chemistry .....	1
Chemical reporter strategy .....	18
Metabolic oligosaccharide engineering (MOE) and selective cancer targeting .....	22
Selective Exo-Enzymatic Labeling (SEEL).....	32
Antibody-drug conjugates (ADCs) .....	34
References:.....	42
2 ONE-STEP SELECTIVE EXOENZYMATIC LABELING (SEEL) STRATEGY FOR THE BIOTINYLATION AND IDENTIFICATION OF GLYCOPROTEINS OF LIVING CELLS .....	62
Abstract .....	63

Introduction.....	64
Results and discussion .....	67
Conclusion .....	78
Experimental section.....	80
References.....	107
 3 NOVEL TWO-STEP SELECTIVE EXOENZYMATIC LABELING (SEEL) USING TETRAZINE FUNCTIONALIZED CMP-NEU5AC DERIVATIVE .....	 110
Abstract.....	111
Introduction.....	112
Results and discussion .....	115
Conclusion .....	130
Experimental section.....	131
Reference .....	157
 4 PREPARATION OF WELL-DEFINED ANTIBODY–DRUG CONJUGATES (ADCS) THROUGH INVERSE ELECTRON DEMAND DIELS-ALDER REACTION (DARINV) AND STRAIN-PROMOTED ALKYNE-NITRONE CYCLOADDITION (SPANC) .....	 160
Abstract.....	161
Introduction.....	162
Results and discussion .....	166
Conclusion .....	182
Experimental section.....	183

Reference .....	205
5 CONCLUSION.....	209

## LIST OF TABLES

	Page
Table 1.1 Reaction rate constants and synthetic accessibility of cyclooctynes.....	10
Table 1.2 Rate constants for the cycloaddition of cyclooctyne with nitrones .....	13
Table 1.3 Tetrazine-Based Inverse-Electron Demand Diels-Alder Reactions with Strained Alkenes and Alkynes.....	16
Table 1.4 Chemical reporters and bioorthogonal reactions used in living systems .....	20
Table 4.1 Properties and fluorescence quenching results of AF488, FITC, TMR, DOX, AF647.....	173
Table 4.2 Properties and fluorescence quenching results of AF488 and DOX. ....	175
Table 4.3 The EC50 values for CD22-ADC-SPANC, CD22-ADC-DARinv and CD22-ADC-SPAAC. .	182

## LIST OF FIGURES

	Page
Figure 1.1 A bioorthogonal chemical reaction.....	2
Figure 1.2 Proposed mechanism of CuAAC. ....	5
Figure 1.3 Accelerating ligands commonly used in the CuAAC reaction.....	6
Figure 1.4 Overview of functionalized cyclooctynes suitable for conjugation reactions.....	8
Figure 1.5 SPAAC with FI-DIBO and the kinetics .....	11
Figure 1.6 SPAAC with TMTH.....	11
Figure 1.7 Normal electron-demand and inverse electron-demand Diels–Alder reaction .....	14
Figure 1.8 Tetrazine bioorthogonal reaction. ....	14
Figure 1.9 Reactivity of tetrazines with different substituents.....	15
Figure 1.10 Fluorogenic conjugation of BODIPY-tetrazine with TCO.....	17
Figure 1.11 DAR <sub>inv</sub> between TCO-DOX and tetrazine.....	18
Figure 1.12 The bioorthogonal chemical reporter strategy.....	19
Figure 1.13 Common classes of animal glycans. Adapted from reference .....	22
Figure 1.14 monosaccharide based chemical reporters .....	24
Figure 1.15 The biosynthetic pathway of sialic acids. Adapted from reference .....	25
Figure 1.16 Metabolic oligosaccharide engineering of cell-surface sialic acids.....	26
Figure 1.17 Two-step in vivo tumor-targeting strategy for nanoparticles via metabolic glycoengineering	



and click chemistry .....	28
Figure 1.18 Targeted imaging of the cancer glycome in vivo.....	29
Figure 1.19 Strategy for tissue-specific release of Ac3ManNAz via enzymatic activation.....	29
Figure 1.20 PSA cleavage of caged azidosugar.....	30
Figure 1.21 HDAC/CTSL-induced degradation of DCL-AAM.....	31
Figure 1.22 Cathepsin B cleavage of DBCO-VC-Dox.....	31
Figure 1.23 Metabolic labeling and SEEL.....	33
Figure 1.24 a) structure of CMP-Neu5Ac9N <sub>3</sub> and S-DIBO-Biotin. b) Enzymatic labeling of fibroblasts. c) Effect of chloroquine on enzymatic labeling.....	34
Figure 1.25 Illustration of antibody drug conjugates .....	35
Figure 1.26 Cleavable linkers .....	37
Figure 1.27. Mechanism of action of ADCs.....	39
Figure 2.1 CMP-sialic acid derivatives with modification at C9 and C5 positions .....	67
Figure 2.2 Preparation of <b>11</b> and <b>13</b> .....	68
Figure 2.3 Preparation of azide modified sialic acid ( <b>16</b> ) and CMP-sialic acid ( <b>1</b> ) at C9 position .....	68
Figure 2.4 Failed trial to prepare Compound <b>5</b> .....	69
Figure 2.5 Preparation of compound <b>5</b> and its unsuccessful transfer to LacNAc .....	69
Figure 2.6 Failed trial to prepare Compound <b>3</b> .....	70
Figure 2.7 Preparation of compound <b>3</b> and its successful transfer to LacNAc .....	70
Figure 2.8 One-pot two-enzyme synthesis of CMP-Neu5N <sub>3</sub> ( <b>22</b> ) .....	71
Figure 2.9 Preparation of compound <b>2</b> and its successful transfer to LacNAc.....	71

Figure 2.10 Preparation of compound <b>6</b> and its successful transfer to LacNAc .....	72
Figure 2.11 Investigation of the tolerance of CMP-sialic acid synthetase at C5 position. ....	72
Figure 2.12 Western blot analysis of One-step SEEL, two-step SEEL, and metabolic labeling.....	74
Figure 2.13 a) Venn diagram for the proteomic analysis of HeLa cells subjected to two-step (cmpd <b>1</b> ) or one-step (cmpd <b>2</b> ) SEEL with ST6Gal1; b) The spectral counts of the 20 most abundant glycoproteins detected using one-step SEEL are plotted relative to the counts detected using two-step SEEL (values for two-step SEEL set to 100%)......	75
Figure 2.14 a) confocal microscopy of one-step SEEL with or without chloroquine; b) Western blot analysis of SEEL labeled HeLa cells under the three conditions tested .....	77
Figure 2.15 a) Western blot analysis of HEK293F cells labeled using sulfo-NHS-biotin or SEEL with ST6Gal1;(b) Quantification of the total proteins identified and their spectral counts under these conditions compared to the total cell surface glycoproteins identified. ....	78
Figure 3.1 Designed synthetic route for TCO attached CMP-sialic acid.....	116
Figure 3.2 Synthesis of <b>5</b> and its hydrogenation using Pd(OH) <sub>2</sub> .....	116
Figure 3.3 Synthesis of TCO attached CMP-sialic acid <b>4</b> and its successful transfer to LacNAc.....	117
Figure 3.4 Inactivation of TCO by attachment with sialic acid moiety. ....	118
Figure 3.5. Synthesis of mono-substituted tetrazine <b>5</b> .....	118
Figure 3.6 Synthesis and decomposition of <b>10</b> .. ....	118
Figure 3.7 Synthesis of disubstituted tetrazine <b>11</b> .....	119
Figure 3.8 Copper Coordination with pyrimidine substituted tetrazine.....	119
Figure 3.9 a) Synthesis and decomposition of <b>7</b> ; b) Proposed mechanism under basic condition .....	120

Figure 3.10 Stability of selected tetrazines in FBS at 37°C after 10 h.....	121
Figure 3.11 Synthesis of tetrazine <b>15</b> .....	121
Figure 3.12 Synthesis of <b>3</b> and its successful transfer to LacNAc.....	122
Figure 3.13 Synthesis of Tetrazine-PEG-CMP-Neu5Ac ( <b>17</b> ).....	123
Figure 3.14 Synthesis of TCO-Biotin. ....	123
Figure 3.15 Synthesis of BCN.. ....	124
Figure 3.16 Synthesis of BCN-Biotin. ....	124
Figure 3.17 Comparison of two click-type reactions.....	125
Figure 3.18 Western blot analysis of previously reported SPAAC two-step SEEL and new two-step SEEL labeled HeLa cells.....	126
Figure 3.19 Western blot analysis of one-step SEEL and two-step SEEL labeled HeLa cells.....	127
Figure 3.20 Western blot analysis of two-step SEEL labeled HeLa cells using tetrazine-CMP-sialic acid ( <b>3</b> ) and tetrazine-PEG <sub>3</sub> -CMP-sialic acid ( <b>17</b> ) following click reaction with TCO-biotin or BCN-biotin.....	128
Figure 3.21 Western blot analysis of Two-step SEEL labeled CD44 using tetrazine-CMP-sialic acid ( <b>3</b> ) and protein-specific antibodies towards CD44.....	129
Figure 4.1 Structure of nitron modified CMP-sialic acid <b>2</b> .....	166
Figure 4.2 Synthesis of nitron modified CMP-sialic acid <b>2</b> and its successful transfer to LacNAc.....	167
Figure 4.3 Synthesis of Tetrazine modified CMP-sialic acid derivative <b>3</b> . ....	167
Figure 4.4 Comparison of three click-type reactions.....	168
Figure 4.5 Structures of modified doxorubicins.....	169

Figure 4.6 Old method to synthesize DIBO attached DOX .....	169
Figure 4.7 New method to synthesize DIBO attached DOX.....	170
Figure 4.8 Synthesis of TCO attached DOX. ....	170
Figure 4.9 Structures of FITC-DIBO and TMR-DIBO .....	171
Figure 4.10 Fluorescence resonance energy transfer (FRET) .....	172
Figure 4.11 Structures of DIBO attached Fluorophores. ....	172
Figure 4.12 Synthesis of AF488-TCO. ....	174
Figure 4.13 Typical Fc-linked glycans present in serum IgG heavy chains.....	175
Figure 4.14 Native PAGE gel analysis of modified control IgGs using SPAAC, SPANC and DARinv..	177
Figure 4.15 reaction rates on antibodies. ....	178
Figure 4.16 Native PAGE gel analysis of modified Anti CD22 IgGs using SPAAC, SPANC and DARinv.	
a) Coomassie blue staining of total protein; b) fluorescence scanning.. ....	180
Figure 4.17. Cytotoxicity of the anti-CD22 antibody conjugated to Dox. ....	182

## LIST OF SCHEMES

	Page
Scheme 1.1 Thermal and metal catalized azide-alkyne cycloaddition reactions. ....	4
Scheme 1.2 Metal free bioorthogonal reactions .....	7
Scheme 2.1 one- and two-step SEEL .....	65
Scheme 2.2 Summary of synthesis of CMP-sialic acid derivatives .....	73
Scheme 3.1 Various SEEL methodologies and compounds used .....	114
Scheme 4.1 Preparation of well-defined ADCs through glycan remodeling and click chemisty.....	164
Scheme 4.2 Comparation of fluorescence absorption spectrum of click product and fluorescence emission spectrum of fluorophores (DOX, TMR, AF647, FITC). ....	173
Scheme 4.3 Comparation of fluorescence absorption spectrum of click product and fluorescence emission spectrum of fluorophores (DOX, AF488). ....	174
Scheme 4.4 Preparation of fluorophones modified control antibodies.....	176
Scheme 4.5 Preparation of control antibody-DOX conjugates. ....	178
Scheme 4.6 Preparation of fluorophones modified anti CD22 antibodies. ....	179
Scheme 4.7 Preparation of anti-CD22 ADCs .....	181

## LIST OF ABBREVIATIONS

Ac	Acetyl
Ac <sub>2</sub> O	Acetic anhydride
AcOH	Acetic acid
BARAC	Biarylazacyclooctynone
BCN	bicyclo[6.1.0]nonyne
Bn	Benzyl
Boc	Tert-butoxycarbonyl
BSA	Bovine serum albumin
BuOH	Butanol
C	Carbon
Cbz	Carboxybenzyl
CH <sub>3</sub> CN	Acetonitrile
CMP	Cytidine monophosphate
CuAAC	Copper-Catalyzed Azide-Alkyne Cycloaddition
CuSO <sub>4</sub>	Copper sulfate
COSY	Correlation spectroscopy
DCC	Dicyclohexyl carbodiimide

DCM	Dichloromethane
DIBO	Dibenzocyclooctyne
DIBAC	Dibenzoazacyclooctyne
DIC	<i>N,N</i> -Diisopropylcarbodiimide
DIFO	Difluorocyclooctyne
DIPEA	<i>N,N</i> -Diisopropylethylamine
DMAP	<i>N, N</i> -Dimethylaminopyridine
DMF	<i>N, N</i> -dimethylamineformamide
DMSO	Dimethyl sulfoxide
EDG	Electron donating group
Et <sub>3</sub> SiH	Triethylsilane
EtOAc	Ethyl acetate
EtOH	Ethanol
Et <sub>2</sub> O	Diethyl ether
EWG	Electron withdrawing group
FI-DIBO	Fluorogenic DIBO
FRET	Förster Resonance Energy Transfer
Gal	Galactose
Glc	Glucose
HBTU	2-(1 <i>H</i> -benzotriazole-1-yl)-oxy-1,1,3,3-tertmet

	hyl hexafluorophosphate
HOBt	Hydroxybenzotriazole
HPLC	High-Performance Liquid Chromatography
HSQC	Heteronuclear single quantum coherence
Hz	Hertz
M	Molar
Man	Mannose
MALDI-TOF-TOF	Atrix assisted laser desorption ionization spectroscopy-time of flight
MeOH	Methanol
MgSO <sub>4</sub>	Magnesium sulfate
MOFO	monofluorinated cyclooctyne
MW	Molecular Weight
NaH	Sodium hydride
NaHCO <sub>3</sub>	Sodium bicarbonate
NaN <sub>3</sub>	Sodium azide
NaOH	Sodium hydroxide
NaOMe	Sodium methoxide
NB	norbornene
NH <sub>3</sub>	Ammonia



NH <sub>2</sub> NH <sub>2</sub>	Hydrazine
NHS	<i>N</i> -hydroxy succinimide
NMR	Nuclear magnetic resonance
OCT	cyclooctyne
Pd	Palladium
Pd(OH) <sub>2</sub>	Palladium hydroxide
PEG	Polyethylene glycol
PNP	p-nitrophenyl carbonate
PBS	Phosphate buffered saline
RuAAC	Ruthenium-catalyzed Azide-Alkyne Cycloaddition
S-DIBO	sulfonylated DIBO
SPAAC	Strain-Promoted Azide-Alkyne Cycloaddition
SPADC	Strain-Promoted Alkyne-Diazocarbonyl Cycloadditions
SPANC	Strain-Promoted Alkyne-Nitrone Cycloaddition
SPANOC	Strain-Promoted Alkyne-Nitrile Oxide Cycloaddition
TBTA	Tris(benzyltriazolyl)methyl amine
TCO	Trans-Cyclooctene

TFA	Trifluoroacetic acid
Tf <sub>2</sub> O	Triflic anhydride
TIPS	Triisopropylsilyl
TLC	Thin layer chromatography
THF	Tetrahydrofuran
TMS	Trimethyl silyl
TMTH	3,3,6,6-tetramethylthiacycloheptyne
Zn	Zinc

## CHAPTER 1

### INTRODUCTION AND LITERATURE OVERVIEW

#### **Bioorthogonal Reactions and Click chemistry**

Biomolecule labeling using chemical probes with specific biological activities has played important roles for the better understanding of living systems. Selective bioconjugation strategies are demanded highly in the construction of various small-molecule probes to elucidate complicated biological processes.<sup>1</sup> In past decades, many bioorthogonal reactions that undergo fast and selective ligation under bio-compatible conditions have been developed.<sup>2-4</sup> These bioorthogonal reactions must meet stringent requirements:<sup>5</sup> (i) the two components of the reaction must be highly selective, and not affect any biomolecules and metabolites in the surrounding environment; (ii) the reaction must proceed rapidly and efficiently under physiological conditions (aqueous system exposed to O<sub>2</sub>, pH = 6~8, temperature = 37 °C); (iii), all reagents and products, should be biocompatible and inert to other surrounding molecules within a cellular environment; (iv), the functional groups should be smaller enough to avoid possible perturbations to the labeled biomolecules.

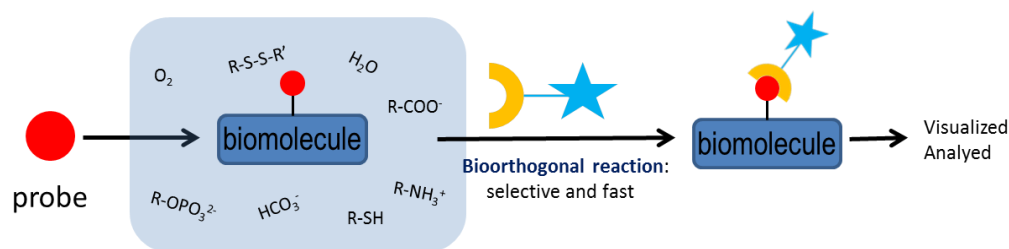


Figure 1.1 A bioorthogonal chemical reaction.

The process of a bioorthogonal chemical reaction was described here: A unique functional group (red circle) appended to a target biomolecule is covalently ligated with a complementary probe (orange arc). The two reagents must react selectively with one another in the presence of all the functionality found within living systems. This method enables the selective visualization, detection or identification of biomolecules in complex environments depending on the choice of tags (blue star).<sup>6</sup> As a result, bioorthogonal reaction selectivity and speed are very important parameters.

Under such rigorous criteria, only a handful of chemical reactions stand out as qualified bioorthogonal reactions, and a prime example is presented by a family of reactions collectively termed “click chemistry”. Click Chemistry has now become a tool for universal modification of nucleic acids, glycans, lipids, proteins, conjugate preparation, and fluorescent labeling, which was introduced by K. B. Sharpless in 2001.<sup>7</sup>

To be qualified as click reactions, Sharpless and coworkers gave a very clear definition:<sup>7,8</sup> they must be modular, stereospecific, wide in scope, have high yields, and generate only inoffensive byproducts that can be removed by nonchromatographic methods. The concept and methodology were widely accepted and developed quickly, and until recently, several types of

reactions have been identified that fulfill these criteria, the most used ones include thiol-ene reaction,<sup>9,10</sup> hydrazone/oxime ether formation,<sup>11-15</sup> nucleophilic substitution,<sup>16</sup> Diels–Alder reaction<sup>17,18</sup> and Huisgen 1, 3-dipolar cycloaddition.<sup>8,19</sup>

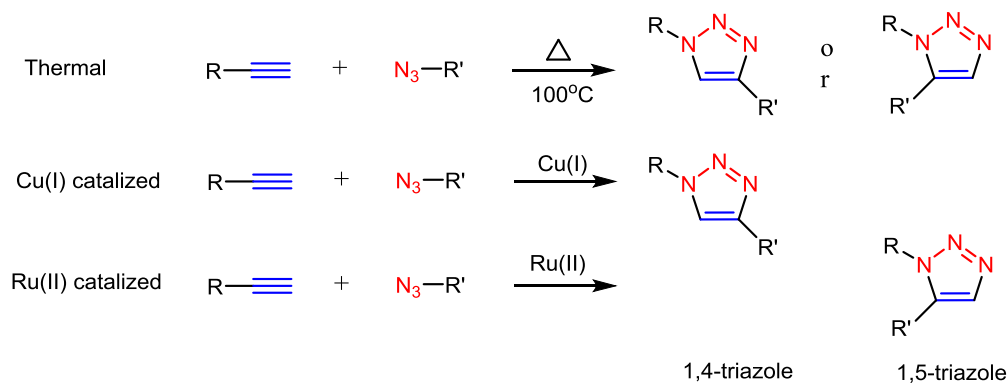
Click chemistry provides the potential to attach a probe or substrate of interest to a specific biomolecule, making it a very powerful tool in almost all fields of research and technology, including drug discovery,<sup>20</sup> polymer science,<sup>21,22</sup> Nanoscience,<sup>23</sup> and bioconjugation.<sup>24,25</sup>

#### Copper-catalyzed azide-alkyne cycloaddition (CuAAC)

Up until now, the most famous and commonly used bioorthogonal reaction is copper-catalyzed azide-alkyne cycloaddition (CuAAC), mainly because of its relatively fast kinetics, high selectivity between azide and alkyne. Moreover, azides and alkynes are hardly found in native biomolecules, and they are small, not very polar, and incapable of significant hydrogen bonding, making them unlikely to significantly change the properties of structures to which they are attached.<sup>8,26,27</sup> They can be easily introduced into biomolecules such as glycans, proteins, lipids and nucleic acids by biosynthetic pathways.

CuAAC is a variant of the Huisgen 1, 3-dipolar cycloaddition reaction, using a Cu(I) as catalyst to form 1,4-disubstituted-1,2,3-triazoles specifically. This is a big improvement compared to Huisgen non-catalyzed 1, 3-dipolar cycloaddition, which gives both 1, 4- and 1, 5-isomers and requires a temperature of 100 degrees celsius and long reaction time (Scheme 1.1).<sup>28,29</sup> Later in 2005, Sharpless and coworkers reported the ruthenium-catalyzed cycloaddition of azides to

alkynes to form the complementary 1, 5-disubstituted triazoles,<sup>30</sup> however, this click reaction, termed RuAAC has not yet found a wide application.



Scheme 1.1 Thermal and metal catalyzed azide-alkyne cycloaddition reactions.

CuAAC has become a commonly employed method for the synthesis of complex molecular architectures under complicated conditions. The CuAAC reaction is so versatile that almost any copper source can be used as a catalyst/ precatalyst, which has been well studied in recent decades. For example, Cu(I) salts,<sup>26</sup> Cu(II) salts,<sup>8,31,32</sup> polymeric copper(I) acetate,<sup>33</sup> preformed Cu(I) complexes,<sup>34,35</sup> metallic copper,<sup>27,36</sup> have been used in CuAAC. But the most widely applied method is the *in situ* reduction of CuSO<sub>4</sub>·5H<sub>2</sub>O with sodium ascorbate in water/alcohol mixtures.<sup>8</sup> The presence of an organic co-solvent (alcohol or DMSO) ensures the solubility of most hydrophobic reactants. Meanwhile, the aqueous compatibility allows for the application of CuAAC in bioconjugation.

The reaction mechanism of CuAAC has been studied from the beginning of this century. The first mechanism was proposed in 2002, which only included one copper atom.<sup>8,37,38</sup> Later in 2013, isotope studies have suggested the contribution of two functionally distinct copper atoms in the mechanism.<sup>39</sup>

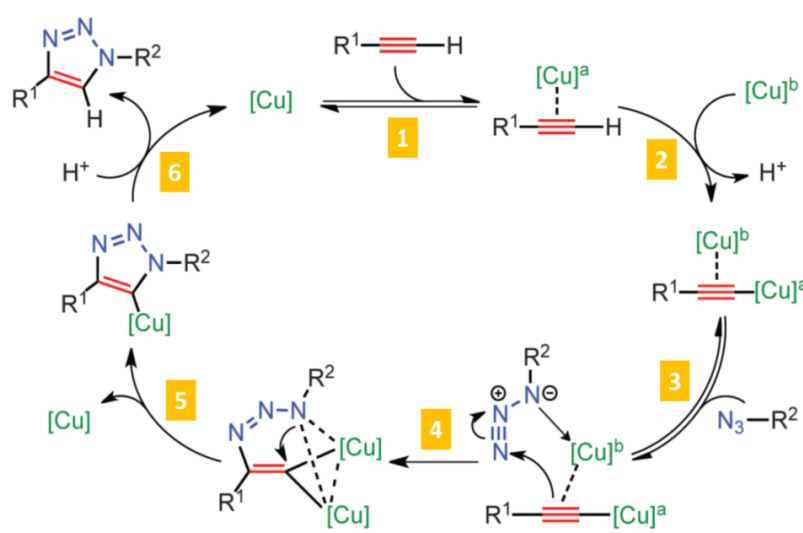


Figure 1.2 Proposed mechanism of CuAAC. Adapted from reference [39]<sup>39</sup>

First, the  $\sigma$ -bound copper acetylide bearing the  $\pi$ -bound enriched copper atom reversibly coordinates an organic azide, forming a complex with two copper atoms, which was confirmed by TOF-MS study. Next,  $\beta$ -carbon of the acetylide attacks N-3 of the azide forms the first covalent C–N bond. The second copper atom acts as a stabilizing donor ligand. Next, Ring contraction gives the second covalent C–N bond, forming copper triazolide, followed by protonolysis that delivers the final triazole product and closes the catalytic cycle.

Cu(I) has greatly improved the efficiency of the Huisgen 1, 3-dipolar cycloaddition reaction as catalyst, however, it raises the issue of potential toxicity *in vivo* systems at the same time and hinders the applications of CuAAC in living cells. Oxidative stress and biological damage associated with CuAAC has been attributed to Cu(I)-promoted generation of reactive oxygen species (ROS) from  $O_2$ ,<sup>40</sup> the oxidation of unstable Cu(I) to Cu(II) by either  $O_2$  or  $H_2O_2$  facilitates the production of superoxide and hydroxyl radicals,<sup>41</sup> which can affect the structural and functional integrity of biomolecules, causing degradation of amino acids and cleavage of

peptide chains.<sup>42</sup> Furthermore, the oxidized form of ascorbate-reducing agent used in these reactions can also cause damage by reacting with lysine, arginine, and cysteine side chains,<sup>43</sup> leading to protein crosslinking.<sup>44</sup>

To address this issue, and further improve the reaction kinetics and efficiency, several ligands, which can increase the reactivity of Cu(I) by stabilizing the Cu(I) oxidation state and thereby reduce the amount of Cu(I) to decrease the toxicity, have been developed.

The first applied ligand was TBTA, which could efficiently stabilize the catalyst and result in the utilization of CuAAC in biological fields, however, it suffers from poor water solubility due to its lipophilic structure.<sup>45,46</sup> Luckily, inspired by TBTA, studies of catalytic ligands<sup>47-51</sup> with various structures soon followed, and some of them were mainly focused on improvement of the biocompatibility issues by stabilizing Cu(I).<sup>52</sup>

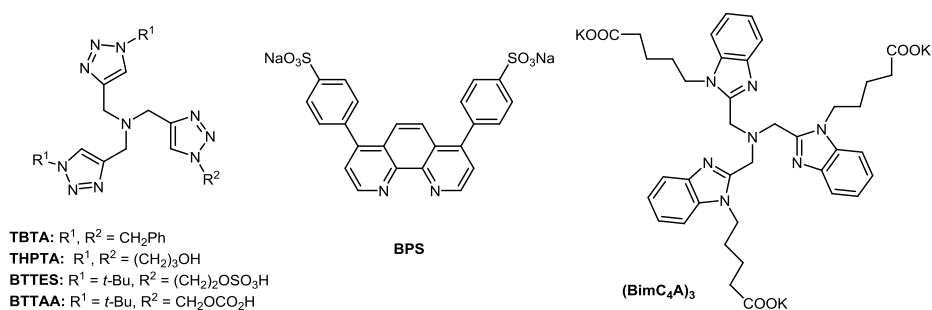


Figure 1.3 Accelerating ligands commonly used in the CuAAC reaction.

### Metal free click chemistry

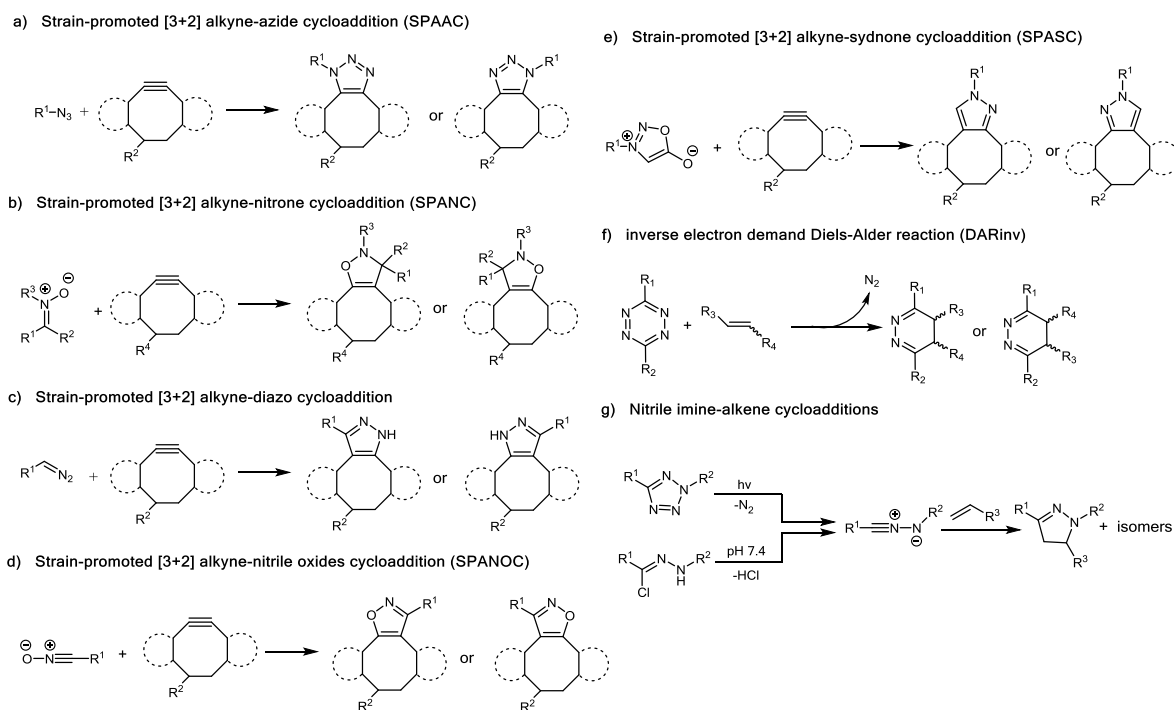
There is no doubt that the use of ligands has broadened the biological applications of CuAAC.<sup>53</sup> However, the most effective way to address the cytotoxicity problem is to develop metal free bioorthogonal reactions. This kind of reactions does not require any metal catalyst to



perform an efficient ligation reaction, and therefore, avoids undesirable effects in living cells.

The reactions include alternative strain-promoted 1, 3-dipolar cycloaddition reactions (the strained alkyne can react with azide (SPAAC),<sup>54</sup> nitron (SPANC),<sup>55,56</sup> nitrile oxides (SPANOC),<sup>57,58</sup>. Diazoalkanes (SPADC),<sup>59,60</sup> and syndones (SPASC).<sup>61</sup>), inverse electron demand Diels–Alder reaction (DARinv),<sup>17,18,62–65</sup> Nitrile imine–alkene cycloadditions (nitrile imines can be generated by photolysis of tetrazoles or decomposition of hydrazonoyl chlorides).

66-72



Scheme 1.2 Metal free bioorthogonal reactions

### Stain Promoted Azide-Alkyne Cycloaddition (SPAAC)

The strain-promoted azidealkyne cycloaddition (SPAAC)<sup>54,73</sup> has been used to label abundant biomolecules within complex biological systems, including live mammalian cells and

animals.<sup>74,75</sup> In the past decade, efforts have been focused on increasing the reaction rate, water solubility, biocompatibility, and pharmacokinetic properties of the alkyne reagents used in SPAAC.

Bertozzi's group first considered an alternative means of activating alkynes for catalyst-free [3 + 2] cycloaddition with azides: ring strain.<sup>54</sup> When cyclooctyne-the smallest of the stable cycloalkynes, reacts with azide, the destabilization of the ground state versus the transition state provides immense rate acceleration compared to unstrained alkynes. OCT was initially investigated as the first generation of cyclooctynes, followed by MOFO and DIFO,<sup>73,74</sup> which has increased reaction rate by appending electron withdrawing groups at the propargylic position.

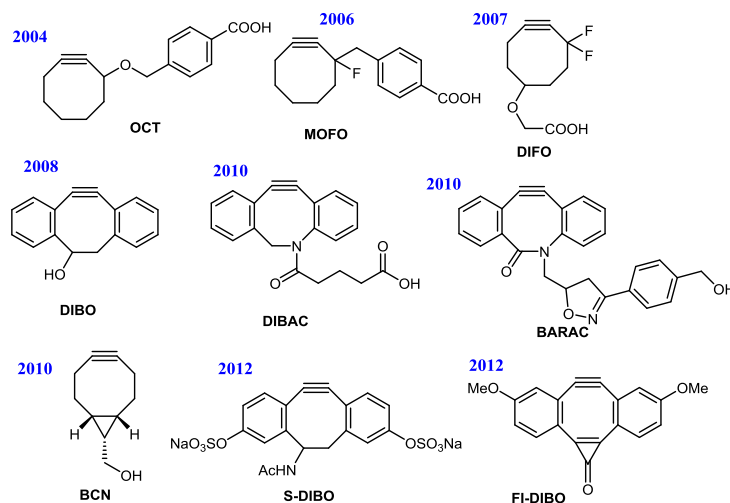


Figure 1.4 Overview of functionalized cyclooctynes suitable for conjugation reactions.

In 2008, our group employed a different approach to modulate the alkyne. Instead of using fluoro-activation, fused phenyl rings were introduced on both sides of the alkyne group to

increase the ring strain, turned DIBO.<sup>76</sup> DIBO analogues are especially attractive cyclooctyne derivatives due to their synthetic accessibility, and increased stability.

Inspired by DIBO, DIBAC<sup>77</sup> which has a nitrogen atom within the strained ring system, was developed by Delft's group. The nitrogen atom can interrupt the hydrophobic surface area and provides a convenient site for probe conjugation. Also, the exocyclic amide linkage can provide one more sp<sup>2</sup>-like center to the dibenzocyclooctyne ring, thus giving a further rate-enhancing effect. Soon after, Bertozzi's group investigated another cyclooctyne probes, BARAC<sup>78</sup> which has an endocyclic amide bond, showing exceptional reaction kinetics. Amides have a significant resonance structure wherein the lone pair of electrons on the nitrogen atom is delocalized between the nitrogen and carbonyl, giving the C-N bond partial  $\pi$ -character, which causes the C-N bond to be slightly shorter as compared to the C-C bond in DIBO. As a result, the amide linkage effectively reduces the size of the ring, which in turn exerts more strain onto the alkyne. However, the superior reaction rate of BARAC is counterbalanced by its instability toward hydrolysis in phosphate buffered saline ( $t_{1/2}$  = 24 h) and its tendency for intramolecular rearrangement under acidic conditions.<sup>79</sup> As a result, it must be stored at 0 °C, protected from light and oxygen.

Furthermore, Delft's group described a novel cyclooctyne probe, BCN,<sup>80</sup> with a cyclopropyl group attached on the backbone of cyclooctyne to increase the ring strain. This new analogue has a smaller size, decreased lipophilicity and exhibit excellent reaction kinetics in strain-promoted cycloaddition reactions.<sup>81</sup>

Table 1.1 Reaction rate constants (with BnN<sub>3</sub> or similar aliphatic azide) and synthetic accessibility of cyclooctynes.

Year	Cyclooctyne	$k_2$ (M <sup>-1</sup> s <sup>-1</sup> )	#steps	Yield%
2004	OCT	0.0024	4	52
2006	MOFO	0.0043	5	15
2007	DIFO	0.076	10	1
2008	DIBO	0.057	4	23
2010	DIBAC	0.31	9	41
2010	BARAC	0.96	6	18
2010	BCN	0.14	4	15
2012	S-DIBO	0.116	7	13
2012	FI-DIBO	0.019	5	35

Despite the many attractive features of cyclooctynes, their hydrophobic nature and relatively large size represent a serious shortcoming, which can affect their distribution and change the biological properties of the species to which they are attached. In particular, it can cause sequestration by membranes or nonspecific binding to serum proteins, thereby reducing bioavailability.<sup>82</sup> Thus, S-DIBO<sup>83</sup> was synthesized to address this problem by adding two sulfate groups to the aromatic rings. This new analog reacts fast with azides, has excellent stabilities under moderately acidic and basic conditions, and can be employed for labeling azido-modified glycoconjugates of living cells without passing the cell membrane, offering unique opportunities for glycomics and glycoproteomics studies.

In 2012, our group also prepared a modified dibenzocyclooctyne (FI-DIBO) that undergoes fast strain-promoted cycloadditions with azides to yield strongly fluorescent

triazoles.<sup>84</sup> The fluorescence was only generated after click reaction with azide, which provides many attractive features such as eliminating the need for probe washout, reducing background labeling and offering opportunities for monitoring biological processes in real time.

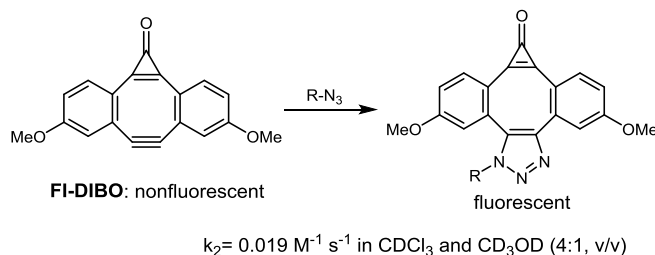


Figure 1.5 SPAAC with FI-DIBO and the kinetics.

Moreover, the application of SPAAC in bioconjugation has been largely amplified, especially after the commercial availability of a variety of derivatives, including those with pendant and orthogonal reactive functionality such as NHS ester or maleimide.

In addition to cyclooctynes, other stained alkyne, such as TMTH,<sup>85</sup> also investigated as a probe to react with azide through 1, 3 dipolar cycloaddition. Its reaction with benzyl azide in  $\text{CD}_3\text{CN}$  proceeded cleanly with a second-order rate constant of  $4.0 \text{ M}^{-1} \text{ s}^{-1}$ , the fastest reported cycloalkyne–azide reaction to date, but it also suffers from poor stability.

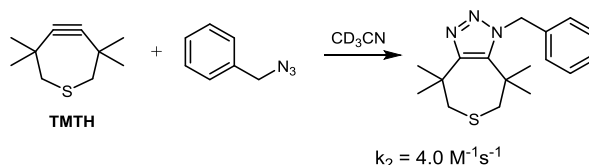


Figure 1.6 SPAAC with TMTH.

### Stain Promoted Azide-Nitrone Cycloaddition (SPANAC)

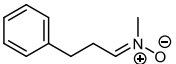
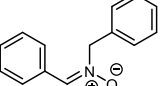
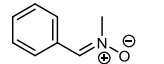
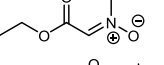
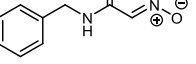
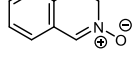
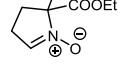
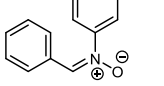
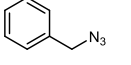
The efforts focusing on increasing the SPAAC reaction rate have achieved great success, which has lowered the concentrations of the labelling reagents for bioorthogonal reactions,

thereby lowering the risk of potential toxicity, interference with cellular processes, and non-specific labelling. In the past decade, most efforts have focused on increasing the reactivity of the cyclooctyne reagent. Their reacting partner, azide, is considered bioorthogonal and is widely used in both CuAAC and SPAAC due to its small size and noninterference. However, utilizing more reactive alternatives to azides can greatly enhance the reaction rate leading to the use of even lower concentrations of labelling reagents. Nitrones have been used in place of azides as partners in strain-promoted alkyne-nitrone cycloaddition (SPANC) for applications such as protein modification.<sup>55,86</sup>

SPANC reactions represent versatile tools for chemical biology and define their utility by the observation of rapid reaction kinetics ( $k_2$  up to  $60 \text{ M}^{-1} \text{ s}^{-1}$ ),<sup>87</sup> biological stability of reagents and products, compatibility with living systems, and systematic tunability through substitution of groups on both the carbon and nitrogen atoms of the nitrone dipole.<sup>88</sup> Compared to SPAAC, the 1,3-dipolar nitrones bear up to three R-groups that can modulate nitrone reactivity.

Generally speaking, acyclic aromatic nitrones bearing electron-withdrawing groups at  $\alpha$ -C position reacted more rapidly than the unsubstituted parent nitrone and those bearing electron-donating groups. Endocyclic nitrones showed increased reactivity relative to their acyclic counterparts.<sup>55,87</sup> And the highest kinetics was obtained when the *N*-methyl group was replaced by a phenyl group (**1c** to **1h**). Of course, the reactions between nitrones and BARAC are even faster than those with DIBO.

Table 1.2 Rate constants for the cycloaddition of cyclooctyne with nitrones.

	Substrate	DIBO	BARAC
1a		0.032	
1b		0.088	2.8
1c		0.13	6.8
1d		3.9	
1e		2.2	
1f		1.5	22
1g		7.7	47
1h		too fast for accurate determination	59
		0.057	0.96

The application scope of SPANC is not that big when compared to SPAAC. But it has been successfully used for *N*-terminal peptide modification,<sup>55</sup> direct protein labeling, and pretargeted labeling of ligand-receptor interactions on cell surfaces,<sup>89</sup> while metabolic incorporation of the nitron functional group has proven challenging in mammalian cells. Furthermore, nitron reactivity is tunable to allow for simultaneous SPANC reactions for rapid, selective, and bioorthogonal multiplex labeling.<sup>55,90</sup>

In addition to nitrones, other 1, 3-dipoles have emerged such as diazo-compounds and nitrile oxides for use in place of azides in strain-promoted cycloadditions with cyclooctynes. They also have many applications in labeling cellular components.<sup>57,60,91,92</sup>

### Inverse electron-demand Diels–Alder reaction (DARinv)

The Diels–Alder reaction is defined as a [4+2] cycloaddition between a conjugated diene and a substituted dienophile (alkene or alkyne), in which two new chemical bonds and a six-membered ring are formed. Based on the electronic effects of the substituent on the diene and dienophile, Diels-Alder reactions can be classified as normal electron-demand and inverse electron demand reactions.

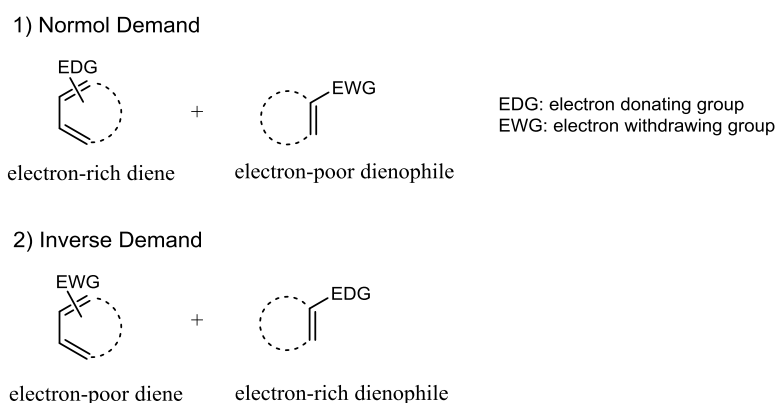


Figure 1.7 Normal electron-demand and inverse electron-demand Diels–Alder reaction.

The most commonly used Diels-Alder bioorthogonal reactions are DARinv. Tetrazine ligations, the most representative within the Diels-Alder reaction family, were first reported to be bioorthogonal independently by Fox group and Hilderbrand's group in 2008.<sup>17,18</sup> They are reported as the fastest bioorthogonal reactions to date, with rate constants between  $10^3$  and  $10^6$   $\text{M}^{-1}\text{s}^{-1}$ .<sup>6,93</sup>

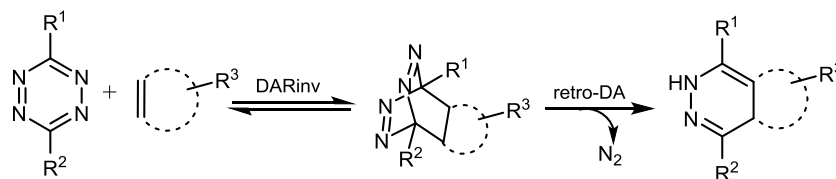


Figure 1.8 Tetrazine bioorthogonal reaction.



As shown in Figure 1.8, s-tetrazine (1,2,4,5-tetrazine) and a strained alkene undergoes an inverse electron-demand Diels-Alder cycloaddition followed by a retro-Diels-Alder reaction to yield a stable dihydropyridazine adduct and release N<sub>2</sub>. This reaction proceeds very fast at room temperature in aqueous environments without a catalyst with high yield, moreover, the reactive components are compatible with a variety of functional groups and challenging conditions.

In general, monosubstituted tetrazines ( $R^1 = \text{aryl}$ ,  $R^2 = \text{H}$ ) show the highest reactivity due to less steric hindrance, but also suffer from poor stability in the presence of water or biologically relevant nucleophiles. Tetrazine stability is dramatically enhanced by changing the substituents to, for example, alkyl groups.<sup>65,94,95</sup> In other words, compounds with stronger electron withdrawing groups showed lower stability than hydrogen substituted tetrazines (monosubstituted tetrazines) and the electron donating alkyl substituted tetrazines showed the highest stability, but lowest reactivity.

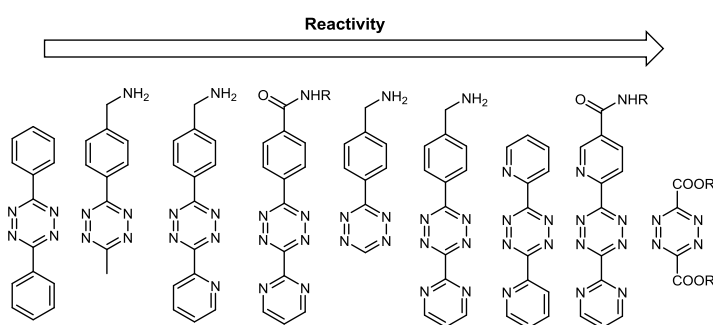
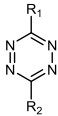
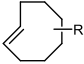
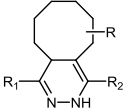

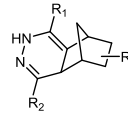
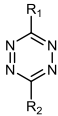
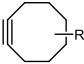
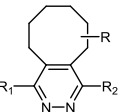
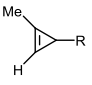
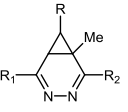

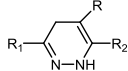
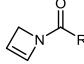
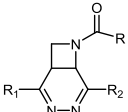


Figure 1.9 Reactivity of tetrazines with different substituents.

In terms of dienophile reaction partner, trans-cyclooctenes (TCOs) afford the highest kinetics reported by Fox and coworkers. Increasing the strain in the trans-cyclooctene moiety through cyclopropyl fusion resulted in a 50-fold rate enhancement.<sup>96</sup> A potential limitation of

these highly reactive trans-cyclooctenes is isomerization to the more stable, but less reactive cis isomer by heat or by light.<sup>97</sup>

Table 1.3 Tetrazine-Based Inverse-Electron Demand Diels-Alder Reactions with Strained Alkenes and Alkynes.

Tetrazine	Dienophile	Product	Kinetics ( $M^{-1}s^{-1}$ )	Year
			210-2,800,000	2008
			0.12-9.5	2008
			3.3-41	2012
			0.03-13	2012
			0.02-0.04	2013
			0.39	2014

Coinciding with the initial report on TCO, Hilderbrand and co-workers described another strained alkene, norbornene (NB) as a probe to react with tetrazines through DARinv.<sup>18</sup> The reaction rate is much smaller than TCO, but NB is far more stable in solution and upon storage.

In 2012, cyclopropenes have been described, which possess a distinct advantage over TCO owing to their smaller size, better stability and broad compatibility with cellular enzymes.<sup>63,64</sup> The kinetics is also tunable depending on the substituents on the cyclopropene ring. Furthermore, tetrazines also undergo cycloadditions with sterically unhindered cyclooctynes,<sup>95</sup>

and *N*-acylazetidine,<sup>98</sup> which were reported in 2012 and 2014 respectively.

Even more impressive, tetrazines absorb visible light, with an absorption maximum of around 520 nm. Weissleder and coworkers showed that a series of green-to-red fluorophores are efficiently quenched by tetrazines via FRET (fluorescence resonance energy transfer), and with up to a 20-fold enhancement in fluorescence after destruction of the tetrazine upon DARinv.<sup>62</sup> This fluorogenic property when conjugated to certain fluorophores, could facilitate highly useful applications in bimolecular imaging.

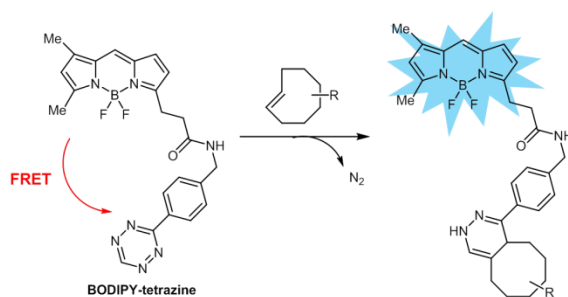


Figure 1.10 Fluorogenic conjugation of BODIPY-tetrazine with TCO.

In 2013, Robillard and coworkers developed a bioorthogonal elimination reaction that enables instantaneous, self-immolative, and traceless release of a substance from trans-cyclooctene following tetrazine ligation.<sup>99,100</sup> They prepared a TCO containing a carbamate-linked drug at the allylic position. After cycloaddition with tetrazine, the formed 1,4-dihydropyridazine product undergoes a  $\beta$ -elimination of carbamate, which liberates the free amine substituted drug after decarboxylation. The cycloaddition rate was decreased 20-fold compared to the parent TCO due to the steric hindrance from the carbamate, meanwhile efficient enough such that a majority of the cargo was released within minutes after the addition of tetrazine.

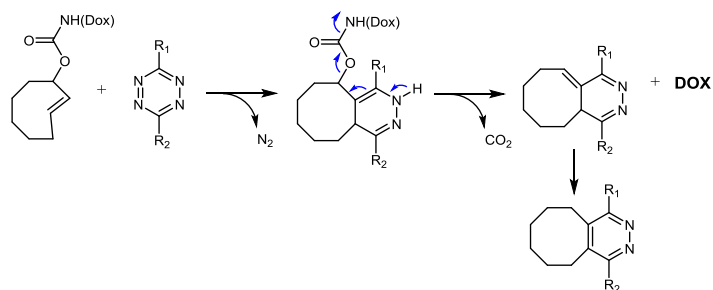


Figure 1.11 DARinv between TCO-DOX and tetrazine.

The trans-cyclooctene component, also suffers from some disadvantages, such as size and hydrophobicity, just like cyclooctynes used for SPAAC. However, tetrazines react reasonably well with the much smaller moieties (terminal alkenes, cyclopropenes), making the components of the tetrazine ligation reaction not much more perturbing than azides and alkynes used in CuAAC. Moreover, the reaction rate of DARinv is highly tunable across many orders of magnitude by chemically manipulating the substituents of the tetrazine's 3,6 positions, or by employing different dienophiles, enabling DARinv to meet the needs of many different applications in living systems. Furthermore, the availability of the tetrazine component has been dramatically improved by new synthetic methods,<sup>101-103</sup> and by the commercial availability of a few derivatives.

For these reasons, tetrazine bioorthogonal reactions are attracting significant interest for labeling and detecting various kinds of biomolecules in vitro and in vivo.

### Chemical reporter strategy

There are many components in living systems, such as interacting biopolymers, ions and metabolites, which drive a complex array of cellular processes. Many of these components cannot be observed when the biomolecules are examined in their purified, isolated forms.<sup>104</sup>

Accordingly, researchers have moved forward to study these biological processes in the context of living cells or whole animals. As a result, several methods have been developed to remodel cellular molecules with proper tags for detection and isolation from biological samples.

One popular tagging strategy for cellular monitoring discrete proteins involves the use of the green fluorescent protein (GFP) and its related variants.<sup>105,106</sup> The fusion of these probes to a target protein makes it possible to visualize this protein by fluorescence microscopy and quantification by flow cytometry. However, GFPs can cause significant perturbations to a protein's structure due to their relatively large size and have no direct extension to other classes of biomolecules such as lipids, glycans, nucleic acids. Therefore, methods to visualize both proteins and their modifiers would contribute to a more holistic understanding of cellular biochemistry.

Nowadays, the most popular strategy to dissect complex cellular processes is chemical reporter strategy, which involves the incorporation of unique chemical functionality—a bioorthogonal chemical reporter—into a target biomolecule using the cell's own biosynthetic machinery.

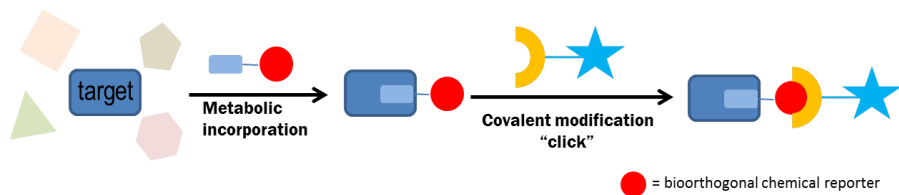
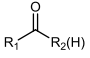
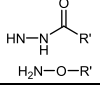
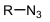
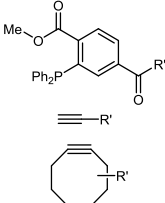
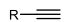
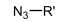
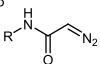
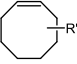
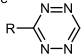
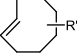
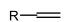
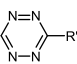

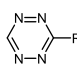


Figure 1.12 The bioorthogonal chemical reporter strategy.

A chemical reporter (red circle), often as small as a single functional group, linked to a substrate (light blue box) is introduced into a biomolecule of interest (dard blue box) through cellular metabolism. Subsequent covalent reaction between the reporter and an exogenously

delivered probe (yellow arc) that has a complementary bioorthogonal reactive moiety enables the target biomolecule to be visualized or retrieved. Here, the choice of the chemical reporters is the most important part for the success of this strategy, which should be non-perturbing handles that can be modified through highly selective reactions with exogenously delivered probes in living systems.

Table 1.4 Chemical reporters and bioorthogonal reactions used in living systems.

Chemical reporter	Probe	Reaction
Ketone/aldehyde 		Hydrazone formation Oxime formation
Azide 		Staudinger ligation CuAAC SPAAC
Terminal alkyne 		CuAAC
Diazo 		SPAAC
Tetrazine 		DAInv
Terminal alkene 		DAInv
Cyclopropene 		DAInv

To date, only a few of broadly applicable reporters have been identified, owing to their rigorous demands. Ketones and aldehydes have been utilized to label proteins and glycans on cell surfaces and in the extracellular environment that can be ligated with hydrazine and hydroxylamine derivatives to form hydrazones and oximes.<sup>107-109</sup> However, the reactions are not

truly bioorthogonal because keto and aldehydic metabolites are abundant in cells and biological fluids. That, along with the fact that the reactions' pH optima are 3-5, has limited their use *in vivo*.

Azide has emerged as the most popular chemical reporter of choice. Azides can be readily affixed to metabolic precursors owing to their remarkable biocompatibility and unique reactivity. Once installed, these motifs can undergo highly selective reactions such as the Staudinger ligation with triarylphosphines, the copper-catalyzed azide-alkyne 1, 3-dipolar cycloaddition (CuAAC), and Cu-free click chemistry with strained alkynes.<sup>110-113</sup>

In a similar way, terminal alkyne can provide a bioorthogonal reporter that can be chemoselectively labeled with azido-containing probes through CuAAC.<sup>114-117</sup> By using both azide and alkyne as chemical reporters, dual marking of biomolecules can be achieved with sequential combination of SPAAC and CuAAC reactions.<sup>118,119</sup> Besides azide, diazo was also developed as chemical reporter group for bioorthogonal labelling of biomolecules through SPAAC with strained alkyne.<sup>120</sup> In addition to 1, 3-dipolar cycloadditions, the development of tetrazine reagents has enabled selective and rapid bioorthogonal labeling of activated alkynes and alkenes through the Diels-Alder reaction.<sup>18,121,122</sup> Moreover, cyclopropenes and terminal alkenes can be metabolic incorporated to into cell surface oligosaccharides due to their small size.<sup>63,64,123,124</sup>

The bioorthogonal reporter strategy has proved to be a powerful tool to image glycans,<sup>107,125-127</sup> proteins,<sup>108,110,128</sup> lipids<sup>111</sup> and other biomolecules.

## Metabolic oligosaccharide engineering (MOE) and selective cancer targeting

As we know, all cell surfaces are decorated with a dense layer of glycans in vertebrates, which are complex biopolymers made of different monosaccharide building blocks, and glycosylation is one of the most common and complex forms of protein modification in biology. The glycans mediate a wide range of cellular functions, such as adhesion, differentiation, cell-cell interactions, and recognition of external molecules, by mediating intracellular signaling events. In addition, glycosylation plays an important role inside cells by regulating protein trafficking, turnover and signal transduction.<sup>129,130</sup>

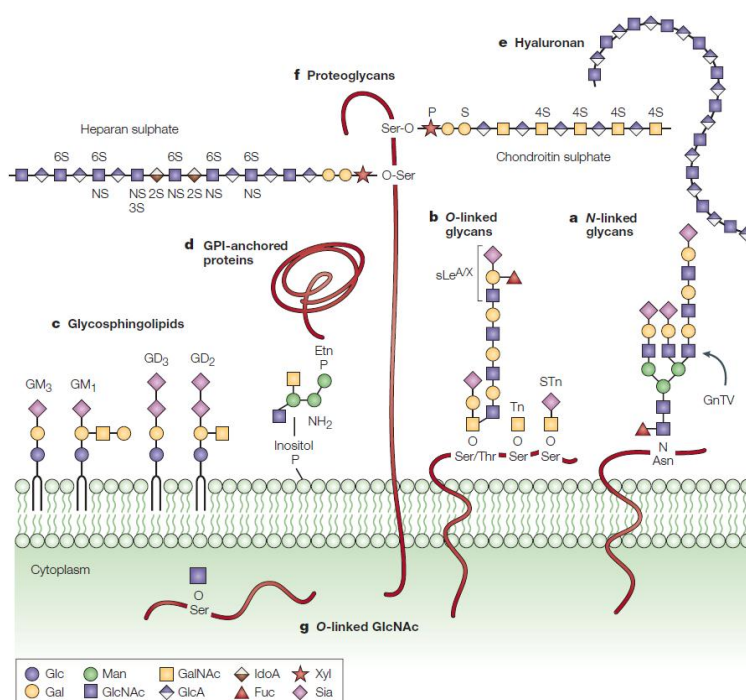


Figure 1.13 Common classes of animal glycans. Adapted from reference [131]<sup>131</sup>

There are several common classes of animal glycans (Figure 1.13): **a.** *N*-linked glycans; **b.** *O*-linked glycans; **c.** Glycosphingolipids; **d.** Glycosylphosphatidylinositol (GPI)-linked proteins; **e.** hyaluronan; **f.** proteoglycans (heparan sulphate, chondroitin sulphate and dermatan sulphate)



and **g.** *O*-linked *N*-acetylglucosamine (*O*-GlcNAc). They all have their own functionalities in biological processes. However, the roles of cell-surface glycans remain elusive compared to proteins or lipids because of their diverse and dynamic nature,<sup>132</sup> since each oligosaccharide chain has multiple linkage types along with intricate stereochemistry. Moreover, the biosynthesis of glycans is not genetically encoded, and as a result, their imaging or quantitative analysis are not as straightforward as those for doing DNA and proteins with conventional biochemical methods.<sup>104,133</sup> In this regard, metabolic incorporation of unnatural monosaccharides in the cellular glycosynthetic pathway, termed metabolic oligosaccharide engineering (MOE), has emerged as an invaluable chemical biology tool that enables metabolic installation of useful functionalities into cell-surface.<sup>134</sup>

This metabolic approach stemmed from the early work by Reutter and coworkers,<sup>135-138</sup> who used the *N*-acyl derivatives of *N*-acetyl-D-mannosamine and *N*-acetyl-D-glucosamine in metabolic synthesis of sialic acids *in vitro* and *in vivo*. ManNAc by an additional methylene (CH<sub>2</sub>) group, has intensively been used and applied to neuroblastoma, nonneuronal glia, and cerebellar cells.<sup>139,140</sup>

On the other hand, Bertozzi and coworkers have explored a powerful elegant methodology,<sup>107,141-143</sup> that combines metabolic engineering and bioorthogonal reactions. This methodology includes the metabolic introduction of monosaccharide based chemical reporters, for example Peracetylated *N*-azidoacetyl-D-mannosamine (Ac<sub>4</sub>ManNAz), onto cellular surface glycans followed by bioorthogonal, chemoselective coupling with a fluorescent dye or an affinity tag bearing phosphine (Staudinger ligation) /alkyne (CuAAC or SPAAC) group.<sup>112,114,125</sup> This

remarkable study has inspired the development of many other azide- and alkyne-functionalized chemical reporters, including monosaccharide reporters Ac<sub>4</sub>GalNAz for mucin-type O-linked glycoproteins,<sup>75,85,144</sup> Ac<sub>4</sub>6-ethynyl-L-fucose for fucosylated glycans,<sup>50,113,116,145</sup> and Ac<sub>4</sub>GlcNAIk for intracellular O-GlcNAc-modified proteins,<sup>146</sup> enabling *in situ* imaging or proteomic enrichment of one glycan type and has been applied to many different cell lines (e.g., Jurkat, CHO and HeLa cells) and organisms (e.g., microbes, mice and zebrafish).

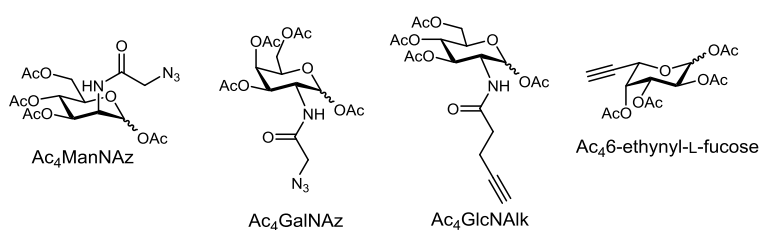


Figure 1.14 monosaccharide based chemical reporters.

Specifically, metabolic remodeling of cell-surface sialic acids through sialic acids biosynthetic pathway has been widely developed. sialic acids are a family of negatively charged nine-carbon monosaccharides that often reside at the outermost ends of glycan chains.<sup>147</sup> They have more than 50 naturally occurring forms, among which Neu5Ac is the most abundant one in humans.<sup>148</sup>

Cell-surface sialic acids are essential in mediating a variety of physiological and pathological processes, whose generation is governed by the sialic acid biosynthetic machinery.

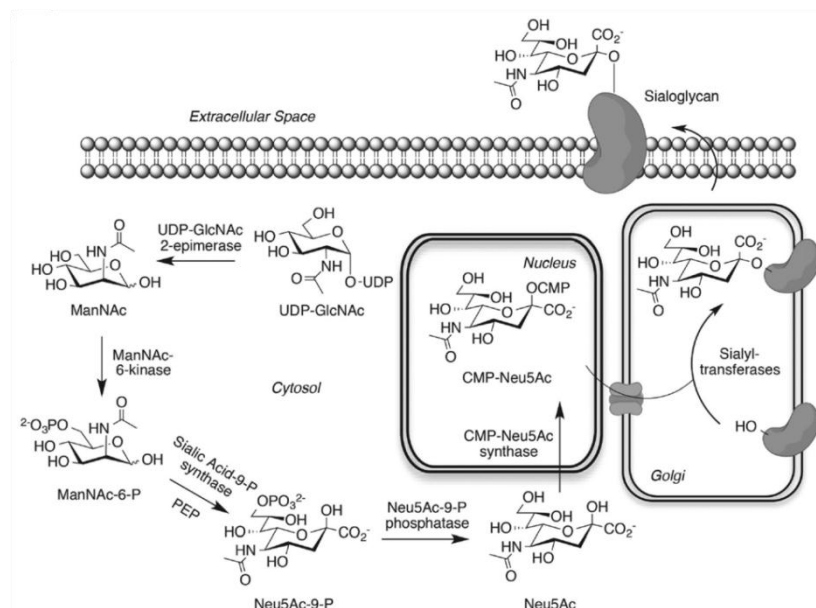


Figure 1.15 The biosynthetic pathway of sialic acids. Adapted from reference [149]<sup>149</sup>

The biosynthesis of Neu5Ac involves enzymatic conversion of UDP-*N*-acetylglucosamine (UDP-GlcNAc) into *N*-acetylmannosamine (ManNAc), which is phosphorylated to give ManNAc-6-phosphate. Condensation of ManNAc-6-phosphate with phosphoenolpyruvate yields Neu5Ac-9-phosphate, followed by dephosphorylation to give Neu5Ac, which is converted into the nucleotide sugar donor CMP-Neu5Ac in the nucleus with CMP-Neu5Ac synthetase. CMP-sialic acid is transported into the Golgi compartment, in which it serves as the substrate for sialylation catalyzed by sialyltransferases. The resulting sialoglycoconjugates, such as sialylated proteins and lipids, are then delivered to the cell surfaces.

Sialic acids play critical roles in diverse cellular processes as ligands, including cell differentiation, host–pathogen interactions, and signaling transduction.<sup>129,150</sup> In contrast to displaying ligands, sialic acids can also mask the underlying glycan epitopes, therefore

preventing protein binding.<sup>151</sup> For example, sialic acid can "hide" mannose antigens on the surface of host cells or bacteria from mannose-binding lectin. Additionally, metastatic cancer cells often express glycoproteins containing a high density of negatively charged sialic acids. The resulting repulsion between these late-stage cancer cells facilitates their entry into the blood stream.<sup>152</sup>

The cellular level of sialoglycans is dynamically regulated by the expression and activity of enzymes involved in sialoglycan biosynthesis, such as sialyltransferases and post-Golgi glycosidases such as sialidases.<sup>153-155</sup> Despite the involvement of sialoglycans in so many important biological processes, elucidating the dynamics and function of sialylation remains a challenge due to its structural diversity and versatility. However, the chemical reporter strategy has opened a door for intensive exploitation of the functions of sialic acids.

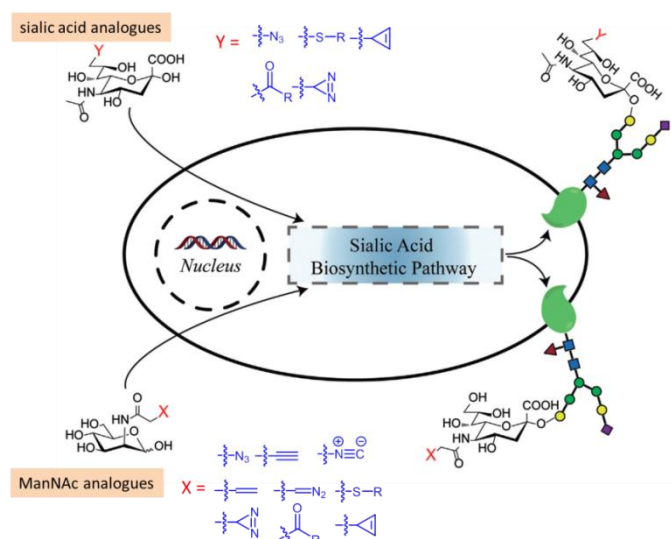


Figure 1.16 Metabolic oligosaccharide engineering of cell-surface sialic acids.

Adapted from reference [149]

An unnatural analogue of the precursor (ManNAc analogues) or intermediate (sialic acid analogues) containing a chemical functional group X or Y, is taken up by the cell and intercepts

the biosynthetic pathway. The biosynthetic enzymes tolerate the subtle chemical modification on the analogue and install it into cellular sialoglycans in the same way as its natural counterpart. For example, it is known that sialyltransferases tolerate modifications at C-5 and C-9 positions of sialic acid.<sup>156</sup> The outcome is the display of an unnatural functionality (X or Y) on cell-surface sialic acids. The incorporated unnatural functionality can be exploited to modulate the properties of cell-surface sialoglycans and the underlying cellular processes such as receptor binding, cell growth, and signal transduction.

Relying on passive diffusion into the interiors of cells, MOE based unnatural analogue cannot selectively label glycans in a specific tissue of interest *in vivo*, but are instead incorporated into sialoglycans in various tissues.<sup>112</sup> This limits MOE for *in vivo* glycan imaging in which probing of sialylation in a specific tissue or cell type is desired. To overcome this limitation, several groups have developed cell-selective MOE strategy and enabled selective *in vitro* or *in vivo* cancer targeting.

Kim and coworkers proposed a two-step strategy for *in vivo* tumor-targeting via metabolic glycoengineering and click chemistry.<sup>157,158</sup> First, an intravenous injection of glycol chitosan nanoparticle (Ac<sub>4</sub>ManNAz-CNP) generates azide groups on tumor tissue by site-specific metabolic glycoengineering. This is based on the fact that nanoparticles exhibit higher accumulation in angiogenic disease sites like tumors than normal tissues as a result of enhanced permeation and retention (EPR) effect.<sup>159</sup> These azide groups enhance the tumor-targeting ability of a second intravenous injection of BCN-Ce6-CNPs by copper-free click chemistry *in vivo*. Thus, a large amount of drugs can be delivered in tumor tissue.

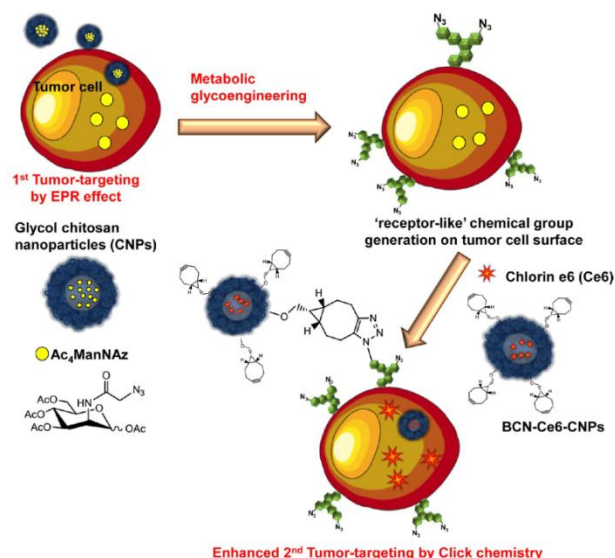


Figure 1.17 Two-step in vivo tumor-targeting strategy for nanoparticles via metabolic glycoengineering and click chemistry.<sup>157</sup> Adapted from reference [157]

Xing Chen's group developed a strategy for the targeted imaging of tumor-associated glycans by using ligand-targeted liposomes encapsulating unnatural sugar (9Az-Neu5Ac).<sup>160-162</sup> The liposomes encapsulating azidosugars are intravenously injected into the tumor-bearing mice. The ligands (e.g., cRGDyK) are selectively recognized by the cell-surface receptors (e.g.,  $\alpha\text{V}\beta 3$ ) only expressed or up-regulated on the tumors, but not expressed or down-regulated on normal cells, which induces the internalization of the liposomal azidosugars into the cancer cells. Next, the azido functional groups are metabolically installed into the tumor-associated glycans and then directly visualized by copper-free click chemistry *in vivo*. They claimed that this strategy not only provide tissue selectivity, but dramatically improves the metabolic labeling efficiency in vivo.

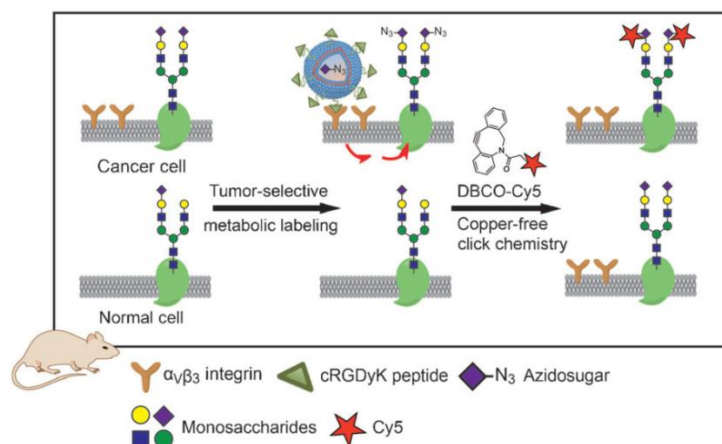


Figure 1.18 Targeted imaging of the cancer glycome in vivo. Adapted from reference [161]<sup>161</sup>

Bertozzi's group described a small-molecule-based strategy for the use of a caged metabolic precursor that is activated for cellular metabolism by enzymatic cleavage.<sup>163,164</sup> A nonmetabolizable caged azidosugar serves as a substrate for a secreted, cancer-specific protease, releasing  $Ac_3ManNAz$ , which is then metabolized by the cell and incorporated into cell-surface glycans and visualized by copper-free click chemistry.

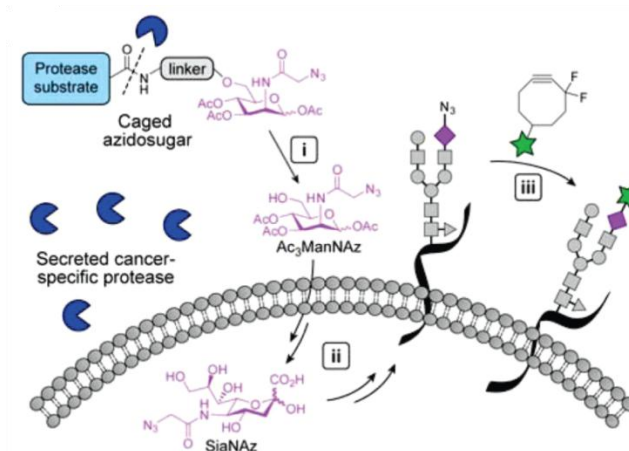


Figure 1.19 Strategy for tissue-specific release of  $Ac_3ManNAz$  via enzymatic activation. Adapted from reference [164]<sup>164</sup>

PSA (prostate-specific antigen) is a serine protease that is secreted at low levels by normal prostatic glandular cells but is highly upregulated by prostate cancer cells.<sup>165</sup> The

hexapeptide Mu-HSSKLY (Mu=morpholino ureidyl) was chosen as a PSA substrate based on reports of its high selectivity for this enzyme over other ubiquitous serine proteases.<sup>166</sup> Upon cleavage of the peptide, the PABA linker (*p*-aminobenzyl alcohol) spontaneously fragments to release Ac3ManNAz, CO<sub>2</sub>, and an iminoquinone methide intermediate that will be subsequently quenched by water.

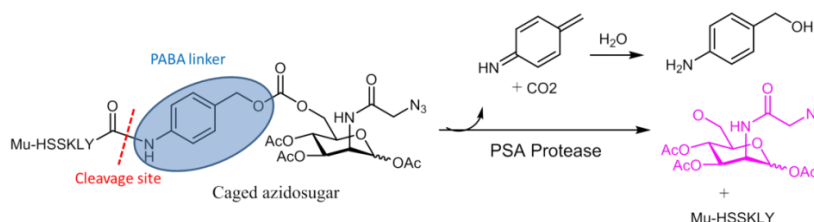


Figure 1.20 PSA cleavage of caged azidosugar. Adapted from reference [164]

This approach gave an important direction for use in tissue-specific glycan imaging with greatly reduced size of the receptor or targeting moieties. Recently, Cheng and coworkers amplified this strategy to other cancer cell type, other than prostate cancer, using a more stable linker.<sup>167</sup> Specifically, they converted the anomeric acetyl group of Ac<sub>4</sub>ManAz to a caged ether bond (DCL-AAM) to inhibit its cell-labeling activity. The ether bond can be selectively cleaved by cancer-overexpressed enzymes (HDAC: histone deacetylase and CTSL: cathepsin L) and thus enables the overexpression of azido groups in cancer cells. This dual-enzymatically triggering design ensures improved cancer selectivity of DCL-AAM labeling, and this method could distinguish many cancer cells, like HeLa, LS174T, MCF-7, MCF-10A, 4T1, MDA-MB-231, TNBC et al.



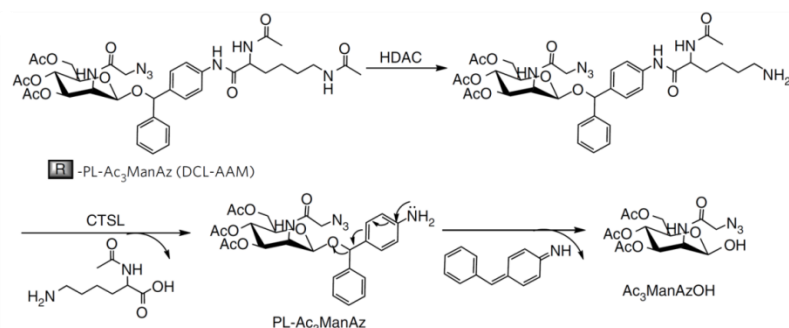


Figure 1.21 HDAC/CTSL-induced degradation of DCL-AAM. Adapted from reference [167]<sup>167</sup>

The following exploration of cancer-targeted therapy using DCL-AAM and a DBCO–doxorubicin conjugate (DBCO-VC-Dox) indicated that the two molecules gave greater antitumor efficacy than DBCO-VC-Dox alone, with significantly reduced tumor volume and increased survival time of mice.

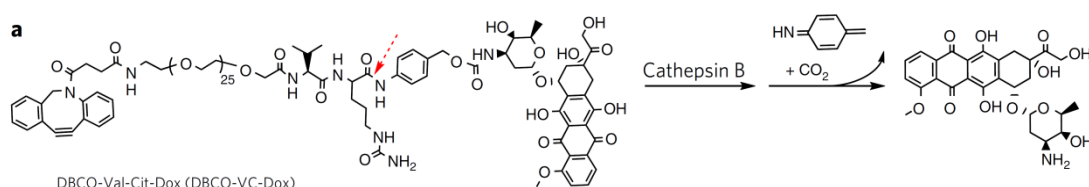


Figure 1.22 Cathepsin B cleavage of DBCO-VC-Dox. Adapted from reference [167]<sup>167</sup>

This small-molecule-based targeting technology could be a complementary to antibody–antigen targeting technology with several obvious advantages, such as greatly reduced size of the receptor or targeting moieties, low cost and nonimmunogenicity, ease of handling and synthesis of both azido sugars and targeting small-molecule substrates.

MOE of sialoglycans in live cells and living animals has emerged as a powerful tool for studying sialic acid chemistry and biology. On the other hand, important issues need to be taken into consideration when applying MOE *in vivo*. For example, the exogenous sialic acid analogues may alter the levels and functions of cellular sialoglycans in specific biological

systems, and their distribution between sialylated glycolipids and glycoproteins should be carefully examined.<sup>149</sup>

### **Selective Exo-Enzymatic Labeling (SEEL)**

Metabolic oligosaccharide engineering has solved numerous of problems in glycobiology. However, it also has some drawbacks, for example, metabolic labeling of ManNAz results in the tagging of azido functional groups in different classes of glycans, including N- and O-linked glycoproteins, proteoglycans and glycolipids, since they are derived from a common pool of nucleotide sugars.<sup>168</sup> But the fact is that various types of glycoconjugates localize and recycle differently in the context of diseased cells, as evidenced by their accumulation within distinct intracellular compartments and vesicles.<sup>169,170</sup> Thus, technology that allows selective labeling of specific classes of glycoconjugate will be very useful to offer a better understanding of many disease processes.

In 2014, our Group developed a strategy, termed SEEL (selective exoenzymatic labeling), which takes advantage of a recombinant glycosyltransferase and a corresponding functionalized nucleotide sugar to install chemical reporters on cell surface *N*-linked glycoproteins.<sup>171</sup> It was found that sialyltransferases usually tolerate modifications at C-5 and C-9 positions of CMP-sialic acid.<sup>172,173</sup> Of course, the transfer efficiency greatly depends on the size of the substituents and the enzymes used. Generally, increasing the size or steric bulk of the unnatural functional groups decreases the transfer efficiency. As we have talked earlier, the azide group is small in size and chemically stable and does not naturally exist in cells, which make it a perfect

substituent to modify CMP-sialic acid and can be incorporated to cell-surface glycans with high efficiency. On the other hand, recombinant ST6GalI sialyltransferase<sup>174-176</sup> can readily accept a CMP-sialic acid analogue modified at C-9 by an azide moiety. And the exogenously administered sialyltransferase only modified N-linked glycans at the cell surface and extracellular matrix, which provide the selectivity upon other glycoconjugates.

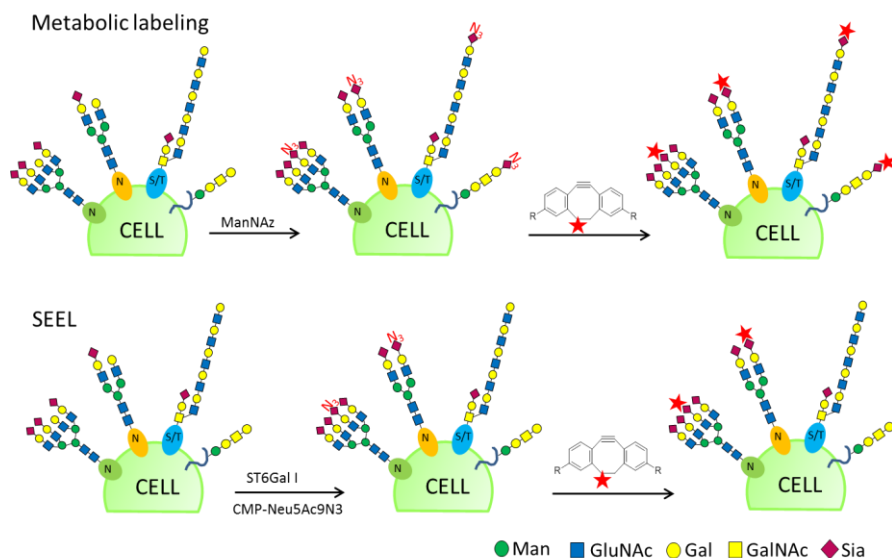


Figure 1.23 Metabolic labeling and SEEL.

CMP-Neu5Ac9N<sub>3</sub> was synthesized and showed marginal impact on the *K<sub>m</sub>* value (0.39 mM for CMP-Neu5Ac9N<sub>3</sub> vs. 0.18 mM for CMP-Neu5Ac) by Kinetic analysis of the enzymatic transformation. It showed a comparable labeling ability versus metabolic labeling, but only labeled *N*-glycans on cell surface. The visualization of trafficking of *N*-linked glycoconjugates of Fibroblasts also carried out by following treatment of S-DIBO-Biotin (or DIBO-biotin: can pass through the cell membrane) and streptavidin-Alexa Fluor 568. Both S-DIBO-Biotin and DIBO-biotin gave robust staining of the cell surface and fibrillar network, but no staining of intracellular structures, confirming that exogenously administered ST6Gal I only labels cell

surface glycans. It should be noted that chloroquine could raise the lysosomal pH and prevent efficient catabolism within this compartment, which was showed in Figure 1c, highlighting the fact that this technology can be employed to study the trafficking of cell surface glycoconjugates.

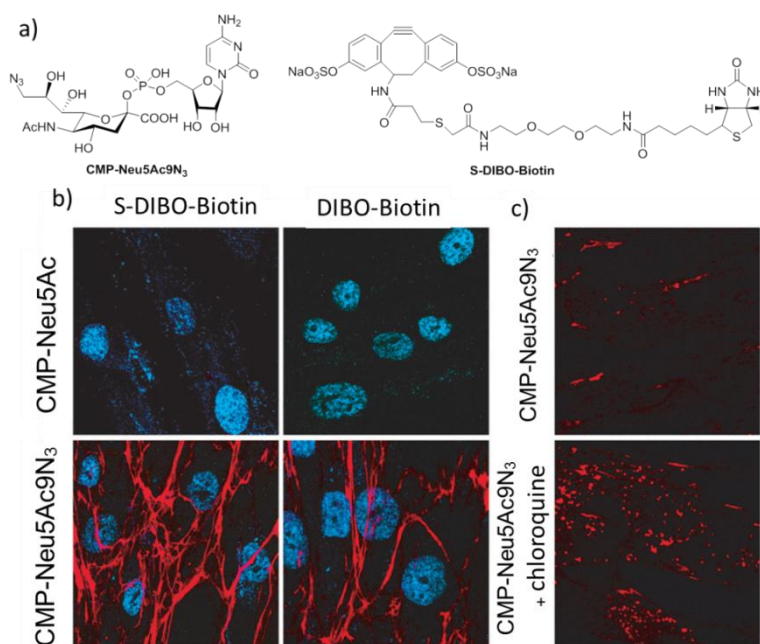


Figure 1.24 a) structure of CMP-Neu5Ac9N<sub>3</sub> and S-DIBO-Biotin. b) Enzymatic labeling of fibroblasts. c) Effect of chloroquine on enzymatic labeling. Adapted from reference [171]

The SEEL methodology provides a unique opportunity to track, capture, and identify subsets of cell surface glycoconjugates. Furthermore, many sialyltransferases exhibit unique substrate specificities,<sup>177-179</sup> for example, ST3Gal I only modify O-linked glycoproteins. As a result, SEEL could be extended to other types of glycoconjugates.

### Antibody-drug conjugates (ADCs)

We have describe selectively target tumor cells using metabolic oligosaccharide engineering and click chemistry, another commonly used technology which can distinguish normal cells and tumor cells is using antibody-drug conjugates (ADCs).

ADCs represent an innovative therapeutic application that combines the unique, high specificity and antitumor activity of monoclonal antibodies (mAbs) with potent cytotoxic drugs which are too toxic to be used on their own.<sup>180,181</sup> This platform enables targeting cancer cells and selective delivery of highly cytotoxic drugs, resulting in a broad therapeutic window.

The approvals of brentuximab vedotin (Adcetris) and ado-trastuzumab emtansine (Kadcyla)<sup>182</sup> plus emerging data for many molecules in clinical trials highlight the potential for ADCs to offer new therapeutic options for patients. Currently, more than 60 ADCs are being evaluated in early- or late-stage clinical trials,<sup>183</sup> and even more in preclinical and/or are ready to enter first-in-human trials.

Antibody-drug conjugates have a complex structure with many moving components. The key components of antibody-drug conjugates include a monoclonal antibody, a stable and cleavable linker and a cytotoxic agent to target a variety of cancers.<sup>184,185</sup> Each component of the ADC must be optimized to fully realize the goal of a targeted therapy with improved efficacy and tolerability.



Figure 1.25 Illustration of antibody drug conjugates.

### The Antibody

Antibody therapies offer many advantages, the main one of which is the specificity of each antibody for its target antigen. A lot of antibody-based therapies are against oncology targets because a number of antigens have been identified as being overexpressed in cancer cells

compared to normal tissues. At the same time, mAbs also suffers from some disadvantages, such as poor cytotoxicity and poor penetration into tumors.

The most commonly used antibody format currently is human IgG isotypes and in particular IgG1<sup>186</sup>. Given the mechanism of action, the ideal antibody needs to have sufficient antigen affinity, can retain their original properties and activate immune functions, such as antibody dependent cellular cytotoxicity, even they are part of the ADC. In summary, the antibody acts as a sort of GPS system, and the theory is that this should increase delivery of potent cell-killing drugs to the tumor, while reducing the exposure of normal cells.

#### The linker

Over the past decades, one of the biggest challenges in the development of ADCs has been the generation of suitable linkers to conjugate the antibodies to the drugs. The successful construction of ADC needs a linker having the following properties: 1) The linker should be extremely stable in circulation since release of the cytotoxic payload before reaching the target cells would lead to nonspecific cell killing. 2) After reaching the target cells, the linker must also be able to efficiently release the drug in its active form to allow the drug to kill cells.<sup>187</sup> 3) The linker should have good hydrophilicity.<sup>188</sup> Hydrophobic linkers coupled with hydrophobic payloads often promote aggregation of ADC molecules.<sup>189</sup> This problem can be overcome by employing hydrophilic linkers containing negatively charged sulfonate groups,<sup>190</sup> polyethylene glycol (PEG) groups,<sup>191</sup> or pyrophosphate diester groups.<sup>192</sup>

Currently, there are the two main classes of linkers being explored, which take advantage of different mechanisms for the release of the drug from the antibody. The first is a cleavable

linker strategy, with three different types of release mechanism within this class: lysosomal protease sensitive linkers (amide bonds), glutathione sensitive linkers (disulfide bonds) or acid sensitive linkers (hydrazones).<sup>193,194</sup> Once inside the cell, each linker is cleaved by a specific mechanism.

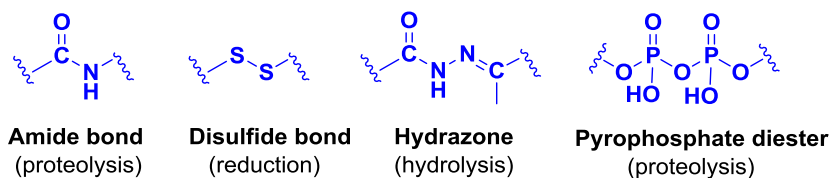


Figure 1.26 Cleavable linkers.

Depending on their sequence, lysosomal protease sensitive linkers can be broken by site-specific proteolysis. This strategy utilizes lysosomal proteases, such as cathepsin B (catB), which can recognize and cleave a dipeptide bond (amide bond) to release the free drug from the conjugate.<sup>195</sup>

Glutathione sensitive linkers can be broken by the reducing environment of the cytosol. This strategy takes advantage of the higher concentration of thiols, such as glutathione, inside the cell compare to the bloodstream. Disulfide bonds within the linker are relatively stable in circulation, and will be reduced by intracellular glutathione to liberate the drug. To further increase plasma stability, the disulfide bond can be flanked with methyl groups that sterically hinder premature cleavage in the bloodstream.<sup>196</sup>

Acid sensitive linkers, such as a hydrazone, can be cleaved by acid-mediated hydrolysis, which can trigger hrdolysis of an acid labile group within the linker in the low pH environment of lysosomal compartment to release the drug.

Recently, Garbaccio and co-workers developed a novel cleavable linker with a pyrophosphate diester structure.<sup>192</sup> This anionic linker has greater aqueous solubility than traditional linkers and excellent circulatory stability. Upon internalization, the pyrophosphate diester gets promptly cleaved through the endosomal-lysosomal pathway to release unmodified drug payload.

The second strategy is one that uses noncleavable linkers (thioether bond).<sup>197,198</sup> This approach depends on complete degradation of the antibody after internalization of the ADC, resulting in release of the free drug payload with the linker attached to an amino acid residue from the antibody. So this approach is best applied to payloads that can conserve their antitumor activity even they are modified chemically. This type of strategy has been used successfully with Kadcyla1 (trastuzumab- MCC-DM1).

### The drug

To ensure that tumor cell killing can be mediated at acceptably low doses of antibody-drug conjugates, very potent cytotoxic agents are typically used. The drug is designed to induce tumor cell death by causing irreversible DNA damage or interfering with cell division.<sup>199</sup> Drugs that interfere with microtubule dynamics, such as monomethyl auristatin E and F (MMAE and MMAF) and the maytansinoids, DM1 and DM4, have proven the most popular ADC payload.<sup>187</sup> Furthermore, drug resistance is a persistent issue in cancer therapy and has been shown to exist against the majority of ADC payloads in clinical trials including calicheamicin, DM1, MMAE, doxorubicin and daunomycin.<sup>200</sup> Therefore, there is a clear need for a wide spectrum of payloads operating by different mechanisms.<sup>201</sup>



In summary, the combination of cytotoxic drugs with mAbs would provide the best of both worlds: use the specificity of a mAb for its antigen to selectively deliver a highly toxic drug to the cancer cell, thus increasing the therapeutic window of both drug and antibody.

#### How do they work?

Conventional chemotherapeutic drugs do not selectively localize to tumors. And as their systemic drug distribution may result in damage to healthy tissue and organs, drug dose escalation to therapeutically active levels may be impossible. By conjugating the drug to antigen specific antibody to form ADC, the side effect on normal tissues can be dramatically reduced.

The mechanism of action of ADCs is described below:

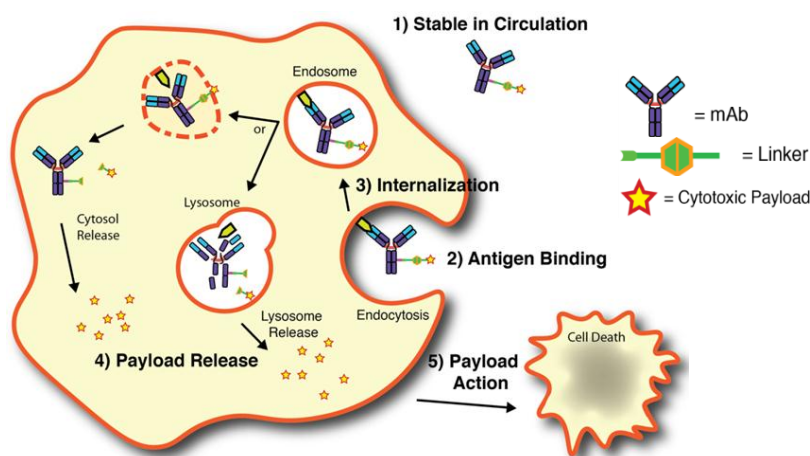


Figure1.27. Mechanism of action of ADCs. Adapted from reference [184]<sup>184</sup>

ADCs are prodrugs that require release of the cytotoxic drug inside the tumor cell.<sup>202</sup> Conjugation of the drug to the antibody inactivates the drug so that it is not toxic while in circulation. The antibody guides the ADC to target the tumor cells, where it binds to the cell surface antigens. Then the ADC is internalized, the antibody is degraded to the level of an amino acid, these drugs are released chemically or enzymatically and become active. Then the drugs

can then kill tumor cells through their established cytotoxic mechanisms. Alternatively, antibodies can be fused directly to cytokines; and these antibody-drug conjugates can act extracellularly by recruiting cytotoxic immune cells to the tumor site, thereby indirectly killing tumor cells.<sup>203</sup>

In general, ADCs offer a unique opportunity to combine the best features of both small-molecule drugs and antibodies to create a single therapy that is highly specific and cytotoxic.

### Conjugation strategies

The history of ADCs can be traced back over a century, although the number of ADCs in clinical trials has steadily increased since 2005, many have failed to reach the later stages of clinical development. Mylotarg has been withdrawn from the market in 2002, and only Adcetris and Kadcyra are currently approved by the FDA for cancer treatment. Emerging preclinical data suggests that heterogeneity, a property shared by most ADCs currently in clinical development, may ultimately limit their potential as therapeutic agents.<sup>204</sup>

Typically, cytotoxic drugs are linked to antibodies through modification of lysine or cysteine residues by using *N*-hydroxysuccinimide ester or maleimide activated drugs, respectively.<sup>205</sup> These conjugation methods lack selectivity and give heterogeneous mixtures of products which will significantly impact the pharmacokinetic properties of ADCs, such as solubility, stability and PK.<sup>206</sup>

Another important factor is the drug-antibody ratio (DAR). In other words, how many of the drug molecules should be loaded onto the antibody. Too few drug molecules will lead to poor

efficacy, and too many drug molecules will make the ADC become unstable with altered pharmacokinetic properties, increased plasma clearance, reduced half-life and increased systemic toxicity.<sup>193</sup> The optimal DAR is undetermined and highly dependent on other ADC variables; however, more commonly the ADCs aim to attain a DAR close to 4.<sup>207</sup>

As a result, site-specific conjugation enabled the construction of homogeneous ADCs with the desired DAR, has been an important step in ADC development. Moreover, site-specific conjugation at defined sites in the antibody results in stable ADCs in vivo.<sup>208-210</sup> In the past decade, the field of site-specific ADC development is advancing rapidly due to fast development in protein engineering, bioorthogonal chemistry, and analytical methods. To date, four methods are commonly used to prepare site-specific ADCs: (a) cysteine residue engineering at specific residues;<sup>211-216</sup> (b) replacement of residues with unnatural amino acids with bio-orthogonal reactivity;<sup>217-220</sup> (c) modification of peptide tags;<sup>221-226</sup> and d) conjugation to glycans.<sup>20,227-230</sup>

ADCs are becoming one of the fastest growing classes of oncology therapeutics. The limited success of first-generation ADCs informed strategies to bring second-generation ADCs to the world, which have higher levels of cytotoxic drug conjugation and more-stable linkers between the drug and the antibody.<sup>231</sup> The third-generation ADCs was introduced recently with the concerns of improved pharmacokinetics, improved stability, defined DAR, high potency and less toxicity.<sup>232</sup> It is safe to say that ADCs has the prospect for improving treatment outcomes for many diseases.

## References

- (1) Kalia, J.; Raines, R. T. *Current organic chemistry* **2010**, *14*, 138.
- (2) Ramil, C. P.; Lin, Q. *Chem Commun (Camb)* **2013**, *49*, 11007.
- (3) Debets, M. F.; van Hest, J. C.; Rutjes, F. P. *Organic & biomolecular chemistry* **2013**, *11*, 6439.
- (4) Shieh, P.; Bertozzi, C. R. *Organic & biomolecular chemistry* **2014**, *12*, 9307.
- (5) Li, L.; Zhang, Z. *Molecules* **2016**, *21*.
- (6) Patterson, D. M.; Nazarova, L. A.; Prescher, J. A. *Acs Chem Biol* **2014**, *9*, 592.
- (7) Kolb, H. C.; Finn, M. G.; Sharpless, K. B. *Angewandte Chemie* **2001**, *40*, 2004.
- (8) Rostovtsev, V. V.; Green, L. G.; Fokin, V. V.; Sharpless, K. B. *Angewandte Chemie* **2002**, *41*, 2596.
- (9) Lowe, A. B. *Polym Chem-Uk* **2010**, *1*, 17.
- (10) Nair, D. P.; Podgorski, M.; Chatani, S.; Gong, T.; Xi, W. X.; Fenoli, C. R.; Bowman, C. N. *Chem Mater* **2014**, *26*, 724.
- (11) Kalia, J.; Raines, R. T. *Angew Chem Int Edit* **2008**, *47*, 7523.
- (12) Oliveira, P. F. M.; Baron, M.; Chamayou, A.; Andre-Barres, C.; Guidetti, B.; Baltas, M. *Rsc Adv* **2014**, *4*, 56736.
- (13) Collins, J.; Xiao, Z. Y.; Mullner, M.; Connal, L. A. *Polym Chem-Uk* **2016**, *7*, 3812.
- (14) Grover, G. N.; Lam, J.; Nguyen, T. H.; Segura, T.; Maynard, H. D. *Biomacromolecules* **2012**, *13*, 3013.

- (15) Ulrich, S.; Boturyn, D.; Marra, A.; Renaudet, O.; Dumy, P. *Chem-Eur J* **2014**, *20*, 34.
- (16) Kashemirov, B. A.; Bala, J. L. F.; Chen, X.; Ebetino, F. H.; Xia, Z.; Russell, R. G. G.; Coxon, F. P.; Roelofs, A. J.; Rogers, M. J.; McKenna, C. E. *Bioconjugate Chemistry* **2008**, *19*, 2308.
- (17) Blackman, M. L.; Royzen, M.; Fox, J. M. *J Am Chem Soc* **2008**, *130*, 13518.
- (18) Devaraj, N. K.; Weissleder, R.; Hilderbrand, S. A. *Bioconjug Chem* **2008**, *19*, 2297.
- (19) Tornøe, C. W.; Christensen, C.; Meldal, M. *Journal of Organic Chemistry* **2002**, *67*, 3057.
- (20) Li, X.; Fang, T.; Boons, G. J. *Angewandte Chemie* **2014**, *53*, 7179.
- (21) Ledin, P. A.; Kolishetti, N.; Hudlikar, M. S.; Boons, G. J. *Chemistry* **2014**, *20*, 8753.
- (22) Ledin, P. A.; Kolishetti, N.; Boons, G. J. *Macromolecules* **2013**, *46*, 7759.
- (23) Hoogenboom, R. *Angewandte Chemie* **2010**, *49*, 3415.
- (24) Ahmad Fuaad, A. A.; Azmi, F.; Skwarczynski, M.; Toth, I. *Molecules* **2013**, *18*, 13148.
- (25) Tong, R.; Tang, L.; Ma, L.; Tu, C.; Baumgartner, R.; Cheng, J. *Chemical Society reviews* **2014**, *43*, 6982.
- (26) Tornøe, C. W.; Christensen, C.; Meldal, M. *The Journal of organic chemistry* **2002**, *67*, 3057.
- (27) Appukkuttan, P.; Dehaen, W.; Fokin, V. V.; Van der Eycken, E. *Organic letters* **2004**, *6*, 4223.
- (28) Huisgen, R. *Angew Chem Int Edit* **1963**, *75*, 742.
- (29) Huisgen, R. *Angew Chem Int Edit* **1963**, *75*, 604.

- (30)Zhang, L.; Chen, X.; Xue, P.; Sun, H. H.; Williams, I. D.; Sharpless, K. B.; Fokin, V. V.; Jia, G. *J Am Chem Soc* **2005**, *127*, 15998.
- (31)Pujari, S. S.; Ingale, S. A.; Seela, F. *Bioconjug Chem* **2014**, *25*, 1855.
- (32)Haldon, E.; Nicasio, M. C.; Perez, P. J. *Organic & biomolecular chemistry* **2015**, *13*, 9528.
- (33)Shao, C. W.; Cheng, G. L.; Su, D. Y.; Xu, J. M.; Wang, X. Y.; Hu, Y. F. *Advanced synthesis & catalysis* **2010**, *352*, 1587.
- (34)Lal, S.; Diez-Gonzalez, S. *The Journal of organic chemistry* **2011**, *76*, 2367.
- (35)Barre, G.; Taton, D.; Lastecoueres, D.; Vincent, J. M. *J Am Chem Soc* **2004**, *126*, 7764.
- (36)Paxton, W. F.; Spruell, J. M.; Stoddart, J. F. *J Am Chem Soc* **2009**, *131*, 6692.
- (37)Himo, F.; Lovell, T.; Hilgraf, R.; Rostovtsev, V. V.; Noodleman, L.; Sharpless, K. B.; Fokin, V. V. *J Am Chem Soc* **2005**, *127*, 210.
- (38)Rodionov, V. O.; Presolski, S. I.; Diaz, D. D.; Fokin, V. V.; Finn, M. G. *J Am Chem Soc* **2007**, *129*, 12705.
- (39)Worrell, B. T.; Malik, J. A.; Fokin, V. V. *Science* **2013**, *340*, 457.
- (40)Brewer, G. J. *Chemical research in toxicology* **2010**, *23*, 319.
- (41)McKay, C. S.; Finn, M. G. *Chemistry & biology* **2014**, *21*, 1075.
- (42)Stadtman, E. R. *Free radical research* **2006**, *40*, 1250.
- (43)Kay, P.; Wagner, J. R.; Gagnon, H.; Day, R.; Klarskov, K. *Chemical research in toxicology* **2013**, *26*, 1333.
- (44)Corti, A.; Casini, A. F.; Pompella, A. *Archives of biochemistry and biophysics* **2010**, *500*,

107.

(45)Wang, Q.; Chan, T. R.; Hilgraf, R.; Fokin, V. V.; Sharpless, K. B.; Finn, M. G. *J Am Chem Soc* **2003**, *125*, 3192.

(46)Link, A. J.; Tirrell, D. A. *J Am Chem Soc* **2003**, *125*, 11164.

(47)Rodionov, V. O.; Presolski, S. I.; Gardinier, S.; Lim, Y. H.; Finn, M. G. *J Am Chem Soc* **2007**, *129*, 12696.

(48)Lewis, W. G.; Magallon, F. G.; Fokin, V. V.; Finn, M. G. *J Am Chem Soc* **2004**, *126*, 9152.

(49)Hong, V.; Presolski, S. I.; Ma, C.; Finn, M. G. *Angewandte Chemie* **2009**, *48*, 9879.

(50)Soriano Del Amo, D.; Wang, W.; Jiang, H.; Besanceney, C.; Yan, A. C.; Levy, M.; Liu, Y.; Marlow, F. L.; Wu, P. *J Am Chem Soc* **2010**, *132*, 16893.

(51)Besanceney-Webler, C.; Jiang, H.; Zheng, T.; Feng, L.; Soriano del Amo, D.; Wang, W.; Klivansky, L. M.; Marlow, F. L.; Liu, Y.; Wu, P. *Angewandte Chemie* **2011**, *50*, 8051.

(52)Presolski, S. I.; Hong, V.; Cho, S. H.; Finn, M. G. *J Am Chem Soc* **2010**, *132*, 14570.

(53)Hong, V.; Steinmetz, N. F.; Manchester, M.; Finn, M. G. *Bioconjug Chem* **2010**, *21*, 1912.

(54)Agard, N. J.; Prescher, J. A.; Bertozzi, C. R. *J Am Chem Soc* **2004**, *126*, 15046.

(55)Ning, X.; Temming, R. P.; Dommerholt, J.; Guo, J.; Ania, D. B.; Debets, M. F.; Wolfert, M. A.; Boons, G. J.; van Delft, F. L. *Angewandte Chemie* **2010**, *49*, 3065.

(56)Sherratt, A. R.; Chigrinova, M.; MacKenzie, D. A.; Rastogi, N. K.; Ouattara, M. T.; Pezacki, A. T.; Pezacki, J. P. *Bioconjug Chem* **2016**, *27*, 1222.

- (57) Sanders, B. C.; Friscourt, F.; Ledin, P. A.; Mbua, N. E.; Arumugam, S.; Guo, J.; Boltje, T. J.; Popik, V. V.; Boons, G. J. *J Am Chem Soc* **2011**, *133*, 949.
- (58) Jawalekar, A. M.; Reubsaet, E.; Rutjes, F. P.; van Delft, F. L. *Chem Commun (Camb)* **2011**, *47*, 3198.
- (59) Friscourt, F.; Fahrni, C. J.; Boons, G. J. *Chemistry* **2015**, *21*, 13996.
- (60) McGrath, N. A.; Raines, R. T. *Chemical science* **2012**, *3*, 3237.
- (61) Wallace, S.; Chin, J. W. *Chemical science* **2014**, *5*, 1742.
- (62) Devaraj, N. K.; Hilderbrand, S.; Upadhyay, R.; Mazitschek, R.; Weissleder, R. *Angewandte Chemie* **2010**, *49*, 2869.
- (63) Patterson, D. M.; Nazarova, L. A.; Xie, B.; Kamber, D. N.; Prescher, J. A. *J Am Chem Soc* **2012**, *134*, 18638.
- (64) Yang, J.; Seckute, J.; Cole, C. M.; Devaraj, N. K. *Angewandte Chemie* **2012**, *51*, 7476.
- (65) Lang, K.; Davis, L.; Torres-Kolbus, J.; Chou, C.; Deiters, A.; Chin, J. W. *Nature chemistry* **2012**, *4*, 298.
- (66) Wang, Y.; Vera, C. I.; Lin, Q. *Organic letters* **2007**, *9*, 4155.
- (67) Song, W.; Wang, Y.; Qu, J.; Lin, Q. *J Am Chem Soc* **2008**, *130*, 9654.
- (68) Song, W.; Wang, Y.; Qu, J.; Madden, M. M.; Lin, Q. *Angewandte Chemie* **2008**, *47*, 2832.
- (69) Yu, Z.; Pan, Y.; Wang, Z.; Wang, J.; Lin, Q. *Angewandte Chemie* **2012**, *51*, 10600.
- (70) Kaya, E.; Vrabel, M.; Deiml, C.; Prill, S.; Fluxa, V. S.; Carell, T. *Angewandte Chemie* **2012**, *51*, 4466.



- (71) Lee, Y. J.; Wu, B.; Raymond, J. E.; Zeng, Y.; Fang, X.; Wooley, K. L.; Liu, W. R. *Acs Chem Biol* **2013**, *8*, 1664.
- (72) Wang, X. S.; Lee, Y. J.; Liu, W. R. *Chem Commun (Camb)* **2014**, *50*, 3176.
- (73) Agard, N. J.; Baskin, J. M.; Prescher, J. A.; Lo, A.; Bertozzi, C. R. *Acs Chem Biol* **2006**, *1*, 644.
- (74) Baskin, J. M.; Prescher, J. A.; Laughlin, S. T.; Agard, N. J.; Chang, P. V.; Miller, I. A.; Lo, A.; Codelli, J. A.; Bertozzi, C. R. *Proc Natl Acad Sci U S A* **2007**, *104*, 16793.
- (75) Laughlin, S. T.; Baskin, J. M.; Amacher, S. L.; Bertozzi, C. R. *Science* **2008**, *320*, 664.
- (76) Ning, X.; Guo, J.; Wolfert, M. A.; Boons, G. J. *Angewandte Chemie* **2008**, *47*, 2253.
- (77) Debets, M. F.; van Berkel, S. S.; Schoffelen, S.; Rutjes, F. P.; van Hest, J. C.; van Delft, F. L. *Chem Commun (Camb)* **2010**, *46*, 97.
- (78) Jewett, J. C.; Sletten, E. M.; Bertozzi, C. R. *J Am Chem Soc* **2010**, *132*, 3688.
- (79) Chigrinova, M.; McKay, C. S.; Beaulieu, L. P.; Udachin, K. A.; Beauchemin, A. M.; Pezacki, J. P. *Organic & biomolecular chemistry* **2013**, *11*, 3436.
- (80) Dommerholt, J.; Schmidt, S.; Temming, R.; Hendriks, L. J.; Rutjes, F. P.; van Hest, J. C.; Lefeber, D. J.; Friedl, P.; van Delft, F. L. *Angewandte Chemie* **2010**, *49*, 9422.
- (81) Poole, T. H.; Reisz, J. A.; Zhao, W.; Poole, L. B.; Furdui, C. M.; King, S. B. *J Am Chem Soc* **2014**, *136*, 6167.
- (82) Chang, P. V.; Prescher, J. A.; Sletten, E. M.; Baskin, J. M.; Miller, I. A.; Agard, N. J.; Lo, A.; Bertozzi, C. R. *Proc Natl Acad Sci U S A* **2010**, *107*, 1821.
- (83) Friscourt, F.; Ledin, P. A.; Mbua, N. E.; Flanagan-Steet, H. R.; Wolfert, M. A.; Steet, R.;

Boons, G. J. *J Am Chem Soc* **2012**, *134*, 5381.

(84)Friscourt, F.; Fahrni, C. J.; Boons, G. J. *J Am Chem Soc* **2012**, *134*, 18809.

(85)de Almeida, G.; Sletten, E. M.; Nakamura, H.; Palaniappan, K. K.; Bertozzi, C. R. *Angewandte Chemie* **2012**, *51*, 2443.

(86)Temming, R. P.; Eggermont, L.; van Eldijk, M. B.; van Hest, J. C.; van Delft, F. L. *Organic & biomolecular chemistry* **2013**, *11*, 2772.

(87)McKay, C. S.; Moran, J.; Pezacki, J. P. *Chem Commun (Camb)* **2010**, *46*, 931.

(88)MacKenzie, D. A.; Sherratt, A. R.; Chigrinova, M.; Cheung, L. L.; Pezacki, J. P. *Current opinion in chemical biology* **2014**, *21*, 81.

(89)McKay, C. S.; Blake, J. A.; Cheng, J.; Danielson, D. C.; Pezacki, J. P. *Chem Commun (Camb)* **2011**, *47*, 10040.

(90)McKay, C. S.; Chigrinova, M.; Blake, J. A.; Pezacki, J. P. *Organic & biomolecular chemistry* **2012**, *10*, 3066.

(91)Andersen, K. A.; Aronoff, M. R.; McGrath, N. A.; Raines, R. T. *J Am Chem Soc* **2015**, *137*, 2412.

(92)Feuer, H. *Nitrile Oxides, Nitrones, and Nitronates in Organic Synthesis: Novel Strategies in Synthesis, 2nd Edition* **2008**, Vii.

(93)Lang, K.; Chin, J. W. *Acs Chem Biol* **2014**, *9*, 16.

(94)Karver, M. R.; Weissleder, R.; Hilderbrand, S. A. *Bioconjug Chem* **2011**, *22*, 2263.

(95)Chen, W.; Wang, D.; Dai, C.; Hamelberg, D.; Wang, B. *Chem Commun (Camb)* **2012**, *48*, 1736.

- (96) Taylor, M. T.; Blackman, M. L.; Dmitrenko, O.; Fox, J. M. *J Am Chem Soc* **2011**, *133*, 9646.
- (97) Rossin, R.; van den Bosch, S. M.; Ten Hoeve, W.; Carvelli, M.; Versteegen, R. M.; Lub, J.; Robillard, M. S. *Bioconjug Chem* **2013**, *24*, 1210.
- (98) Engelsma, S. B.; Willems, L. I.; van Paaschen, C. E.; van Kasteren, S. I.; van der Marel, G. A.; Overkleeft, H. S.; Filippov, D. V. *Organic letters* **2014**, *16*, 2744.
- (99) Versteegen, R. M.; Rossin, R.; ten Hoeve, W.; Janssen, H. M.; Robillard, M. S. *Angewandte Chemie* **2013**, *52*, 14112.
- (100) Rossin, R.; van Duijnhoven, S. M.; Ten Hoeve, W.; Janssen, H. M.; Kleijn, L. H.; Hoeben, F. J.; Versteegen, R. M.; Robillard, M. S. *Bioconjug Chem* **2016**, *27*, 1697.
- (101) Wu, H.; Yang, J.; Seckute, J.; Devaraj, N. K. *Angewandte Chemie* **2014**, *53*, 5805.
- (102) Yang, J.; Karver, M. R.; Li, W.; Sahu, S.; Devaraj, N. K. *Angewandte Chemie* **2012**, *51*, 5222.
- (103) Yang, J.; Liang, Y.; Seckute, J.; Houk, K. N.; Devaraj, N. K. *Chemistry* **2014**, *20*, 3365.
- (104) Prescher, J. A.; Bertozzi, C. R. *Nature chemical biology* **2005**, *1*, 13.
- (105) Lippincott-Schwartz, J.; Patterson, G. H. *Science* **2003**, *300*, 87.
- (106) Zhang, J.; Campbell, R. E.; Ting, A. Y.; Tsien, R. Y. *Nature reviews. Molecular cell biology* **2002**, *3*, 906.
- (107) Mahal, L. K.; Yarema, K. J.; Bertozzi, C. R. *Science* **1997**, *276*, 1125.
- (108) Zhang, Z.; Smith, B. A.; Wang, L.; Brock, A.; Cho, C.; Schultz, P. G. *Biochemistry*

**2003**, 42, 6735.

- (109) Chen, I.; Howarth, M.; Lin, W.; Ting, A. Y. *Nature methods* **2005**, 2, 99.
- (110) Link, A. J.; Vink, M. K.; Tirrell, D. A. *J Am Chem Soc* **2004**, 126, 10598.
- (111) Kho, Y.; Kim, S. C.; Jiang, C.; Barma, D.; Kwon, S. W.; Cheng, J.; Jaunbergs, J.; Weinbaum, C.; Tamanoi, F.; Falck, J.; Zhao, Y. *Proc Natl Acad Sci U S A* **2004**, 101, 12479.
- (112) Prescher, J. A.; Dube, D. H.; Bertozzi, C. R. *Nature* **2004**, 430, 873.
- (113) Rabuka, D.; Hubbard, S. C.; Laughlin, S. T.; Argade, S. P.; Bertozzi, C. R. *J Am Chem Soc* **2006**, 128, 12078.
- (114) Chang, P. V.; Chen, X.; Smyrniotis, C.; Xenakis, A.; Hu, T.; Bertozzi, C. R.; Wu, P. *Angewandte Chemie* **2009**, 48, 4030.
- (115) Speers, A. E.; Cravatt, B. F. *Chemistry & biology* **2004**, 11, 535.
- (116) Hsu, T. L.; Hanson, S. R.; Kishikawa, K.; Wang, S. K.; Sawa, M.; Wong, C. H. *Proc Natl Acad Sci U S A* **2007**, 104, 2614.
- (117) Sawa, M.; Hsu, T. L.; Itoh, T.; Sugiyama, M.; Hanson, S. R.; Vogt, P. K.; Wong, C. H. *Proc Natl Acad Sci U S A* **2006**, 103, 12371.
- (118) Lion, C.; Simon, C.; Huss, B.; Blervacq, A. S.; Tirot, L.; Toybou, D.; Spriet, C.; Slomianny, C.; Guerardel, Y.; Hawkins, S.; Biot, C. *Cell chemical biology* **2017**, 24, 326.
- (119) Wu, B.; Wang, Z.; Huang, Y.; Liu, W. R. *Chembiochem : a European journal of chemical biology* **2012**, 13, 1405.
- (120) Josa-Cullere, L.; Wainman, Y. A.; Brindle, K. M.; Leeper, F. J. *Rsc Adv* **2014**, 4, 52241.

- (121) Rossin, R.; Verkerk, P. R.; van den Bosch, S. M.; Vulders, R. C.; Verel, I.; Lub, J.; Robillard, M. S. *Angewandte Chemie* **2010**, *49*, 3375.
- (122) Schoch, J.; Wiessler, M.; Jaschke, A. *J Am Chem Soc* **2010**, *132*, 8846.
- (123) Cole, C. M.; Yang, J.; Seckute, J.; Devaraj, N. K. *Chembiochem : a European journal of chemical biology* **2013**, *14*, 205.
- (124) Niederwieser, A.; Spate, A. K.; Nguyen, L. D.; Jungst, C.; Reutter, W.; Wittmann, V. *Angewandte Chemie* **2013**, *52*, 4265.
- (125) Saxon, E.; Luchansky, S. J.; Hang, H. C.; Yu, C.; Lee, S. C.; Bertozzi, C. R. *J Am Chem Soc* **2002**, *124*, 14893.
- (126) Luchansky, S. J.; Hang, H. C.; Saxon, E.; Grunwell, J. R.; Yu, C.; Dube, D. H.; Bertozzi, C. R. *Methods in enzymology* **2003**, *362*, 249.
- (127) Luchansky, S. J.; Goon, S.; Bertozzi, C. R. *Chembiochem : a European journal of chemical biology* **2004**, *5*, 371.
- (128) Griffin, B. A.; Adams, S. R.; Tsien, R. Y. *Science* **1998**, *281*, 269.
- (129) Varki, A. *Nature* **2007**, *446*, 1023.
- (130) Murrey, H. E.; Hsieh-Wilson, L. C. *Chemical reviews* **2008**, *108*, 1708.
- (131) Fuster, M. M.; Esko, J. D. *Nature reviews. Cancer* **2005**, *5*, 526.
- (132) Kang, K.; Joo, S.; Choi, J. Y.; Geum, S.; Hong, S. P.; Lee, S. Y.; Kim, Y. H.; Kim, S. M.; Yoon, M. H.; Nam, Y.; Lee, K. B.; Lee, H. Y.; Choi, I. S. *Proc Natl Acad Sci U S A* **2015**, *112*, E241.
- (133) Bertozzi, C. R.; Kiessling, L. L. *Science* **2001**, *291*, 2357.

- (134) Zheng, M.; Zheng, L.; Zhang, P.; Li, J.; Zhang, Y. *Molecules* **2015**, *20*, 3190.
- (135) Kayser, H.; Zeitler, R.; Kannicht, C.; Grunow, D.; Nuck, R.; Reutter, W. *J Biol Chem* **1992**, *267*, 16934.
- (136) Wieser, J. R.; Heisner, A.; Stehling, P.; Oesch, F.; Reutter, W. *FEBS letters* **1996**, *395*, 170.
- (137) Keppler, O. T.; Horstkorte, R.; Pawlita, M.; Schmidt, C.; Reutter, W. *Glycobiology* **2001**, *11*, 11R.
- (138) Grunholz, H. J.; Harms, E.; Opetz, M.; Reutter, W.; Cerny, M. *Carbohydrate research* **1981**, *96*, 259.
- (139) Collins, B. E.; Fralich, T. J.; Itonori, S.; Ichikawa, Y.; Schnaar, R. L. *Glycobiology* **2000**, *10*, 11.
- (140) Buttner, B.; Kannicht, C.; Schmidt, C.; Loster, K.; Reutter, W.; Lee, H. Y.; Nohring, S.; Horstkorte, R. *The Journal of neuroscience : the official journal of the Society for Neuroscience* **2002**, *22*, 8869.
- (141) Shieh, P.; Hangauer, M. J.; Bertozzi, C. R. *J Am Chem Soc* **2012**, *134*, 17428.
- (142) Saxon, E.; Bertozzi, C. R. *Science* **2000**, *287*, 2007.
- (143) Chang, P. V.; Prescher, J. A.; Hangauer, M. J.; Bertozzi, C. R. *J Am Chem Soc* **2007**, *129*, 8400.
- (144) Hang, H. C.; Yu, C.; Kato, D. L.; Bertozzi, C. R. *Proc Natl Acad Sci U S A* **2003**, *100*, 14846.
- (145) Dehnert, K. W.; Beahm, B. J.; Huynh, T. T.; Baskin, J. M.; Laughlin, S. T.; Wang,

W.; Wu, P.; Amacher, S. L.; Bertozzi, C. R. *Acs Chem Biol* **2011**, 6, 547.

(146) Laughlin, S. T.; Bertozzi, C. R. *Proc Natl Acad Sci U S A* **2009**, 106, 12.

(147) Angata, T.; Varki, A. *Chemical reviews* **2002**, 102, 439.

(148) Chen, X.; Varki, A. *Acs Chem Biol* **2010**, 5, 163.

(149) Cheng, B.; Xie, R.; Dong, L.; Chen, X. *Chembiochem : a European journal of chemical biology* **2016**, 17, 11.

(150) Higashi, K.; Asano, K.; Yagi, M.; Yamada, K.; Arakawa, T.; Ehashi, T.; Mori, T.; Sumida, K.; Kushida, M.; Ando, S.; Kinoshita, M.; Kakehi, K.; Tachibana, T.; Saito, K. *J Biol Chem* **2014**, 289, 25833.

(151) Croci, D. O.; Cerliani, J. P.; Dalotto-Moreno, T.; Mendez-Huergo, S. P.; Mascanfroni, I. D.; Dergan-Dylon, S.; Toscano, M. A.; Caramelo, J. J.; Garcia-Vallejo, J. J.; Ouyang, J.; Mesri, E. A.; Junttila, M. R.; Bais, C.; Shipp, M. A.; Salatino, M.; Rabinovich, G. A. *Cell* **2014**, 156, 744.

(152) Eylar, E. H.; Madoff, M. A.; Brody, O. V.; Oncley, J. L. *J Biol Chem* **1962**, 237, 1992.

(153) Cha, S. K.; Ortega, B.; Kurosu, H.; Rosenblatt, K. P.; Kuro, O. M.; Huang, C. L. *Proc Natl Acad Sci U S A* **2008**, 105, 9805.

(154) Gadhoom, S. Z.; Sackstein, R. *Nature chemical biology* **2008**, 4, 751.

(155) Miyagi, T.; Yamaguchi, K. *Glycobiology* **2012**, 22, 880.

(156) Kajihara, Y.; Kamitani, T.; Sato, R.; Kamei, N.; Miyazaki, T.; Okamoto, R.; Sakakibara, T.; Tsuji, T.; Yamamoto, T. *Carbohydrate research* **2007**, 342, 1680.

- (157) Lee, S.; Koo, H.; Na, J. H.; Han, S. J.; Min, H. S.; Lee, S. J.; Kim, S. H.; Yun, S. H.; Jeong, S. Y.; Kwon, I. C.; Choi, K.; Kim, K. *ACS nano* **2014**, 8, 2048.
- (158) Koo, H.; Lee, S.; Na, J. H.; Kim, S. H.; Hahn, S. K.; Choi, K.; Kwon, I. C.; Jeong, S. Y.; Kim, K. *Angewandte Chemie* **2012**, 51, 11836.
- (159) Maeda, H. *Journal of controlled release : official journal of the Controlled Release Society* **2012**, 164, 138.
- (160) Xie, R.; Hong, S.; Feng, L.; Rong, J.; Chen, X. *J Am Chem Soc* **2012**, 134, 9914.
- (161) Xie, R.; Dong, L.; Huang, R.; Hong, S.; Lei, R.; Chen, X. *Angewandte Chemie* **2014**, 53, 14082.
- (162) Xie, R.; Dong, L.; Du, Y.; Zhu, Y.; Hua, R.; Zhang, C.; Chen, X. *Proc Natl Acad Sci U S A* **2016**, 113, 5173.
- (163) Breidenbach, M. A.; Gallagher, J. E.; King, D. S.; Smart, B. P.; Wu, P.; Bertozzi, C. R. *Proc Natl Acad Sci U S A* **2010**, 107, 3988.
- (164) Chang, P. V.; Dube, D. H.; Sletten, E. M.; Bertozzi, C. R. *J Am Chem Soc* **2010**, 132, 9516.
- (165) Jones, G. B.; Crasto, C. F.; Mathews, J. E.; Xie, L.; Mitchell, M. O.; El-Shafey, A.; D'Amico, A. V.; Bubley, G. J. *Bioorganic & medicinal chemistry* **2006**, 14, 418.
- (166) Denmeade, S. R.; Lou, W.; Lovgren, J.; Malm, J.; Lilja, H.; Isaacs, J. T. *Cancer research* **1997**, 57, 4924.
- (167) Wang, H.; Wang, R.; Cai, K.; He, H.; Liu, Y.; Yen, J.; Wang, Z.; Xu, M.; Sun, Y.; Zhou, X.; Yin, Q.; Tang, L.; Dobrucki, I. T.; Dobrucki, L. W.; Chaney, E. J.; Boppart, S. A.; Fan,



- T. M.; Lezmi, S.; Chen, X.; Yin, L.; Cheng, J. *Nature chemical biology* **2017**, *13*, 415.
- (168) Jewett, J. C.; Bertozzi, C. R. *Chemical Society reviews* **2010**, *39*, 1272.
- (169) Hara, A.; Kitazawa, N.; Taketomi, T. *Journal of lipid research* **1984**, *25*, 175.
- (170) McGlynn, R.; Dobrenis, K.; Walkley, S. U. *The Journal of comparative neurology* **2004**, *480*, 415.
- (171) Mbua, N. E.; Li, X.; Flanagan-Steet, H. R.; Meng, L.; Aoki, K.; Moremen, K. W.; Wolfert, M. A.; Steet, R.; Boons, G. J. *Angewandte Chemie* **2013**, *52*, 13012.
- (172) Gross, H. J.; Rose, U.; Krause, J. M.; Paulson, J. C.; Schmid, K.; Feeney, R. E.; Brossmer, R. *Biochemistry* **1989**, *28*, 7386.
- (173) Gross, H. J.; Brossmer, R. *Glycoconjugate journal* **1995**, *12*, 739.
- (174) Roth, J.; Taatjes, D. J.; Lucocq, J. M.; Weinstein, J.; Paulson, J. C. *Cell* **1985**, *43*, 287.
- (175) Dall'Olio, F. *Glycoconjugate journal* **2000**, *17*, 669.
- (176) Zhuo, Y.; Bellis, S. L. *J Biol Chem* **2011**, *286*, 5935.
- (177) Harduin-Lepers, A.; Vallejo-Ruiz, V.; Krzewinski-Recchi, M. A.; Samyn-Petit, B.; Julien, S.; Delannoy, P. *Biochimie* **2001**, *83*, 727.
- (178) Takashima, S. *Bioscience, biotechnology, and biochemistry* **2008**, *72*, 1155.
- (179) Harduin-Lepers, A.; Mollicone, R.; Delannoy, P.; Oriol, R. *Glycobiology* **2005**, *15*, 805.
- (180) Ducry, L.; Stump, B. *Bioconjugate Chemistry* **2010**, *21*, 5.
- (181) Iyer, U.; Kadambi, V. J. *J Pharmacol Tox Met* **2011**, *64*, 207.

- (182) Zolot, R. S.; Basu, S.; Million, R. P. *Nat Rev Drug Discov* **2013**, *12*, 259.
- (183) Tsuchikama, K.; An, Z. *Protein & cell* **2016**.
- (184) Gordon, M. R.; Canakci, M.; Li, L.; Zhuang, J.; Osborne, B.; Thayumanavan, S. *Bioconjug Chem* **2015**, *26*, 2198.
- (185) Liu, X.; Gao, W. *Biomedical Nanomaterials* **2016**.
- (186) Hughes, B. *Nat Rev Drug Discov* **2010**, *9*, 665.
- (187) Hamilton, G. S. *Biologicals : journal of the International Association of Biological Standardization* **2015**, *43*, 318.
- (188) Lu, J.; Jiang, F.; Lu, A.; Zhang, G. *Int J Mol Sci* **2016**, *17*, 561.
- (189) King, H. D.; Dubowchik, G. M.; Mastalerz, H.; Willner, D.; Hofstead, S. J.; Firestone, R. A.; Lasch, S. J.; Trail, P. A. *Journal of medicinal chemistry* **2002**, *45*, 4336.
- (190) Zhao, R. Y.; Wilhelm, S. D.; Audette, C.; Jones, G.; Leece, B. A.; Lazar, A. C.; Goldmacher, V. S.; Singh, R.; Kovtun, Y.; Widdison, W. C.; Lambert, J. M.; Chari, R. V. *Journal of medicinal chemistry* **2011**, *54*, 3606.
- (191) Lyon, R. P.; Bovee, T. D.; Doronina, S. O.; Burke, P. J.; Hunter, J. H.; Neff-LaFord, H. D.; Jonas, M.; Anderson, M. E.; Setter, J. R.; Senter, P. D. *Nature biotechnology* **2015**, *33*, 733.
- (192) Kern, J. C.; Cancilla, M.; Dooney, D.; Kwasnjuk, K.; Zhang, R.; Beaumont, M.; Figueroa, I.; Hsieh, S.; Liang, L.; Tomazela, D.; Zhang, J.; Brandish, P. E.; Palmieri, A.; Stivers, P.; Cheng, M.; Feng, G.; Geda, P.; Shah, S.; Beck, A.; Bresson, D.; Firdos, J.; Gately, D.; Knudsen, N.; Manibusan, A.; Schultz, P. G.; Sun, Y.; Garbaccio, R. M. *J Am Chem Soc* **2016**, *138*,

1430.

(193) Perez, H. L.; Cardarelli, P. M.; Deshpande, S.; Gangwar, S.; Schroeder, G. M.; Vite, G. D.; Borzilleri, R. M. *Drug Discov Today* **2014**, *19*, 869.

(194) Shadid, M.; Bowlin, S.; Bolleddula, J. *Bioorganic & medicinal chemistry* **2017**, *25*, 2933.

(195) Dubowchik, G. M.; Firestone, R. A.; Padilla, L.; Willner, D.; Hofstead, S. J.; Mosure, K.; Knipe, J. O.; Lasch, S. J.; Trail, P. A. *Bioconjug Chem* **2002**, *13*, 855.

(196) Saito, G.; Swanson, J. A.; Lee, K. D. *Advanced drug delivery reviews* **2003**, *55*, 199.

(197) LoRusso, P. M.; Weiss, D.; Guardino, E.; Girish, S.; Sliwkowski, M. X. *Clinical cancer research : an official journal of the American Association for Cancer Research* **2011**, *17*, 6437.

(198) Ponte, J. F.; Sun, X.; Yoder, N. C.; Fishkin, N.; Laleau, R.; Coccia, J.; Lanieri, L.; Bogalhas, M.; Wang, L.; Wilhelm, S.; Widdison, W.; Pinkas, J.; Keating, T. A.; Chari, R.; Erickson, H. K.; Lambert, J. M. *Bioconjug Chem* **2016**, *27*, 1588.

(199) Zolot, R. S.; Basu, S.; Million, R. P. *Nat Rev Drug Discov* **2013**, *12*, 259.

(200) Shefet-Carasso, L.; Benhar, I. *Drug resistance updates : reviews and commentaries in antimicrobial and anticancer chemotherapy* **2015**, *18*, 36.

(201) Howard, D.; Garcia-Parra, J.; Healey, G. D.; Amakiri, C.; Margarit, L.; Francis, L. W.; Gonzalez, D.; Conlan, R. S. *Interface focus* **2016**, *6*, 20160054.

(202) Sutherland, M. S. K.; Sanderson, R. J.; Gordon, K. A.; Andreyka, J.; Cervený, C. G.;

Yu, C. P.; Lewis, T. S.; Meyer, D. L.; Zabinski, R. F.; Doronina, S. O.; Senter, P. D.; Law, C. L.; Wahl, A. F. *J Biol Chem* **2006**, *281*, 10540.

(203) Kovtun, Y. V.; Goldmacher, V. S. *Cancer Lett* **2007**, *255*, 232.

(204) Sassoon, I.; Blanc, V. *Methods in molecular biology* **2013**, *1045*, 1.

(205) Ducry, L.; Stump, B. *Bioconjug Chem* **2010**, *21*, 5.

(206) Pabst, M.; McDowell, W.; Manin, A.; Kyle, A.; Camper, N.; De Juan, E.; Parekh, V.; Rudge, F.; Makwana, H.; Kantner, T.; Parekh, H.; Michelet, A.; Sheng, X.; Popa, G.; Tucker, C.; Khayrabad, F.; Pollard, D.; Kozakowska, K.; Resende, R.; Jenkins, A.; Simoes, F.; Morris, D.; Williams, P.; Badescu, G.; Baker, M. P.; Bird, M.; Frigerio, M.; Godwin, A. *Journal of controlled release : official journal of the Controlled Release Society* **2017**, *253*, 160.

(207) Teicher, B. A.; Chari, R. V. *Clinical cancer research : an official journal of the American Association for Cancer Research* **2011**, *17*, 6389.

(208) Junutula, J. R.; Raab, H.; Clark, S.; Bhakta, S.; Leipold, D. D.; Weir, S.; Chen, Y.; Simpson, M.; Tsai, S. P.; Dennis, M. S.; Lu, Y.; Meng, Y. G.; Ng, C.; Yang, J.; Lee, C. C.; Duenas, E.; Gorrell, J.; Katta, V.; Kim, A.; McDorman, K.; Flagella, K.; Venook, R.; Ross, S.; Spencer, S. D.; Lee Wong, W.; Lowman, H. B.; Vandlen, R.; Sliwkowski, M. X.; Scheller, R. H.; Polakis, P.; Mallet, W. *Nature biotechnology* **2008**, *26*, 925.

(209) Thompson, P.; Fleming, R.; Bezabeh, B.; Huang, F.; Mao, S.; Chen, C.; Harper, J.; Zhong, H.; Gao, X.; Yu, X. Q.; Hinrichs, M. J.; Reed, M.; Kamal, A.; Strout, P.; Cho, S.; Woods, R.; Hollingsworth, R. E.; Dixit, R.; Wu, H.; Gao, C.; Dimasi, N. *Journal of controlled release : official journal of the Controlled Release Society* **2016**, *236*, 100.

- (210) Shen, B. Q.; Xu, K.; Liu, L.; Raab, H.; Bhakta, S.; Kenrick, M.; Parsons-Reponce, K. L.; Tien, J.; Yu, S. F.; Mai, E.; Li, D.; Tibbitts, J.; Baudys, J.; Saad, O. M.; Scales, S. J.; McDonald, P. J.; Hass, P. E.; Eigenbrot, C.; Nguyen, T.; Solis, W. A.; Fuji, R. N.; Flagella, K. M.; Patel, D.; Spencer, S. D.; Khawli, L. A.; Ebens, A.; Wong, W. L.; Vandlen, R.; Kaur, S.; Sliwkowski, M. X.; Scheller, R. H.; Polakis, P.; Junutula, J. R. *Nature biotechnology* **2012**, *30*, 184.
- (211) Stimmel, J. B.; Merrill, B. M.; Kuyper, L. F.; Moxham, C. P.; Hutchins, J. T.; Fling, M. E.; Kull, F. C., Jr. *J Biol Chem* **2000**, *275*, 30445.
- (212) Voynov, V.; Chennamsetty, N.; Kayser, V.; Wallny, H. J.; Helk, B.; Trout, B. L. *Bioconjug Chem* **2010**, *21*, 385.
- (213) Jeffrey, S. C.; Burke, P. J.; Lyon, R. P.; Meyer, D. W.; Sussman, D.; Anderson, M.; Hunter, J. H.; Leiske, C. I.; Miyamoto, J. B.; Nicholas, N. D.; Okeley, N. M.; Sanderson, R. J.; Stone, I. J.; Zeng, W.; Gregson, S. J.; Masterson, L.; Tiberghien, A. C.; Howard, P. W.; Thurston, D. E.; Law, C. L.; Senter, P. D. *Bioconjug Chem* **2013**, *24*, 1256.
- (214) Shiraishi, Y.; Muramoto, T.; Nagatomo, K.; Shinmi, D.; Honma, E.; Masuda, K.; Yamasaki, M. *Bioconjug Chem* **2015**, *26*, 1032.
- (215) Shinmi, D.; Taguchi, E.; Iwano, J.; Yamaguchi, T.; Masuda, K.; Enokizono, J.; Shiraishi, Y. *Bioconjug Chem* **2016**, *27*, 1324.
- (216) Dimasi, N.; Fleming, R.; Zhong, H.; Bezabeh, B.; Kinneer, K.; Christie, R. J.; Fazenbaker, C.; Wu, H.; Gao, C. *Molecular pharmaceutics* **2017**, *14*, 1501.
- (217) Zimmerman, E. S.; Heibeck, T. H.; Gill, A.; Li, X.; Murray, C. J.; Madlansacay, M.

R.; Tran, C.; Uter, N. T.; Yin, G.; Rivers, P. J.; Yam, A. Y.; Wang, W. D.; Steiner, A. R.; Bajad, S. U.; Penta, K.; Yang, W.; Hallam, T. J.; Thanos, C. D.; Sato, A. K. *Bioconjug Chem* **2014**, 25, 351.

(218) Tian, F.; Lu, Y.; Manibusan, A.; Sellers, A.; Tran, H.; Sun, Y.; Phuong, T.; Barnett, R.; Hehli, B.; Song, F.; DeGuzman, M. J.; Ensari, S.; Pinkstaff, J. K.; Sullivan, L. M.; Biroc, S. L.; Cho, H.; Schultz, P. G.; DiJoseph, J.; Dougher, M.; Ma, D.; Dushin, R.; Leal, M.; Tchistiakova, L.; Feyfant, E.; Gerber, H. P.; Sapra, P. *Proc Natl Acad Sci U S A* **2014**, 111, 1766.

(219) VanBrunt, M. P.; Shanebeck, K.; Caldwell, Z.; Johnson, J.; Thompson, P.; Martin, T.; Dong, H.; Li, G.; Xu, H.; D'Hooze, F.; Masterson, L.; Bariola, P.; Tiberghien, A.; Ezeadi, E.; Williams, D. G.; Hartley, J. A.; Howard, P. W.; Grabstein, K. H.; Bowen, M. A.; Marelli, M. *Bioconjug Chem* **2015**, 26, 2249.

(220) Levengood, M. R.; Zhang, X.; Hunter, J. H.; Emmerton, K. K.; Miyamoto, J. B.; Lewis, T. S.; Senter, P. D. *Angewandte Chemie* **2017**, 56, 733.

(221) Dennler, P.; Chiotellis, A.; Fischer, E.; Bregeon, D.; Belmant, C.; Gauthier, L.; Lhospice, F.; Romagne, F.; Schibli, R. *Bioconjug Chem* **2014**, 25, 569.

(222) Farias, S. E.; Strop, P.; Delaria, K.; Galindo Casas, M.; Dorywalska, M.; Shelton, D. L.; Pons, J.; Rajpal, A. *Bioconjug Chem* **2014**, 25, 240.

(223) Paterson, B. M.; Alt, K.; Jeffery, C. M.; Price, R. I.; Jagdale, S.; Rigby, S.; Williams, C. C.; Peter, K.; Hagemeyer, C. E.; Donnelly, P. S. *Angewandte Chemie* **2014**, 53, 6115.

(224) Mao, H.; Hart, S. A.; Schink, A.; Pollok, B. A. *J Am Chem Soc* **2004**, 126, 2670.

(225) Mohlmann, S.; Mahlert, C.; Greven, S.; Scholz, P.; Harrenga, A. *ChemBiochem : a European journal of chemical biology* **2011**, 12, 1774.

- (226) Drake, P. M.; Albers, A. E.; Baker, J.; Banas, S.; Barfield, R. M.; Bhat, A. S.; de Hart, G. W.; Garofalo, A. W.; Holder, P.; Jones, L. C.; Kudirka, R.; McFarland, J.; Zmolek, W.; Rabuka, D. *Bioconjug Chem* **2014**, *25*, 1331.
- (227) Zuberbuhler, K.; Casi, G.; Bernardes, G. J.; Neri, D. *Chem Commun (Camb)* **2012**, *48*, 7100.
- (228) Zhou, Q.; Stefano, J. E.; Manning, C.; Kyazike, J.; Chen, B.; Gianolio, D. A.; Park, A.; Busch, M.; Bird, J.; Zheng, X.; Simonds-Mannes, H.; Kim, J.; Gregory, R. C.; Miller, R. J.; Brondyk, W. H.; Dhal, P. K.; Pan, C. Q. *Bioconjug Chem* **2014**, *25*, 510.
- (229) Zeglis, B. M.; Davis, C. B.; Aggeler, R.; Kang, H. C.; Chen, A.; Agnew, B. J.; Lewis, J. S. *Bioconjug Chem* **2013**, *24*, 1057.
- (230) Okeley, N. M.; Toki, B. E.; Zhang, X.; Jeffrey, S. C.; Burke, P. J.; Alley, S. C.; Senter, P. D. *Bioconjug Chem* **2013**, *24*, 1650.
- (231) Beck, A.; Goetsch, L.; Dumontet, C.; Corvaia, N. *Nat Rev Drug Discov* **2017**, *16*, 315.
- (232) Lambert, J. M. *Therapeutic delivery* **2016**, *7*, 279.

## CHAPTER 2

### ONE-STEP SELECTIVE EXOENZYMATIC LABELING (SEEL) STRATEGY FOR THE BIOTINYLATION AND IDENTIFICATION OF GLYCOPROTEINS OF LIVING CELLS <sup>1</sup>

<sup>1</sup>Sun, T.; Yu, S. H.; Zhao, P.; Meng, L.; Moremen, K. W.; Wells, L.; Steet, R.; Boons, G. J. *J Am Chem Soc* **2016**, *138*, 11575.

Authors contribution. G-J.B. conceived the idea of one-step SEEL; G-J.B., R.S., L.W., and K.W.M. designed research plan; T.S., S-H.Y., P.Z., and L.M. performed research; T.S., S-H.Y., P.Z., and L.M. analyzed data; and G-J.B. and R.S. wrote the paper

Reprinted here with permission of the publisher.



## **Abstract**

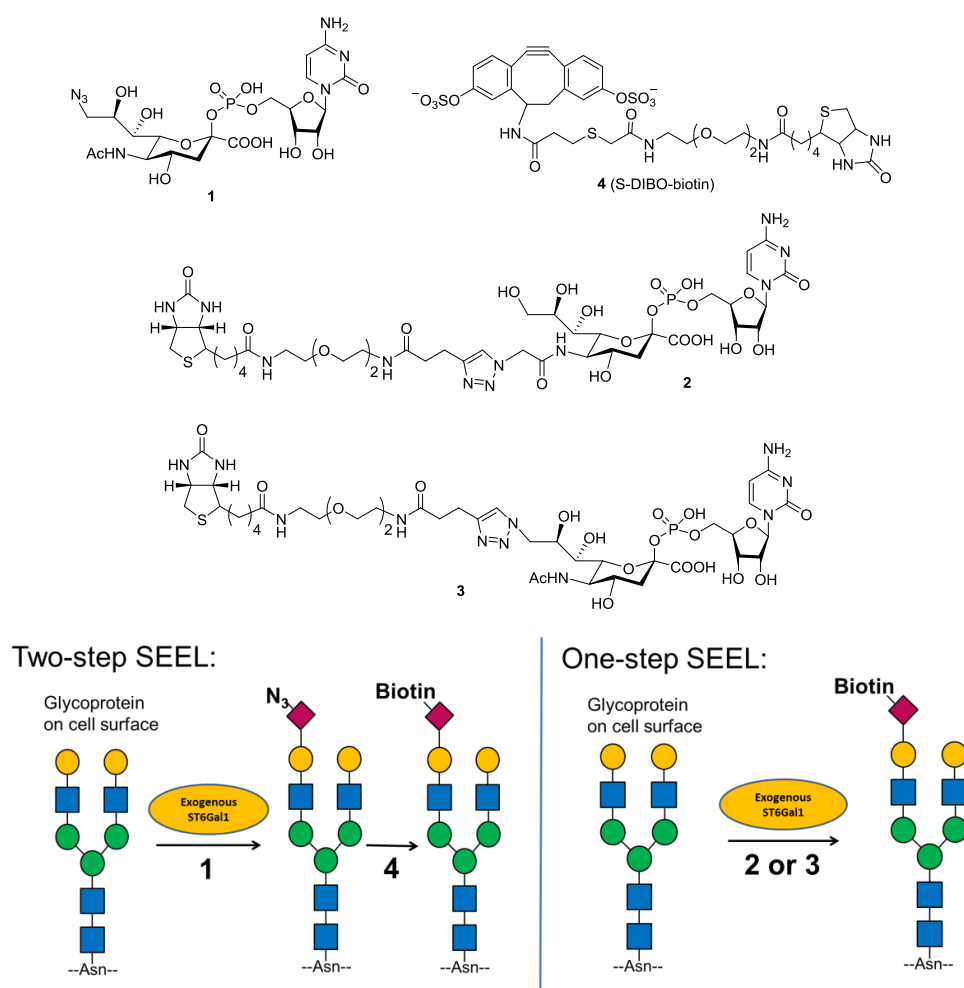
Technologies that can visualize, capture, and identify subsets of biomolecules that are not encoded by the genome in the context of healthy and diseased cells will offer unique opportunities to uncover the molecular mechanism of a multitude of physiological and disease processes. We describe here a chemical reporter strategy for labeling of cell surface glycoconjugates that takes advantage of recombinant glycosyltransferases and a corresponding sugar nucleotide functionalized by biotin. The exceptional efficiency of this method, termed one-step selective exoenzymatic labeling, or SEEL, greatly improved the ability to enrich and identify large numbers of tagged glycoproteins by LC-MS/MS. We further demonstrated that this labeling method resulted in far superior enrichment and detection of glycoproteins at the plasma membrane compared to a sulfo-NHS-activated biotinylation or two-step SEEL. This new methodology will make it possible to profile cell surface glycoproteomes with unprecedented sensitivity in the context of physiological and disease states.

## Introduction

The bioorthogonal chemical reporter strategy offers exciting possibilities to interrogate biomolecules of living cells that are not encoded by the genome.<sup>1,2</sup> In this approach, the biosynthetic machinery of a cell is hijacked by feeding a metabolic precursor functionalized with a chemical reporter for incorporation into a target class of biomolecules, such as lipids or glycoconjugates. Next, a bioorthogonal reaction is performed to modify the reporter with a biophysical probe for visualization or enrichment. To date, azido modification is the most widely employed bioorthogonal chemical reporter because of its small size and inertness to most components in a biological environment. It can for example be tagged by Staudinger ligation using modified phosphines,<sup>3,4</sup> copper(I)-catalyzed cycloaddition with terminal alkynes (CuAAC),<sup>5-7</sup> or strain-promoted alkyne–azide cycloaddition (SPAAC).<sup>8,9</sup> In particular, SPAAC is attractive because it avoids the cellular toxicity associated with copper ions without compromising alkyne reactivity.

In an alternative approach, chemical reporters can be introduced into biomolecules of living cells by performing glycosyltransferase reactions at the cell surface.<sup>10-19</sup> This process, for which we coined the term SEEL (selective exoenzymatic labeling), takes advantage of recombinant glycosyltransferases and a corresponding functionalized nucleotide sugar to install chemical reporters on cell surface acceptor glycans. For example, we have demonstrated that recombinant ST6Gal1 sialyltransferase and CMP-Neu5Ac9N<sub>3</sub> (1) can be exploited for the selective labeling of *N*-linked glycans of living cells with azido-modified sialic acid.<sup>16</sup> The

attraction of the SEEL approach is that it only labels a specific class of cell surface molecules (e.g., *N*- vs *O*-glycans) and does not rely on feeding with metabolic substrates that must compete with natural sugar precursor pools. In light of the direct nature of this method, we explored whether SEEL can be accomplished in a single step by employing CMP-Neu5Ac modified by biotin.<sup>20,21</sup> Such an approach would circumvent possible limitations associated with bioorthogonal reactions, such as side reactions,<sup>22</sup> and decrease the time needed for labeling.



Scheme 2.1 one- and two-step SEEL.

We sought to explore whether SEEL could be accomplished in a single step by employing CMP-Neu5Ac modified by biotin. Surprisingly, the one-step SEEL procedure,

employing exogenously administered CMP-Neu5Ac analogues modified at C-5 or C-9 with biotin (compounds **2** and **3**, Scheme 2.1)<sup>13,21</sup> not only is feasible but dramatically improves cell surface labeling of glycoconjugates compared to two-step SEEL or metabolic labeling. The new methodology offers exciting possibilities to track, capture, and identify subsets of cell surface glycoconjugates with unprecedented sensitivity in whole cells. We have exploited the high efficiency labeling with compound **2** to enrich and identify tagged glycoproteins by LC-MS/MS, and could monitor the internalization and degradation of labeled cell surface glycoproteins over time, and identify a subset of glycoproteins that are subject to accumulation upon lysosomal disruption by chloroquine. Lastly, the new labeling strategy was compared with a commonly employed kit for cell surface biotinylation and was found to be vastly superior for enrichment of cell surface glycoproteins. Many diseases exhibit lysosomal dysfunction and altered recycling of cell surface glycoproteins.<sup>23-25</sup> For example, Niemann-Pick type C (NPC) disease is characterized by impaired cholesterol efflux from late endosomes and lysosomes and secondary accumulation of lipids. Previously, we employed the chemical reporter strategy to demonstrate an unrecognized accumulation of glycoconjugates in endocytic compartments of NPC1-null and NPC2-deficient fibroblasts.<sup>25</sup> The endosomal accumulation of sialylated glycoproteins was attributed to impaired recycling as opposed to altered fusion of vesicles. It is our expectation that identification of altered cell surface residency of glycoproteins in diseases such as NPC using the new SEEL methodology will uncover the molecular mechanisms that cause the phenotypes of these diseases, which in turn may lead to the design of new therapeutic strategies.

## Results and discussion

### Synthesis of Modified Sugar Nucleotides.

It is known that sialyltransferases tolerate modifications at C-5 and C-9,<sup>20</sup> and it has for example been demonstrated that a CMP-sialic acid derivative having biotin at C-9 can be transferred to LacNAc.<sup>13,21</sup> Therefore, Compounds **3**, **2**, **5** and **6** with modification at C9 and C5 positions of CMP-sialic acid were synthesized through CuAAC and SPAAC.

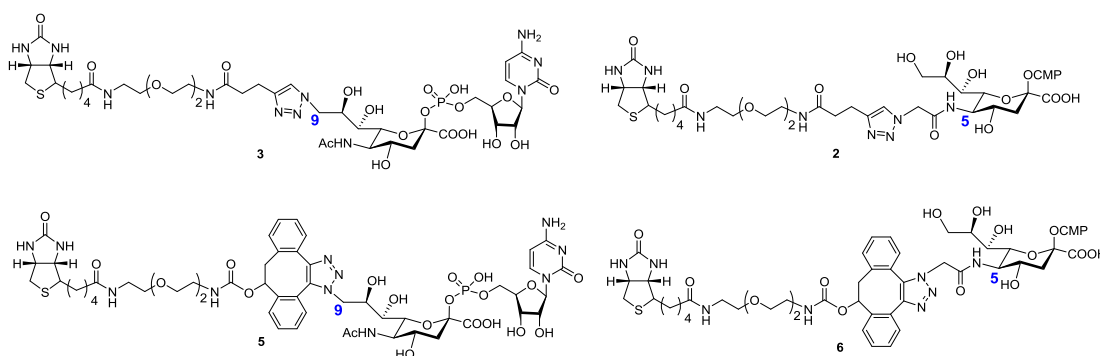


Figure 2.1 CMP-sialic acid derivatives with modification at C9 and C5 positions.

### Biotinylation at C9 position of CMP-sialic acid.

The preparation of the alkyne moieties attached with biotin (**11** and **13**) was very straightforward (Figure 2.2). 2,2'-(Ethylenedioxy)diethylamine (**7**) was firstly protected with Boc group at one side, followed by condensation reaction with biotin in the presence of HBTU and DIPEA to give compound **9**. After removal of the Boc protecting group, compound **10** could be either coupled with 4-Pentynoic acid to give biotin attached terminal alkyne **11**, or with activated DIBO (**12**)<sup>26</sup> to give biotin attached DIBO **13**.

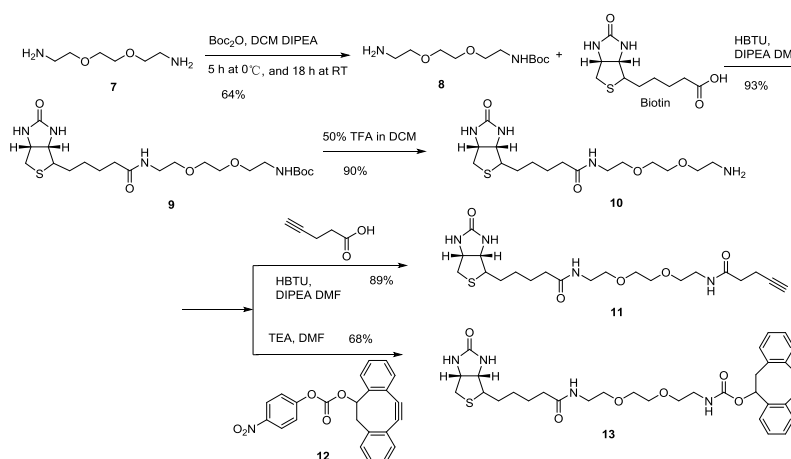


Figure 2.2 Preparation of **11** and **13**.

CMP-sialic acid derivative **1** was prepared according to literature (Figure 2.3).<sup>16</sup> A methylation reaction of sialic acid was firstly carried out, followed by selective tosylation of the C-9 primary hydroxy group to give **15**, which was treated with sodium azide in a mixture of acetone and water, and heated under reflux to afford **16** in an almost quantitative yield. In this step, the methyl ester was removed under these conditions to give the required free carboxylic acid. Condensation of **16** with CTP in the presence of recombinant CMP-sialic acid synthetase from *Neisseria meningitidis* [EC 2.7.7.43]<sup>27</sup> and inorganic pyrophosphatase from *Saccharomyces cerevisiae* [EC 3.6.1.1] gave, after purification by size-exclusion column chromatography, CMP-Neu5Ac9N<sub>3</sub> (**1**).

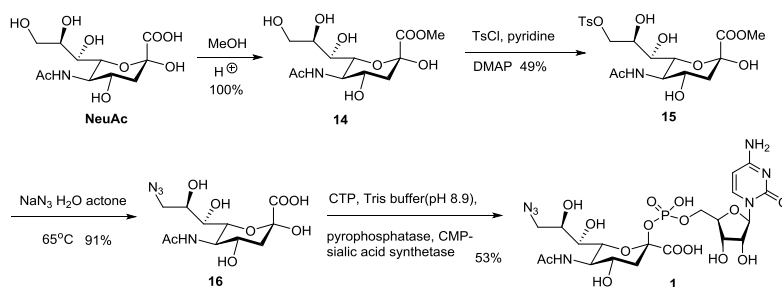


Figure 2.3 Preparation of azide modified sialic acid (**16**) and CMP-sialic acid (**1**) at C9 position.

We initially tried to click biotin-DIBO (**13**) to sialic acid (**16**) in DMF, to give compound **17**, and then install the CMP functionality. But no matter how many synthetase was added, the CMP could not be successfully installed (Figure 2.4), indicating that the synthetase could not tolerate bulky moiety such as DIBO.

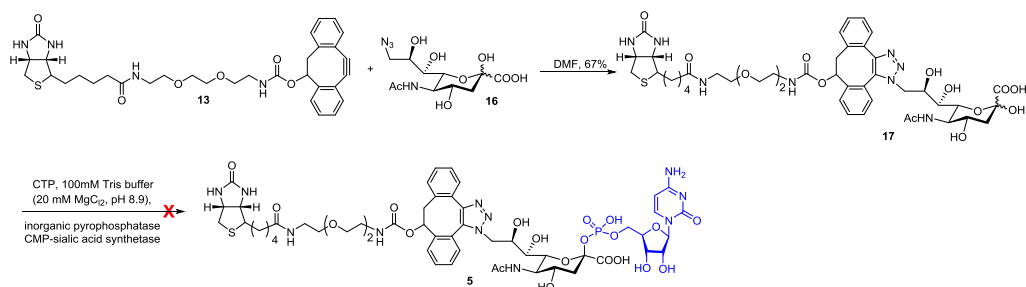


Figure 2.4 Failed trial to prepare Compound **5**.

Next, Biotin-DIBO (**13**) was reacted with CMP-Neu9N<sub>3</sub> (**1**) in the mixture of DMF and 100 mM Tris buffer (pH 7.5), which can stabilize the CMP functionality, to give biotin modified CMP-sialic acid in good yield after purification by size exclusion column chromatography over Biogel P2 (Figure 2.5). However, Incubation of *N*-acetyllactosamine (LacNAc) and **5** in the presence of Recombinant  $\alpha$ -(2,6)-sialyltransferase (ST6GalI) [GenBank P13721] and calf intestine alkaline phosphatase at 37 °C in 5 hours did not give the transferred product, indicating that the C-9 modification by SPAAC could not be tolerated by the enzyme.

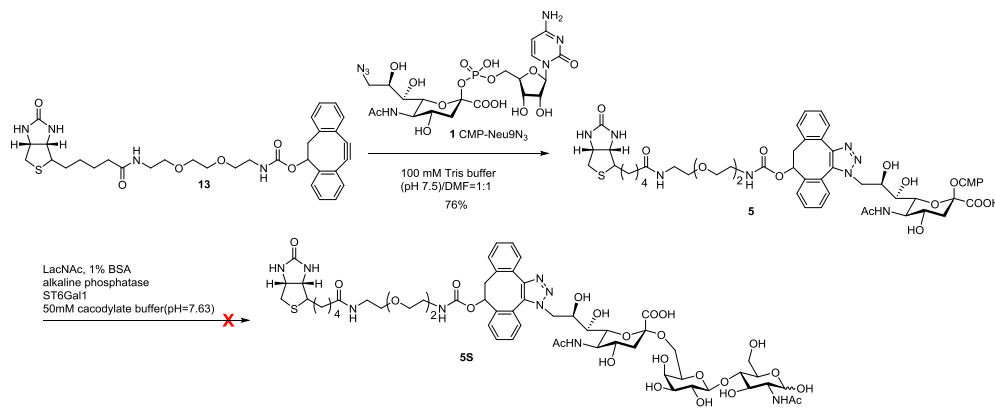


Figure 2.5 Preparation of compound **5** and its unsuccessful transfer to LacNAc.

Then we tried to construct the Biotin modified CMP-sialic acid through CuAAC. Firstly, terminal alkyne **11** reacted with sialic acid derivative **16** in the presence of CuSO<sub>4</sub>, sodium ascorbate and TBTA in the mixture of DMF and water, biotin modified sialic acid **18** was obtained (Figure 2.6). However, the following installation of CMP functionality with CMP-sialic acid synthetase also failed, indicating that this enzyme could not tolerate the triazole group with a biotin linker at C9 position.

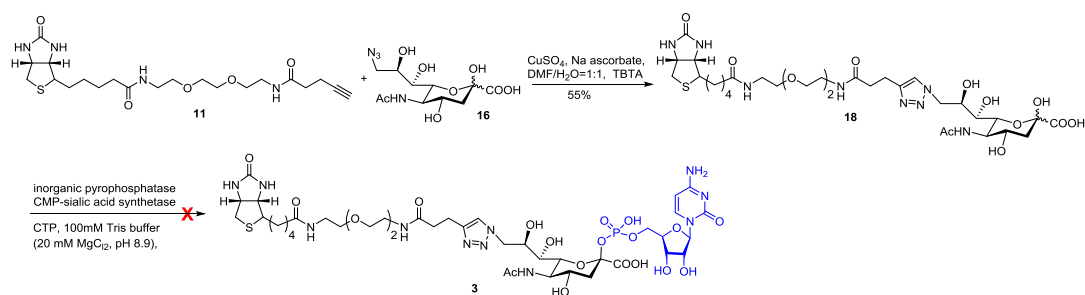


Figure 2.6 Failed trial to prepare Compound **3**.

Next, compound **11** was reacted with CMP-Neu9N<sub>3</sub> (**1**) in the presence of Cu(I) in the mixture of DMF and 100 mM Tris buffer (pH 7.5), CMP-sialic acid derivative **3** was obtained in a good yield after purification by size exclusion column chromatography (Figure 2.7). And excitingly, **3** could be transferred to LacNAc by ST6Gal1 efficiently, highlighting the fact that the C-9 triazole moiety of **3** is tolerated by the enzyme.

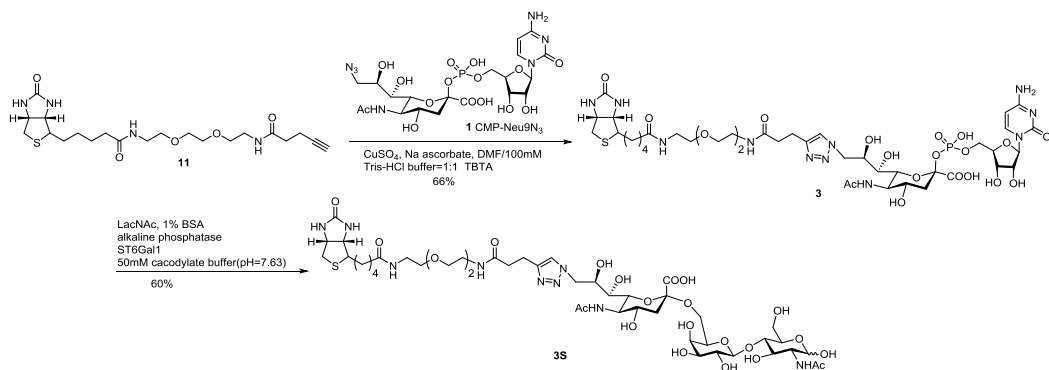


Figure 2.7 Preparation of compound **3** and its successful transfer to LacNAc.



### Biotinylation at C5 position of CMP-sialic acid.

With the C9 position biotinylated CMP-sialic acid **3** in hand, we also want to explore the modification at C5 position. CMP-Neu5N<sub>3</sub> (**22**) was prepared according to literature (Figure 2.8),<sup>27</sup> by a one-pot two-enzyme system, from mannose derivative (**21**), with a recombinant sialic acid aldolase cloned from *E. coli* K12 and CMP-sialic acid synthetase.

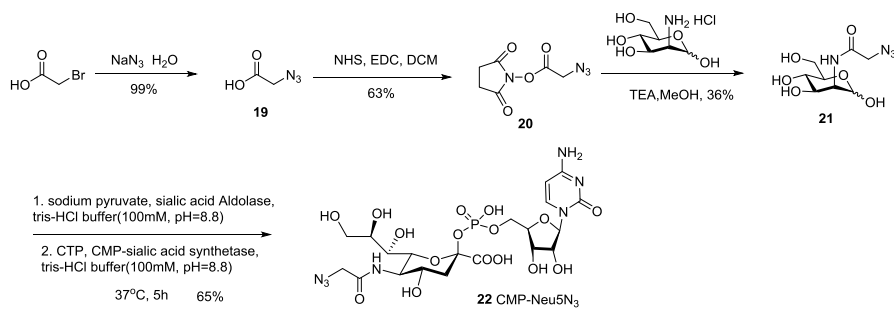


Figure 2.8 One-pot two-enzyme synthesis of CMP-Neu5N<sub>3</sub> (**22**)

The CuAAC between terminal alkyne **11** and CMP-Neu5N<sub>3</sub> (**23**) gave CMP-sialic acid derivative **2** (Figure 2.9). And as expected, **2** could be successfully transferred to LacNAc by ST6Gal1, indicating that this enzyme could tolerate the triazole modification at C5 position.

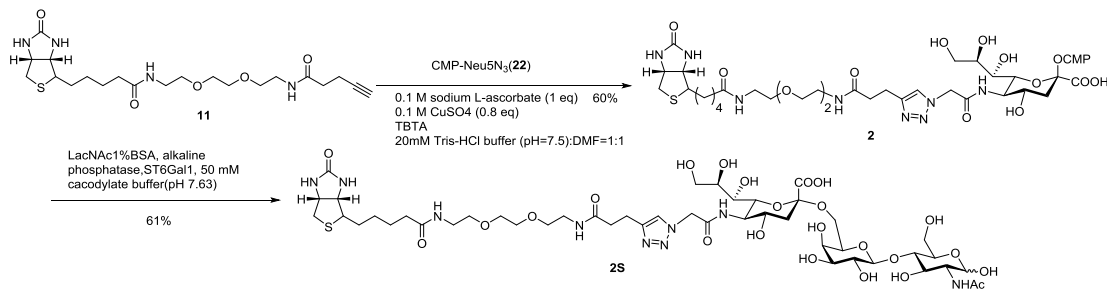


Figure 2.9 Preparation of compound **2** and its successful transfer to LacNAc.

Surprisingly, CMP-sialic acid derivative **2** constructed by SPAAC from Biotin-DIBO (**13**) and CMP-NeuNeu5N<sub>3</sub> (**23**), could also be transferred to LacNAc by ST6Gal1 efficiently (Figure

2.10), highlighting the fact that Modification at C5 position is much more tolerable than C9 position to ST6Gal1.

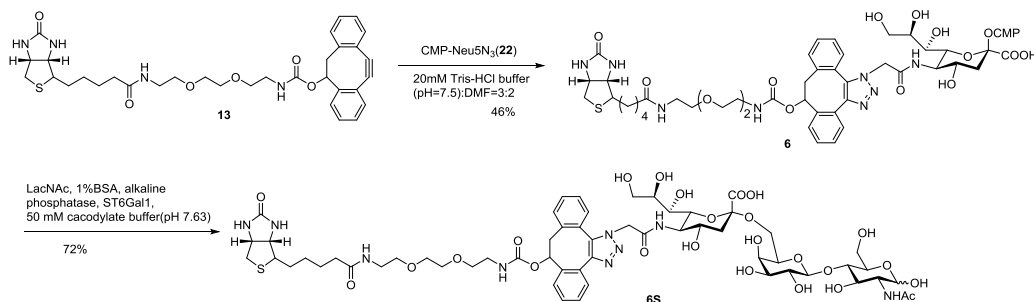


Figure 2.10 Preparation of compound **6** and its successful transfer to LacNAc.

We also investigated the tolerance of CMP-sialic acid synthetase at C5 position. After getting the sialic acid derivatives **23** and **24** through CuAAC and SPAAC respectively, the installation of CMP functionality failed on both compounds because the enzyme did not tolerate these substituents (Figure 2.11).

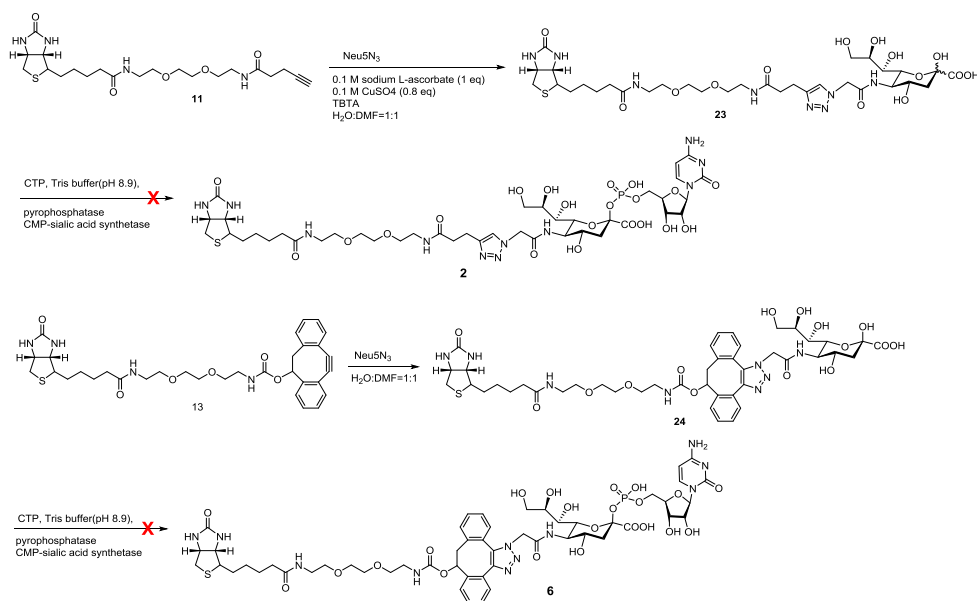
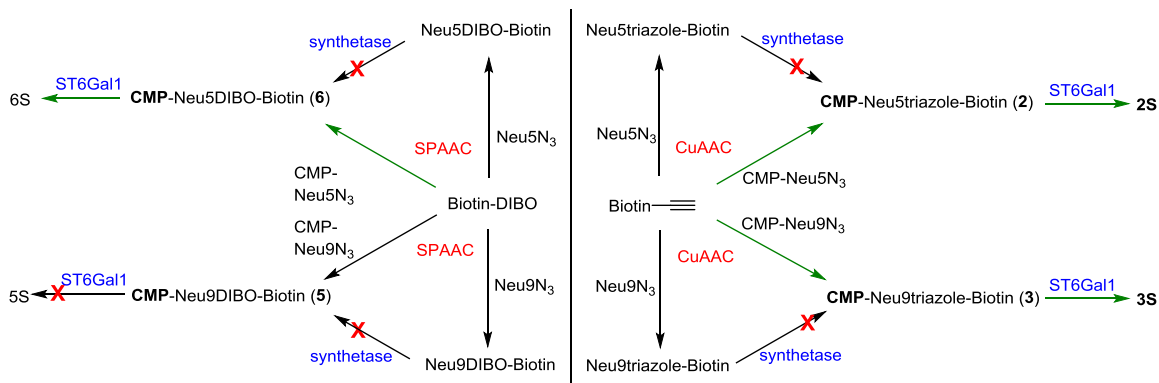


Figure 2.11 Investigation of the tolerance of CMP-sialic acid synthetase at C5 position.

Now, we have successfully prepared 3 CMP-sialic acid derivatives (**2**, **3** and **6**) that can

be transferred to LacNAc. The tolerance of enzymes is playing a very important role which can be summarized in the following scheme:



Scheme 2.2 Summary of synthesis of CMP-sialic acid derivatives

Next, we investigated the use of the one-step SEEL technology with compounds **2** and **3** for the visualization of trafficking of *N*-linked glycoconjugates. Kinetic analysis of the enzymatic transformation showed that the modifications of **2** and **3** had no or a marginal impact on the *K<sub>m</sub>* value (**2**, **3**, and CMP-Neu5Ac, *K<sub>m</sub>* = 53, 108, and 54  $\mu$ M, respectively) with no appreciable influence on *V<sub>max</sub>*.

### Labeling and Trafficking of Cell Surface Glycoproteins of Living Cells.

HeLa cells were incubated with CMP-Neu5Ac derivatives **1**, **2**, and **3** (Scheme 2.1) in the presence of ST6Gal1 for 2 h at 37 °C to examine the efficiency of one-step SEEL in comparison to the previously reported<sup>16</sup> two-step SEEL method. The labeling was performed with and without prior treatment with *Vibrio cholerae* sialidase. In addition, cells were metabolically labeled with azido containing sialosides by feeding Ac4ManNAz.<sup>3</sup> The cells modified by

azido-containing glycoconjugates were biotinylated by exposure to sulfated dibenzocyclooctynylamide containing biotin (S-DIBO-biotin **4**, 30  $\mu$ M, Scheme 2.1) for 1 h. The efficiency of the various surface-labeling procedures was determined by SDS-PAGE of cell lysates followed by Western blotting using an anti-biotin antibody conjugated with HRP. These experiments demonstrated that prior neuraminidase treatment of the cells increased the efficiency of labeling for both one- and two-step SEEL (consistent with the presence of abundant highly sialylated Nglycan structures in these cells which reduce the abundance of SEEL acceptors). Remarkably, the one-step labeling procedure using **2** and **3** gave a robust biotin signal even after exposure of the blot for only seconds, whereas the two-step protocol with compound **1** or metabolic labeling with ManNAz gave a faint biotin signal and longer exposure time was required to make the glycoproteins visible (Figure 2.12). Furthermore, labeling with **2** was more efficient than with **3** probably because it is a better substrate for ST6Gal1.

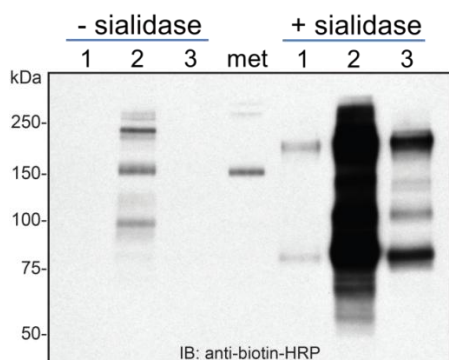


Figure 2.12 Western blot analysis of One-step SEEL, two-step SEEL, and metabolic labeling.

Next, we performed proteomic analysis on HeLa cells labeled by two-step SEEL or one-step SEEL (with ST6Gal1) to compare the labeling efficiency of the two methods. 294 proteins were assigned at <1% false-discovery rate using one-step SEEL, whereas 174 proteins

were assigned with two-step SEEL (Figure 2.13a). One-step SEEL detected 140 glycoproteins not observed using the two-step method, while two-step SEEL identified only 20 unique glycoproteins. The total spectral count of all assigned proteins from one-step SEEL was 2.1 times higher than that from two-step SEEL. Out of the 154 commonly found proteins in both methods, 85 proteins showed more than 2-fold increase in their spectral counts, while 57 proteins showed more than 3-fold increase and 25 proteins showed more than 5-fold increase in one-step SEEL. The relative spectral counts of the top 20 most abundant commonly assigned glycoproteins were compared in Figure 2.13b. Among these 20 proteins, PTPRF (752%), BSG (423%), ROBO1 (359%), and IGF2R (342%) showed at least a 3-fold improvement in assigned spectral counts. These data demonstrate the remarkably superior labeling efficiency of sialoglycoproteins at the cell surface when one-step SEEL is utilized.

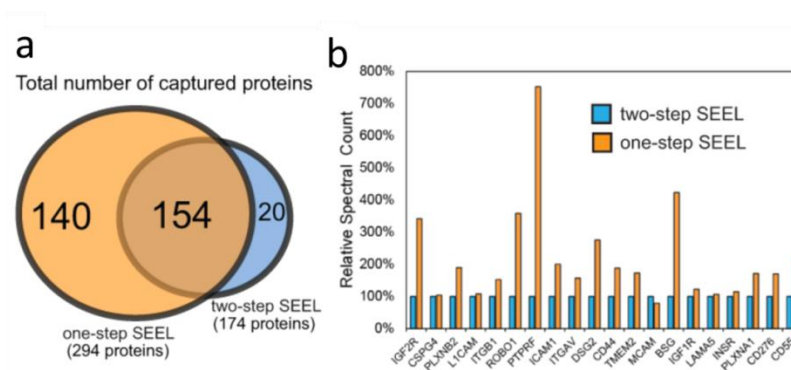


Figure 2.13 a) Venn diagram for the proteomic analysis of HeLa cells subjected to two-step (cmpd 1) or one-step (cmpd 2) SEEL with ST6Gal1; b) The spectral counts of the 20 most abundant glycoproteins detected using one-step SEEL are plotted relative to the counts detected using two-step SEEL (values for two-step SEEL set to 100%).

### Proteomic Analysis of Labeled Glycoproteins Following Lysosomal Disruption.

Next, attention was focused on the use of the new compounds to visualize trafficking of *N*-linked glycoconjugates in normal and chloroquine-treated cells. HeLa cells were

enzymatically labeled with ST6Gal1 and CMP-sialic acid derivative **2**, and the resulting biotin-modified N-glycoproteins were visualized by confocal microscopy following incubation with a fluorophore conjugated anti-biotin antibody (Figure 2.14a).

As expected, robust staining at the cell surface was observed. Labeled cells were then incubated with or without chloroquine for 16 h to allow labeled glycoproteins to be internalized from the cell surface. Chloroquine is known to disrupt lysosomal pH and prevent efficient catabolism within this compartment. In the absence of chloroquine, a clear decrease in the intensity of labeling at the cell surface was detected, indicating that the SEEL-tagged glycoproteins can be internalized and/or degraded. In the chloroquine-treated cells, the labeled glycoconjugates instead accumulated within intracellular vesicles, consistent with late endosomes/lysosomes.

The high labeling efficiency achieved by the one-step SEEL procedure provides opportunities to enrich and identify cell surface glycoproteins and investigate how different glycoproteins respond to biological processes such as lysosomal disruption. For enrichment of tagged glycoproteins, immunoprecipitation was performed with an anti-biotin antibody, which was followed by SDS-PAGE and silver staining (Figure 2.14b). The results clearly show a loss of labeled *N*-linked glycoproteins following incubation in the absence of chloroquine (indicative of endocytosis and degradation of these glycoproteins) but a substantial reduction in the degradation of many labeled proteins in the presence of chloroquine. This observation was confirmed by Western blotting analysis of the same samples using an anti-biotin antibody (Figure 2.14b).

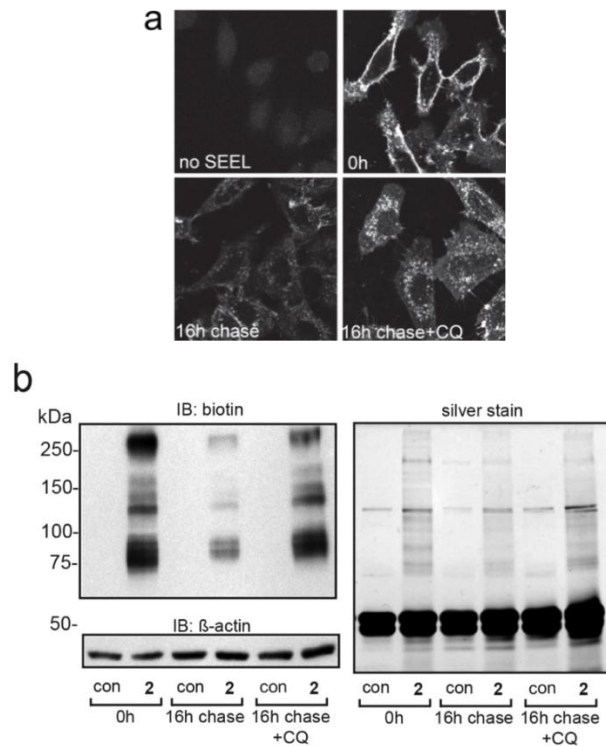


Figure 2.14 a) confocal microscopy of one-step SEEL with or without chloroquine;  
b) Western blot analysis of SEEL labeled HeLa cells under the three conditions tested.

### Proteomic Analysis of Cell Surface Proteins Labeled by SEEL and Amino-Reactive Reagents

Existing strategies for the enrichment of cell surface glycoproteins utilize reagents such as sulfo-NHS-activated biotin to tag lysine residues on available proteins.<sup>28</sup> These reagents suffer from lack of selectivity and often isolate cytosolic proteins. Using nonadherent HEK293F cells, a direct comparison of the SEEL and amino labeling method was performed. As shown in Figure 2.15a, labeling with the sulfo-NHS-biotin reagent resulted in the detection of numerous proteins across a broad molecular weight. On the other hand, a more restricted profile of proteins was visualized by one-step SEEL labeling with ST6Gal1. Analysis of the total proteins detected (vs total cell surface glycoproteins detected), however, revealed a clear enrichment in the detection of cell surface glycoproteins using SEEL. Nearly 95% of the total proteins detected following

SEEL with ST6Gal1 (367) were bona fide cell surface glycoproteins whereas only 18% of the total proteins detected using the sulfo-NHS-biotin reagent were cell surface glycoproteins (Figure 2.15b, top panel). Analysis of total spectral counts recovered using the two methodologies further enforced the obvious advantage of using SEEL-based labeling to enrich and detect cell surface glycoproteins (Figure 2.15b, bottom panel).

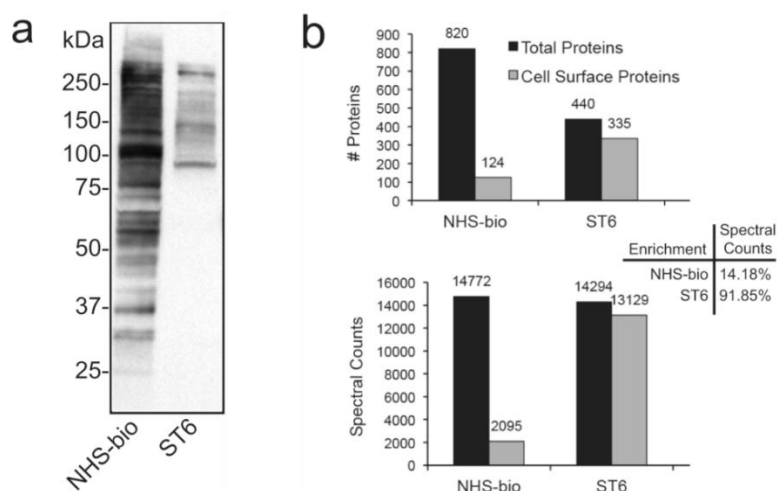


Figure 2.15 a) Western blot analysis of HEK293F cells labeled using sulfo-NHS-biotin or SEEL with ST6Gal1; (b) Quantification of the total proteins identified (top panel) and their spectral counts (bottom panel) under these conditions compared to the total cell surface glycoproteins identified.

## Conclusion

The findings reported here demonstrate a remarkable labeling efficiency of cell surface glycoproteins by employing CMP-sialic acid modified by biotin and an appropriate sialyltransferase. The approach made it possible to track, capture, and identify subsets of cell surface glycoconjugates with unprecedented sensitivity in whole cells. The efficiency of the enzymatic transfer by ST6Gal1 is not substantially altered by the presence of the biotin (or azide) tag, and therefore we believe that the inferior labeling with the two-step SEEL method lies in the



bioorthogonal reaction step. The use of the biotin conjugated CMP-sialic acid derivatives also decreases the total labeling time which makes it suitable for SEEL on cell types that may be sensitive to the conditions needed for this type of labeling. The SEEL approach requires galactosyl acceptors at the cell surface, which *in situ* can be generated by performing the reactions in the presence of a bacterial neuraminidase that is capable of removing the natural sialic acids but not the biotin-bearing sialic acids. The ability to effectively label in the presence of the neuraminidase is advantageous since it may limit the effects that desialylation would have on the cell surface residence or endocytosis of glycoproteins.

Immunopurification of labeled glycoconjugates followed by tandem mass spectrometry demonstrated the power of the one-step SEEL approach to efficiently enrich and confidently identify cell surface glycoproteins, as approximately 300 known cell surface glycoproteins were detected. Almost twice as many proteins were identified compared to the two-step SEEL method, and the new approach allows for many lower abundance glycoproteins to be uniquely identified. We believe that this difference arises from the fact that only one glycan of a glycoprotein that may have multiple glycans needs to be labeled for enrichment and subsequent proteomic analysis. In contrast, labeling multiple glycans of a single glycoprotein will greatly influence Western blot detection of a given glycoprotein as each biotin contributes independently to the overall signal.

The SEEL methodology described here is highly selective for cell surface proteins because the employed enzymes and reagents cannot cross the cell membrane. The high labeling efficiency and the selectivity for cell surface proteins achieved is best underscored by the impressive enrichment of cell surface glycoproteins vs total proteins detected (95% using SEEL;

18% using NHS-biotin). Moreover, the procedure is technically simple and allows glycoprotein trafficking and turnover to be easily investigated though of course it is limited to the glycoproteins that can be substrates for the enzyme. Furthermore, the one-step SEEL approach can readily be expanded to the labeling of specific classes of glycoproteins by employing alternative glycosyltransferases that have unique glycosyl acceptor specificities.<sup>29</sup>

## **Experimental section**

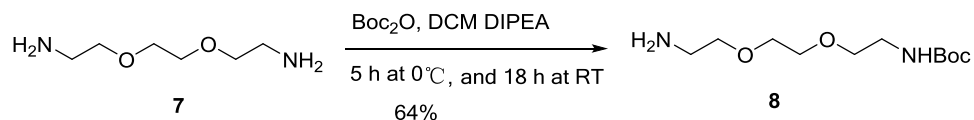
### General methods and materials:

NeuAc and D-mannosamine HCl were purchased from Carbosynth LLC. Other reagents were obtained from commercial sources and used as purchased. Dichloromethane (DCM) was freshly distilled using standard procedures. Other organic solvents were purchased anhydrous and used without further purification. Unless otherwise noted, all reactions were carried out at room temperature (RT) in glassware with magnetic stirring. Organic solutions were concentrated under reduced pressure with bath temperatures < 30 °C. Flash column chromatography was carried out on silica gel G60 (Silicycle, 60-200 µm, 60 Å). Thin-layer chromatography (TLC) was carried out on Silica gel 60 F<sub>254</sub> (EMD Chemicals Inc.) with detection by UV absorption (254 nm) where applicable, by spraying with 20% sulfuric acid in ethanol followed by charring at ~150 °C or by spraying with a solution of (NH<sub>4</sub>)<sub>6</sub>Mo<sub>7</sub>O<sub>24</sub>·H<sub>2</sub>O (25 g/L) in 10% sulfuric acid in ethanol followed by charring at ~150°C. <sup>1</sup>H and <sup>13</sup>C NMR spectra were recorded on a Varian Inova-300 (300/75 MHz), a Varian Inova-500 (500 MHz) and a Varian Inova-600 (600/150 MHz) spectrometer equipped with sun workstations. Multiplicities are quoted as singlet (s), doublet (d), doublet of

doublets (dd), triplet (t) or multiplet (m). All NMR signals were assigned on the basis of  $^1\text{H}$  NMR,  $^{13}\text{C}$  NMR, gCOSY and gHSQC experiments. All chemical shifts are quoted on the  $\delta$ -scale in parts per million (ppm). Residual solvent signals were used as an internal reference. Mass spectra were recorded on an Applied Biosystems 5800 MALDI-TOF or Shimadzu LCMS-IT-TOF mass spectrometer. The matrix used was 2,5-dihydroxy-benzoic acid (DHB). Reverse-Phase HPLC was performed on an Agilent 1200 series system equipped with an auto-sampler, fraction-collector, UV-detector and eclipse XDB-C18 column ( $5\ \mu\text{m}$ ,  $4.6 \times 250\ \text{mm}$  or  $9.4 \times 250\ \text{mm}$ ).

#### Biotinylation at C5 position of CMP-sialic acid.

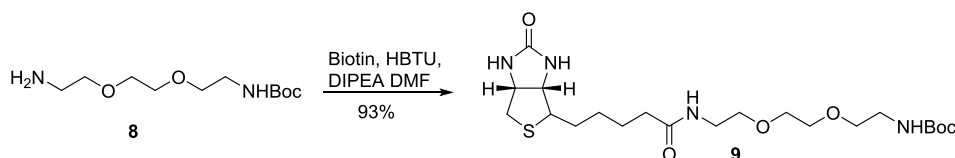
##### ***N*-Boc-3,6-dioxaoctane-1,8-diamine (8)**



A solution of di-tert-butyl dicarbonate (di-Boc) (873 mg, 4 mmol, 1 equiv) in  $\text{CH}_2\text{Cl}_2$  (40 mL) was added dropwise to a mixture of tris(ethylene glycol)-1,8-diamine (3 mL, 20 mmol, 5 equiv) and diisopropylethylamine (5.4 mL, 31.2 mmol) at  $0^\circ\text{C}$ . the reaction mixture was stirred for 5 hours at  $0^\circ\text{C}$ , then the temperature was raised to room temperature and the reaction mixture was stirred overnight, after which it was washed with water (80 mL \*3) to remove the unreacted diamine, dried over  $\text{MgSO}_4$ , filtered and concentrated in vacuo. The residue was purified by flash silica gel column chromatography ( $\text{CH}_2\text{Cl}_2/\text{CH}_3\text{OH}$ , 10/1, v/v) to afford **8** (640 mg, 64%) as a colorless oil.  $^1\text{H}$  NMR (300 MHz,  $\text{d}_2\text{O}$ )  $\delta$  3.66 (s, 4H,  $\text{OCH}_2\text{CH}_2\text{O}$ ), 3.56 (td,  $J = 5.4, 3.7\ \text{Hz}$ , 4H,

OCH<sub>2</sub>CH<sub>2</sub>N \*2), 3.27 (t, *J* = 5.6 Hz, 2H, OCH<sub>2</sub>CH<sub>2</sub>N), 2.84 (t, *J* = 5.3 Hz, 2H, OCH<sub>2</sub>CH<sub>2</sub>N), 1.48 (s, 9H, Boc); <sup>13</sup>C NMR (75 MHz, d<sub>2</sub>O) δ 73.6, 71.5, 71.3, 42.3, 41.4, 28.9; MALDI HRMS: *m/z* 271.2365 [M + Na<sup>+</sup>]. Calcd for C<sub>11</sub>H<sub>24</sub>N<sub>2</sub>NaO<sub>4</sub> 271.1634.

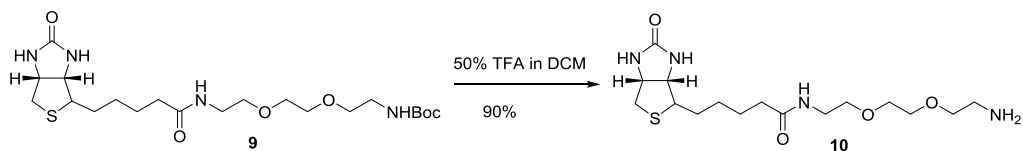
***N*-Boc-*N'*-biotinyl-3,6-dioxaoctane-1,8-diamine (**9**)**



A solution of vitamin H (Biotin) (590 mg, 2.41 mmol), O-benzotriazol-1-yl-N,N,N',N'-tetramethyluronium hexapfluorophosphate (HBTU) (918.2 mg, 2.41 mmol), and DIPEA (0.476 mL, 2.73 mmol) in DMF (20 mL) was stirred for 10 min at room temperature before being adding dropwise to a solution of *N*-Boc-3,6-dioxaoctane-1,8-diamine (**8**, 397 mg, 1.6 mmol) in DMF (10 mL). The reaction mixture was stirred for 2 h at room temperature, after which the DMF was removed in vacuo to give an oily residue ,which was purified by flash silica gel column chromatography (CH<sub>2</sub>Cl<sub>2</sub>/CH<sub>3</sub>OH, 25/1, v/v) to afford **9** (710 mg, 93%) as a white solid.

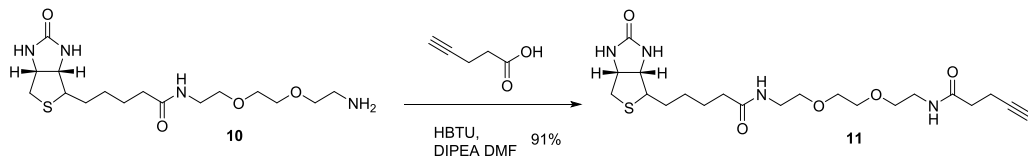
<sup>1</sup>H NMR (300 MHz, d<sub>2</sub>O) δ 4.52 (dd, *J* = 7.7, 4.8 Hz, 1H, CHNH, biotin), 4.33 (dd, *J* = 7.8, 4.5 Hz, 1H, CHNH, biotin), 3.64 (s, 4H, OCH<sub>2</sub>CH<sub>2</sub>O), 3.61 – 3.52 (m, 4H, OCH<sub>2</sub>CH<sub>2</sub>N \*2), 3.39 (d, *J* = 9.1 Hz, 2H, OCH<sub>2</sub>CH<sub>2</sub>N), 3.25 (t, *J* = 5.6 Hz, 3H, OCH<sub>2</sub>CH<sub>2</sub>N + CHS, biotin), 2.96 (dd, *J* = 12.7, 5.0 Hz, 1H, CHHS), 2.73 (d, *J* = 12.7 Hz, 1H, CHHS), 2.25 (t, *J* = 7.3 Hz, 2H, CH<sub>2</sub>CH<sub>2</sub>CH<sub>2</sub>CH<sub>2</sub>C=O, biotin), 1.83 – 1.49 (m, 6H, CH<sub>2</sub>CH<sub>2</sub>CH<sub>2</sub>CH<sub>2</sub>C=O, biotin), 1.47 (s, 9H, Boc); MALDI HRMS: *m/z* 497.3021 [M + Na<sup>+</sup>]. Calcd for C<sub>21</sub>H<sub>38</sub>N<sub>4</sub>NaO<sub>6</sub>S 497.2410.

### ***N*-Biotinyl-3,6-dioxaoctane-1,8-diamine (10)**



*N*-Boc-*N'*-biotinyl-3,6-dioxaoctane-1,8-diamine (**9**, 700 mg, 1.47 mmol) was dissolved in 50% TFA in CH<sub>2</sub>Cl<sub>2</sub> (8 mL) and stirred for 1 h at room temperature. The solvents were evaporated under reduced pressure to give an oily residue, which was purified by flash silica gel column chromatography (CH<sub>2</sub>Cl<sub>2</sub>/CH<sub>3</sub>OH, 10/1, v/v) to afford **10** (497 mg, 90%) as a white solid. <sup>1</sup>H NMR (300 MHz, dmso) δ 7.83 (d, *J* = 5.5 Hz, 3H, NH<sub>2</sub> + NH), 6.38 (d, *J* = 11.3 Hz, 2H, NH \*2, Biotin), 4.29 – 4.33 (m, 1H, CHNH, biotin), 4.10 – 4.15 (m, 1H, CHNH, biotin), 3.58 (dd, *J* = 11.0, 5.8 Hz, 6H, OCH<sub>2</sub>CH<sub>2</sub>O + OCH<sub>2</sub>CH<sub>2</sub>N), 3.40 (t, *J* = 6.0 Hz, 2H, OCH<sub>2</sub>CH<sub>2</sub>N), 3.19 (q, *J* = 5.5 Hz, 2H, OCH<sub>2</sub>CH<sub>2</sub>N), 3.13 – 3.04 (m, 1H, CHS, biotin), 2.97 (s, 2H, OCH<sub>2</sub>CH<sub>2</sub>N), 2.82 (dd, *J* = 12.4, 5.1 Hz, 1H, CHHS), 2.57 (d, *J* = 12.4 Hz, 1H, CHHS), 2.06 (t, *J* = 7.3 Hz, 2H, CH<sub>2</sub>CH<sub>2</sub>CH<sub>2</sub>CH<sub>2</sub>C=O, biotin), 1.71 – 1.15 (m, 6H, CH<sub>2</sub>CH<sub>2</sub>CH<sub>2</sub>CH<sub>2</sub>C=O, biotin); MALDI HRMS: *m/z* 397.1962 [*M* + Na<sup>+</sup>]. Calcd for C<sub>16</sub>H<sub>30</sub>N<sub>4</sub>NaO<sub>4</sub>S 397.1885.

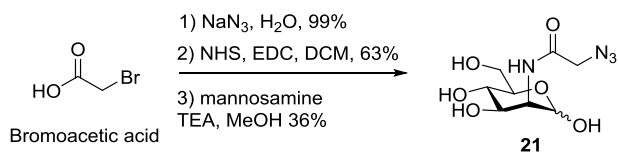
### **4-Pentynamide, *N*-[2-[2-[2-[(1-biotinyl)amino]ethoxy]ethoxy]ethyl]- (11):**



Pentynoic acid (100 mg, 1 mmol), 1-[bis(dimethylamino)methylene]-1*H*-1,2,3-triazolo[4,5-*b*]pyridinium 3-oxid hexafluorophosphate (HATU, 380 mg, 1 mmol) and *N,N*-diisopropylethylamine (DIPEA) (204 μL, 1.17mmol) in DMF (10 mL) was stirred for 10 min at room temperature before being adding dropwise to a solution of

*N*-biotinyl-3,6-dioxaoctane-1,8-diamine (**10**) (255 mg, 0.68 mmol) in DMF (5 mL). The resulting solution was stirred for another 2 hours, after which the DMF was removed under reduced pressure and the residue was purified by silica gel column chromatography using a gradient of methanol in CH<sub>2</sub>Cl<sub>2</sub> (5% → 25%) to give **11** as a white solid (280 mg, 91%). <sup>1</sup>H NMR (300 MHz, D<sub>2</sub>O) δ 4.52 (dd, *J* = 7.8, 4.7 Hz, 1H, *CH*NH, biotin), 4.33 (dd, *J* = 7.8, 4.5 Hz, 1H, *CH*NH biotin), 3.65 (s, 4H, OCH<sub>2</sub>CH<sub>2</sub>O), 3.58 (t, *J* = 5.5 Hz, 4H, NHCH<sub>2</sub>CH<sub>2</sub>O + OCH<sub>2</sub>CH<sub>2</sub>NH), 3.40 (dd, *J* = 5.4, 2.8 Hz, 4H, NHCH<sub>2</sub>CH<sub>2</sub>O + OCH<sub>2</sub>CH<sub>2</sub>NH), 3.30 – 3.18 (m, 2H, CHS, biotin + C≡CH), 2.95 (dd, *J* = 12.8, 5.0 Hz, 1H, CHHS), 2.73 (d, *J* = 12.7 Hz, 1H, CHHS), 2.53 – 2.38 (m, 4H, C=OCH<sub>2</sub>CH<sub>2</sub>C≡C), 2.25 (t, *J* = 7.3 Hz, 2H, CH<sub>2</sub>CH<sub>2</sub>CH<sub>2</sub>CH<sub>2</sub>C=O, biotin), 1.85 – 1.43 (m, 6H, CH<sub>2</sub>CH<sub>2</sub>CH<sub>2</sub>CH<sub>2</sub>C=O, biotin). <sup>13</sup>C NMR (75 MHz, D<sub>2</sub>O) δ 71.5, 71.5, 70.9, 70.8, 63.7, 61.8, 57.3, 49.6, 41.1, 40.9, 40.5, 40.5, 36.8, 36.3, 36.2, 29.9, 27.1, 27.1, 15.8. MALDI-MS: *m/z* calcd for C<sub>21</sub>H<sub>34</sub>N<sub>4</sub>O<sub>5</sub>S [M+H]<sup>+</sup>: 455.2323; found 455.2786.

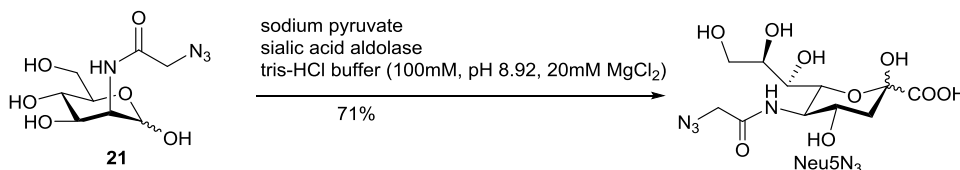
### *N*-azidoacetyl-D-mannosamine (**21**)



Bromoacetic acid (8.34 g, 60 mmol) was added to a solution of sodium azide (7.8 g, 120 mmol) in water (60mL) at 0 °C. The temperature was allowed to increase to room temperature and the reaction mixture was stirred overnight before it was acidified to pH =2 by adding 1 M HCl, and extracted with ethyl ether (300mL \* 3). The combined ether fractions were dried with MgSO<sub>4</sub>, filtered and concentrated under reduced pressure to give 2-azidoacetic acid (6.3 g, 99%) as colorless oil. 2-azidoacetic acid (1.5 g, 14.1 mmol) was dissolved in dry DCM (80 mL),

*N*-(3-Dimethylaminopropyl)-*N'*-ethylcarbodiimide hydrochloride (EDC) (2.98 g, 15.5 mmol) and *N*-Hydroxysuccinimide (NHS) (1.79 g, 15.5 mmol) were added. The reaction mixture was stirred overnight at room temperature, before it was washed with water (100 mL \*2) and brine, and dried over MgSO<sub>4</sub>, filtered and concentrated under reduced pressure to give azidoacetic acid NHS ester (1.76 g, 63%) as a white solid. Mannosamine hydrochloride salt (160 mg, 0.74 mmol) was dissolved in 5 mL of dry MeOH under argon. To this solution was added 0.21 mL of triethylamine. The mixture was stirred for 10 min until the solution turned clear. Azidoacetic acid NHS ester (220 mg, 1.11 mmol) was then added and the resulting solution was stirred at room temperature for overnight until the completion of the reaction. The reaction mixture was then concentrated and the product was purified by flash chromatography (MeOH/CH<sub>2</sub>Cl<sub>2</sub> = 20:1 to 10:1) to give **21** (70 mg, 36%) as a white solid. <sup>1</sup>H NMR (500 MHz, d<sub>2</sub>O) δ 5.06 (d, *J* = 1.5 Hz, 0.5H, H-1), 4.97 (d, *J* = 1.6 Hz, 0.5H, H-1), 4.41 (dd, *J* = 4.5, 1.6 Hz, 0.5H, H-2), 4.29 (dd, *J* = 4.6, 1.6 Hz, 0.5H, H-2), 4.04 – 3.96 (m, 3H), 3.82 – 3.68 (m, 3H), 3.52 (t, *J* = 9.8 Hz, 0.5H), 3.42 (t, *J* = 9.8 Hz, 0.5H). <sup>13</sup>C NMR (126 MHz, d<sub>2</sub>O) δ 92.9, 92.9, 72.0, 68.8, 66.7, 66.5, 60.3, 60.3, 54.3, 53.4, 51.7, 51.1.

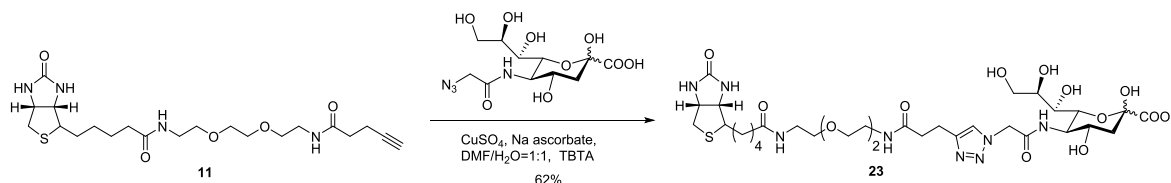
**5-azidoacetamido-3, 5- dideoxy -D-glycero-D-galacto-2-nonulosonic acid (Neu5N<sub>3</sub>):**



To a solution of *N*-azidoacetyl-D-mannosamine (5 mg, 0.019 mmol) and sodium pyruvate (10.5 mg, 0.095 mmol) in tris-HCl buffer (100 mM, pH 8.9, 20 mM MgCl<sub>2</sub>, 1 mL) was added sialic

acid aldolase (0.2U/ $\mu$ L, 5  $\mu$ L). The reaction mixture was incubated at 37 °C, and progress of the reaction was monitored by TLC (EtOH :  $\text{NH}_4\text{HCO}_3$  (1 M), 7:3, v:v), which after 12 hour indicated completion of the reaction. Lyophilization of this mixture provide a residue that was purified by silica gel column chromatography using a gradient of to methanol in  $\text{CH}_2\text{Cl}_2$  (10%  $\rightarrow$ 50%) to give Neu5N<sub>3</sub> as a white amorphous solid (4.7 mg, 71%). <sup>1</sup>H NMR (300 MHz, D<sub>2</sub>O)  $\delta$  4.05 – 3.80 (m, 4H), 3.71 (dd,  $J$  = 11.5, 2.8 Hz, 1H, H-9a), 3.67 – 3.62 (m, 4H), 3.48 (dd,  $J$  = 11.6, 6.2 Hz, 1H, H-9b), 3.39 (d,  $J$  = 8.9 Hz, 1H), 2.10 (dd,  $J$  = 12.9, 4.6 Hz, 1H, H-3eq), 1.78 – 1.63 (m, 1H, H-3ax). <sup>13</sup>C NMR (75 MHz, d<sub>2</sub>o)  $\delta$  69.9, 68.9, 68.3, 67.2, 63.2, 63.1, 61.4, 52.4, 39.5, 38.6. HRMS (ESI):  $m/z$  calcd for C<sub>11</sub>H<sub>18</sub>N<sub>4</sub>O<sub>9</sub> [M-H]<sup>-</sup>: 349.1001; found 349.2042.

**5-[[[2-[4-[2-[2-[2-[2-[(1-biotinyl)amino]ethoxy]ethoxy]ethylamino]oxoethyl]-1H-1,2,3-triazol-1-yl]acetyl]amino]-3, 5-dideoxy-D-glycero-D-galacto-2-nonulosonic acid (23):**

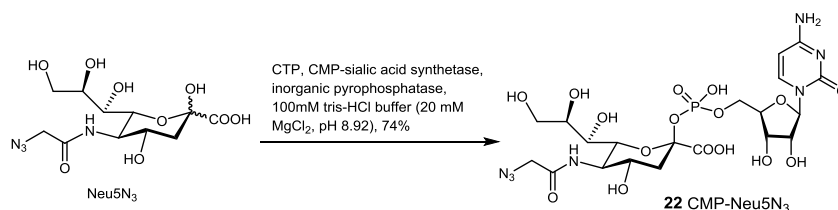


The solution of compound **11** (20 mg, 0.044 mmol) in DMF (1 mL) was added to the solution of Neu5N<sub>3</sub> (12 mg, 0.034 mmol) in H<sub>2</sub>O (pH 7.5, 1 mL). To this mixture was added  $\text{CuSO}_4$  (100 mM, 270  $\mu$ L), sodium L-ascorbate (100 mM, 340  $\mu$ L) and TBTA (3.7 mg, 0.007 mmol). After stirring for 3 hours at ambient temperature, the reaction mixture was centrifuged and the supernatant was collected and concentrated under reduced pressure to give a residue that was purified by silica gel column chromatography using a gradient of methanol in  $\text{CH}_2\text{Cl}_2$  (10%  $\rightarrow$ 50%) to give **8** as a white solid (17 mg, 62%). <sup>1</sup>H NMR (500 MHz, D<sub>2</sub>O)  $\delta$  7.74 (s, 1H, CH=C,



triazole), 5.17 (s, 2H, triazole-CH<sub>2</sub>-CONH), 4.48 (dd, *J* = 7.9, 4.8 Hz, 1H, CHNH, biotin), 4.30 (dd, *J* = 7.8, 4.4 Hz, 1H, CHNH, biotin), 3.96 (d, *J* = 10.6 Hz, 2H), 3.86 (t, *J* = 10.2 Hz, 1H), 3.74–3.64 (m, 2H), 3.52 (dq, *J* = 14.7, 5.3 Hz, 7H, H-9b + OCH<sub>2</sub>CH<sub>2</sub>O+NHCH<sub>2</sub>CH<sub>2</sub>O), 3.46 (t, *J* = 5.4 Hz, 2H, OCH<sub>2</sub>CH<sub>2</sub>NH), 3.26 (dt, *J* = 14.7, 5.2 Hz, 4H, NHCH<sub>2</sub>CH<sub>2</sub>O+ OCH<sub>2</sub>CH<sub>2</sub>NH), 3.20 (dt, *J* = 9.8, 5.3 Hz, 1H, CHS, biotin), 2.92 (t, *J* = 7.3 Hz, 2H, triazole-CH<sub>2</sub>CH<sub>2</sub>C=O), 2.87 (dd, *J* = 13.0, 4.9 Hz, 1H, CHHS), 2.65 (d, *J* = 13.0 Hz, 1H, CHHS), 2.53 (t, *J* = 7.2 Hz, 2H, triazole CH<sub>2</sub>CH<sub>2</sub>C=O), 2.15 (t, *J* = 7.2 Hz, 3H, CH<sub>2</sub>CH<sub>2</sub>CH<sub>2</sub>CH<sub>2</sub>C=O, biotin, H-3eq), 1.70 (q, *J* = 11.5, 10.7 Hz, 1H, H-3ax), 1.64–1.39 (m, 4H, CH<sub>2</sub>CH<sub>2</sub>CH<sub>2</sub>CH<sub>2</sub>C=O, biotin), 1.34–1.23 (m, 2H, CH<sub>2</sub>CH<sub>2</sub>CH<sub>2</sub>CH<sub>2</sub>C=O, biotin). <sup>13</sup>C NMR (126 MHz, D<sub>2</sub>O) δ 124.8, 70.5, 70.0, 69.4, 68.9, 68.9, 63.2, 63.0, 62.1, 60.2, 55.3, 52.6, 51.9, 39.7, 39.7, 39.3, 38.9, 38.8, 35.4, 35.0, 27.8, 27.7, 27.6, 25.0, 21.0. HRMS (ESI): *m/z*: calcd for C<sub>32</sub>H<sub>52</sub>N<sub>8</sub>O<sub>14</sub>S [M-H]<sup>+</sup>: 803.3251; found: 803.3567.

**Cytidine-5'-monophospho-5-azidoacetamido-3, 5- dideoxy-β-D-glycero-D-galacto-2-nonulopyranosonic acid (22).**



CMP-sialic acid synthetase (0.1U/μL, 10μL) and inorganic pyrophosphatase (0.2U/μL, 5μL) were added to a mixture of Neu5N<sub>3</sub> (10.5 mg, 0.03mmol) in tris-HCl buffer (100mM, pH 8.92, 20mM MgCl<sub>2</sub>, 2 mL), containing CTP (33 mg, 0.063mmol). The tube was incubated at 37 °C, and progress of the reaction was monitored by TLC (i-PrOH : 20mM NH<sub>4</sub>Cl = 4:1, v:v), which after 4 hour indicated completion of the reaction. EtOH (14 mL) was added, and the mixture

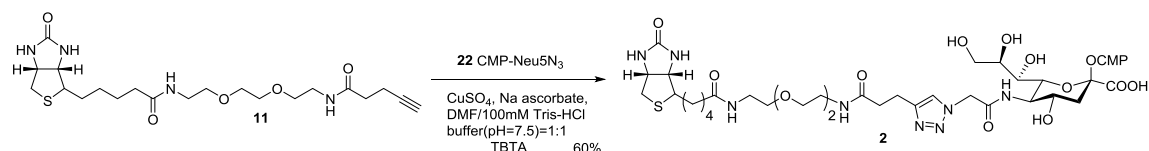
was kept on ice for 2 hours prior to centrifugation and the supernatant was decanted and the pellet (mostly inorganic salts) was re-suspended in EtOH (8mL), cooled on ice for 1 h and centrifuged. The combined ethanol extracts were concentrated under reduced pressure. The residue was redissolved in 1.5 mL distilled water followed by lyophilization to provide a crude material, which was applied on a Biogel fine P-2 column (75\*1.5 cm, eluted with 0.1 M  $\text{NH}_4\text{HCO}_3$  at 4 °C in dark.). The product was detected by TLC, and appropriate fractions were combined and lyophilized to provide **22** as a white solid (14.5 mg, 74%).

**One-pot two-enzyme system approach for synthesis of compound 22.**<sup>27</sup> Sialic acid aldolase (0.2U/ $\mu\text{L}$ , 5  $\mu\text{L}$ ), and CMP-sialic acid synthetase (0.2U/ $\mu\text{L}$ , 5  $\mu\text{L}$ ) were added to a mixture of *N*-azidoacetyl-D-mannosamine (**21**, 5 mg, 0.019 mmol) in tris-HCl buffer (100mM, pH 8.9, 20mM  $\text{MgCl}_2$ , 1.9 mL), containing sodium pyruvate (10.5 mg, 0.095 mmol) and CTP (10 mg, 0.019 mmol). The tube was incubated at 37 °C, and progress of the reaction was monitored by TLC (EtOH : aq.  $\text{NH}_4\text{HCO}_3$  (1 M) 7:3, v:v), which after 5 hour indicated completion of the reaction. EtOH (3 mL) was added, and the precipitate was removed by centrifugation and the supernatant was concentrated under reduced pressure. The residue was redissolved in distilled water (500  $\mu\text{L}$ ) followed by lyophilization to provide a crude material that was applied to a Biogel fine P-2 column (50\* 1 cm, eluted with 0.1 M  $\text{NH}_4\text{HCO}_3$  at 4 °C in dark.). The product was detected by TLC, and appropriate fractions were combined and lyophilized to provide **22** as an amorphous white solid (10.1 mg, 81%).  $^1\text{H}$  NMR (500 MHz,  $\text{d}_2\text{o}$ )  $\delta$  7.86 (d,  $J$  = 7.6 Hz, 1H, H-6, cyt), 6.02 (d,  $J$  = 7.5 Hz, 1H, H-5, cyt), 5.88 (d,  $J$  = 4.5 Hz, 1H, H-1, rib), 4.27 – 4.19 (m, 2H, H-2 + H-3, rib), 4.12 (dd,  $J$  = 9.1, 7.6 Hz, 4H), 4.08 – 3.97 (m, 3H, H-4 +  $\text{N}_3\text{CH}_2\text{CO}$ ), 3.92 (t,

$J = 10.3$  Hz, 1H), 3.83 (ddd,  $J = 9.4, 6.5, 2.6$  Hz, 1H), 3.78 (dd,  $J = 11.8, 2.5$  Hz, 1H), 3.52 (dd,  $J = 11.9, 6.6$  Hz, 1H), 3.34 (dd,  $J = 9.6, 1.2$  Hz, 1H), 2.40 (dd,  $J = 13.2, 4.8$  Hz, 1H, H-3eq), 1.55 (ddd,  $J = 13.3, 11.3, 5.8$  Hz, 1H, H-3ax). HRMS (ESI):  $m/z$  calcd for  $C_{20}H_{30}N_7O_{16}P$  [M-H]<sup>-</sup>: 654.1414; found: 654.2023.

**Cytidine-5'-monophospho-5-[[2-[4-[2-[2-[2-[(1-biotinyl)amino]ethoxy]ethoxy]ethylamino]oxoethyl]-1H-1,2,3-triazol-1-yl]acetyl]amino]-3,**

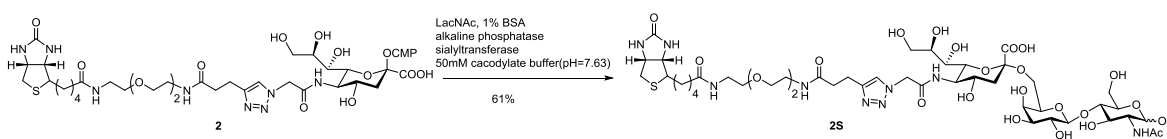
**5-dideoxy-D-glycero-D-galacto-2-nonulopyranosonic acid (2):**



A solution of compound **11** (9 mg, 0.02 mmol) in DMF (1 mL) was added to the solution of CMP-Neu5N<sub>3</sub> (**22**, 10 mg, 0.015 mmol) in Tris-HCl buffer (100 mM, pH 7.5, 1 mL). To this mixture was added CuSO<sub>4</sub> (100 mM, 120 μL), sodium L-ascorbate (100 mM, 150 μL) and TBTA (2.4 mg, 0.0045 mmol). After stirring for 3 hours at ambient temperature, the reaction mixture was lyophilized to provide a residue that was applied to a Biogel fine P-2 column (75\*1.5 cm) and eluted with 0.1 M NH<sub>4</sub>HCO<sub>3</sub> at 4 °C in dark. The product was detected by TLC (i-PrOH : aq. NH<sub>4</sub>Cl (20 M) 4 : 1, v:v), and appropriate fractions were combined and lyophilized to provide **2** as a white solid (9.9 mg, 60%). <sup>1</sup>H NMR (500 MHz, D<sub>2</sub>O) δ 7.86 (d,  $J = 7.6$  Hz, 1H, H-6, cyt), 7.73 (s, 1H, CH=C, triazole), 6.01 (d,  $J = 7.6$  Hz, 1H, H-5, cyt), 5.88 (d,  $J = 4.5$  Hz, 1H, H-1, rib), 5.17 (d,  $J = 2.7$  Hz, 2H, triazole-CH<sub>2</sub>-C=O), 4.48 (dd,  $J = 8.0, 4.9$  Hz, 1H, CHNH, biotin), 4.30 (dd,  $J = 8.0, 4.5$  Hz, 1H, CHNH, biotin), 4.23 (t,  $J = 4.9$  Hz, 1H, H-3, rib), 4.19 (t,  $J = 4.8$  Hz, 1H, H-2, rib), 4.15 – 4.07 (m, 4H, H-4 rib, H-5 rib, H-6 Neu), 4.06 – 3.98 (m, 1H, H-4), 3.90 (t,  $J =$

10.3 Hz, 1H, H-5), 3.83 (ddd,  $J = 9.3, 6.4, 2.5$  Hz, 1H, H-8), 3.77 (dd,  $J = 11.8, 2.5$  Hz, 1H, H-9a), 3.59 – 3.49 (m, 7H, H-9b +  $\text{OCH}_2\text{CH}_2\text{O} + \text{NHCH}_2\text{CH}_2\text{O}$ ), 3.45 (t,  $J = 5.4$  Hz, 2H,  $\text{OCH}_2\text{CH}_2\text{NH}$ ), 3.35 (dd,  $J = 9.6, 1.1$  Hz, 1H, H-7), 3.30 – 3.22 (m, 4H,  $\text{NHCH}_2\text{CH}_2\text{O} + \text{OCH}_2\text{CH}_2\text{NH}$ ), 3.22 – 3.17 (m, 1H, CHS, biotin), 2.92 (t,  $J = 7.3$  Hz, 2H, triazole- $\text{CH}_2\text{CH}_2\text{C}=\text{O}$ ), 2.87 (dd,  $J = 13.1, 5.0$  Hz, 1H, CHHS), 2.66 (d,  $J = 13.0$  Hz, 1H, CHHS), 2.52 (t,  $J = 7.4$  Hz, 2H, triazole- $\text{CH}_2\text{CH}_2\text{C}=\text{O}$ ), 2.39 (dd,  $J = 13.3, 4.8$  Hz, 1H, H-3eq), 2.15 (t,  $J = 7.3$  Hz, 2H,  $\text{CH}_2\text{CH}_2\text{CH}_2\text{CH}_2\text{C}=\text{O}$ , biotin), 1.66 – 1.39 (m, 5H, H-3ax +  $\text{CH}_2\text{CH}_2\text{CH}_2\text{CH}_2\text{C}=\text{O}$ , biotin), 1.34 – 1.23 (m, 2H,  $\text{CH}_2\text{CH}_2\text{CH}_2\text{CH}_2\text{C}=\text{O}$ , biotin).  $^{13}\text{C}$  NMR (126 MHz,  $\text{D}_2\text{O}$ )  $\delta$  141.7, 124.7, 96.6, 89.1, 82.9, 74.3, 71.6, 69.6, 69.5, 69.4, 68.9, 68.9, 68.8, 66.8, 64.9, 62.9, 62.9, 62.1, 60.2, 55.3, 52.2, 52.0, 41.1, 41.1, 39.7, 39.7, 38.9, 38.9, 35.5, 35.1, 27.8, 27.7, 27.7, 25.1, 21.0. HRMS (ESI):  $m/z$  calcd for  $\text{C}_{41}\text{H}_{63}\text{N}_{11}\text{O}_{21}\text{PS}$   $[\text{M}-\text{H}]^-$ : 1108.3664; found  $m/z$ : 1108.2461.

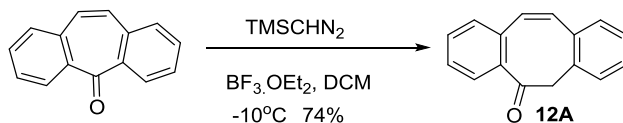
#### Biotinyl Neu5Ac $\alpha$ (2,6)Gal $\beta$ (1,4)GlcNAc (2S):



Recombinant  $\alpha$ -(2,6)-sialyltransferase (ST6Gal I) [GenBank P13721] (0.63 mg/mL, 23.2  $\mu\text{L}$ )<sup>16</sup> and calf intestine alkaline phosphatase (10000 U/mL, 2.5  $\mu\text{L}$ ) were added to a mixture of LacNAc (0.43 mg, 1.13  $\mu\text{mol}$ ) in cacodylate buffer (50 mM, pH 7.63, 96  $\mu\text{L}$ ) containing 0.1% BSA and **2** (2.5 mg, 2.26  $\mu\text{mol}$ ) in an Eppendorf tube. The tube was incubated at 37 °C, and progress of the reaction was monitored by TLC ( $\text{EtOAc} : \text{CH}_3\text{OH} : \text{H}_2\text{O} : \text{AcOH} = 4:2:1:0.5$ , v:v:v:v), which after 5 hour indicated completion of the reaction.  $\text{CH}_3\text{OH}$  (0.5  $\mu\text{L}$ ) was added and the mixture was lyophilization to provide a residue that was applied to a Biogel fine P-2

column (50\* 1 cm), which was eluted with H<sub>2</sub>O at room temperature. The product was detected by TLC and appropriate fractions were combined and lyophilized to provide **2S** as a white solid (0.8 mg, 61%). <sup>1</sup>H NMR (600 MHz, d<sub>2</sub>O) δ 7.69 (s, 1H, CH=C, triazole), 5.19 – 5.06 (m, 2H, H-1', H-1''), 4.61 – 4.57 (m, 1H, H5), 4.45 (ddd, *J* = 8.0, 5.0, 0.9 Hz, 1H, CHNH, biotin), 4.30 (dd, *J* = 7.9, 2.3 Hz, 1H), 4.27 (dd, *J* = 7.9, 4.5 Hz, 1H, CHNH, biotin), 3.87 – 3.79 (m, 2H), 3.79 – 3.70 (m, 5H), 3.70 – 3.64 (m, 2H), 3.56 (m, 3H), 3.54 – 3.45 (m, 10H), 3.44 – 3.35 (m, 5H), 3.24 (dd, *J* = 6.2, 4.7 Hz, 2H, NHCH<sub>2</sub>CH<sub>2</sub>O), 3.21 (t, *J* = 5.2 Hz, 2H, OCH<sub>2</sub>CH<sub>2</sub>NH), 3.17 (dt, *J* = 9.7, 5.2 Hz, 1H, CHS, biotin), 2.92 – 2.87 (m, 2H, triazole-CH<sub>2</sub>CH<sub>2</sub>C=O), 2.83 (dd, *J* = 13.1, 5.1 Hz, 1H, CHHS), 2.62 (d, *J* = 13.3 Hz, 1H, CHHS), 2.53 (dd, *J* = 12.4, 4.7 Hz, 1H, H-3eq), 2.49 (td, *J* = 7.3, 1.9 Hz, 2H, triazole-CH<sub>2</sub>CH<sub>2</sub>C=O), 2.11 (t, *J* = 7.3 Hz, 2H, CH<sub>2</sub>CH<sub>2</sub>CH<sub>2</sub>CH<sub>2</sub>C=O, biotin), 1.87 (s, 3H, Ac), 1.62–1.37 (m, 5H, H-3ax, CH<sub>2</sub>CH<sub>2</sub>CH<sub>2</sub>CH<sub>2</sub>C=O, biotin), 1.25 (dd, *J* = 8.6, 7.8 Hz, 2H, CH<sub>2</sub>CH<sub>2</sub>CH<sub>2</sub>CH<sub>2</sub>C=O, biotin). <sup>13</sup>C NMR (151 MHz, D<sub>2</sub>O) δ 124.6, 103.4, 80.7, 73.6, 72.5, 72.4, 72.2, 71.6, 70.7, 69.8, 69.5, 69.3, 69.3, 68.8, 68.8, 68.3, 68.3, 68.2, 68.0, 67.3, 66.8, 63.4, 63.4, 62.8, 62.0, 61.2, 60.0, 55.2, 53.4, 52.0, 51.9, 40.0, 39.5, 39.5, 38.8, 38.8, 35.3, 35.0, 27.8, 27.7, 27.6, 25.2, 22.0, 21.0. HRMS (ESI): *m/z* calcd for C<sub>46</sub>H<sub>74</sub>N<sub>9</sub>O<sub>24</sub>S [M-H]<sup>-</sup>: 1168.4573; found: 1168.3288.

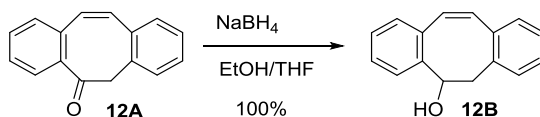
#### 6*H*-Dibenzo[*a,e*]cyclooctatrien-5-one (**12A**)



A solution of trimethylsilyl diazomethane (11 mL, 21.9 mmol) in CH<sub>2</sub>Cl<sub>2</sub> (20 mL) was added dropwise to a stirred solution of dibenzosuberone (2.88 g, 14.0 mmol) and BF<sub>3</sub>·OEt<sub>2</sub> (2.59 mL,

21.0 mmol) in CH<sub>2</sub>Cl<sub>2</sub> (30 mL) at -10°C over a period of 1 h in dark. The reaction mixture was stirred at -10°C for 2 h, and then poured into ice water. The aqueous layer was extracted with CH<sub>2</sub>Cl<sub>2</sub> (3\*100 mL) and the combined organic layers washed with brine, dried (MgSO<sub>4</sub>), filtered and the filtrate was concentrated under reduced pressure. The crude product was purified by flash chromatography over silica gel (2:1→1:2, v/v, hexanes/CH<sub>2</sub>Cl<sub>2</sub>) to give compound **12A** (2.28 g, 74 %) as an amorphous solid. <sup>1</sup>H NMR (500 MHz, cdcl<sub>3</sub>) δ 8.26 (dd, *J* = 8.0, 1.5 Hz, 1H, PhH), 7.50 (ddd, *J* = 7.8, 7.1, 1.5 Hz, 1H, PhH), 7.46 – 7.41 (m, 1H, PhH), 7.37 (dd, *J* = 7.8, 1.4 Hz, 1H, PhH), 7.30 (dtd, *J* = 7.6, 6.7, 6.3, 1.7 Hz, 2H, PhH), 7.27 – 7.19 (m, 2H, PhH), 7.10 – 7.00 (m, 2H, CH=CH), 4.06 (s, 2H, CH<sub>2</sub>).

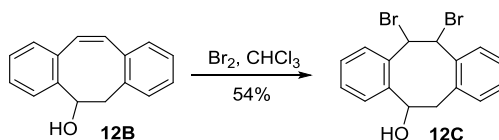
#### 5,6-Dihydro-dibenzo[a,e]cycloocten-5-ol (**12B**)



Sodium borohydride (946 mg, 25 mmol) was slowly added to a stirred solution of **12A** (2.25 g, 10 mmol) in a mixture of EtOH and THF (1:1, v/v, 120 mL). The reaction mixture was stirred for 7 h, after which TLC analysis indicated completion of the reaction. The reaction was quenched by slow addition of acetic acid (1 mL) and the solvents were evaporated. The residue was dissolved in DCM (100 mL) and the resulting solution was washed with brine (100 mL), which was back extracted with DCM (4\*100 mL). The combined organic phases were dried (MgSO<sub>4</sub>), filtered and concentrated under reduced pressure to give **12B** as a white solid (2.22 g, 100%), which was directly used in the next step without further purification. <sup>1</sup>H NMR (300 MHz, cdcl<sub>3</sub>) δ 7.51 – 7.42 (m, 1H, PhH), 7.28 – 7.06 (m, 7H, PhH), 6.92 – 6.78 (m, 2H, CH=CH), 5.29

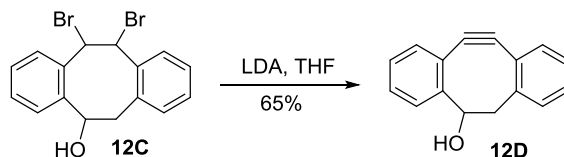
(dd,  $J = 10.0, 6.3$  Hz, 1H, CHO), 3.46 (dd,  $J = 13.8, 6.2$  Hz, 1H, CHH), 3.33 (dd,  $J = 13.7, 10.0$  Hz, 1H, CHH).

### 11,12-Dibromo-5,6,11,12-tetrahydro-dibenzo[a,e]cycloocten-5-ol (**12C**)



Bromine (0.28 mL, 5.4 mmol) was added dropwise to a stirred solution of **12B** (1.2 g, 5.4 mmol) in  $\text{CHCl}_3$  (25 mL). After stirring the mixture for 0.5 h in dark, TLC analysis indicated completion of the reaction. The reaction mixture was washed with sat. aq  $\text{Na}_2\text{S}_2\text{O}_5$ , brine, dried ( $\text{MgSO}_4$ ), filtered and the filtrate was concentrated under reduced pressure and the residue was purified by flash chromatography over silica gel (10:1→2:1, v/v, hexanes/DCM) to give **12C** as a light-yellow oil (1.22 g, 54%).  $^1\text{H}$  NMR (300 MHz,  $\text{cdCl}_3$ )  $\delta$  7.68 (d,  $J = 7.8$  Hz, 1H, PhH), 7.44 – 7.33 (m, 1H, PhH), 7.24 – 6.83 (m, 6H, PhH), 5.82 (d,  $J = 2.2$  Hz, 1H, CHBr), 5.76 (dd,  $J = 2.3, 1.1$  Hz, 1H, CHBr), 5.46 (dd,  $J = 3.8, 2.5$  Hz, 1H, CHO), 3.75 (ddd,  $J = 16.4, 2.5, 1.2$  Hz, 1H, CHH), 3.09 (dd,  $J = 16.1, 3.7$  Hz, 1H, CHH).  $^{13}\text{C}$  NMR (75 MHz,  $\text{cdCl}_3$ )  $\delta$  132.7, 132.3, 128.2, 127.3, 126.7, 126.6, 122.4, 120.3, 85.6, 80.3, 60.5, 46.8.

### 5,6-Dihydro-11,12-didehydro-dibenzo[a,e]cycloocten-5-ol (**12D**)

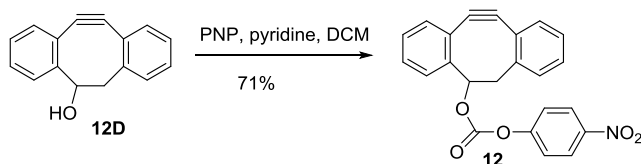


Lithium diisopropylamide in tetrahydrofuran (2 M; 6.4 mL, 12.8 mmol) was added dropwise to a stirred solution of **12C** (1.22 g, 3.2 mmol) in tetrahydrofuran (32 mL) under an atmosphere of argon. The reaction mixture was stirred for 0.5 h, after which it was quenched by the dropwise

addition of water (0.5 mL). The solvents were evaporated under reduced pressure, and the residue was purified by flash chromatography on silica gel (hexanes/DCM 5:1→2:3, v/v) to give **12D** as a white amorphous solid (0.45 g, 65%). <sup>1</sup>H NMR (300 MHz, cdcl<sub>3</sub>) δ 7.68 (d, *J* = 7.7 Hz, 1H, PhH), 7.42 – 7.17 (m, 7H, PhH), 4.61 – 4.50 (m, 1H, CHO), 3.04 (dd, *J* = 14.7, 2.2 Hz, 1H, CHH), 2.87 (dd, *J* = 14.7, 3.7 Hz, 1H, CHH), 2.13 (d, *J* = 4.5 Hz, 1H, OH). <sup>13</sup>C NMR (75 MHz, D<sub>2</sub>O) δ 126.9, 125.3, 124.2, 124.1, 123.9, 123.4, 121.5, 121.0, 72.5, 45.9.

**Carbonic acid, 5,6-dihydro-11,12-didehydro-dibenzo[a,e]cycloocten-5-yl ester,**

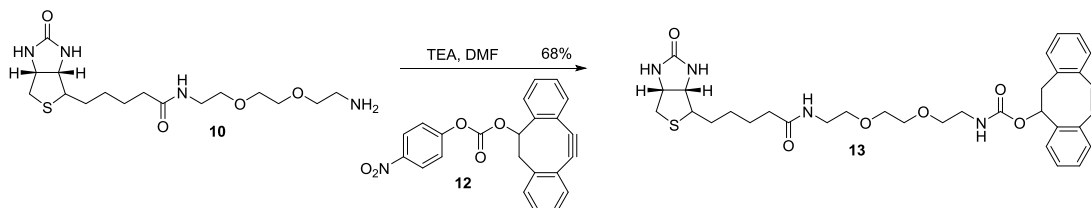
**4-nitrophenyl ester (**12**)**



4-Nitrophenyl chloroformate (275 mg, 1.36 mmol) and pyridine (0.27 mL, 3.4 mmol) were added to a solution of **12D** (145 mg, 0.68 mmol) in DCM (20 mL). After being stirred for 3 h at room temperature, the mixture was washed with brine (2\*10 mL) and the organic layer was dried (MgSO<sub>4</sub>). The solvents were evaporated under reduced pressure, and the residue was purified by silica gel column chromatography (hexane/ethyl acetate, 15:1, v/v) to afford **12** (186 mg, 71%) as a white solid. <sup>1</sup>H NMR (300 MHz, cdcl<sub>3</sub>) δ 8.28 (d, *J* = 9.1 Hz, 2H, PhH), 7.67 – 7.58 (m, 1H, PhH), 7.48 – 7.29 (m, 9H, PhH), 5.64 – 5.54 (m, 1H, CHO), 3.34 (dd, *J* = 15.4, 2.2 Hz, 1H, CHH), 3.13 – 2.97 (m, 1H, CHH). <sup>13</sup>C NMR (75 MHz, cdcl<sub>3</sub>) δ 129.9, 128.0, 127.9, 127.3, 127.0, 127.0, 125.3, 123.4, 121.6, 81.6, 45.7.

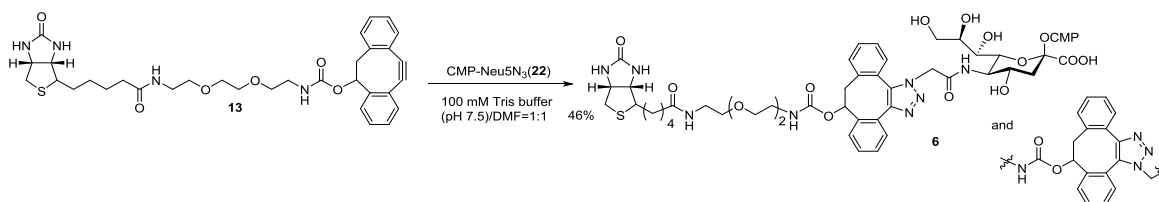


**Carbonyl acid 7,8-didehydro-1,2:5,6-dibenzocyclooctene-3-yl ester, 8'-biotinyamine-3',6'-dioxaoctane 1'-amide (13)**



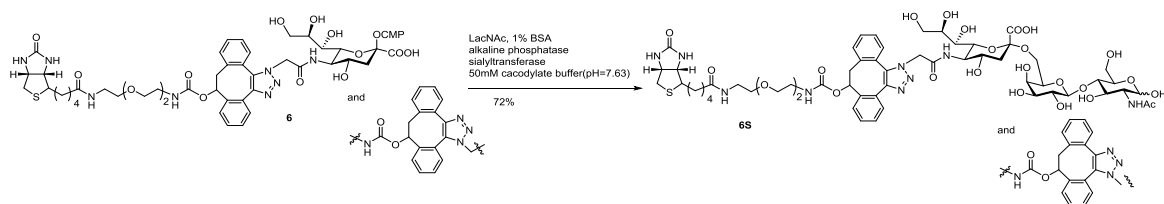
To a solution of **10** (112.4 mg, 0.3 mmol) and  $\text{NEt}_3$  (125.5  $\mu\text{L}$ , 0.9 mmol) in DMF (20 mL) was added **12** (115.6 mg, 0.3 mmol) under an atmosphere of Argon. After stirring the reaction mixture overnight at ambient temperature, the solvent was removed under reduced pressure and the residue was purified by silica gel column chromatography ( $\text{CH}_2\text{Cl}_2/\text{CH}_3\text{OH}$ , 20/1  $\rightarrow$  15/1, v/v) to afford **13** (127 mg, 68%) as a white solid.  $^1\text{H}$  NMR (300 MHz,  $\text{d}_2\text{O}$ )  $\delta$  7.59 (d,  $J = 7.6$  Hz, 1H, PhH), 7.46 – 7.26 (m, 7H, PhH), 5.45 (1H, m, CHOH DIBO), 4.53 – 4.41 (m, 1H, CHNH biotin), 4.30 – 4.19 (m, 1H, CHNH biotin), 3.65 (s, 4H,  $\text{OCH}_2\text{CH}_2\text{O}$ ), 3.61 – 3.51 (m, 4H,  $\text{OCH}_2\text{CH}_2\text{N}$  \*2), 3.37 (m, 4H,  $\text{OCH}_2\text{CH}_2\text{NH}$  \*2), 3.18-3.23 (m, 2H, CHS biotin, CHH DIBO), 2.97 – 2.80 (m, 2H, CHH DIBO, CHHS Biotin), 2.69 (d,  $J = 12.6$  Hz, 1H, CHHS Biotin), 2.20 (t,  $J = 7.2$  Hz, 2H,  $\text{CH}_2\text{CH}_2\text{CH}_2\text{CH}_2\text{C}=\text{O}$  biotin), 1.82 – 1.53 (m, 4H,  $\text{CH}_2$ \*2, biotin), 1.42 (q,  $J = 7.2$  Hz, 2H,  $\text{CH}_2$  biotin). MALDI HRMS:  $m/z$  643.2575 [ $\text{M} + \text{Na}^+$ ]. Calcd for  $\text{C}_{33}\text{H}_{40}\text{N}_4\text{NaO}_6\text{S}$  643.2566.

**Biotin-DIBO-CMP-Neu5N<sub>3</sub> (6)**



The solution of **13** (5.7 mg, 0.0092 mmol)<sup>26</sup> in DMF (300  $\mu$ L) was added to the solution of CMP-Neu5N<sub>3</sub> (**22**, 4.0 mg, 0.006 mmol) in 100 mM Tris-HCl buffer (pH 7.5, 300  $\mu$ L). After stirring for 3 hours at ambient temperature, the reaction mixture was lyophilized to provide a crude material, which was applied on a Biogel fine P-2 column (50\*1.5 cm) and eluted with 0.1 M NH<sub>4</sub>HCO<sub>3</sub> at 4 °C in dark. The product was detected by TLC (EtOH: 1 M NH<sub>4</sub>HCO<sub>3</sub>, 7:3, v:v), and appropriate fractions were combined and lyophilized to provide **6** (3.5 mg, 46%) as a white solid. <sup>1</sup>H NMR (500 MHz, d<sub>2</sub>O)  $\delta$  7.99 – 7.90 (m, 1H, H-6, cyt), 7.61 – 7.11 (m, 8H, PhH), 6.12 – 6.02 (m, 1H, H-5, cyt), 5.86 (t, *J* = 4.1 Hz, 1H, H-1, rib), 5.40 – 5.21 (m, 1H, CHO, DIBO), 4.33 (m, 0.4H), 4.28 – 4.18 (m, 2H), 4.18 – 4.06 (m, 4H), 4.06 – 3.89 (m, 3H), 3.89 – 3.70 (m, 1H), 3.71 – 3.64 (m, 4H), 3.62 (m, 1H), 3.61 – 3.42 (m, 6H), 3.42 – 3.31 (m, 1H), 3.26 (d, *J* = 28.6 Hz, 4H), 2.96 (d, *J* = 13.3 Hz, 1H), 2.91 – 2.80 (m, 1H), 2.80 – 2.62 (m, 1H), 2.54 (dd, *J* = 28.5, 12.5 Hz, 1H), 2.46 – 2.29 (m, 1H, H-3eq), 2.20 – 1.88 (m, 2H, CH<sub>2</sub>CH<sub>2</sub>CH<sub>2</sub>CH<sub>2</sub>C=O, biotin), 1.59 – 0.97 (m, 7H, H-3ax + CH<sub>2</sub>CH<sub>2</sub>CH<sub>2</sub>CH<sub>2</sub>C=O, biotin). <sup>13</sup>C NMR (126 MHz, d<sub>2</sub>O)  $\delta$  142.8, 132.4, 130.9, 130.0, 129.0, 128.2, 127.7, 96.0, 89.2, 83.1, 74.3, 69.5, 69.5, 69.4, 69.4, 69.3, 69.2, 69.0, 68.9, 68.6, 66.5, 64.7, 63.3, 62.9, 62.7, 61.0, 60.6, 60.2, 59.6, 59.5, 59.3, 50.5, 50.3, 41.3, 41.2, 41.1, 39.9, 39.7, 39.6, 39.5, 39.4, 39.1, 36.5, 35.5, 35.1, 27.7, 27.5, 27.4, 25.1, 25.0, 25.0, 24.9. HRMS (ESI): calcd for C<sub>53</sub>H<sub>69</sub>N<sub>11</sub>O<sub>22</sub>PS [M-H]<sup>-</sup>: m/z: 1274.4082; found m/z: 1274.2560.

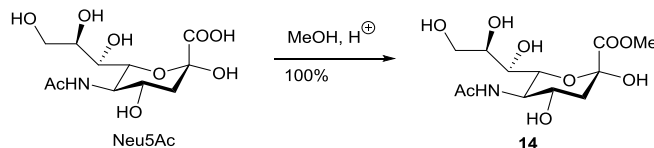
### Biotinyl (DIBO) Neu5N<sub>3</sub> $\alpha$ (2,6)Gal $\beta$ (1,4)GlcNAc (**6S**)



Recombinant  $\alpha$ -(2, 6)-sialyltransferase (ST6Gal I) from HEK 293 expression [GenBank P13721] (0.63 mg/mL, 23.2  $\mu$ L) and calf intestine alkaline phosphatase (10000 U/mL, 2.5  $\mu$ L) were added to a mixture of LacNAc (0.33 mg, 0.86  $\mu$ mol) in cacodylate buffer (50 mM, pH 7.63, 96  $\mu$ L) containing 0.1% BSA and **6** (2.2 mg, 1.7  $\mu$ mol) in an Eppendorf tube. The tube was incubated at 37 °C, and progress of the reaction was monitored by TLC (EtOAc : CH<sub>3</sub>OH : H<sub>2</sub>O : AcOH = 4:2:1:0.5, v:v:v:v), which after 5 hour indicated completion of the reaction. CH<sub>3</sub>OH (0.5  $\mu$ L) was added and followed by lyophilization to provide a crude material, which was applied on a Biogel fine P-2 column (50\* 1 cm, using H<sub>2</sub>O as eluent) at room temperature. The product was detected by TLC, and appropriate fractions were combined and lyophilized to provide **6S** (0.8 mg, 72%) as a white solid. <sup>1</sup>H NMR (500 MHz, d<sub>2</sub>o)  $\delta$  7.64 – 7.10 (m, 8H, PhH), 6.15 – 5.70 (m, 1H, CHO, DIBO), 5.41 – 5.11 (m, 1H, H1), 5.11 – 5.00 (m, 1H, H1), 4.33 (dt,  $J$  = 7.8, 4.4 Hz, 1H), 4.23 (dd,  $J$  = 7.9, 4.5 Hz, 1H), 4.02 – 3.67 (m, 10H), 3.64 – 3.36 (m, 15H), 3.24 (q,  $J$  = 17.4, 13.2 Hz, 4H), 3.11 – 2.91 (m, 1H), 2.91 – 2.63 (m, 1H), 2.63 – 2.45 (m, 2H), 2.20 – 2.01 (m, 2H), 1.86 (s, 5H), 1.66 – 0.91 (m, 6H). <sup>13</sup>C NMR (151 MHz, d<sub>2</sub>o)  $\delta$  133.2, 132.3, 131.6, 131.3, 131.1, 129.7, 129.5, 128.9, 127.7, 126.9, 103.4, 91.5, 80.9, 77.9, 74.4, 73.6, 72.3, 72.1, 72.0, 71.9, 70.6, 70.4, 70.3, 69.9, 69.4, 69.2, 68.4, 68.3, 68.1, 68.0, 67.1, 63.4, 63.3, 61.6, 60.3, 60.3, 60.1, 60.0, 55.9, 55.0, 55.0, 53.4, 52.1, 50.5, 39.9, 39.9, 39.8, 39.7, 39.4, 39.4, 38.9, 38.9, 35.3, 35.3, 35.3, 27.7, 27.6, 27.5, 25.0, 24.9, 16.6. HRMS (ESI): calcd for C<sub>58</sub>H<sub>80</sub>N<sub>9</sub>O<sub>25</sub>S [M-H]<sup>-</sup>: m/z: 1334.4992; found m/z: 1334.3517.

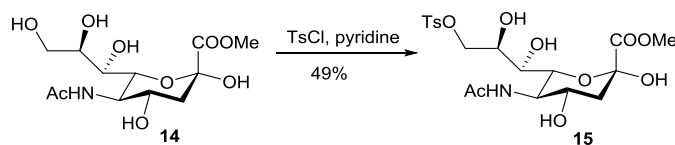
## Biotinylation at C9 position of CMP-sialic acid

### **5-Acetamido-3,5-di-deoxy-D-glycero-D-galacto-2-nonulosonic acid (**14**):**



To a suspension of Neu5Ac (5 g, 16.2 mmol) in dry methanol (250 mL) was added Dowex 50W  $\times$  8-200 (2.5 g). The mixture was stirred at RT for 18 h. The resin was removed by filtration and the filtrate was concentrated under reduced pressure to give **14** as a white amorphous solid (5.2 g, 100%).  $^1\text{H}$  NMR (300 MHz,  $\text{d}_2\text{O}$ )  $\delta$  4.04 (dd,  $J$  = 10.6, 4.8 Hz, 2H, H-4, H-6), 3.91 – 3.78 (m, 5H, H-5, H-9a,  $\text{OCH}_3$ ), 3.77 – 3.71 (m, 1H, H-8), 3.66 (dd,  $J$  = 11.0, 5.6 Hz, 1H, H-9b), 3.52 (d,  $J$  = 9.0 Hz, 1H, H-7), 2.26 (dd,  $J$  = 12.9, 4.9 Hz, 1H, H-3eq), 2.05 (s, 3H, Ac), 1.99 – 1.87 (m, 1H, H-3ax).  $^{13}\text{C}$  NMR (75 MHz,  $\text{d}_2\text{O}$ )  $\delta$  72.3, 71.8, 70.4, 68.1, 65.0, 54.5, 53.4, 40.8, 22.8.

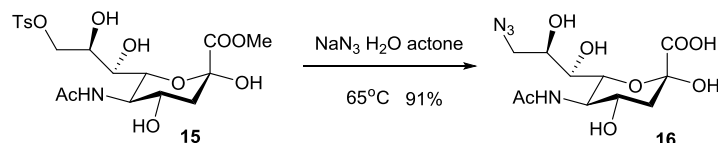
### **5-Acetamido-9-tosyl-3,5,9-tri-deoxy-D-glycero-D-galacto-2-nonulosonic acid (**15**):**



**14** (1 g, 3.09 mmol) in pyridine (25 mL) was cooled to 0 °C and *p*-toluenesulfonyl chloride (824.7 mg, 4.33 mmol) was added. The mixture was allowed to warm to RT and stirred overnight. The reaction was quenched by adding 15 mL MeOH. After removal of solvent under reduced pressure, the residue was purified by flash chromatography ( $\text{EtOAc}:\text{MeOH}$ , 20:1  $\rightarrow$  5:1, v/v) to afford **15** as a white amorphous solid (723 mg, 49%).  $^1\text{H}$  NMR (300 MHz,  $\text{d}_2\text{O}$ )  $\delta$  7.81 (d,  $J$  = 8.1 Hz, 2H, PhH), 7.47 (d,  $J$  = 8.0 Hz, 2H, PhH), 4.31 (dd,  $J$  = 10.1, 2.3 Hz, 1H), 4.12 – 4.00 (m, 2H), 3.96 (d,  $J$  = 10.5 Hz, 1H), 3.92 – 3.84 (m, 1H), 3.79 (s, 4H), 3.50 – 3.42 (m, 1H), 2.48 (s, 3H,

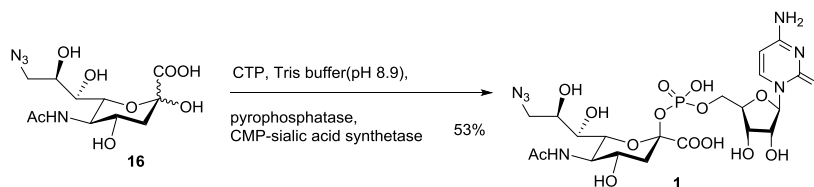
CH<sub>3</sub>-Ph), 2.23 (dd, *J* = 12.9, 4.9 Hz, 1H, H-3eq), 2.03 (s, 3H,Ac), 1.89 (dd, *J* = 12.7, 11.5 Hz, 1H, H-3ax). MALDI-FTMS (C<sub>19</sub>H<sub>27</sub>NO<sub>11</sub>S), calculated (M+Na<sup>+</sup>): 500.1203, found: 500.1321.

### 5-Acetamido-9-azido-3,5,9-tri-deoxy-D-glycero-D-galacto-2-nonulosonic acid (**16**)



Sodium azide (413 mg, 6.35 mmol) and **15** (740 mg, 1.55 mmol) were dissolved in a mixture of water (3.2 mL) and acetone (9.6 mL). The solution was heated under reflux overnight. The solvents were concentrated under reduced pressure and the residue was purified by flash chromatography to give **16** as a yellow solid (470 mg, 91%). <sup>1</sup>H NMR (300 MHz, d<sub>2</sub>O) δ 4.08 – 3.89 (m, 3H), 3.89 – 3.80 (m, 1H), 3.52 (dd, *J* = 12.8, 2.4 Hz, 1H), 3.44 – 3.37 (m, 2H), 2.21 – 2.09 (m, 1H, H-3eq), 2.03 (s, 3H, Ac), 1.90 (d, *J* = 9.1 Hz, 1H, H-3ax). <sup>13</sup>C NMR (75 MHz, d<sub>2</sub>O) δ 71.9, 71.2, 71.2, 68.8, 55.9, 54.2, 42.0, 23.0. MALDI-FTMS (C<sub>11</sub>H<sub>18</sub>N<sub>4</sub>O<sub>8</sub>): Calculated (M+Na<sup>+</sup>): 357.1022, found: 357.1432.

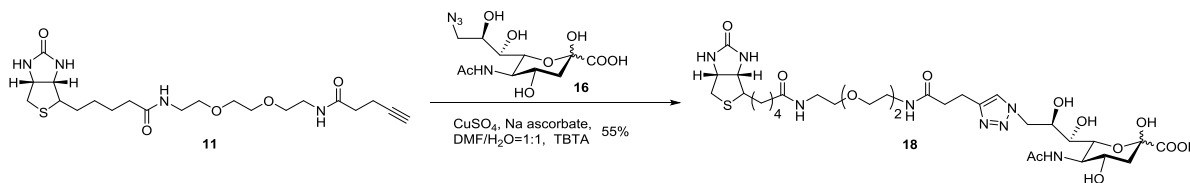
### Cytidine-5'-(5-acetamido-9-azido-3,5,9-tri-deoxy-β-D-glycero-D-galacto-2-nonulopyranosylonic acid monophosphate (**1**)



CTP (33 mg, 0.063 mmol) was added to a solution of **16** (10 mg, 0.03 mmol) in a Tris-HCl buffer (0.1 M, 2 mL, pH 8.92) containing MgCl<sub>2</sub> (20 mM). The recombinant CMP-sialic acid synthetase

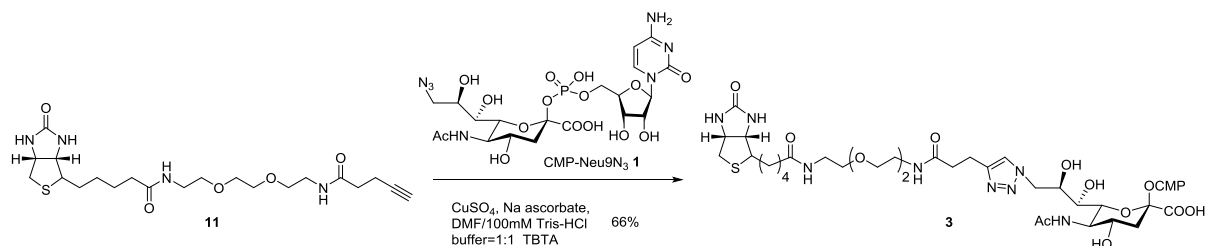
from *N. meningitis* (1.0 U) and the inorganic pyrophosphatase from *S. cerevisiae* (1.0 U) were added and the reaction mixture was incubated at 37 °C with shaking. The progress of the reaction was monitored by TLC (isopropanol: 20 mM NH<sub>4</sub>OH, 4:1, v:v), which after 3 h indicated completion of the reaction. Ethanol (5 mL) was added and the mixture was kept on ice for 1 h prior to centrifugation. The supernatant was decanted and the combined ethanol extracts were concentrated *in vacuo* providing crude material, which was purified on a column of extra-fine Biogel P-2 eluted with 0.1 M NH<sub>4</sub>HCO<sub>3</sub> at 4 °C. The appropriate fractions were detected by UV and TLC (as above), collected and lyophilized to afford **1** (10 mg, 53%) as a white solid. <sup>1</sup>H NMR (600 MHz, d<sub>2</sub>O) δ 7.78 (d, *J* = 7.6 Hz, 1H, H-6, cyt), 5.95 (d, *J* = 7.6 Hz, 1H, H-5, cyt), 5.81 (d, *J* = 4.5 Hz, 1H, H-1 rib), 4.16 (t, *J* = 4.9 Hz, 1H, H-3 rib), 4.12 (t, *J* = 4.8 Hz, 1H, H-2 rib), 4.06 (dq, *J* = 6.2, 2.6 Hz, 3H, H-4, H-5 rib), 3.96 (dd, *J* = 10.4, 1.2 Hz, 1H, H-6), 3.93 – 3.87 (m, 2H, H-4, H-8), 3.77 (t, *J* = 10.3 Hz, 1H, H-5), 3.46 (dd, *J* = 13.1, 2.7 Hz, 1H, H-9a), 3.33 (dd, *J* = 13.1, 6.0 Hz, 1H, H-9b), 3.31 – 3.28 (m, 1H, H-7), 2.31 (dd, *J* = 13.3, 4.8 Hz, 1H, H-3eq), 1.88 (s, 3H, Ac), 1.47 (ddd, *J* = 13.2, 11.3, 5.7 Hz, 1H, H-3ax). <sup>13</sup>C NMR (151 MHz, d<sub>2</sub>O) δ 141.2, 95.7, 88.2, 82.2, 73.3, 70.6, 68.4, 68.1, 66.7, 66.7, 63.7, 52.0, 50.5, 39.6, 21.2. HRMS (ESI): *m/z*: calcd for C<sub>20</sub>H<sub>29</sub>N<sub>7</sub>O<sub>15</sub>P [M-H]<sup>-</sup>: 638.1459; found: 638.1056.

**5-Acetamido-9-[4-[2-[2-[2-[2-[(1-biotinyl)amino]ethoxy]ethoxy]ethylamino]oxoethyl]-1*H*-1,2,3-triazol-1-yl]-3,5,9-tri-deoxy-D-glycero-D-galacto-2-nonulosonic acid (18):**



A solution of compound **11** (50 mg, 0.11 mmol) in DMF (5 mL) was added to the solution of **16** (28.0 mg, 0.08 mmol) in H<sub>2</sub>O (5 mL). To this mixture was added CuSO<sub>4</sub> (100 mM, 640 µL), sodium L-ascorbate (100, mM 800 µL) and TBTA (5 mg, 0.02 mmol). After stirring for 3.5 hours at ambient temperature, the reaction mixture was concentrated under reduced pressure to provide a crude material, and this residue was purified by silica gel column chromatography (MeOH/DCM, 5:1, v/v). The product was detected by TLC (<sup>i</sup>PrOH : 20 mM NH<sub>4</sub>Cl, 4:1, v:v), and appropriate fractions were combined and concentrated to provide **18** as a white solid (37 mg, 55%). <sup>1</sup>H NMR (500 MHz, CD<sub>3</sub>OD) δ 7.93 (m, 1H, CH=C, triazole), 4.51 (s, 1H, CHNH, biotin), 4.35 – 4.30 (m, 2H), 4.02 (m, 4H), 3.62 (s, 4H, OCH<sub>2</sub>CH<sub>2</sub>O), 3.59 – 3.52 (m, 4H, NHCH<sub>2</sub>CH<sub>2</sub>O, OCH<sub>2</sub>CH<sub>2</sub>NH), 3.45 – 3.33 (m, 6H, NHCH<sub>2</sub>CH<sub>2</sub>O, OCH<sub>2</sub>CH<sub>2</sub>NH, H-9), 3.28 – 3.18 (m, 1H, CHS biotin), 3.01 (m, 2H, C=OCH<sub>2</sub>CH<sub>2</sub>-triazole), 2.94 (dd, *J* = 12.6, 4.3 Hz, 1H, CHHS), 2.73 (d, *J* = 12.6 Hz, 1H, CHHS), 2.59 (m, 2H, C=OCH<sub>2</sub>CH<sub>2</sub> triazole), 2.24 (t, *J* = 7.1 Hz, 2H, CH<sub>2</sub>CH<sub>2</sub>CH<sub>2</sub>CH<sub>2</sub>C=O, biotin), 2.19 – 1.88 (m, 5H, NCH<sub>3</sub>, H-3), 1.83 – 1.41 (m, 6H, CH<sub>2</sub>CH<sub>2</sub>CH<sub>2</sub>CH<sub>2</sub>C=O). <sup>13</sup>C NMR (126 MHz, CD<sub>3</sub>OD) δ 70.3, 69.9, 69.3, 68.7, 62.7, 60.3, 55.6, 53.9, 53.4, 52.7, 52.7, 39.7, 39.7, 38.9, 35.4, 35.0, 28.4, 28.1, 28.1, 25.4, 21.5, 21.3. HRMS (ESI): *m/z* calcd for C<sub>32</sub>H<sub>52</sub>N<sub>8</sub>O<sub>13</sub>S [M-H]<sup>-</sup>: 787.3302; found: 787.1547.

**Cytidine-5'-monophospho-5-Acetamido-9-[4-[2-[2-[2-[2-[(1-biotinyl)amino]ethoxy]ethoxy]ethylamino]oxoethyl]-1*H*-1,2,3-triazol-1-yl]-3,5,9-tri-deoxy-D-glycero-D-galacto-2-nonulopyranosonic acid (3):**

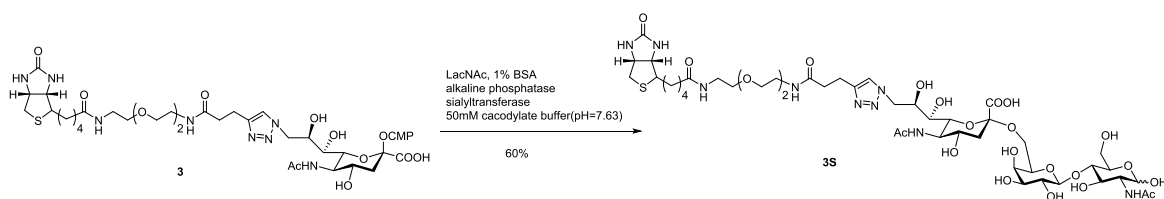


The solution of **11** (5.9 mg, 0.013 mmol) in DMF (500  $\mu$ L) was added to the solution of CMP-Neu9N<sub>3</sub> (**1**, 8.0 mg, 0.012 mmol)<sup>30</sup> in Tris-HCl buffer (100 mM, pH 7.5, 500  $\mu$ L). To this mixture was added CuSO<sub>4</sub> (100 mM, 80  $\mu$ L), sodium L-ascorbate (100 mM, 100  $\mu$ L) and TBTA (1.6 mg, 0.003 mmol). After stirring for 3.5 hours at ambient temperature, the reaction mixture was lyophilized to provide a crude material, which was applied on a Biogel fine P-2 column (75\*1.5 cm) and eluted with 0.1 M aqueous NH<sub>4</sub>HCO<sub>3</sub> at 4 °C in dark. The product was detected by TLC (<sup>i</sup>PrOH: aq. NH<sub>4</sub>Cl (20 mM), 4:1, v:v), and appropriate fractions were combined and lyophilized to provide **3** as a white solid (9.1 mg, 66%). <sup>1</sup>H NMR (600 MHz, D<sub>2</sub>O)  $\delta$  7.67 (d, *J* = 7.6 Hz, 1H, H-6, cyt), 7.62 (s, 1H, CH=C, triazole), 5.83 (d, *J* = 7.6 Hz, 1H, H-5, cyt), 5.78 (d, *J* = 5.0 Hz, 1H, H-1, rib), 4.62-4.59 (m, 3H, H-4 rib + H-5 rib), 4.40 (dd, *J* = 8.0, 5.2 Hz, 1H, CHNH, biotin), 4.25 – 4.18 (m, 2H, CHNH biotin, H-3, rib), 4.06 – 4.03 (m, 1H, H-2, rib), 4.03 – 3.92 (m, 3H, H-5, H-7, H-8), 3.89 (td, *J* = 11.0, 4.0 Hz, 1H, H-4), 3.75 (t, *J* = 10.3 Hz, 1H, H-6), 3.50 – 3.40 (m, 7H, H-9a, OCH<sub>2</sub>CH<sub>2</sub>O, NHCH<sub>2</sub>CH<sub>2</sub>O), 3.36 (dd, *J* = 6.8, 3.9 Hz, 2H, OCH<sub>2</sub>CH<sub>2</sub>NH), 3.23–3.08 (m, 6H, NHCH<sub>2</sub>CH<sub>2</sub>O, OCH<sub>2</sub>CH<sub>2</sub>NH, H-9b, CHS biotin), 2.86–2.73 (m, 3H, triazole-CH<sub>2</sub>CH<sub>2</sub>C=O, CHHS), 2.57 (dd, *J* = 13.1, 3.1 Hz, 1H, CHHS), 2.46 – 2.37 (m, 2H, triazole-CH<sub>2</sub>CH<sub>2</sub>C=O), 2.29 (dt, *J* = 13.2, 3.9 Hz, 1H, H-3eq), 2.06 (td, *J* = 7.3, 3.0 Hz, 2H, CH<sub>2</sub>CH<sub>2</sub>CH<sub>2</sub>CH<sub>2</sub>C=O, biotin), 1.84 (d, *J* = 3.0 Hz, 3H, NAc), 1.54 – 1.32 (m, 5H, H-3ax, CH<sub>2</sub>CH<sub>2</sub>CH<sub>2</sub>CH<sub>2</sub>C=O, biotin), 1.19 (ddt, *J* = 15.3, 9.2, 7.8, 4.3 Hz, 2H, CH<sub>2</sub>CH<sub>2</sub>CH<sub>2</sub>CH<sub>2</sub>C=O,



biotin).  $^{13}\text{C}$  NMR (600 MHz,  $\text{D}_2\text{O}$ )  $\delta$  141.2, 123.9, 96.4, 88.6, 83.0, 74.4, 71.5, 71.5, 69.8, 69.5, 69.3, 69.0, 68.7, 68.4, 66.5, 65.1, 61.9, 60.1, 55.2, 51.9, 41.1, 39.9, 39.6, 38.7, 38.4, 35.2, 35.1, 27.8, 25.2, 24.9, 22.1, 21.0. HRMS (ESI):  $m/z$  calcd for  $\text{C}_{41}\text{H}_{64}\text{N}_{11}\text{O}_{20}\text{PS}$   $[\text{M}-\text{H}]^-$ , 1092.3715; found: 1092.3482.

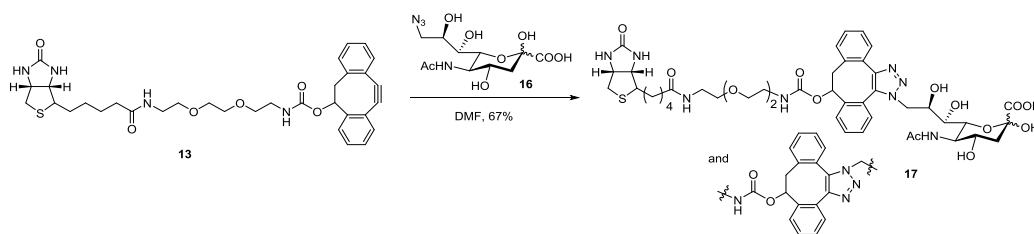
### biotinyl Neu9N $_3\alpha$ (2,6)Gal $\beta$ (1,4)GlcNAc (**3S**)



Recombinant  $\alpha$ -(2,6)-sialyltransferase (ST6Gal I) [GenBank P13721] (2.18 mg/mL, 6.7  $\mu\text{L}$ ) and calf intestine alkaline phosphatase (1000 U/mL, 24.5  $\mu\text{L}$ ) were added to a mixture of LacNAc (0.5 mg, 1.3  $\mu\text{mol}$ ) in cacodylate buffer (50 mM, pH 7.63, 96  $\mu\text{L}$ ) containing 0.1% BSA and **3** (2.8 mg, 2.6  $\mu\text{mol}$ ) in an Eppendorf tube. The tube was incubated at 37  $^{\circ}\text{C}$ , and progress of the reaction was monitored by TLC (EtOAc :  $\text{CH}_3\text{OH}$  :  $\text{H}_2\text{O}$  : AcOH = 4:2:1:0.5, v:v:v:v), which after 5 hour indicated completion of the reaction.  $\text{CH}_3\text{OH}$  (0.5  $\mu\text{L}$ ) was added and the resulting solution was lyophilization to provide a residue that was applied on a Biogel fine P-2 column (50\* 1 cm), which was eluted with  $\text{H}_2\text{O}$  at room temperature. The product was detected by TLC, and appropriate fractions were combined and lyophilized to provide **3S** as a white solid (0.9 mg, 60%).  $^1\text{H}$  NMR (600 MHz,  $\text{D}_2\text{O}$ )  $\delta$  7.92 (s, 1H,  $\text{CH}=\text{C}$ , triazole), 5.76 (q,  $J$  = 1.9 Hz, 0.2H, H-1'), 5.28 (dd,  $J$  = 3.3, 1.3 Hz, 0.8H, H-1'), 4.86 – 4.80 (m, 1H, H-1''), 4.71 – 4.65 (m, 1H,  $\text{CHNH}$ , biotin), 4.59 (dddd,  $J$  = 17.2, 9.4, 5.2, 1.3 Hz, 1H), 4.56 – 4.47 (m, 2H), 4.38 – 4.23 (m, 1H,

H-5), 4.09 – 4.00 (m, 2H), 3.97 (qd,  $J = 5.8, 1.8$  Hz, 2H), 3.94 – 3.86 (m, 2H), 3.86 – 3.78 (m, 4H, OCH<sub>2</sub>CH<sub>2</sub>O), 3.77 – 3.67 (m, 10H), 3.67 – 3.57 (m, 3H), 3.49 – 3.37 (m, 5H, NHCH<sub>2</sub>CH<sub>2</sub>O, OCH<sub>2</sub>CH<sub>2</sub>NH, CHS biotin), 3.10 (t,  $J = 7.4$  Hz, 2H, triazole-CH<sub>2</sub>CH<sub>2</sub>C=O), 3.06 (ddt,  $J = 13.0, 5.1, 1.4$  Hz, 1H, CHHS), 2.85 (d,  $J = 13.1$  Hz, 1H, CHHS), 2.75 – 2.68 (m, 3H, H-3eq + triazole-CH<sub>2</sub>CH<sub>2</sub>C=O), 2.36 – 2.32 (m, 2H, CH<sub>2</sub>CH<sub>2</sub>CH<sub>2</sub>CH<sub>2</sub>C=O, biotin), 2.14 (d,  $J = 12.0$  Hz, 3H, NAc), 2.09 (d,  $J = 1.3$  Hz, 3H, NAc), 1.83 – 1.60 (m, 5H, H-3ax + CH<sub>2</sub>CH<sub>2</sub>CH<sub>2</sub>CH<sub>2</sub>C=O, biotin), 1.47 (ddt,  $J = 12.4, 9.3, 7.0$  Hz, 2H CH<sub>2</sub>CH<sub>2</sub>CH<sub>2</sub>CH<sub>2</sub>C=O, biotin). <sup>13</sup>C NMR (600 MHz, D<sub>2</sub>O)  $\delta$  124.1, 107.5, 103.4, 94.6, 90.5, 80.8, 74.5, 73.6, 72.9, 72.4, 70.6, 69.9, 69.8, 69.5, 69.5, 69.4, 69.3, 68.8, 68.7, 67.9, 67.3, 67.2, 63.4, 63.4, 62, 60.3, 60.3, 60.1, 60.1, 59.2, 55.3, 53.4, 52.8, 52.8, 52.7, 51.8, 40, 40, 39.6, 39.6, 38.8, 38.8, 35.3, 35.1, 27.8, 27.6, 27.6, 25, 22, 21.9, 21. HRMS (ESI):  $m/z$  calcd for C<sub>46</sub>H<sub>75</sub>N<sub>9</sub>O<sub>23</sub>S [M-H]<sup>-</sup>: 1152.4624; found: 1152.2786.

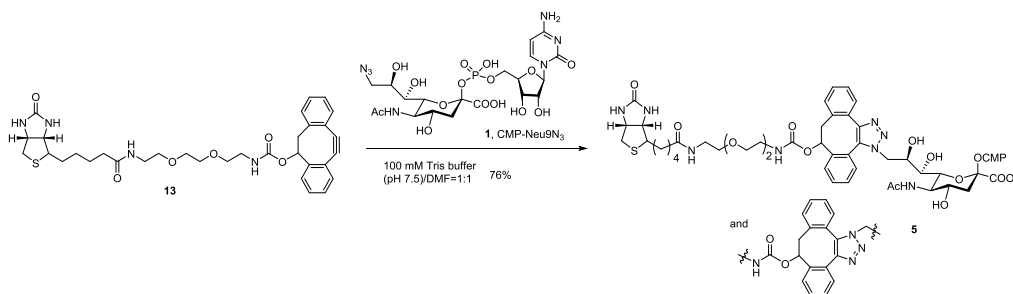
### Biotin-DIBO-Neu9N<sub>3</sub> (**17**)



Neu9N<sub>3</sub> (**16**, 27 mg, 0.08 mmol) was added to the solution of **13** (50 mg, 0.08 mmol) in DMF (2mL) at room temperature. After stirring for 3 hours, the reaction mixture was concentrated under reduced pressure and the residue was purified by silica gel column chromatography using a gradient of 10% to 50% methanol in CH<sub>2</sub>Cl<sub>2</sub> to give **17** as a white solid (51 mg, 67%). <sup>1</sup>H NMR (500 MHz, cd<sub>3</sub>od)  $\delta$  7.72 – 7.14 (m, 8H, PhH), 6.22 – 5.97 (m, 1H, CH<sub>2</sub>CHO, DIBO), 4.48 (m, 1H, CHNH, biotin), 4.32 – 4.24 (m, 1H, CHNH biotin), 4.09 – 3.79 (m, 4H, H-4 + H-5 +

H-7 + H-8), 3.64 – 3.48 (m, 9H, H-9a + OCH<sub>2</sub>CH<sub>2</sub>O + NHCH<sub>2</sub>CH<sub>2</sub>O + OCH<sub>2</sub>CH<sub>2</sub>NH), 3.42 (t, *J* = 7.8 Hz, 1H, H-6), 3.36 – 3.26 (m, 7H, NHCH<sub>2</sub>CH<sub>2</sub>O + OCH<sub>2</sub>CH<sub>2</sub>NH + H-9b + CH<sub>2</sub>CHO, DIBO), 3.18 (tt, *J* = 10.0, 5.0 Hz, 1H, CHS, biotin), 2.95 – 2.84 (m, 1H, CHHS), 2.73 – 2.65 (m, 1H, CHHS), 2.21 (d, *J* = 7.1 Hz, 2H, CH<sub>2</sub>CH<sub>2</sub>CH<sub>2</sub>CH<sub>2</sub>C=O, biotin), 2.17 – 2.09 (m, 1H, H-3eq), 2.04 – 1.96 (m, 3H, NAc), 1.92 (d, *J* = 12.0 Hz, 1H, H-3ax), 1.77 – 1.52 (m, 4H, CH<sub>2</sub>CH<sub>2</sub>CH<sub>2</sub>CH<sub>2</sub>C=O, biotin), 1.48 – 1.39 (m, 2H, CH<sub>2</sub>CH<sub>2</sub>CH<sub>2</sub>CH<sub>2</sub>C=O, biotin). <sup>13</sup>C NMR (500 MHz, cd<sub>3</sub>od) δ 132.1, 131.4, 129.6, 129.6, 128.6, 128.2, 127.2, 126.2, 77.9, 70.4, 69.9, 69.8, 69.7, 69.7, 69.5, 67.4, 62, 60.3, 55.6, 54.3, 54.3, 52.7, 40.4, 40.3, 40.3, 39.8, 39.7, 38.9, 35.4, 28.4, 28.1, 25.4, 21.5. HRMS (ESI): calcd for C<sub>44</sub>H<sub>58</sub>N<sub>8</sub>O<sub>14</sub>S [M-H]<sup>-</sup>:m/z: 953.3720; found m/z: 953.1340.

### Biotin-DIBO-CMP-Neu9N<sub>3</sub> (**5**)



The solution of **13** (13.0 mg, 0.021 mmol) in DMF (300 μL) was added to the solution of CMP-Neu9N<sub>3</sub> (8.9 mg, 0.014 mmol) in 100 mM Tris-HCl buffer (pH 7.5, 500 μL). After stirring for 3 hours at ambient temperature, the reaction mixture was lyophilized to provide a crude material, which was applied on a Biogel fine P-2 column (75\*1.5 cm) and eluted with 0.1 M NH<sub>4</sub>HCO<sub>3</sub> at 4 °C in dark. The product was detected by TLC (i-PrOH : 20 mM NH<sub>4</sub>Cl, 4:1, v:v), and appropriate fractions were combined and lyophilized to provide **5** (13.6 mg, 76%) as a white

solid.  $^1\text{H}$  NMR (600 MHz,  $\text{d}_2\text{O}$ )  $\delta$  7.93 – 6.98 (m, 9H, PhH + H-6, cyt), 5.97 (dq,  $J = 18.5$ , 5.9, 4.7 Hz, 1H), 5.84 – 5.73 (m, 2H), 5.68 – 5.44 (m, 1H), 4.84 – 4.57 (m, 2H), 4.37 – 3.67 (m, 10H), 3.56 – 2.96 (m, 13H), 2.95 – 2.70 (m, 1H), 2.59 (m, 1H, CHHS), 2.46 (dd,  $J = 24.8$ , 12.5 Hz, 1H, CHHS), 2.30 (m, 1H, H-3eq), 2.11 – 1.79 (m, 5H,  $\text{NCH}_3$  +  $\text{CH}_2\text{CH}_2\text{CH}_2\text{CH}_2\text{C}=\text{O}$ , biotin), 1.54 – 0.91 (m, 7H, H-3ax +  $\text{CH}_2\text{CH}_2\text{CH}_2\text{CH}_2\text{C}=\text{O}$ , biotin).  $^{13}\text{C}$  NMR (151 MHz,  $\text{d}_2\text{O}$ )  $\delta$  130.1, 129.7, 129.4, 129.3, 129.2, 128.9, 127.8, 127.4, 105.3, 96.3, 88.8, 88.7, 83.6, 82.5, 78.1, 74.2, 73.9, 72.7, 71.4, 70.1, 70.1, 69.4, 69.3, 69.2, 69.1, 69.0, 68.7, 64.9, 64.8, 62.8, 62.7, 61.7, 61.6, 60.0, 55.1, 54.9, 52.1, 51.6, 51.3, 40.9, 40.8, 39.8, 39.4, 35.2, 35.1, 27.6, 27.5, 27.4, 24.8, 24.7, 22.0, 22.0. HRMS (ESI): calcd for  $\text{C}_{53}\text{H}_{70}\text{N}_{11}\text{O}_{21}\text{PS}$   $[\text{M-H}]^-$ :  $m/z$ : 1258.4133; found  $m/z$ : 1258.1899.

## References

- (1) Sletten, E. M.; Bertozzi, C. R. *Angewandte Chemie* **2009**, *48*, 6974.
- (2) Grammel, M.; Hang, H. C. *Nature chemical biology* **2013**, *9*, 475.
- (3) Saxon, E.; Bertozzi, C. R. *Science* **2000**, *287*, 2007.
- (4) Schilling, C. I.; Jung, N.; Biskup, M.; Schepers, U.; Brase, S. *Chemical Society reviews* **2011**, *40*, 4840.
- (5) Meldal, M.; Tornøe, C. W. *Chemical reviews* **2008**, *108*, 2952.
- (6) Soriano Del Amo, D.; Wang, W.; Jiang, H.; Besanceney, C.; Yan, A. C.; Levy, M.; Liu, Y.; Marlow, F. L.; Wu, P. *J Am Chem Soc* **2010**, *132*, 16893.
- (7) Kennedy, D. C.; McKay, C. S.; Legault, M. C.; Danielson, D. C.; Blake, J. A.; Pegoraro, A. F.; Stolorow, A.; Mester, Z.; Pezacki, J. P. *J Am Chem Soc* **2011**, *133*, 17993.
- (8) Jewett, J. C.; Bertozzi, C. R. *Chemical Society reviews* **2010**, *39*, 1272.
- (9) Debets, M. F.; van Berkel, S. S.; Dommerholt, J.; Dirks, A. T.; Rutjes, F. P.; van Delft, F. L. *Accounts of chemical research* **2011**, *44*, 805.
- (10) Whiteheart, S. W.; Hart, G. W. *Analytical biochemistry* **1987**, *163*, 123.
- (11) Gross, H. J.; Brossmer, R. *European journal of biochemistry* **1988**, *177*, 583.
- (12) Gross, H. J.; Brossmer, R. *Glycoconjugate journal* **1995**, *12*, 739.
- (13) Blixt, O.; Allin, K.; Bohorov, O.; Liu, X.; Andersson-Sand, H.; Hoffmann, J.; Razi, N. *Glycoconjugate journal* **2008**, *25*, 59.
- (14) Zheng, T.; Jiang, H.; Gros, M.; del Amo, D. S.; Sundaram, S.; Lauvau, G.; Marlow, F.;

Liu, Y.; Stanley, P.; Wu, P. *Angewandte Chemie* **2011**, *50*, 4113.

(15)Chaubard, J. L.; Krishnamurthy, C.; Yi, W.; Smith, D. F.; Hsieh-Wilson, L. C. *J Am Chem Soc* **2012**, *134*, 4489.

(16)Mbua, N. E.; Li, X.; Flanagan-Steet, H. R.; Meng, L.; Aoki, K.; Moremen, K. W.; Wolfert, M. A.; Steet, R.; Boons, G. J. *Angewandte Chemie* **2013**, *52*, 13012.

(17)Mercer, N.; Ramakrishnan, B.; Boeggeman, E.; Verdi, L.; Qasba, P. K. *Bioconjug Chem* **2013**, *24*, 144.

(18)Li, Q.; Li, Z.; Duan, X.; Yi, W. *J Am Chem Soc* **2014**, *136*, 12536.

(19)Rouhanifard, S. H.; Lopez-Aguilar, A.; Wu, P. *Chembiochem : a European journal of chemical biology* **2014**, *15*, 2667.

(20)Yu, C. C.; Withers, S. G. *Advanced synthesis & catalysis* **2015**, *357*, 1633.

(21)Kajihara, Y.; Kamitani, T.; Sato, R.; Kamei, N.; Miyazaki, T.; Okamoto, R.; Sakakibara, T.; Tsuji, T.; Yamamoto, T. *Carbohydrate research* **2007**, *342*, 1680.

(22)Yao, J. Z.; Uttamapinant, C.; Poloukhine, A.; Baskin, J. M.; Codelli, J. A.; Sletten, E. M.; Bertozzi, C. R.; Popik, V. V.; Ting, A. Y. *J Am Chem Soc* **2012**, *134*, 3720.

(23)Fraldi, A.; Annunziata, F.; Lombardi, A.; Kaiser, H. J.; Medina, D. L.; Spanpanato, C.; Fedele, A. O.; Polishchuk, R.; Sorrentino, N. C.; Simons, K.; Ballabio, A. *The EMBO journal* **2010**, *29*, 3607.

(24)Cabeza, C.; Figueroa, A.; Lazo, O. M.; Galleguillos, C.; Pissani, C.; Klein, A.; Gonzalez-Billault, C.; Inestrosa, N. C.; Alvarez, A. R.; Zanolungo, S.; Bronfman, F. C. *Molecular neurodegeneration* **2012**, *7*, 11.

- (25)Mbua, N. E.; Flanagan-Steet, H.; Johnson, S.; Wolfert, M. A.; Boons, G. J.; Steet, R. *Proc Natl Acad Sci U S A* **2013**, *110*, 10207.
- (26)Ning, X.; Guo, J.; Wolfert, M. A.; Boons, G. J. *Angewandte Chemie* **2008**, *47*, 2253.
- (27)Yu, H.; Yu, H.; Karpel, R.; Chen, X. *Bioorganic & medicinal chemistry* **2004**, *12*, 6427.
- (28)Elia, G. *Proteomics* **2008**, *8*, 4012.
- (29)Moremen, K. W.; Tiemeyer, M.; Nairn, A. V. *Nature reviews. Molecular cell biology* **2012**, *13*, 448.
- (30)Rauvolfova, J.; Venot, A.; Boons, G. J. *Carbohydrate research* **2008**, *343*, 1605.

## CHAPTER 3

### NOVEL TWO-STEP SELECTIVE EXOENZYMATIC LABELING (SEEL) USING TETRAZINE FUNCTIONALIZED CMP-NEU5AC DERIVATIVE

Sun, T.; Yu, S. H.; Moremen, K. W.; Steet, R.; Boons, G. J. To be submitted to *Journal of the American Chemical Society*.



## Abstract

We describe here a chemical reporter strategy for labeling of cell surface glycoconjugates that takes advantage of recombinant glycosyltransferases, a corresponding sugar-nucleotide functionalized by tetrazine, and fast inverse electron demand Diels–Alder click reaction.

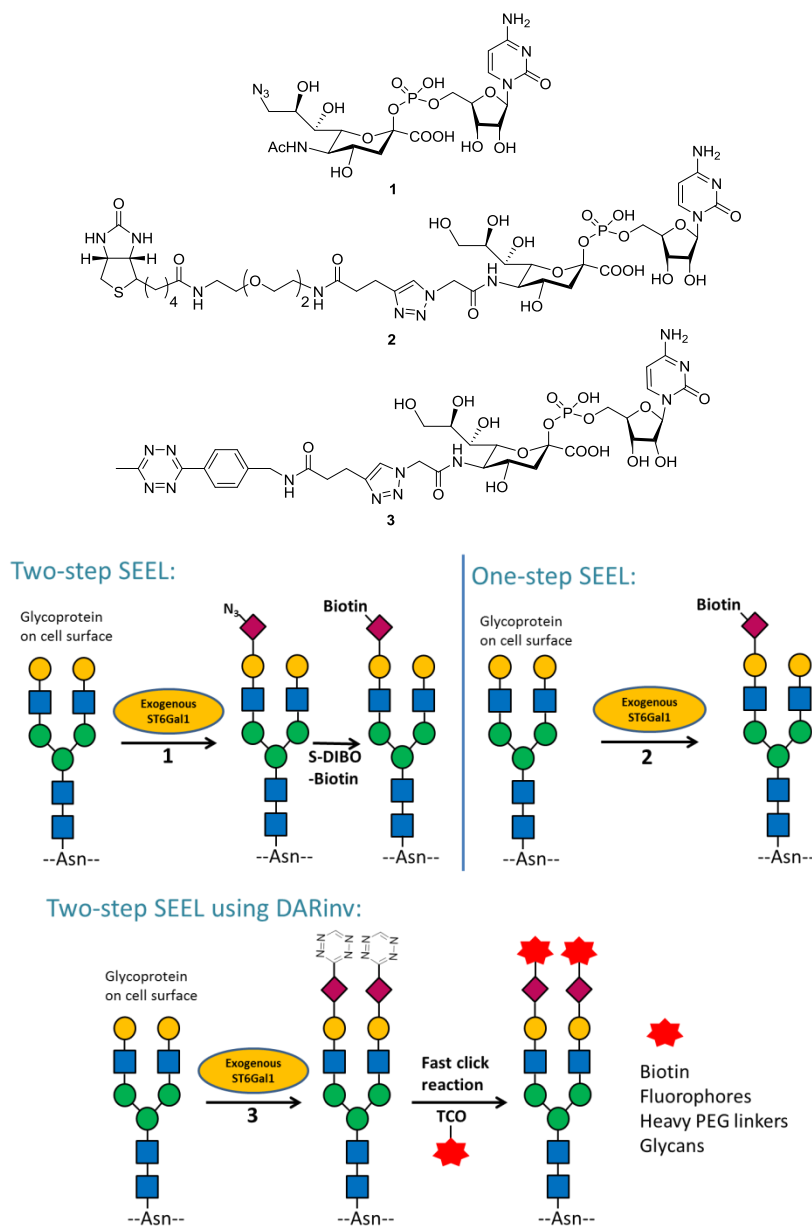
This new two-step selective exoenzymatic labeling strategy (two-step SEEL) provides a platform that is able to selectively and efficiently decorate the cell surface with different functionalities, such as biotin, fluorophores, heavy PEG linkers and glycans. Specifically, modifications of cell surface glycoproteins with a 5KDa PEG linker followed by western blot analysis with protein-specific antibodies have very broad applications. For example, with this technology, protein by protein glycosylation status on *N*- and *O*- glycans can be easily analyzed using different sialyltransferases (ST3Gal1, ST6Gal1, ST6GalNAc1, *etc.*) in different cell types.

## Introduction

The bioorthogonal chemical reporter strategy<sup>1,2</sup> provides the possibility to selectively target desired biomolecules in living systems. This is a two-step process, which involves the incorporation of a bioorthogonal chemical reporter into the target of interest using the cell's own biosynthetic machinery followed by a bioorthogonal reaction with specific function groups for detection. This strategy was found to be extremely useful to image proteins, lipids, glycans and other biomolecules.<sup>3-5</sup> Metabolic oligosaccharide engineering (MOE), developed by Reutter and Bertozzi's group,<sup>6,7</sup> metabolically incorporates unnatural monosaccharides in the cellular glycosynthetic pathway, which enables installation of useful small functionalities, like azide or terminal alkyne into cell-surface.<sup>8-11</sup> However, this approach cannot selectively label glycans in a specific manner, as the monosaccharides are incorporated into a variety of glycosylated biomolecules, such as glycolipids, *N*-linked glycans and *O*-linked glycans.<sup>1</sup> This limits MOE for *in vivo* glycan imaging in which probing of sialylation in a specific tissue or cell type is desired.

In 2013, our group described a methodology termed SEEL (selective exo-enzymatic labeling),<sup>12</sup> which takes advantage of recombinant glycosyltransferases and a corresponding functionalized nucleotide sugar (**1**) to install chemical reporters on cell surface acceptor glycans. This approach only labels a specific class of cell surface molecules (e.g., *N*- vs *O*-glycans) and does not rely on feeding with metabolic substrates that must compete with natural sugar precursor pools. In 2016, we developed a more efficient strategy, termed one-step SEEL,<sup>13</sup> by employing a biotin modified CMP-sialic acid derivative **2**. We found that this approach has

exceptional efficiency compared to two-step SEEL or metabolic labeling, which greatly improved the ability to enrich and identify large numbers of tagged glycoproteins by LC-MS/MS. The one-step approach offers exciting possibilities to study the trafficking and identification of subsets of cell surface glycoconjugates with unprecedented sensitivity in whole cells. However, this approach also faces some limitations, such as difficulties in synthesis. Multiple synthesis must be carried out if other functionalities other than biotin are needed to modify the cell surface, and each compound has long synthetic route, which is time consuming and costly. Furthermore, one glycan chain of *N*-linked glycoprotein usually has multiple branched sites to transfer CMP-sialic acid derivatives, all which are in close proximity to each other. If the functionality of modified CMP-sialic acid is too bulky, it may decrease the efficiency of the enzymatic transfer of the second moiety. Herein, we explored a new two-step SEEL, which takes advantage of a sugar nucleotide functionalized by tetrazine (**3**), and a fast bioorthogonal reaction-DARinv (inverse electron demand Diels-Alder reaction).<sup>14</sup> This approach first remodels the cell surface with high reactive tetrazines, and is followed by a click reaction with trans-cyclooctenes (TCO) modified functionalities.



Scheme 3.1 Various SEEL methodologies and compounds used.

DARinv is a reaction between electron-poor diene and electron-rich dienophile, in which two new chemical bonds and a six-membered ring are formed. This reaction does not employ toxic metal catalysts, and the reaction between tetrazine and TCO was reported as the fastest bioorthogonal reactions to date,<sup>14,15</sup> with rate constants between  $10^3$  and  $10^6 \text{ M}^{-1}\text{s}^{-1}$  (compared with  $\text{N}_3 + \text{DIBO}$ ,  $k_2 = 0.057 \text{ M}^{-1}\text{s}^{-1}$  in MeOH). The reaction rate of DARinv is highly tunable

across many orders of magnitude by chemically manipulating the substituents of the tetrazine's 3 and 6 positions, or by employing different dienophiles,<sup>16</sup> enabling DARinv to meet the needs of many different applications in living systems.<sup>17-19</sup> Moreover, the reactive partners are unreactive and compatible with a variety of functional groups and challenging conditions. The fast kinetics guarantee the shorter click time and high labeling efficiency.

The new two-step SEEL provides a platform that is able to selectively and efficiently decorate the cell surface with different functionalities, such as biotin, fluorophores, heavy PEG linkers and even glycans, and simplifies the synthesis at the same time. Any functionality that is about to conjugate to the glycoprotein, can simply be attached to TCO, instead of conjugating to CMP-sialic acid, which is really time consumed and costly. We found that this new two-step SEEL procedure using tetrazine modified CMP sialic acid derivative **3** and TCO-PEG5K can easily analyze protein by protein glycosylation status (*N*- vs. *O*-linked glycans) with different sialyltransferases (ST3Gal1, ST6Gal1, ST6GalNAc1 *et al*) in different cell types. Moreover, with this fast bioorthogonal click reaction, PEG5K conjugated CMP-sialic acid derivative can be generated *in situ* and one-step SEEL with this new reagent can be performed. In one word, we can choose one or two-step SEEL depends on the size of decorating functionalities with this CMP sialic acid derivative modified by Tetrazine.

## Results and discussion

### Synthesis of Modified Sugar Nucleotides.

We have confirmed that ST6Gal1 can tolerate a wide range of modifications at the C5

position of sialic acid. Therefore, CMP-sialic acid was modified at C5 position instead of C9 position. Initially, we tried to attach TCO to CMP-sialic acid (**4**), since it has a small size, and has high reactivities with various tetrazines.

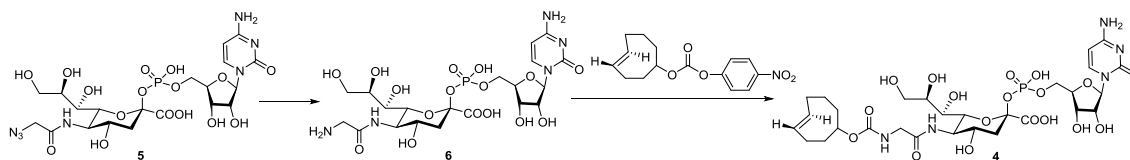


Figure 3.1 Designed synthetic route for TCO attached CMP-sialic acid.

CMP-Neu5N<sub>3</sub> (**5**) was prepared using a one-pot two-enzyme system.<sup>20</sup> X. Chen *et al* found that the CMP-sialic acid synthetases [EC 2.7.7.43] cloned from *Neisseria meningitidis* group B was shown to have the highest expression level, the most flexible substrate specificity, and the highest catalytic efficiency compared to other sources to synthesize CMP-sialic acid derivatives.<sup>20</sup> By using this enzyme, we successfully obtained the modified CMP-sialic acid that has an azide group at the C5 position starting from ManNAz (Figure 3.2). Next, Pd(OH)<sub>2</sub> was used to reduce the azide to free amine. With 5% Pd(OH)<sub>2</sub> and 1 hour's stirring at r.t, **6** was successfully obtained after filtration to remove the catalyst. It should be noted that with more catalyst (20% by mass) and longer reaction time, hydrogenation in cytosine moiety was observed.

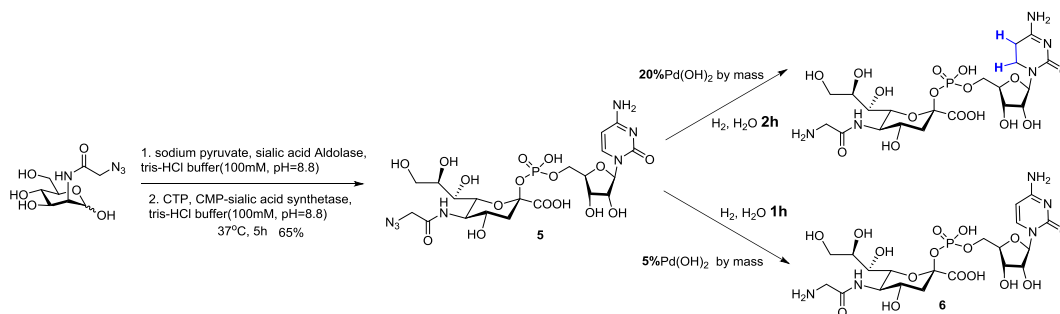


Figure 3.2 Synthesis of **5** and its hydrogenation using Pd(OH)<sub>2</sub>.

The coupling of free amine **6** with PNP (p-nitrophenyl carbonate) activated TCO was carried out in the mixture of DMF and 100 mM  $\text{NH}_4\text{HCO}_3$  for 20 hours, giving product **4** in the yield of 34%. When the reaction was carried out in the solvent of DMSO, complete conversion to product **4** was observed in 3 hours, and the isolated yield was increased to 43% (Figure 3.3). CMP-sialic acid derivative **4** could be successfully transferred to LacNAc by ST6Gal1, indicating that TCO is tolerated by this enzyme.

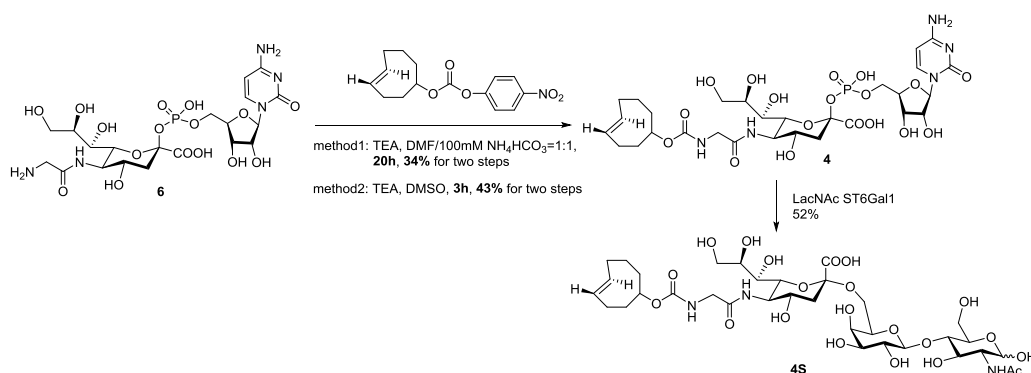


Figure 3.3 Synthesis of TCO attached CMP-sialic acid **4** and its successful transfer to LacNAc.

However, once the TCO was conjugated to CMP-sialic acid or transferred to LacNAc (compound **4** and **4S**), it was found that these compounds were unable to react with tetrazines. This has also been observed in literature,<sup>21</sup> where Haun's group found that the majority of TCOs conjugated to monoclonal antibodies using standard amine-coupling procedures are nonreactive. They proposed several mechanisms which may cause TCO inactivation: (1) conversion of TCO to the *cis* isoform during conjugation which is orders of magnitude less reactive compared to *trans*-cyclooctene, (2) steric hindrance and (3) hydrophobic interaction of the TCO with external or internal domains of the antibody. Similarly, the inactivation of TCO attachment in our case may also be explained by these possibilities. As a result, we decided to attach the tetrazine

moiety to CMP-sialic acid instead of TCO to maintain the click reactivity of TCO.

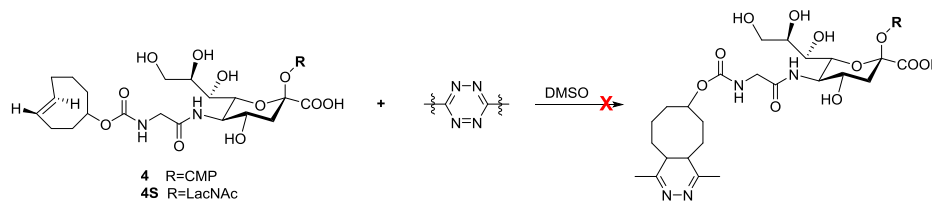


Figure 3.4 Inactivation of TCO by attachment with sialic acid moiety.

Mono-substituted tetrazine **7** was first synthesized according to literature,<sup>22</sup> because monosubstituted tetrazines have the highest reactivity due to less steric hindrance. 4-(aminomethyl)benzonitrile was first protected with Boc group to give nitrile **8**. Zinc triflate was used to catalyze the one-pot synthesis of 1,2,4,5-tetrazine **7** from unactivated nitrile **8** and hydrazine in a high yield.



Figure 3.5. Synthesis of mono-substituted tetrazine **5**.

After deprotection of Boc group and coupling with 4-pentynoic acid to install a terminal alkyne, tetrazine **9** was obtained. CuAAC with CMP-Neu5N<sub>3</sub> (**5**) gave tetrazine modified CMP-sialic acid **10**. However, complete decomposition of **10** was observed after 3 hours in transfer condition (37°C in 50 mM cacodylate buffer, pH 7.63) due to the increased lability of mono-substituted tetrazine.<sup>23</sup>

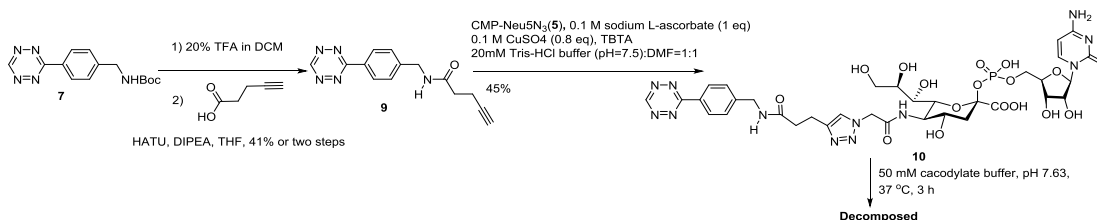


Figure 3.6 Synthesis and decomposition of **10**.



In general, monosubstituted tetrazines show the highest reactivity due to less steric hindrance, but also suffer from poor stability in the presence of water or biologically relevant nucleophiles. Tetrazine stability is dramatically enhanced by changing the substituents.<sup>24-26</sup> As a result, a disubstituted tetrazine **11** was synthesized according to literature.<sup>27</sup> This tetrazine still has high reactivity with TCO due to the stronger electron withdrawing group-pyrimidine.

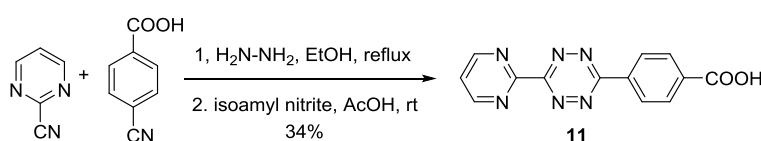


Figure 3.7 Synthesis of disubstituted tetrazine **11**.

Tetrazine **11** was activated by NHS, followed by coupling with 1-amino-3-butyne, giving terminal alkyne attached tetrazine **13**. However, CuAAC of **13** with CMP-Neu5N<sub>3</sub> (**5**) failed due to metal coordination.<sup>28</sup>

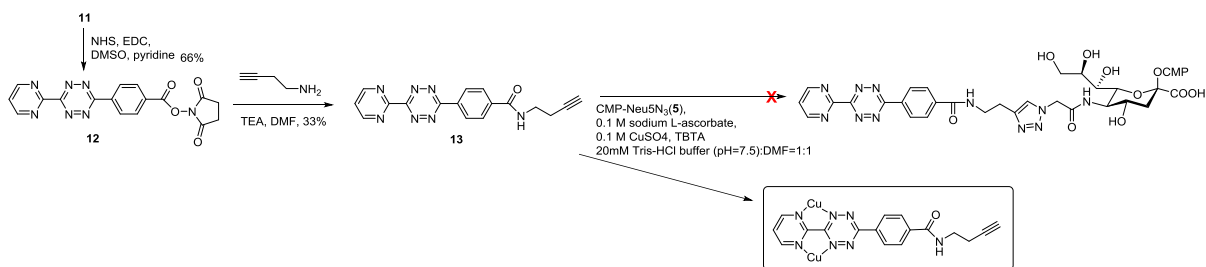


Figure 3.8 Copper Coordination with pyrimidine substituted tetrazine.

To avoid the use of copper, amide coupling was applied to conjugate free amine attached CMP-sialic acid derivative **6** to NHS-activated tetrazine **11**. However, the base TEA used in coupling step caused many problems. During purification, a rearrangement was induced by the base and N<sub>2</sub> was released to form compound **14A**, and additionally basic conditions facilitate the

elimination of CMP to form compound **14B** as confirmed by ESI. The proposed mechanism was shown in Figure 3.9.

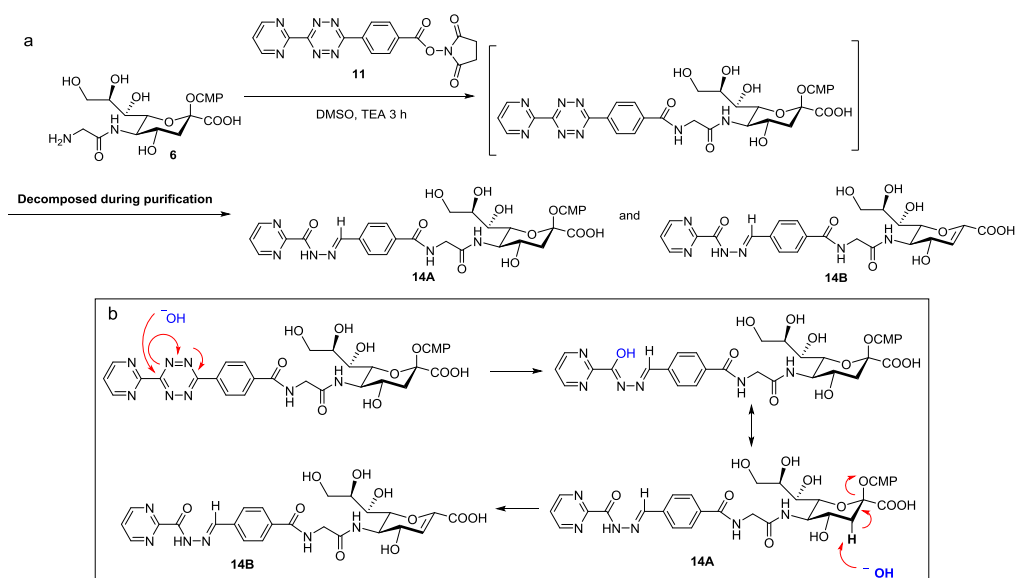


Figure 3.9 a) Synthesis and decomposition of **7**;  
b) Proposed mechanism under basic condition.

We next used a more stable tetrazine, which should not cause any problems during purifications, or decompose during transfer conditions. According to literature,<sup>24</sup> tetrazines with electron donating alkyl substituents exhibit higher stability (Figure 3.10, tetrazines with yellow color) than monosubstituted tetrazines or tetrazines with electron withdrawing substituents. Though this kind of tetrazines will have decreased reactivity, the reaction rates with TCO are still much faster than other type of click reactions. As a result, tetrazine **15** which has an electron donating methyl group was then synthesized using nickel triflate as a catalyst.<sup>22</sup>

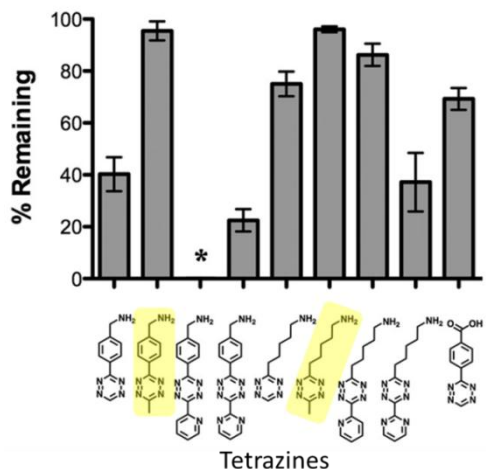


Figure 3.10 Stability of selected tetrazines in FBS at 37°C after 10 h. Adapted from reference [24]<sup>24</sup>

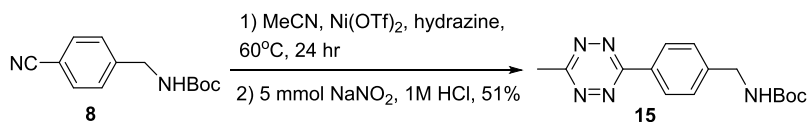


Figure 3.11 Synthesis of tetrazine **15**.

Deprotection of Boc group under acidic condition and followed coupling with 4-pentynoic acid in the presence of HATU and DIPEA gave **16** with a terminal alkyne. The final tetrazine modified CMP-sialic acid **3** was obtained after CuAAC of **16** with CMP-Neu5N<sub>3</sub> (**5**) in moderate yield (Figure 3.12) after C18 chromatography purification. To our delight, **3** was successfully transferred to LacNAc by ST6Gal1, indicating that this compound has enough stability to survive in biological systems and could be employed to modify cell surface glycoproteins.

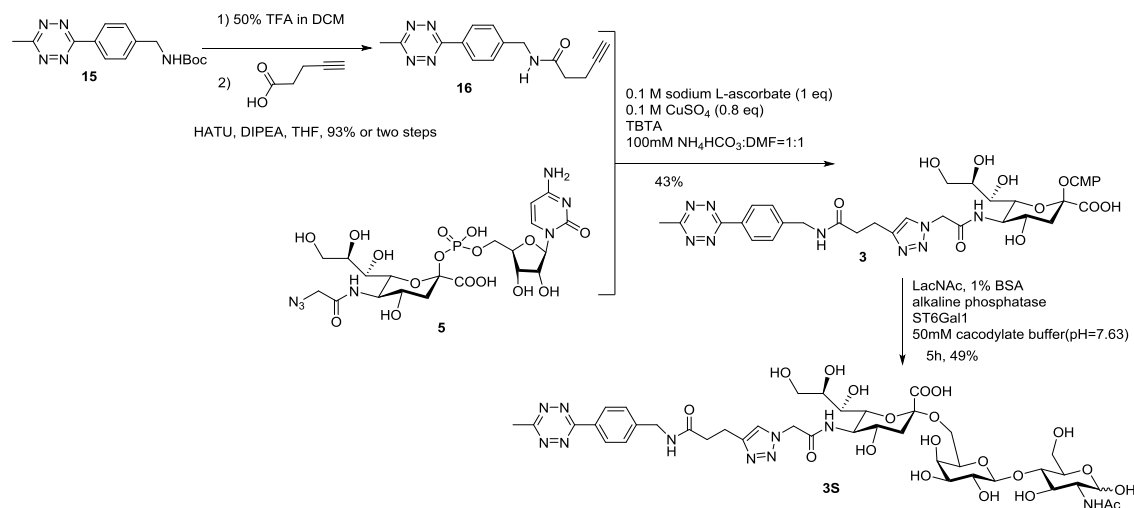


Figure 3.12 Synthesis of **3** and its successful transfer to LacNAc

With tetrazine modified CMP-sialic acid **3** in hand, we sought to further optimize this compound by adding a short PEG linker. This would increase the hydrophilicity of this compound to potentially make it more accessible to the glycoprotein on the cell surface, thus, giving more efficient labeling. *N*-Boc-3,6-dioxaoctane-1,8-diamine was first coupled with pentynoic acid with HATU and DIPEA to give **18**, followed by deprotection and conjugation with succinic anhydride. After silica gel column chromatography using DCM/MeOH as eluent, the free carboxylic acid was methylated to give **19**. The methoxy ester group was saponified using LiOH and **20** was coupled with free amine containing tetrazine **21** to provide tetrazine **22** with a terminal alkyne in 61% yield over three steps. CuAAC of **22** with CMP-Neu5N<sub>3</sub> (**5**) gave the final product **17** in moderate yield.

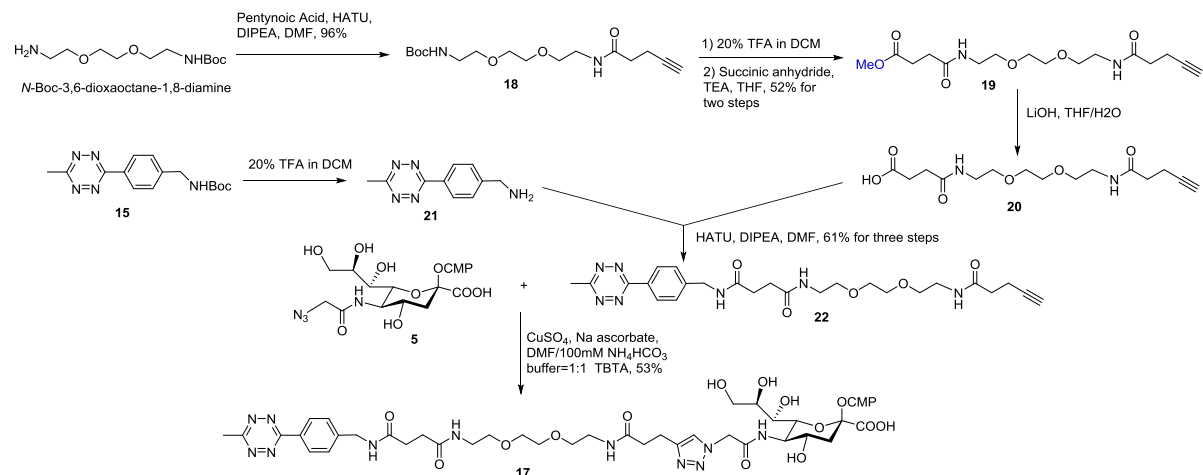


Figure 3.13 Synthesis of Tetrzine-PEG-CMP-Neu5Ac (**17**).

### Synthesis of Biotin Modified strained alkene/alkyne.

To establish the conjugation efficiency to cell surface, biotin modified TCO with a short PEG linker to increase the water solubility was prepared (Figure 3.14).

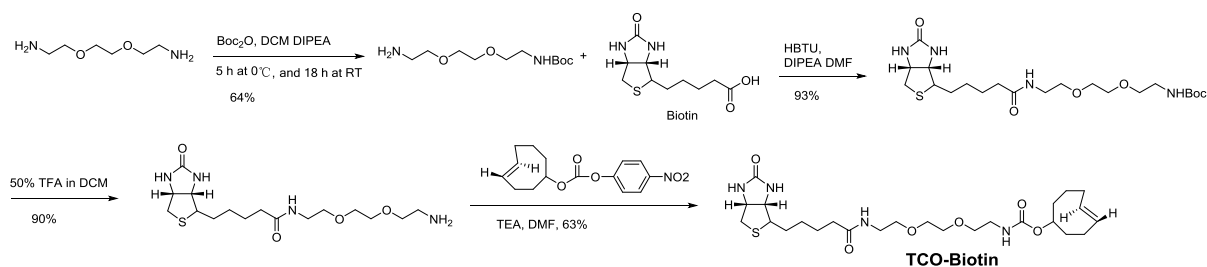


Figure 3.14 Synthesis of TCO-Biotin.

It is known that TCO can have poor stability due to conversion from *trans*-cyclooctene to *cis*-cyclooctene. This can be induced thermally, by light, or in concentrated thiol solutions.<sup>29</sup> From our observation, approximately 50% of the reactivity of TCO towards tetrazine was lost after storage at -78°C in dark for 8 months. Taking this into consideration, we also made a more stable probe, bicyclo[6.1.0]nonyne (BCN)<sup>25</sup> as a novel ring-strained alkyne for inverse

electron-demand Diels-Alder reactions.

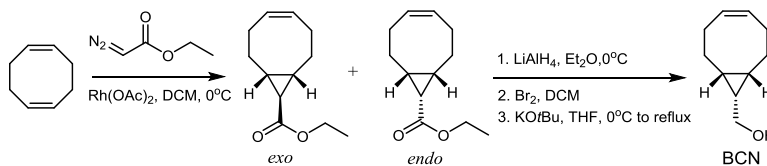


Figure 3.15 Synthesis of BCN.

Biotin attached BCN was also synthesized as showed below.

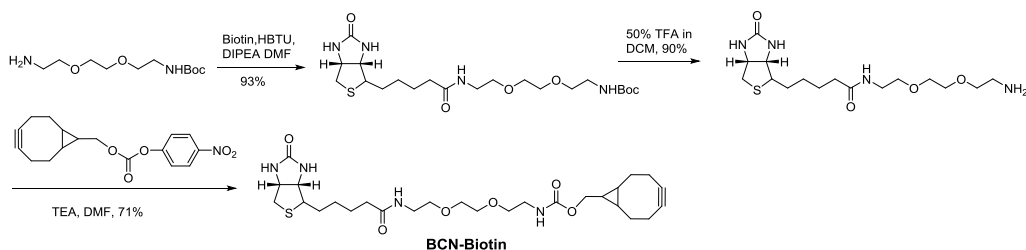


Figure 3.16 Synthesis of BCN-Biotin.

### Kinetics study

With the tetrazine modified sialic acid derivative in hand, we measured its reaction rates with TCO or BCN. To compare the kinetics with SPAAC (DIBO + Azide reaction:  $k_2 = 0.057 \text{ M}^{-1} \text{ s}^{-1}$  in methanol), we measured the reaction constants in MeOH or MeOD by UV spectroscopy or  $^1\text{H}$  NMR at 25°C.

DIBO does not react with disubstituted tetrazine,<sup>30</sup> probably due to the steric hindrance. And no cycloaddition reaction was observed between TCO and azide over a period of 5 hours at rt in MeOH. As a result, the DARinv between TCO and tetrazine **15** and SPAAC between DIBO and azide are orthogonal, which is useful for further study in dual labeling.

BCN reacted with tetrazine through DARinv and also reacted with azide through 1, 3-dipolar cycloaddition (SPAAC). The kinetics of the three click-type reactions was compared

(Figure 3.17) and it was found that TCO-tetrazine pair gave the fastest kinetics, which was 50 times faster than DIBO-azide pair. Consequently, we believe the new two-step SEEL using DARinv will be more advantageous and better labeling capabilities than SPAAC.

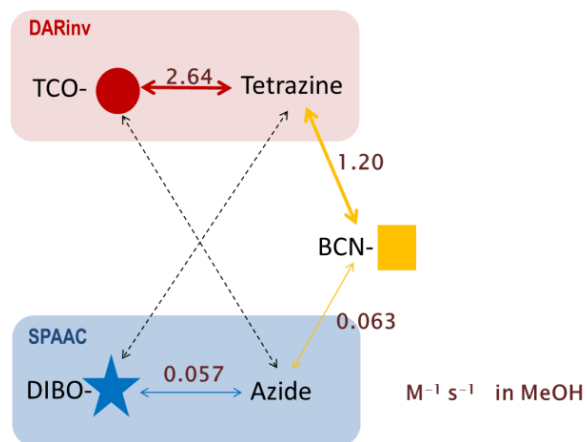


Figure 3.17 Comparison of two click-type reactions.

Dashed lines highlight reactants that do not react with each other under tested conditions.

#### SPAAC two-step SEEL VS New Tetrazine-TCO Two-step SEEL

The efficiency of the previously reported SPAAC two-step SEEL (with azide modified CMP-sialic acid **1**) and tetrazine-TCO two-step SEEL (with tetrazine modified CMP-sialic acid **3**) was compared by western blot analysis (Figure 3.18). HeLa cells were first labeled by ST6Gla1 and CMP-sialic acid derivatives (**1** or **3**) with co-neuraminidase treatment, followed by click reaction with DIBO-biotin or TCO-biotin for 15 min or 60 min. The efficiency of the various surface-labeling procedures was determined by SDS-PAGE of cell lysates followed by Western blotting using an anti-biotin antibody conjugated with HRP.

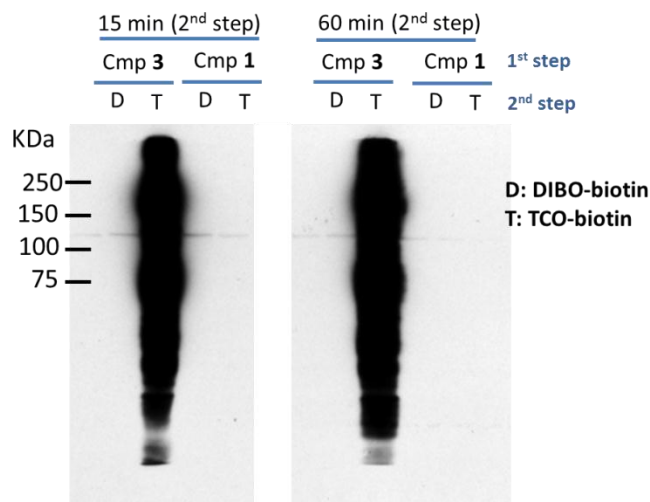


Figure 3.18 Western blot analysis of previously reported SPAAC two-step SEEL and new two-step SEEL labeled HeLa cells.

With 30s exposure, the new two-step SEEL with tetrazine modified CMP-sialic acid and TCO-biotin pair gave robust labeling, while there no labeling was observed for the old two-step SEEL with azide modified CMP-sialic acid, this indicates that the new two-step SEEL is far more efficient than the previous reported two-step SEEL.

#### One-step SEEL VS Tetrazine-TCO Two-step SEEL

The efficiency of one-step SEEL and Tetrazine-TCO Two-step SEEL was also compared by western blot analysis (Figure 3.19). HeLa cells were labeled by ST6Gla1 and CMP-sialic acid derivatives (**2** or **3**) with pre-neuraminidase treatment or co-neuraminidase treatment for 0.5h, 1h and 2h. SEEL labeling with compound **3** was followed by incubation with TCO-biotin for 15 min. The efficiency of the various surface-labeling procedures was determined by SDS-PAGE of cell lysates followed by Western blotting using an anti-biotin antibody conjugated with HRP.



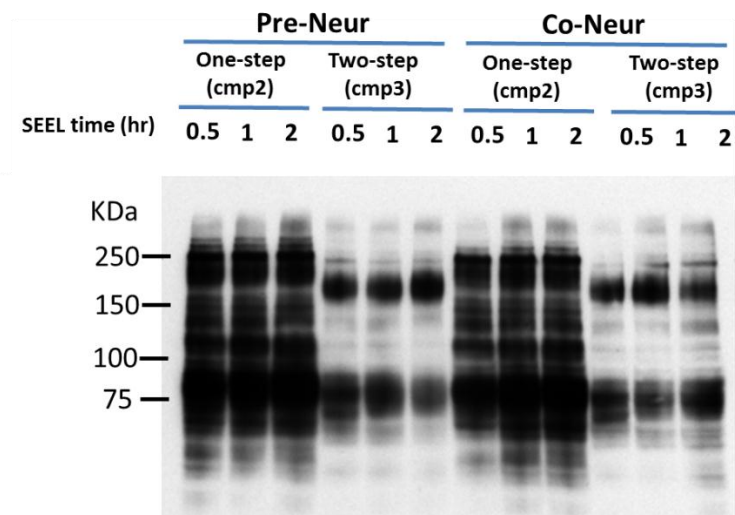


Figure 3.19 Western blot analysis of one-step SEEL and two-step SEEL labeled HeLa cells. SEEL labeling with compound **3** was followed by incubation with TCO-biotin for 15 min.

As we can see, tetrazine-TCO two-step SEEL has approximately 30% of the efficiency of the one-step SEEL. This is not surprising because the two-step SEEL still requires a click reaction after installation of the modified sialic acid. There was no difference between pre-neuraminidase treatment and co-neuraminidase treatment which indicated that the neuraminidase (from *Vibrio cholerae* (VC) or *Arthrobacter ureafaciens* (AU)) cannot remove the modified sialic acid moiety with the tetrazine at C5, similar to the results with the biotin at this position. Furthermore, for both one-step SEEL and new two-step SEEL, 30 min incubation with CMP-sialic acid derivatives is enough to give robust labeling.

#### Western blot using Tetrazine-PEG3-CMP-sialic acid and BCN-Biotin

In addition to the two-step SEEL using tetrazine-CMP-sialic acid (**3**) and TCO-biotin, we also explored labeling efficiency using tetrazine-PEG3-CMP-sialic acid (**17**) and BCN-biotin. HeLa cells were first labeled by ST6Gla1 and CMP-sialic acid derivatives (**3** or **17**) with

co-neuraminidase treatment, followed by click reaction with TCO-biotin or BCN-biotin for 15 min or 30 min. The efficiency of the various surface-labeling procedures was determined by SDS-PAGE of cell lysates followed by Western blotting using an anti-biotin antibody conjugated with HRP.

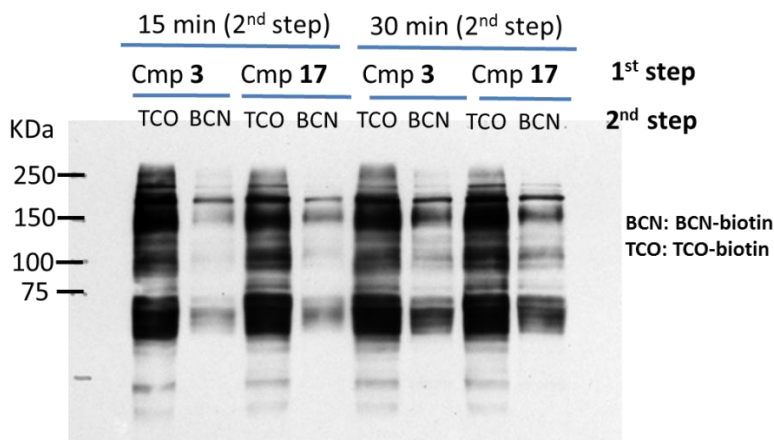


Figure 3.20 Western blot analysis of two-step SEEL labeled HeLa cells using tetrazine-CMP-sialic acid (**3**) and tetrazine-PEG<sub>3</sub>-CMP-sialic acid (**17**) following click reaction with TCO-biotin or BCN-biotin.

The western blot analysis showed that CMP-sialic acid derivative **17** with the short PEG-linker slightly improved the efficiency of labeling. Furthermore, the BCN-tetrazine pair gave a much weaker signal compared to the TCO-Tetrazine pair. For BCN-tetrazine pair, a 30 min incubation of BCN-biotin during the second step resulted in better labeling than a 15 min incubation, while longer incubation time did not affect the labeling efficiency for TCO-tetrazine pair.

#### Glycosylation status analysis of CD44

After confirming the high efficiency of labeling using tetrazine-CMP-sialic acid (**3**), the glycosylation status of one identified glycoprotein (CD44) on HeLa cells was assessed by

Western blotting. CD44 is known as cell surface glycoproteins modified by *N*-glycans. HeLa cells were first labeled by ST6Gal1 and tetrazine-CMP-sialic acid (**3**) with co-neuraminidase treatment, followed by click reaction with TCO-PEG5K with different concentrations: 0, 15, 30, 60  $\mu$ M. The lysates were analyzed by Western blotting using protein-specific antibodies towards CD44. As shown in Figure 3.21, 15  $\mu$ M TCO-PEG5K treatment showed several protein bands which had higher molecular weight than untreated protein, because the conjugations of heavy linker chain on this protein. 30 $\mu$ M TCO-PEG5K gave stronger labeling for the higher molecular weight bands, and less labeling for the lower molecular weight bands, indicating that more glycosylation sites of protein were labeled by PEG5K. 60 $\mu$ M TCO-PEG5K did not give better labeling than 30 $\mu$ M TCO-PEG5K, indicating that 30 $\mu$ M TCO-PEG5K saturated all the glycosylation sites of this protein.

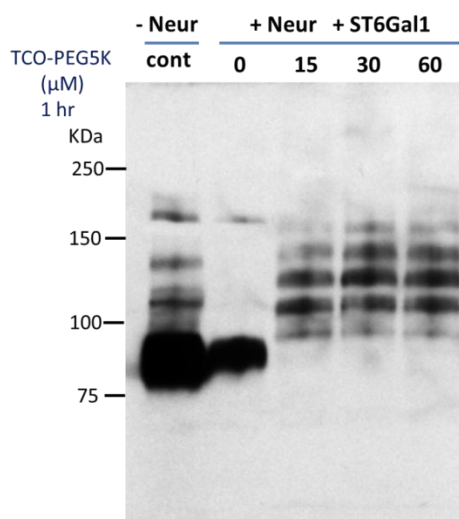


Figure 3.21 Western blot analysis of Two-step SEEL labeled CD44 using tetrazine-CMP-sialic acid (**3**) and protein-specific antibodies towards CD44. The labeling was followed by click reaction with TCO-PEG5K with different concentrations: 0, 15, 30, 60  $\mu$ M.

In this way, we can easily monitor the *N*-glycosylation status of CD44 by using ST6Gal1

and protein-specific antibodies. By using other protein-specific antibodies and glycosyltransferases (ST3Gal1, ST6GalNAc1 *et al*), we can also explore many other proteins' properties, which is very useful for better understanding of involved physiological and disease processes.

## Conclusion

We have demonstrated a remarkable two-step SEEL procedure to analyze cell surface glycoproteins by employing CMP-sialic acid modified by tetrazine and TCO modified by biotin or heavy PEG linker. The fast bioorthogonal click reaction----inverse electron demand Diels-Alder reaction results in a shorter click reaction time and high efficiency labeling compared to previously reported two-step SPAAC labeling conditions. The tetrazine modified sialic acid is also not removed by neuraminidase, similar to biotin-bearing sialic acids, allowing labeling to be carried out in the presence of the neuraminidase, limiting the effects that desialylation would have on the cell surface residence or endocytosis of glycoproteins.

Two-step SEEL with TCO-PEG5K followed by western blot analysis with protein-specific antibodies could easily analyze protein by protein glycosylation status (*N*- vs. *O*-linked glycans) using different sialyltransferases (ST3Gal1, ST6Gal1, ST6GalNAc1 *et al*) in different cell types. Current technologies to study protein glycosylation (e.g. HPLC-MS, MS/MS) rely on many techniques, such as peptide fragmentation, sample preparation, MS analysis, and data interpretation. *et al*,<sup>31,32</sup> and still need to be further optimized. Our new technology has a very simple procedure, and relies on protein-specific antibodies that are

available from many sources. Furthermore, the diversity of TCO attached compounds provides many possibilities that can be used to analyze subsets of cell surface glycoconjugates in details. For example, two-step SEEL with TCO-fluorophore could be employed to study the trafficking of cell surface glycoconjugates, and two-step SEEL with TCO-glycan, for example, TCO-HS (heparan sulfate) could easily engineer the cell surface and mimic the natural HS polymer, and thus modulate cellular functions such as cell differentiation and proliferation, cell-cell adhesion and communication. We believe this new technology will find numerous applications in other areas of biology and biomedicine.

## **Experimental section**

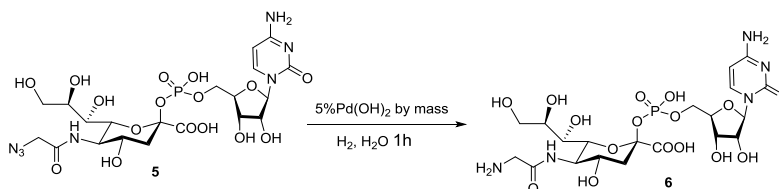
### General methods and materials:

D-mannosamine HCl were purchased from Carbosynth LLC. Other reagents were obtained from commercial sources and used as purchased. Dichloromethane (DCM) was freshly distilled using standard procedures. Other organic solvents were purchased anhydrous and used without further purification. Unless otherwise noted, all reactions were carried out at room temperature (RT) in glassware with magnetic stirring. Organic solutions were concentrated under reduced pressure with bath temperatures < 30 °C. Flash column chromatography was carried out on silica gel G60 (Silicycle, 60-200  $\mu\text{m}$ , 60 Å). Thin-layer chromatography (TLC) was carried out on Silica gel 60 F<sub>254</sub> (EMD Chemicals Inc.) with detection by UV absorption (254 nm) where applicable, by spraying with 20% sulfuric acid in ethanol followed by charring at ~150 °C or by spraying with a solution of (NH<sub>4</sub>)<sub>6</sub>Mo<sub>7</sub>O<sub>24</sub>·H<sub>2</sub>O (25 g/L) in 10% sulfuric acid in ethanol followed by charring at

~150°C.  $^1\text{H}$  and  $^{13}\text{C}$  NMR spectra were recorded on a Varian Inova-300 (300/75 MHz), a Varian Inova-500 (500 MHz) and a Varian Inova-600 (600/150 MHz) spectrometer equipped with sun workstations. Multiplicities are quoted as singlet (s), doublet (d), doublet of doublets (dd), triplet (t) or multiplet (m). All NMR signals were assigned on the basis of  $^1\text{H}$  NMR,  $^{13}\text{C}$  NMR, gCOSY and gHSQC experiments. All chemical shifts are quoted on the  $\delta$ -scale in parts per million (ppm). Residual solvent signals were used as an internal reference. Mass spectra were recorded on an Applied Biosystems 5800 MALDI-TOF or Shimadzu LCMS-IT-TOF mass spectrometer. The matrix used was 2,5-dihydroxy-benzoic acid (DHB). Reverse-Phase HPLC was performed on an Agilent 1200 series system equipped with an auto-sampler, fraction-collector, UV-detector and eclipse XDB-C18 column (5  $\mu\text{m}$ , 4.6  $\times$  250 mm or 9.4  $\times$  250 mm).

### Chemical synthesis.

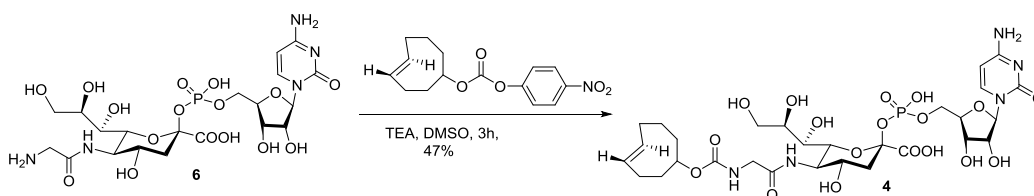
#### **Cytidine-5' -monophospho-5-aminoacetamido-3, 5- dideoxy- $\beta$ -D-glycero-D-galacto-2-nonulopyranosonic acid (6)**



CMP-Neu5N<sub>3</sub> (**5**, 5 mg, 0.0076mmol) was dissolved in water (1mL), Pd(OH)<sub>2</sub> (Palladium hydroxide on carbon, 20 wt. % loading, 0.25 mg, 5% by weight) was added. The reaction flask was thrice evacuated and flushed with hydrogen and the reaction mixture was stirred at room temperature in dark and under hydrogen atmosphere. After 1 hour's stirring, the catalyst was

removed by Acrodisc syringe filter (0.2  $\mu\text{m}$ ), and the solution was concentrated under reduced pressure to give **6** as a white solid (4.4 mg, 92%).  $^1\text{H}$  NMR (300 MHz,  $\text{d}_2\text{O}$ )  $\delta$  8.01 – 7.89 (m, 1H, H-6, cyt), 6.19 – 5.99 (m, 1H, H-5, cyt), 5.86 (d,  $J$  = 4.3 Hz, 1H, H-1, rib), 4.27 – 3.60 (m, 12H), 3.57 – 3.48 (m, 1H, H-9b), 3.33 (d,  $J$  = 9.5 Hz, 1H), 2.39 (dd,  $J$  = 13.1, 4.3 Hz, 1H, H-3eq), 1.51 (m, 1H, H-3ax). HRMS (ESI):  $m/z$  calcd for  $\text{C}_{20}\text{H}_{30}\text{N}_7\text{O}_{16}\text{P}$   $[\text{M}-\text{H}]^-$ : 628.1509; found: 628.1345.

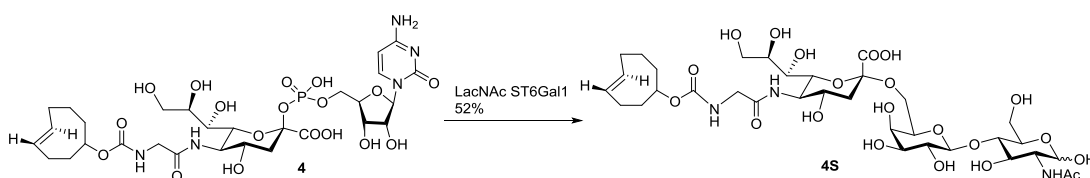
#### TCO-CMP-Neu5NH<sub>2</sub> (**4**)



**6** (5 mg, 0.0079mmol) and TCO-PNP (6.9 mg, 0.0237mmol) were dissolved in DMSO (1mL), TEA (80  $\mu\text{L}$ ) was added. After 3 hours stirring at room temperature in dark, 1 mL 100mM  $\text{NH}_4\text{HCO}_3$  was added and the resulted mixture was lyophilized and the residue was applied to a C18 column, which was eluted with a gradient of methanol in 0.1 M  $\text{NH}_4\text{HCO}_3$  buffer (3%  $\rightarrow$ 20%). Fractions containing product were concentrated under reduced pressure, and the residue was redissolved in 1 mL water and lyophilized to give **4** (2.9 mg, 47%) as a white solid.  $^1\text{H}$  NMR (800 MHz,  $\text{d}_2\text{O}$ )  $\delta$  7.94 (dd,  $J$  = 35.2, 7.7 Hz, 1H, H-6, cyt), 6.10 – 5.99 (m, 1H, H-5, cyt), 5.85 (d,  $J$  = 4.3 Hz, 1H, H-1, rib), 5.63 (d,  $J$  = 11.5 Hz, 1H, H-1 or H-2, TCO), 5.57 (d,  $J$  = 9.8 Hz, 1H, H-2 or H-1, TCO), 4.56 (s, 1H, H-5, TCO), 4.24 – 4.17 (m, 2H, H-2,3 rib), 4.17 – 4.03 (m, 4H, H-4,5 rib, H-6 Neu), 4.03 – 3.92 (m, 1H, H-4), 3.87 (t,  $J$  = 10.0 Hz, 1H, H-5), 3.80 (q,  $J$  = 9.9, 8.6 Hz, 1H, H-8), 3.74 (t,  $J$  = 13.0 Hz, 3H,  $\text{NH}-\text{CH}_2-\text{C}=\text{O}$ , H-9a), 3.49 (d,  $J$  = 10.5 Hz, 1H, H-9b), 3.30 (d,  $J$  = 9.5 Hz, 1H, H-7), 2.36 (dd,  $J$  = 13.3, 4.8 Hz, 1H, H-3eq), 2.28 – 2.17 (m,

1H, H-3a TCO), 2.04 (d,  $J = 6.0$  Hz, 2H, H-8 TCO), 1.97 (dt,  $J = 13.0, 6.4$  Hz, 1H, H-3b TCO), 1.77 (dd,  $J = 20.1, 15.2$  Hz, 2H, H-4 TCO), 1.62 (s, 1H, H-6a TCO), 1.55 – 1.46 (m, 3H, H-6b TCO, H-3ax Neu, H-7a TCO), 1.38 (s, 1H, H-7b TCO).  $^{13}\text{C}$  NMR (201 MHz,  $\text{d}_2\text{O}$ )  $\delta$  142.6, 130.3, 130.0, 96.0, 89.2, 83.1, 77.9, 74.2, 71.6, 69.7, 69.2, 69.2, 68.8, 66.6, 64.7, 64.6, 63.6, 63.2, 63.1, 51.7, 43.7, 41.1, 41.0, 33.3, 33.3, 33.3, 25.1, 24.4, 24.3, 21.5, 21.5.

#### TCO-Neu5Ac $\alpha$ (2,6)Gal $\beta$ (1,4)GlcNAc (**4S**)

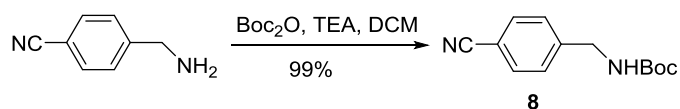


Recombinant  $\alpha$ -(2,6)-sialyltransferase (ST6Gal I) [GenBank P13721] (0.63 mg/mL, 23.2  $\mu\text{L}$ ) and calf intestine alkaline phosphatase (10000 U/mL, 2.5  $\mu\text{L}$ ) were added to a mixture of LacNAc (0.37 mg, 1.0  $\mu\text{mol}$ ) in cacodylate buffer (50 mM, pH 7.63, 96  $\mu\text{L}$ ) containing 0.1% BSA and **4** (1.5 mg, 1.9  $\mu\text{mol}$ ) in an Eppendorf tube. The tube was incubated at 37  $^{\circ}\text{C}$  in dark, and progress of the reaction was monitored by TLC (EtOAc :  $\text{CH}_3\text{OH}$  :  $\text{H}_2\text{O}$  : AcOH = 4:2:1:0.5, v:v:v:v), which after 6 hours indicated completion of the reaction.  $\text{CH}_3\text{OH}$  (0.5  $\mu\text{L}$ ) was added and the mixture was lyophilized to provide a residue that was applied to a C18 column, which was eluted with a gradient of methanol in water (5%  $\rightarrow$ 20%). Fractions containing product were concentrated under reduced pressure, and the residue was redissolved in 1 mL water and lyophilized to provide **4S** as a white solid (0.4 mg, 52%).  $^1\text{H}$  NMR (800 MHz,  $\text{d}_2\text{O}$ )  $\delta$  5.58 (dt,  $J = 29.7, 8.9$  Hz, 2H, H-1, H-2, TCO), 5.06 (d,  $J = 2.8$  Hz, 1H, H-1'), 4.54 – 4.52 (m, 1H, H-5 TCO), 4.31 (dd,  $J = 7.9, 3.0$  Hz, 1H, H-1''), 3.88 – 3.80 (m, 2H), 3.79 (q,  $J = 3.9, 3.2$  Hz, 2H),



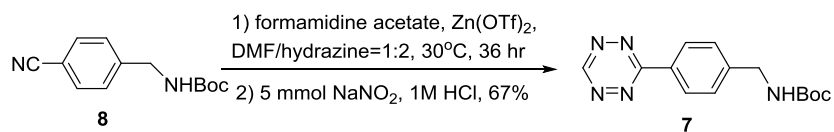
3.77 – 3.65 (m, 7H), 3.64 – 3.45 (m, 7H), 3.44 – 3.37 (m, 3H), 2.53 (dd,  $J = 12.4, 4.7$  Hz, 1H, H-3eq), 2.22 (s, 1H, H-3a TCO), 2.02 (ddd,  $J = 15.6, 10.0, 6.0$  Hz, 2H, H-8 TCO), 1.98 – 1.90 (m, 4H, H-3b TCO, Ac), 1.79 – 1.71 (m, 2H, H-4 TCO), 1.63 – 1.55 (m, 2H, H-6a TCO, H-3ax Neu), 1.51 (d,  $J = 15.4$  Hz, 2H, H-6b, H-7a TCO), 1.36 (s, 1H, H-7b TCO).  $^{13}\text{C}$  NMR (201 MHz,  $\text{d}_2\text{o}$ )  $\delta$  130.0, 129.8, 102.9, 90.8, 80.7, 77.9, 73.4, 72.0, 71.7, 71.7, 69.6, 69.2, 68.8, 63.7, 63.5, 62.7, 60.9, 60.5, 56.1, 53.1, 43.8, 40.2, 40.2, 33.5, 33.5, 33.3, 25.2, 24.7, 24.5, 22.2, 22.1, 21.9. HRMS (ESI):  $m/z$  calcd for  $\text{C}_{46}\text{H}_{74}\text{N}_9\text{O}_{24}\text{S}$   $[\text{M-H}]^-$ : 1168.4573; found: 1168.3288.

***tert*-butyl (4-cyanobenzyl)carbamate (8)**



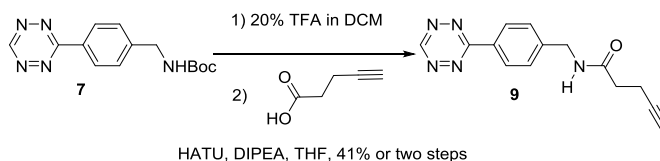
4-(aminomethyl)benzonitrile hydrochloride (1g, 5.9 mmol) was dissolved in DCM under argon. After addition of triethylamine (TEA, 2.1 mL, 14.8 mmol) and Di-*tert*-butyl dicarbonate ( $(\text{Boc})_2\text{O}$ , 1.5 mL, 6.5 mmol), the reaction mixture was stirred at room temperature overnight. Then the reaction mixture was concentrated under reduced pressure to give a residue that was purified by silica gel column chromatography using a gradient of ethyl acetate in hexane (15%  $\rightarrow$  20%) to give **8** as a white solid (1.35 g, 99%).  $^1\text{H}$  NMR (300 MHz,  $\text{cdcl}_3$ )  $\delta$  7.61 (d,  $J = 8.3$  Hz, 2H, phH), 7.38 (d,  $J = 8.1$  Hz, 2H, phH), 4.97 (bs, 1H, NH), 4.36 (d,  $J = 6.3$  Hz, 2H,  $\text{CH}_2$ ), 1.45 (s, 9H, Boc).

***tert*-butyl 4-(1,2,4,5-tetrazin-3-yl)benzylcarbamate (7)**



To a 100 mL flask equipped with a stir bar,  $\text{Zn}(\text{OTf})_2$  (454 mg, 1.25 mmol), formamidine acetate (2.6 g, 25 mmol), **8** (581 mg, 2.5 mmol), DMF (2 mL), and anhydrous hydrazine (4 mL) were added. The flask was sealed and the mixture was stirred at 30 °C for 36 hours. The color was changed from pink to yellow. Sodium nitrite (3.45 g, 50 mmol) in water (50 mL) was slowly added to the solution and followed by slow addition of 1M HCl during which the solution turned bright red in color and gas evolved. 1M HCl was continually added until gas evolution ceased and the pH value was 3. The mixture was extracted with EtOAc and the organic phase dried over sodium sulfate. The EtOAc was removed using rotary evaporation and the residue purified using silica column chromatography (Hexane:EtOAc=7:1) to give **7** (480 mg, 67%) as a purple solid.  $^1\text{H}$  NMR (300 MHz,  $\text{cdcl}_3$ )  $\delta$  10.21 (s, 1H, H-3 tetrazine), 8.59 (d,  $J$  = 8.1 Hz, 2H, pH), 7.52 (d,  $J$  = 8.1 Hz, 2H, pH), 4.97 (bs, 1H, NH), 4.44 (d,  $J$  = 6.1 Hz, 2H,  $\text{CH}_2$ ), 1.49 (s, 9H, Boc).  $^{13}\text{C}$  NMR (126 MHz,  $\text{cdcl}_3$ )  $\delta$  159.1, 128.9, 128.3, 44.5, 28.2. HRMS  $[\text{M}+\text{Na}]^+$   $m/z$  calcd. for  $[\text{C}_{14}\text{H}_{17}\text{N}_5\text{O}_2\text{Na}]^+$  310.1276, found 310.1274.

***N*-(4-(1,2,4,5-tetrazin-3-yl)benzyl)pent-4-ynamide (9)**



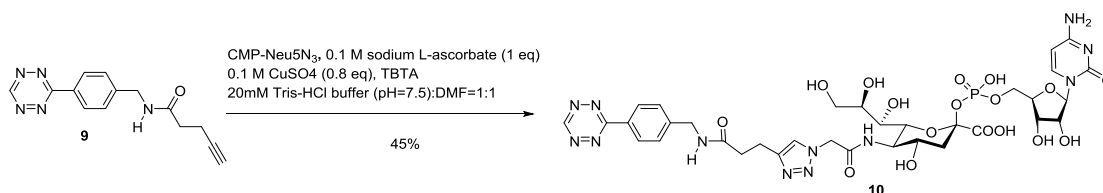
**7** (150 mg, 0.52 mmol) was dissolved in DCM (4 mL), TFA (1 mL) was added. The reaction mixture was stirred at room temperature for 2 hours before it was concentrated under reduced pressure. The residue was then dissolved in dry THF (4 mL), the resulted solution was cooled to 0 °C. 4-pentynoic acid (61.5 mg, 0.63 mmol), 1-[Bis(dimethylamino)methylene]-1H-1,2,3-triazolo[4,5-b]pyridinium 3-oxid hexafluorophosphate (HATU, 240 mg, 0.63 mmol) and

*N,N*-Diisopropylethylamine (370  $\mu$ L, 2.1 mmol) were added. The reaction mixture was then warmed to room temperature and stirred for 18 hours in dark before it was concentrated under reduced pressure to give a residue that was purified by silica gel column chromatography using a gradient of ethyl acetate in hexane (30%  $\rightarrow$ 50%) to give **9** (57 mg, 41%) as a purple solid.

Step 1:  $^1\text{H}$  NMR (500 MHz,  $\text{d}_2\text{o}$ )  $\delta$  10.28 (d,  $J$  = 1.6 Hz, 1H, H-3 tetrazine), 8.41 (d,  $J$  = 8.7 Hz, 2H, PhH), 7.61 (d,  $J$  = 9.1 Hz, 2H, PhH), 4.21 (s, 2H,  $\text{CH}_2$ ).

Step 2:  $^1\text{H}$  NMR (300 MHz,  $\text{cdcl}_3$ )  $\delta$  10.22 (s, 1H, H-3 tetrazine), 8.59 (d,  $J$  = 7.9 Hz, 2H, PhH), 7.53 (d,  $J$  = 7.6 Hz, 2H, PhH), 6.07 (bs, 1H, NH), 4.61 (m, 2H,  $\text{CH}_2\text{NH}$ ), 2.55 (d,  $J$  = 27.9 Hz, 4H,  $\text{CH}_2\text{CH}_2$ ), 2.03 (s, 1H,  $\text{C}\equiv\text{CH}$ ).

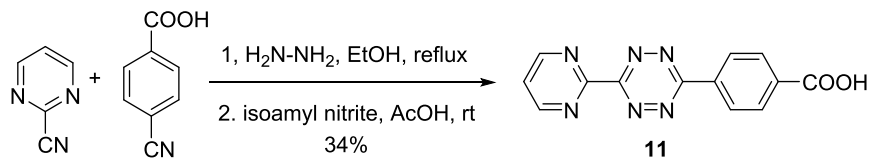
### Tetrazine-CMP-Neu5N<sub>3</sub> (**10**)



A solution of compound **9** (2.7 mg, 0.01 mmol) in DMF (0.5 mL) was added to the solution of CMP-Neu5N<sub>3</sub> (5 mg, 0.076 mmol) in Tris-HCl buffer (100 mM, pH 7.5, 0.5 mL). To this mixture was added CuSO<sub>4</sub> (100 mM, 61  $\mu$ L), sodium L-ascorbate (100 mM, 76  $\mu$ L) and TBTA (1.2 mg, 0.0023 mmol). After stirring for 2 hours at ambient temperature in dark, the reaction mixture was lyophilized to provide a residue that was applied to a C18 column, which was eluted with a gradient of methanol in 0.1 M  $\text{NH}_4\text{HCO}_3$  buffer (1%  $\rightarrow$ 10%). Fractions containing product were concentrated under reduced pressure, and the residue was redissolved in 1 mL water and

lyophilized to provide **10** as a purple solid (3.2 mg, 45%).  $^1\text{H}$  NMR (600 MHz,  $\text{d}_2\text{O}$ )  $\delta$  10.22 (m, 1 H, H-3 tetrazine), 8.31 – 8.23 (m, 2H, PhH), 7.82 (t,  $J = 6.7$  Hz, 1H, H-6, cyt), 7.63 (d,  $J = 5.2$  Hz, 1H, CH=C, triazole), 7.27 (d,  $J = 8.1$  Hz, 2H, PhH), 5.98 (s, 1H, H-5, cyt), 5.83 (t,  $J = 5.6$  Hz, 1H, H-1, rib), 5.14 – 4.99 (m, 2H, triazole- $\text{CH}_2\text{-C=O}$ ), 4.32 – 4.16 (m, 3H, NH- $\text{CH}_2\text{-Ph}$ , H-3, rib), 4.14 (t,  $J = 4.8$  Hz, 1H, H-2, rib), 4.12 – 4.03 (m, 4H, H-4 rib, H-5 rib, H-6 Neu), 3.98 (tt,  $J = 11.0, 5.5$  Hz, 1H, H-4), 3.89 – 3.81 (m, 1H, H-5), 3.77 (ddt,  $J = 9.1, 6.4, 3.6$  Hz, 1H, H-8), 3.71 (dt,  $J = 11.9, 3.6$  Hz, 1H, H-9a), 3.45 (dd,  $J = 12.0, 6.5$  Hz, 1H, H-9b), 3.29 (dd,  $J = 9.1, 7.2$  Hz, 1H, H-7), 2.91 (dt,  $J = 14.4, 7.1$  Hz, 2H, triazole- $\text{CH}_2\text{CH}_2\text{C=O}$ ), 2.57 (dt,  $J = 19.0, 7.3$  Hz, 2H, triazole- $\text{CH}_2\text{CH}_2\text{C=O}$ ), 2.34 (dt,  $J = 13.3, 4.8$  Hz, 1H, H-3eq), 1.49 (td,  $J = 12.5, 5.7$  Hz, 1H, H-3ax).  $^{13}\text{C}$  NMR (151 MHz,  $\text{d}_2\text{O}$ )  $\delta$  157.3, 141.5, 128.4, 128.0, 124.7, 89.0, 82.8, 74.2, 71.4, 69.5, 69.2, 69.1, 66.6, 64.7, 62.8, 62.8, 52.1, 51.9, 42.6, 41.0, 41.0, 35.0, 21.0. HRMS (ESI):  $m/z$  calcd for  $\text{C}_{41}\text{H}_{63}\text{N}_{11}\text{O}_{21}\text{PS}$   $[\text{M-H}]^-$ : 1108.3664; found  $m/z$ : 1108.2461.

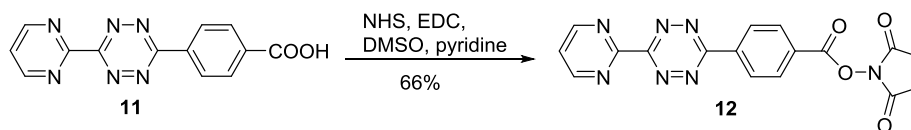
#### 4-(6-(Pyrimidin-2-yl)-1,2,4,5-tetrazin-3-yl)benzoic acid (**11**)



4-Cyanobenzoic acid (3.5 g, 24 mmol) and pyrimidin-2-carbonitrile (2.5 g, 24 mmol) were suspended in dry EtOH (10 mL) and hydrazine (3.84 mL, 120 mmol) was added dropwise. Subsequently, the mixture was stirred at reflux temperature for 18 h. After cooling to room temperature, the formed orange precipitate was filtered off and washed with small volumes of EtOH. In order to remove the symmetrical byproduct bis(pyrimidin-2-yl)-1,2,4,5-dihydropyrimidin-4-one, the solid was stirred in refluxing acetone (15 mL) and filtered off in the heat.

This procedure was repeated once. The filtered off orange solid was suspended in acetic acid (60 mL) and oxidized by slow addition of isopentyl nitrite (3.04 mL, 36 mmol). After stirring overnight, ethyl ether (95 mL) was added in order to precipitate the purple product mixture. The ether layer was removed by centrifugation, and the solid was washed with ethyl ether for three times. **11** (2.3g, 34 %) was collected as purple solid that still contained small amounts of the tetrazinyldibenzoic acid.  $^1\text{H}$  NMR (300 MHz, DMSO- $d_6$ ):  $\delta$  13.35 (br. s, 1 H; COOH), 9.20 (d,  $J$  = 4.9 Hz, 2 H; H-4'' and H-6''), 8.71 (m, 2 H; H-2 and H-6 or H-3 and H-5), 8.25 (m, 2 H; H-2 and H-6 or H-3 and H-5), 7.84 (t,  $J$  = 4.9 Hz, 1 H; H-5'')  $^{13}\text{C}$  NMR (300 MHz, DMSO- $d_6$ ):  $\delta$  166.7, 163.2, 162.9, 159.0, 158.5, 135.3, 134.5, 130.2, 128.3, 127.9, 123.0

**2, 5-Dioxopyrrolidin-1-yl 6-(6-(pyrimidin-2-yl)-1,2,4,5-tetrazin-3-yl)benzoate (**12**)**



**11** (100 mg, 0.357mmol) was suspended in DMSO/pyridine (20:1, 4.2 mL) and N-hydroxysuccinimide (61.6 mg, 0.536 mmol) and EDC HCl (1-ethyl-3-(3-dimethylaminopropyl)carbodiimide hydrochloride) (102.8 mg, 0.536 mmol) were added. The mixture was heated to 40 °C and became clear after a few minutes. After 2 h, the solvent was removed under reduced pressure. The residue was redissolved in  $\text{CH}_2\text{Cl}_2$  and washed once with water. The aqueous layer was extracted once with  $\text{CH}_2\text{Cl}_2$ . The combined organic layers were dried over  $\text{MgSO}_4$ , filtered and the solvent was removed under reduced pressure. The residue was purified by silica gel column chromatography using 1% methanol in  $\text{CH}_2\text{Cl}_2$  to give **12** (89 mg, 66%) as a red crystalline solid.  $^1\text{H}$  NMR (300 MHz,  $\text{cdCl}_3$ )  $\delta$  9.16 (d,  $J$

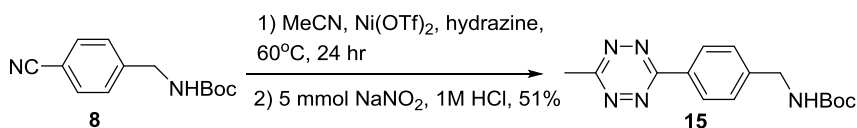
= 5.0 Hz, 2H, H-4'' and H-6''), 8.96 – 8.86 (m, 2H, H-2 and H-6 or H-3 and H-5), 8.40 (d,  $J$  = 8.2 Hz, 2H, H-2 and H-6 or H-3 and H-5), 7.62 (t,  $J$  = 4.9 Hz, 1H, H-5''), 2.95 (s, 4H, CH<sub>2</sub>CH<sub>2</sub>). ESI-TOF-HRMS (pos. mode):  $m/z$  = 378.0918 [M+H]<sup>+</sup>, 400.0748 [M+Na]<sup>+</sup> (calc.  $m/z$  = 378.0945 [M+H]<sup>+</sup>, 400.0765 [M+Na]<sup>+</sup>).

***N*-(but-3-yn-1-yl)-4-(6-(pyrimidin-2-yl)-1,2,4,5-tetrazin-3-yl)benzamide (13)**



To active ester **12** (50 mg, 0.133 mmol) in dry DMF (5 mL), 1-amino-3-butyne (16.3  $\mu$ L, 0.20 mmol) and triethylamine (56.0  $\mu$ L, 0.40 mmol) were added. After stirring for 1.5 hs at room temperature, TLC indicated the completion of the reaction. The solvent was removed under reduced pressure and the residue was purified by silica gel column chromatography using a gradient of methanol in CH<sub>2</sub>Cl<sub>2</sub> (0.5%  $\rightarrow$  1.5%) to give **13** (14.5 mg, 33%) as a purple solid. <sup>1</sup>H NMR (300 MHz, cdcl<sub>3</sub>)  $\delta$  9.15 (d,  $J$  = 4.9 Hz, 2H, H-4'' and H-6''), 8.96 – 8.86 (m, 2H, H-2 and H-6 or H-3 and H-5), 8.41 (d,  $J$  = 8.2 Hz, 2H, H-2 and H-6 or H-3 and H-5), 7.60 (t,  $J$  = 4.9 Hz, 1H, H-5''), 6.54 (bs, 1H, NH), 3.64 (q,  $J$  = 6.2 Hz, 2H, NHCH<sub>2</sub>), 2.55 (td,  $J$  = 6.3, 2.6 Hz, 2H, CH<sub>2</sub>C $\equiv$ C), 2.07 (t,  $J$  = 2.7 Hz, 1H, C $\equiv$ CH).

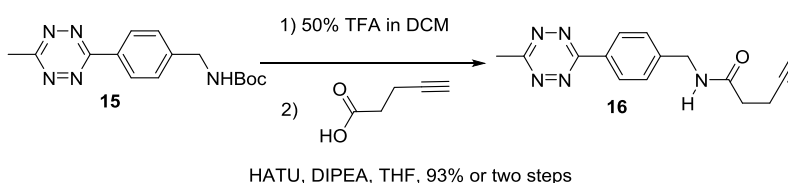
***tert*-butyl 4-(6-methyl-1,2,4,5-tetrazin-3-yl)benzylcarbamate (15)**



To a 10 mL flask equipped with a stir bar, Ni(OTf)<sub>2</sub> (367 mg, 1 mmol), acetonitrile (1.04 mL, 20 mmol), **8** (465 mg, 2 mmol) and anhydrous hydrazine (3.14 mL) were added. The vessel was

sealed and the mixture was stirred in an oil bath at 60 °C for 24 hours. The reaction solution was cooled to r. t. and the seal was removed. Sodium nitrite (2.76 g, 40 mmol) in 10 mL of water was slowly added to the solution followed by dropwise addition of 1M HCl during which the solution turned bright red in color and gas evolved. 1M HCl was continually added until gas evolution ceased and the pH value is 3. The mixture was extracted with EtOAc and the organic phase were washed with water (20mL \*2), brine (20mL), dried over sodium sulfate. The EtOAc was removed using rotary evaporation and the residue purified using silica column chromatography (Hexane:EtOAc=4:1) to give **15** (307mg, 51%) as a purple solid. <sup>1</sup>H NMR (500 MHz, cdcl<sub>3</sub>) δ 8.56 (d, *J* = 8.3 Hz, 2H, PhH), 7.51 (d, *J* = 8.1 Hz, 2H, PhH), 4.97 (bs, 1H, NH), 4.48 – 4.33 (m, 2H, CH<sub>2</sub>NH), 3.10 (s, 3H, CH<sub>3</sub>), 1.49 (s, 9H, Boc). <sup>13</sup>C NMR (126 MHz, cdcl<sub>3</sub>) δ 128.1, 128.0, 44.5, 28.5, 21.1.

***N*-(4-(6-methyl-1,2,4,5-tetrazin-3-yl)benzyl)pent-4-ynamide (16)**



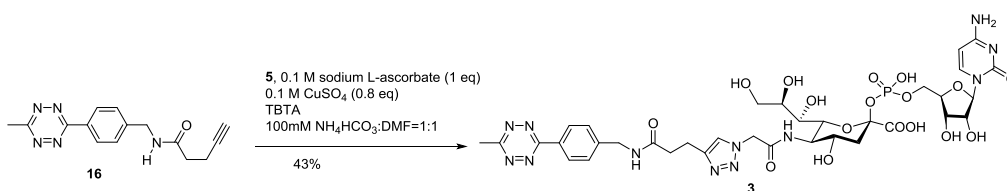
**15** (100 mg, 0.332 mmol) was dissolved in DCM (4 mL), TFA (4 mL) was added. The reaction mixture was stirred at room temperature for 1 hour before it was concentrated under reduced pressure. The residue was then dissolved in dry THF (4 mL), the resulted solution was cooled to 0 °C. 4-pentynoic acid (39 mg, 0.398 mmol), 1-[Bis(dimethylamino)methylene]-1H-1,2,3-triazolo[4,5-b]pyridinium 3-oxid hexafluorophosphate (HATU, 189.4 mg, 0.498 mmol) and *N,N*-Diisopropylethylamine (231 µL,

1.328 mmol) were added. The reaction mixture was then warmed to room temperature and stirred for 2 hours before it was concentrated under reduced pressure. The residue was diluted with ethyl acetate (10 mL), the solution was washed with 1 M HCl (10 mL \*2), brine, dried over MgSO<sub>4</sub> and the solvent was removed under reduced pressure. The residue was purified by silica gel column chromatography using a gradient of ethyl acetate in hexane (25% →50%) to give **16** (87 mg, 93%) as a purple solid.

Step 1: <sup>1</sup>H NMR (300 MHz, cdcl<sub>3</sub>) δ 8.81 (d, *J* = 8.3 Hz, 2H, PhH), 7.90 – 7.76 (m, 2H, PhH), 4.37 (s, 2H, CH<sub>2</sub>NH<sub>2</sub>), 3.27 (s, 3H, CH<sub>3</sub>).

Step 2: <sup>1</sup>H NMR (300 MHz, cdcl<sub>3</sub>) δ 8.56 (d, *J* = 8.3 Hz, 2H, PhH), 7.52 (d, *J* = 8.1 Hz, 2H, PhH), 6.02 (d, *J* = 9.1 Hz, 1H, NH), 4.60 (d, *J* = 6.0 Hz, 2H, CH<sub>2</sub>NH<sub>2</sub>), 3.10 (s, 3H, CH<sub>3</sub>), 2.60 (td, *J* = 6.5, 2.4 Hz, 2H, CH<sub>2</sub>CH<sub>2</sub>C≡C or CH<sub>2</sub>CH<sub>2</sub>C≡C), 2.49 (dd, *J* = 8.3, 6.4 Hz, 2H, CH<sub>2</sub>CH<sub>2</sub>C≡C or CH<sub>2</sub>CH<sub>2</sub>C≡C), 2.02 (t, *J* = 2.6 Hz, 1H, C≡CH).

### Tetrazine-CMP-Neu5N<sub>3</sub> (**3**)

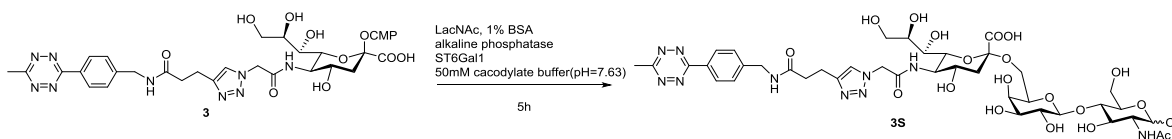


A solution of **16** (4.7 mg, 0.017 mmol) in DMF (1.5 mL) was added to the solution of CMP-Neu5N<sub>3</sub> (**5**, 10 mg, 0.015 mmol) in Tris-HCl buffer (100 mM, pH 7.5, 1.5 mL). To this mixture was added CuSO<sub>4</sub> (100 mM, 123 μL), sodium L-ascorbate (100 mM, 153 μL) and TBTA (1.6 mg, 0.0031 mmol). After stirring for 1 hour at ambient temperature, the reaction mixture was lyophilized to provide a residue that was applied to a C18 column, which was eluted with a



gradient of methanol in 0.1 M  $\text{NH}_4\text{HCO}_3$  buffer (3%  $\rightarrow$ 20%). Fractions containing product were concentrated under reduced pressure, and the residue was redissolved in 1 mL water and lyophilized to provide **3** (6.1 mg, 43%) as a purple solid.  $^1\text{H}$  NMR (600 MHz,  $\text{d}_2\text{O}$ )  $\delta$  8.43 (d,  $J$  = 7.9 Hz, 2H, PhH), 8.16 (dd,  $J$  = 18.3, 7.4 Hz, 1H, H-6, cyt), 7.89 (d,  $J$  = 8.1 Hz, 1H, CH=C, triazole), 7.48 (dd,  $J$  = 8.2, 6.2 Hz, 2H, PhH), 6.30 (m, 1H, H-5, cyt), 6.11 – 6.02 (m, 1H, H-1, rib), 5.33 (t,  $J$  = 4.7 Hz, 2H, triazole- $\text{CH}_2$ -C=O), 4.53 (s, 2H, NH- $\text{CH}_2$ -Ph), 4.42 (dt,  $J$  = 12.0, 3.0 Hz, 2H, H-2,3 rib), 4.38 – 4.26 (m, 4H, H-4, 5 rib, H-6), 4.26 – 4.15 (m, 1H, H-4), 4.08 (t,  $J$  = 10.3 Hz, 1H, H-5), 4.05 – 3.98 (m, 1H, H-8), 3.95 (dd,  $J$  = 11.6, 2.2 Hz, 1H, H-9a), 3.73 – 3.65 (m, 1H, H-9b), 3.54 (d,  $J$  = 9.1 Hz, 1H, H-7), 3.16 (m, 5H,  $\text{O}=\text{CCH}_2\text{CH}_2$ -triazole,  $\text{CH}_3$ ), 2.82 (t,  $J$  = 6.4 Hz, 2H,  $\text{O}=\text{CCH}_2\text{CH}_2$ -triazole), 2.58 (d,  $J$  = 12.5 Hz, 1H, H-3eq), 1.74 (s, 1H, H-3ax).  $^{13}\text{C}$  NMR (151 MHz,  $\text{d}_2\text{O}$ )  $\delta$  142.7, 128.6, 128.0, 126.8, 89.3, 83.1, 74.2, 71.5, 69.6, 69.2, 68.8, 66.6, 64.7, 62.9, 62.9, 52.1, 52.0, 42.6, 41.0, 41.0, 35.7, 21.1, 20.0. HRMS (ESI):  $m/z$  calcd for  $\text{C}_{35}\text{H}_{44}\text{N}_{12}\text{O}_{17}\text{P}$  [ $\text{M}-\text{H}$ ] $^-$ : 935.2690; found  $m/z$ : 935.2063.

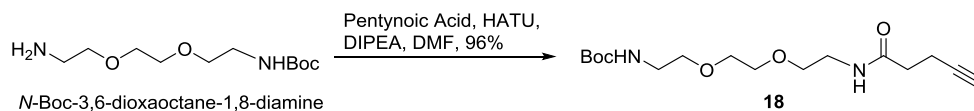
### Tetrazine-Neu5Ac $\alpha$ (2,6)Gal $\beta$ (1,4)GlcNAc (**3S**)



Recombinant  $\alpha$ -(2,6)-sialyltransferase (ST6Gal I) [GenBank P13721] (0.63 mg/mL, 19  $\mu\text{L}$ ) and calf intestine alkaline phosphatase (10000 U/mL, 2  $\mu\text{L}$ ) were added to a mixture of LacNAc (0.57 mg, 1.5  $\mu\text{mol}$ ) in cacodylate buffer (50 mM, pH 7.63, 76  $\mu\text{L}$ ) containing 0.1% BSA and **3** (1.4 mg, 1.5  $\mu\text{mol}$ ) in an Eppendorf tube. The tube was incubated at 37  $^\circ\text{C}$ , and progress of the reaction was monitored by TLC ( $\text{EtOAc} : \text{CH}_3\text{OH} : \text{H}_2\text{O} : \text{AcOH} = 4:2:1:0.5$ , v:v:v:v), which

after 3 hour indicated completion of the reaction. CH<sub>3</sub>OH (1  $\mu$ L) was added and the mixture was lyophilization to provide a residue that was applied to a C18 column, which was eluted with a gradient of methanol in water (5%  $\rightarrow$ 20%). Fractions containing product were concentrated under reduced pressure, and the residue was redissolved in 1 mL water and lyophilized to give **3S** (0.7 mg, 49%) as a purple solid. <sup>1</sup>H NMR (800 MHz, d<sub>2</sub>O)  $\delta$  8.46 – 8.41 (m, 2H, PhH), 7.83 (s, 1H, CH=C, triazole), 7.48 (d,  $J$  = 7.9 Hz, 2H, PhH), 5.28 (m, 2H, triazole-CH<sub>2</sub>-C=O), 5.26 – 5.24 (m, 1H, H-1'), 4.52 (q,  $J$  = 3.7 Hz, 3H, NH-CH<sub>2</sub>-Ph, H-1''), 4.09 – 4.02 (m, 2H), 4.00 (t,  $J$  = 3.9 Hz, 1H), 3.99 – 3.97 (m, 1H), 3.97 – 3.85 (m, 8H), 3.80 – 3.65 (m, 6H), 3.62 (ddtd,  $J$  = 12.6, 10.0, 7.9, 7.3, 2.4 Hz, 3H), 3.16 (s, 3H, CH<sub>3</sub>-tetrazine), 3.16 – 3.13 (m, 2H, O=CCH<sub>2</sub>CH<sub>2</sub>-triazole), 2.80 (q,  $J$  = 6.6, 6.1 Hz, 2H, O=CCH<sub>2</sub>CH<sub>2</sub>-triazole), 2.75 (dt,  $J$  = 12.4, 4.8 Hz, 1H, H-3eq), 2.30 (s, 2H), 2.06 (d,  $J$  = 4.8 Hz, 3H, Ac), 1.79 (td,  $J$  = 12.3, 5.0 Hz, 1H, H-3ax). <sup>13</sup>C NMR (201 MHz, d<sub>2</sub>O)  $\delta$  128.0, 127.9, 124.7, 103.4, 90.5, 80.7, 74.4, 73.6, 72.4, 72.3, 72.2, 71.7, 70.7, 69.9, 69.2, 68.3, 68.3, 68.1, 63.3, 63.3, 62.6, 62.5, 60.2, 60.2, 60.1, 55.9, 53.4, 52.1, 51.9, 42.6, 40.0, 40.0, 35.0, 22.1, 21.0, 20.0. HRMS (ESI):  $m/z$  calcd for C<sub>41</sub>H<sub>63</sub>N<sub>11</sub>O<sub>21</sub>PS [M-H]<sup>-</sup>: 995.3600; found  $m/z$ : 995.3051.

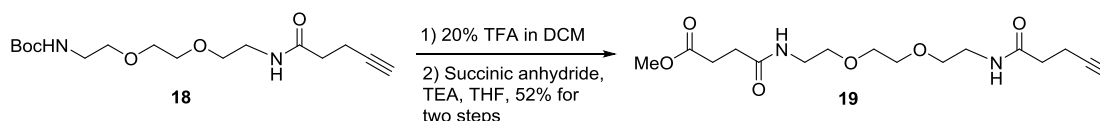
***tert*-butyl (2-(2-(2-(pent-4-ynamido)ethoxy)ethoxy)ethyl)carbamate (**18**)**



4-Pentynoic acid (59.3 mg, 0.604 mmol), HATU (230 mg, 0.604 mmol) and DIPEA (140  $\mu$ L, 0.804 mmol) in DMF (6 mL) was stirred for 10 min at room temperature, before adding dropwise to a solution of *N*-Boc-3,6-dioxaoctane-1,8-diamine (100 mg, 0.403 mmol) in DMF (3

mL). The reaction mixture was stirred at room temperature for another 2 hours before it was concentrated under reduced pressure. The residue was purified by silica gel column chromatography ( $\text{CH}_2\text{Cl}_2/\text{CH}_3\text{OH}$ , 25/1, v/v) to give **18** (126 mg, 96%) as a white solid.  $^1\text{H}$  NMR (500 MHz,  $\text{cd}_3\text{od}$ )  $\delta$  3.64 (s, 4H,  $\text{OCH}_2\text{CH}_2\text{O}$ ), 3.55 (dt,  $J = 16.5, 5.6$  Hz, 4H,  $\text{OCH}_2\text{CH}_2\text{N}$  \*2), 3.40 (q,  $J = 5.3$  Hz, 2H,  $\text{OCH}_2\text{CH}_2\text{N}$ ), 3.28 – 3.21 (m, 2H,  $\text{OCH}_2\text{CH}_2\text{N}$ ), 2.52 – 2.46 (m, 2H,  $\text{COCH}_2\text{CH}_2\text{C}\equiv\text{C}$ ), 2.45 – 2.39 (m, 2H,  $\text{COCH}_2\text{CH}_2\text{C}\equiv\text{C}$ ), 2.29 (d,  $J = 2.6$  Hz, 1H,  $\text{C}\equiv\text{CH}$ ), 1.46 (s, 9H, Boc).  $^{13}\text{C}$  NMR (126 MHz,  $\text{cd}_3\text{od}$ )  $\delta$  69.9, 69.7, 69.2, 69.0, 42.4, 39.0, 34.6, 27.4, 14.3. HRMS (ESI):  $m/z$ : calcd for  $\text{C}_{16}\text{H}_{28}\text{N}_2\text{NaO}_5$   $[\text{M}+\text{Na}]^+$ : 351.1896; found: 351.0699.

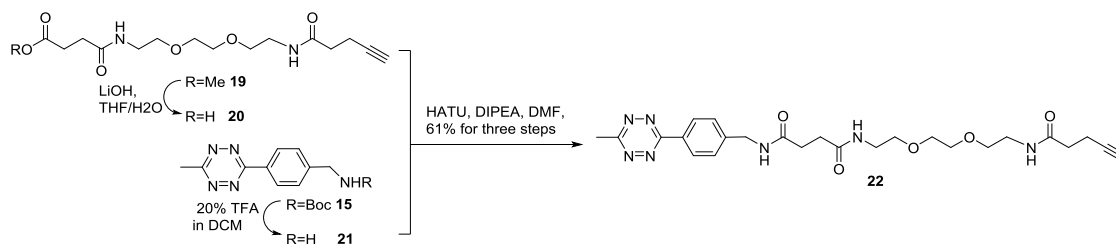
**methyl 4,15-dioxo-8,11-dioxa-5,14-diazanonadec-18-ynoate (19)**



**18** (126 mg, 0.384 mmol) was dissolved in DCM (3 mL), TFA (0.6 mL) was added. The reaction mixture was stirred at room temperature for 2 hours, before it was concentrated under reduced pressure. The residue was dissolved in THF (1 mL), TEA (562  $\mu\text{L}$ , 4.03 mmol) was added. To this solution was added a solution of succinic anhydride (41 mg, 0.403 mmol) in THF (0.5 mL) over a period of 10 min at room temperature. The reaction mixture was stirred overnight before it was concentrated under reduced pressure. The residue was diluted with ethyl acetate (5 mL), acidified by 1 M HCl. The water layer was further extracted with ethyl acetate (5\* 3 mL). The organic layer were combined, dried over  $\text{MgSO}_4$ , filtered, and concentrated under reduced pressure. The residue was purified by silica gel column chromatography ( $\text{CH}_2\text{Cl}_2/\text{CH}_3\text{OH}$ , 10/1, v/v) to give **19** (65 mg, 52%) as a white solid.  $^1\text{H}$  NMR (300 MHz,  $\text{cd}_3\text{od}$ )  $\delta$  3.66 (s, 3H,  $\text{OCH}_3$ ),

3.61 (s, 4H, OCH<sub>2</sub>CH<sub>2</sub>O), 3.54 (td, *J* = 5.5, 3.3 Hz, 4H, OCH<sub>2</sub>CH<sub>2</sub>N\*2), 3.36 (q, *J* = 5.5 Hz, 4H, OCH<sub>2</sub>CH<sub>2</sub>N\*2), 2.60 (dd, *J* = 8.1, 6.4 Hz, 2H, COCH<sub>2</sub>CH<sub>2</sub>CO), 2.54 – 2.35 (m, 6H, COCH<sub>2</sub>CH<sub>2</sub>CO + COCH<sub>2</sub>CH<sub>2</sub>C≡C), 2.24 (t, *J* = 2.5 Hz, 1H, C≡CH). <sup>13</sup>C NMR (75 MHz, cd<sub>3</sub>od) δ 70.0, 69.9, 68.9, 50.8, 39.0, 39.0, 34.5, 30.0, 28.8, 14.3. HRMS (ESI): *m/z*: calcd for C<sub>16</sub>H<sub>26</sub>N<sub>2</sub>NaO<sub>6</sub> [M+Na]<sup>+</sup>: 365.1689; found: 365.0743.

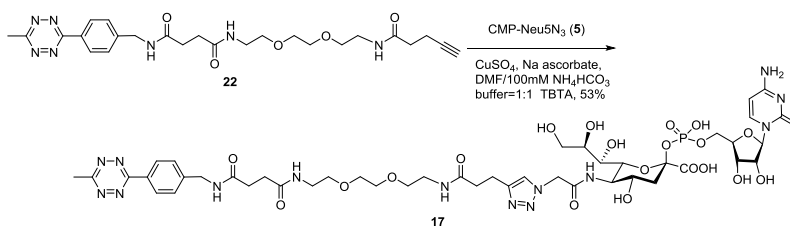
***N*<sup>1</sup>-(4-(6-methyl-1,2,4,5-tetrazin-3-yl)benzyl)-*N*<sup>4</sup>-(2-(2-(2-(pent-4-ynamido)ethoxy)ethoxy)ethyl)succinamide (20)**



**15** (32 mg, 0.106 mmol) was dissolved in DCM (1 mL), TFA (0.2 mL) was added. The reaction mixture was stirred at room temperature for 2 hours, before it was concentrated under reduced pressure to give **21**. **19** (30 mg, 0.088 mmol) was dissolved in the mixture of THF (2 mL) and H<sub>2</sub>O (0.5 mL). LiOH.H<sub>2</sub>O (14.7 mg, 0.35 mmol) was added. The reaction mixture was stirred at room temperature for 1 hour before it was added acidic exchange resin (Amberlite IR120 hydrogen form resin) until the pH value  $\approx$  6. The resin was removed by filtration and the solution was concentrated under reduced pressure to give **20**. **20** and HATU (50 mg, 0.132 mmol), DIPEA (76  $\mu$ L, 0.44 mmol) in DMF (2 mL) was stirred for 10 min at room temperature before it was added the solution of **21** in DMF (1 mL) dropwise. The reaction mixture was stirred for 2 hours at room temperature before it was concentrated under reduced pressure. The residue was purified by silica gel column chromatography using 1% to 5% methanol in CH<sub>2</sub>Cl<sub>2</sub> to give

**22** (27 mg, 61%) as a purple solid.  $^1\text{H}$  NMR (300 MHz,  $\text{cd}_3\text{od}$ )  $\delta$  8.49 (d,  $J$  = 8.3 Hz, 2H, PhH), 7.49 (d,  $J$  = 8.2 Hz, 2H, PhH), 4.47 (d,  $J$  = 5.6 Hz, 2H,  $\text{PhCH}_2\text{NH}$ ), 3.59 (s, 4H,  $\text{OCH}_2\text{CH}_2\text{O}$ ), 3.53 (t,  $J$  = 5.4 Hz, 4H,  $\text{OCH}_2\text{CH}_2\text{N}$  \*2), 3.37 (q,  $J$  = 5.4 Hz, 4H,  $\text{OCH}_2\text{CH}_2\text{N}$ \*2), 3.05 (s, 3H,  $\text{CH}_3$ ), 2.60 – 2.49 (m, 4H,  $\text{COCH}_2\text{CH}_2\text{CO}$ ), 2.49 – 2.32 (m, 4H,  $\text{COCH}_2\text{CH}_2\text{C}\equiv\text{C}$ ), 2.08 (t,  $J$  = 2.5 Hz, 1H,  $\text{C}\equiv\text{CH}$ ).  $^{13}\text{C}$  NMR (75 MHz,  $\text{cd}_3\text{od}$ )  $\delta$  128.0, 127.9, 70.0, 69.4, 69.4, 42.8, 39.1, 39.1, 35.6, 31.9, 31.0, 20.4, 14.6. HRMS (ESI):  $m/z$ : calcd for  $\text{C}_{25}\text{H}_{33}\text{N}_7\text{NaO}_5$   $[\text{M}+\text{Na}]^+$ : 534.2441; found: 534.0616.

### Tetrazine-PEG<sub>3</sub>-CMP-Neu5N<sub>3</sub> (**17**)

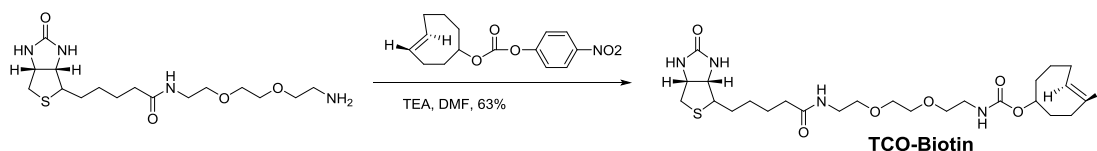


A solution of **22** (5.8 mg, 0.0113 mmol) in DMF (0.75 mL) was added to the solution of CMP-Neu5N<sub>3</sub> (**5**, 6.2 mg, 0.00945 mmol) in Tris-HCl buffer (100 mM, pH 7.5, 0.75 mL). To this mixture was added  $\text{CuSO}_4$  (100 mM, 75.6  $\mu\text{L}$ ), sodium L-ascorbate (100 mM, 94.5  $\mu\text{L}$ ) and TBTA (1 mg, 0.0019 mmol). After stirring for 3 hour at ambient temperature, the reaction mixture was lyophilized to provide a residue that was applied to a Biogel fine P-2 column (75\*1.5 cm) and eluted with 0.1 M  $\text{NH}_4\text{HCO}_3$  at 4 °C in dark. The product was detected by TLC ( $i\text{-PrOH}$  : aq.  $\text{NH}_4\text{Cl}$  (20 M) 4 : 1, v:v), and appropriate fractions were combined and lyophilized to provide **17** (5.8 mg, 53%) as a purple solid.  $^1\text{H}$  NMR (500 MHz,  $\text{d}_2\text{O}$ )  $\delta$  8.26 (d,  $J$  = 8.1 Hz, 2H, PhH), 8.01 (d,  $J$  = 7.4 Hz, 1H, H-6, cyt), 7.69 (s, 1H,  $\text{CH}=\text{C}$ , triazole), 7.43 (d,  $J$  = 8.0 Hz, 2H, PhH), 6.30 (m, 1H, H-5, cyt), 5.84 (s, 1H, H-1, rib), 5.18 – 5.08 (m, 2H, triazole- $\text{CH}_2\text{-C}=\text{O}$ ), 4.38

(s, 2H, PhCH<sub>2</sub>NH), 4.21 (m, 2H, H-2+H-3, rib), 4.18 – 4.05 (m, 4H, H-4+H-5 rib + H-6 Neu), 4.00 (d, *J* = 12.5 Hz, 1H, H-4 Neu), 3.89 (t, *J* = 10.3 Hz, 1H, H-5 Neu), 3.81 (s, 1H, H-8 Neu), 3.75 (d, *J* = 11.7 Hz, 1H, H-9a Neu), 3.52 – 3.38 (m, 9H, H-9b Neu + OCH<sub>2</sub>CH<sub>2</sub>O + OCH<sub>2</sub>CH<sub>2</sub>N\*2), 3.34 (d, *J* = 9.2 Hz, 1H, H-7 Neu), 3.26 – 3.16 (m, 4H, OCH<sub>2</sub>CH<sub>2</sub>N\*2), 2.95 (s, 3H, CH<sub>3</sub>), 2.84 (s, 2H, triazole-CH<sub>2</sub>CH<sub>2</sub>CO), 2.52 (t, *J* = 6.7 Hz, 2H, COCH<sub>2</sub>CH<sub>2</sub>CO), 2.46 (t, *J* = 5.7 Hz, 4H, triazole-CH<sub>2</sub>CH<sub>2</sub>CO + COCH<sub>2</sub>CH<sub>2</sub>CO), 2.39 (d, *J* = 13.4 Hz, 1H, H-3eq, Neu), 1.53 (s, 1H, H-3ax, Neu). <sup>13</sup>C NMR (126 MHz, d<sub>2</sub>O) δ 143.3, 128.1, 127.9, 83.2, 74.3, 71.6, 69.6, 69.3, 69.2, 68.9, 68.7, 68.7, 66.5, 64.7, 62.9, 62.9, 52.0, 51.9, 42.7, 40.9, 40.9, 38.9, 38.9, 34.9, 31.1, 31.1, 21.0, 20.0. HRMS (ESI): *m/z*: calcd for C<sub>45</sub>H<sub>62</sub>N<sub>14</sub>O<sub>21</sub>P [M-H]<sup>-</sup>: 1165.3957; found: 1165.0985.

#### (*E*)-cyclooct-4-en-1-yl

#### (2-(2-(2-(5-((3*aS*,6*aR*)-2-oxohexahydro-1*H*-thieno[3,4-*d*]imidazol-4-yl)pentanamido)ethoxy)ethoxy)ethyl)carbamate (TCO-Biotin)

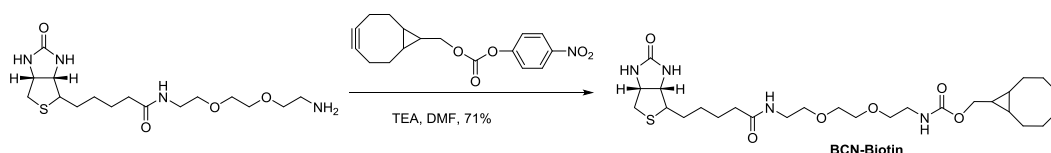


To a solution of **8** (5 mg, 0.0133 mmol) and NEt<sub>3</sub> (6 μL, 0.043 mmol) in DMF (1 mL) was added TCO-PNP (4.3 mg, 0.0147 mmol) under an atmosphere of Argon. After stirring the reaction mixture for 3.5 hours at ambient temperature, the solvent was removed under reduced pressure and the residue was purified by silica gel column chromatography (CH<sub>2</sub>Cl<sub>2</sub>/CH<sub>3</sub>OH, 50/1→10/1, v/v) to afford TCO-biotin (4.4 mg, 63%). <sup>1</sup>H NMR (600 MHz, cd<sub>3</sub>od) δ 5.71 – 5.53 (m, 2H, H-1, H-2 TCO), 4.66 (td, *J* = 9.1, 4.3 Hz, 1H, H-5 TCO), 4.47 (dd, *J* = 7.9, 4.9 Hz, 1H, CHNH biotin), 4.29 (dd, *J* = 7.9, 4.5 Hz, 1H, CHNH biotin), 3.60 (s, 4 H, OCH<sub>2</sub>CH<sub>2</sub>O) 3.55 – 3.47 (m, 4H,

OCH<sub>2</sub>CH<sub>2</sub>N \*2), 3.36 – 3.34 (m, 2H, OCH<sub>2</sub>CH<sub>2</sub>NH), 3.25 (p, *J* = 5.8 Hz, 2H, OCH<sub>2</sub>CH<sub>2</sub>NH), 3.21 – 3.16 (m, 1H, CHS biotin), 2.91 (dd, *J* = 12.8, 5.0 Hz, 1H, CHHS Biotin), 2.69 (d, *J* = 12.7 Hz, 1H, CHHS Biotin), 2.39 – 2.26 (m, 2H), 2.23 – 2.18 (m, 2H, CH<sub>2</sub>CH<sub>2</sub>CH<sub>2</sub>CH<sub>2</sub>C=O biotin), 2.16 (dt, *J* = 8.2, 4.1 Hz, 1H), 2.07 (ddt, *J* = 14.1, 6.9, 3.2 Hz, 1H), 2.01 – 1.78 (m, 3H), 1.77 – 1.51 (m, 7H), 1.43 (p, *J* = 7.7 Hz, 2H). <sup>13</sup>C NMR (151 MHz, cd<sub>3</sub>od) δ 129.3, 129.3, 75.8, 69.9, 69.4, 69.3, 62.0, 60.2, 55.6, 40.9, 40.2, 39.9, 39.7, 38.9, 38.3, 38.2, 35.4, 33.9, 33.9, 33.8, 33.6, 32.1, 28.3, 28.1, 28.1, 25.4, 25.2, 21.9, 21.9.

### bicyclo[6.1.0]non-4-yn-9-ylmethyl

(2-(2-(2-(5-((3a*S*,6a*R*)-2-oxohexahydro-1*H*-thieno[3,4-*d*]imidazol-4-yl)pentanamido)ethoxy)ethoxy)ethyl)carbamate (BCN-Biotin)



To a solution of **8** (10.1 mg, 0.027 mmol) and NEt<sub>3</sub> (11.3 μL, 0.081 mmol) in DMF (3 mL) was added BCN-PNP (8.5 mg, 0.027 mmol) under an atmosphere of Argon. After stirring the reaction mixture overnight at ambient temperature, the solvent was removed under reduced pressure and the residue was purified by silica gel column chromatography (CH<sub>2</sub>Cl<sub>2</sub>/CH<sub>3</sub>OH, 30/1→15/1, v/v) to afford BCN-biotin (10.5 mg, 71%). <sup>1</sup>H NMR (500 MHz, cdcl<sub>3</sub>) δ 6.50 (d, *J* = 79.4 Hz, 2H, NH \*2), 5.36 (s, 1H, NH), 4.58 – 4.47 (m, 1H, CHNH biotin), 4.34 (t, *J* = 6.0 Hz, 1H, CHNH biotin), 3.99 (d, *J* = 7.0 Hz, 2H, OCH<sub>2</sub>-BCN), 3.69 – 3.61 (m, 4H, OCH<sub>2</sub>CH<sub>2</sub>O), 3.59 (dt, *J* = 6.7, 3.5 Hz, 4H, OCH<sub>2</sub>CH<sub>2</sub>N \*2), 3.47 (dd, *J* = 12.7, 7.3 Hz, 2H, OCH<sub>2</sub>CH<sub>2</sub>NH), 3.39 (q, *J* = 7.2, 6.3 Hz, 2H, OCH<sub>2</sub>CH<sub>2</sub>NH), 3.21 – 3.06 (m, 1H, CHS biotin), 2.92 (dd, *J* = 12.9, 4.9 Hz, 1H, CHHS Biotin),

2.77 (d,  $J = 12.8$  Hz, 1H, CHHS Biotin), 2.41 (dt,  $J = 13.6, 3.0$  Hz, 2H), 2.33 – 2.11 (m, 7H), 1.72 (dtt,  $J = 32.1, 17.4, 7.4$  Hz, 4H), 1.51 – 1.19 (m, 6H).  $^{13}\text{C}$  NMR (126 MHz,  $\text{cdcl}_3$ )  $\delta$  70.2, 70.0, 69.2, 61.8, 60.3, 55.6, 40.8, 40.5, 40.5, 39.2, 35.9, 33.3, 33.3, 33.3, 29.8, 28.2, 28.1, 28.1, 25.6, 21.5, 21.4, 21.4, 21.4, 21.4, 8.7, 8.6.

### Kinetics measurement by UV

The reaction between TCO and tetrazine, BCN and Tetrazine were monitored by UV-Vis spectroscopy using a ten-fold (or more than ten-fold) excess of reactant B (TCO/BCN). The reaction was conducted at 25 °C ( $\pm 0.5$  °C) in a 1-mL UV cuvette. Prepared solution A (500  $\mu\text{L}$ ) and B (500  $\mu\text{L}$ ) was rapidly mixed ( $t=0$ ) and immediately inserted into a 1 mL UV cuvette. Next, UV-absorption was measured at preset time intervals (in general every 15 seconds). The graphs obtained showed a decrease of the absorption over time.

The kinetics was measured in triplicate, with different concentration of reactant B.

The pseudo-first order rates were calculated according to equation (1):

$$[A]_t = [A]_0 e^{-k(\text{obs})t} \quad (1)$$

With  $k(\text{obs})$  = pseudo-first order rate constant ( $\text{s}^{-1}$ ),  $t$  = reaction time (s),  $[A]_0$  = the initial concentration of substrate A (mmol/mL).

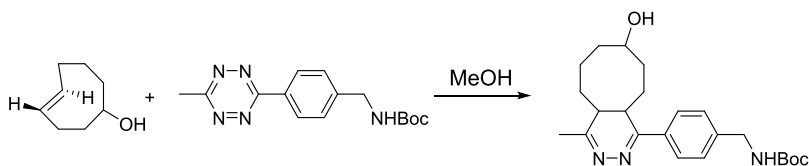
The second order rates were calculated according to equation (2):

$$k = k(\text{obs})/[B]_0 \quad (2)$$

With  $k$  = 2nd order rate constant ( $\text{M}^{-1}\text{s}^{-1}$ ),  $[B]_0$  = the initial concentration of substrate B (mmol/mL).



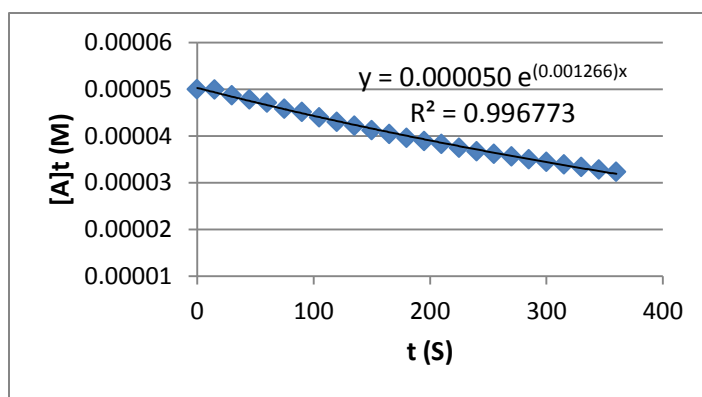
### Tetrazine + TCO:



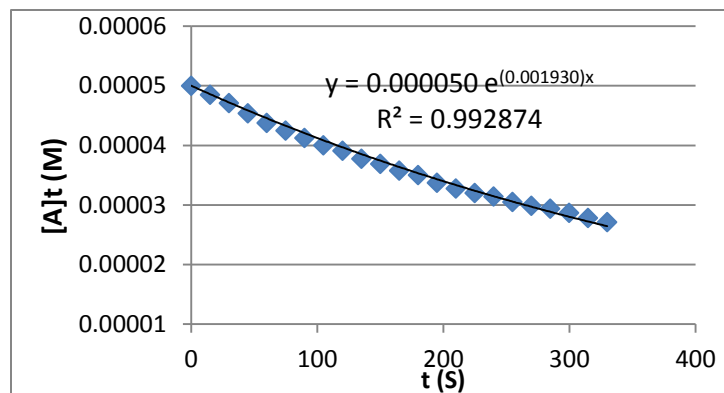
The reaction rates were measured by UV-Vis spectroscopy at 267 nm.

Stock solution A (100  $\mu\text{M}$ ): Tetrazine **15** (1.2 mg, 0.00499 mmol) was dissolved in 0.996 mL MeOH to give a 4 mM solution. And this 4 mM solution was diluted with MeOH to give a 100  $\mu\text{M}$  solution.

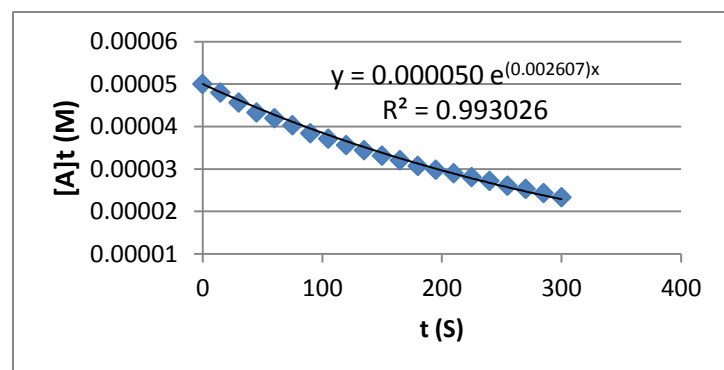
Stock solution B (1 mM, 1.4 mM and 2 mM): TCO (1 mg, 0.00793 mmol) was dissolved in 2.643 mL MeOH to give a 3 mM solution, and this 3 mM solution was diluted with MeOH to give 1 mM, 1.4 mM and 2 mM solutions.



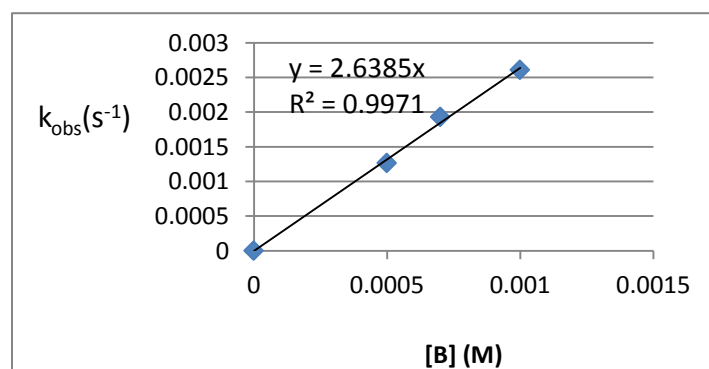
Exponential plot of the reaction between tetrazine ( $[A]_0 = 50 \mu\text{M}$ ) and TCO ( $[B]_0 = 500 \mu\text{M}$ ).  
 $k(\text{obs}) = 0.001266 \text{ s}^{-1}$



Exponential plot of the reaction between tetrazine ( $[A]_0=50\text{ }\mu\text{M}$ ) and TCO ( $[B]_0=700\text{ }\mu\text{M}$ ).  
 $k(\text{obs})=0.001930\text{ s}^{-1}$



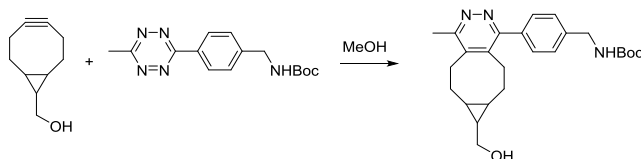
Exponential plot of the reaction between tetrazine ( $[A]_0=50\text{ }\mu\text{M}$ ) and TCO ( $[B]_0=1000\text{ }\mu\text{M}$ ).  
 $k(\text{obs})=0.002607\text{ s}^{-1}$



Linear plot of the reaction between TCO and tetrazine,  $k=2.64\text{ M}^{-1}\text{ s}^{-1}$ .

The second order rate constant was calculated to be  $2.64\text{ M}^{-1}\text{ s}^{-1}$ .

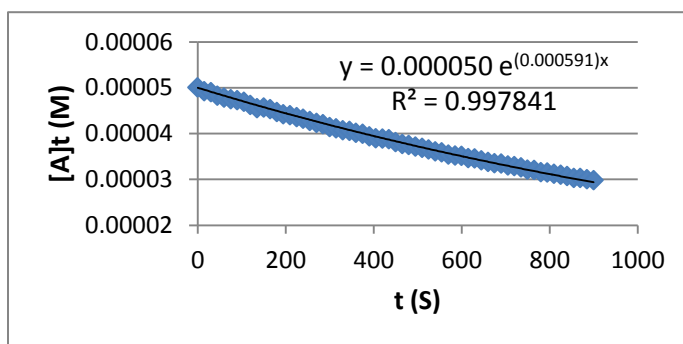
## Tetrazine + BCN:



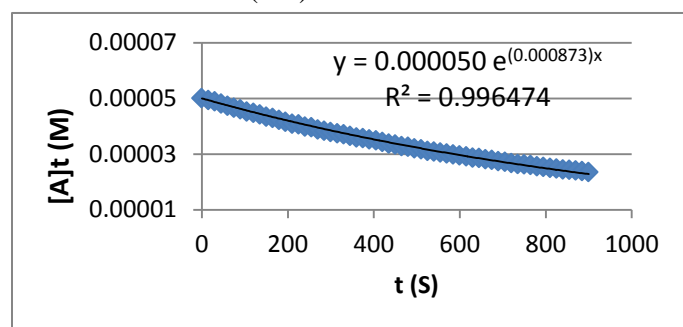
The reaction rates were measured by UV-Vis spectroscopy at 267 nm.

Stock solution A (100  $\mu\text{M}$  and 200  $\mu\text{M}$ ): Tetrazine **15** (0.9 mg, 0.00299 mmol) was dissolved in 2.99 mL MeOH to give a 1 mM solution. And this 1 mM solution was diluted with MeOH to give a 100  $\mu\text{M}$  and 200  $\mu\text{M}$  solutions.

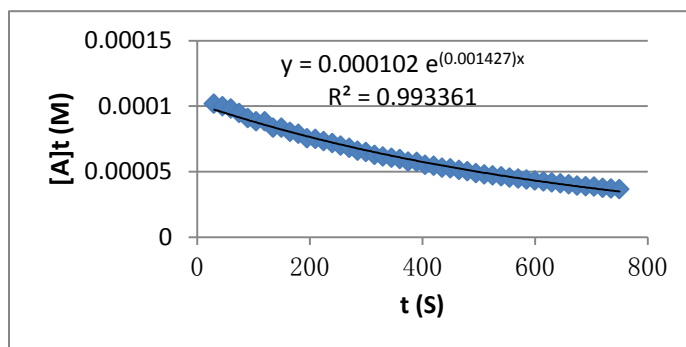
Stock solution B (1 mM, 1.5 mM and 2.333 mM): BCN-OH (1.2 mg, 0.008 mmol) was dissolved in 2.665 mL MeOH to give a 3 mM solution, and this 3 mM solution was diluted with MeOH to give 1 mM, 1.5 mM and 2.333 mM solutions.



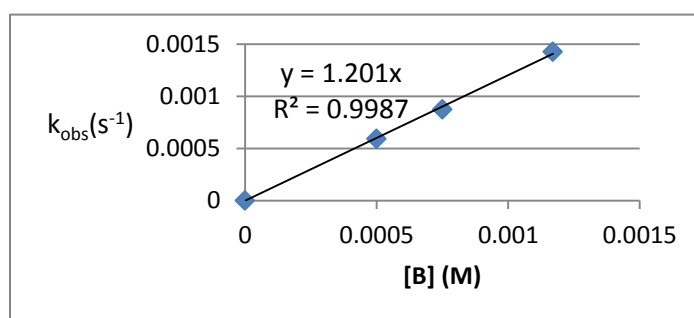
Exponential plot of the reaction between tetrazine ( $[A]_0 = 50 \mu\text{M}$ ) and BCN ( $[B]_0 = 500 \mu\text{M}$ ).  
 $k(\text{obs}) = 0.000591 \text{ s}^{-1}$



Exponential plot of the reaction between tetrazine ( $[A]_0 = 50 \mu\text{M}$ ) and BCN ( $[B]_0 = 750 \mu\text{M}$ ).  
 $k(\text{obs}) = 0.000873 \text{ s}^{-1}$



Exponential plot of the reaction between tetrazine ( $[A]_0 = 100 \mu\text{M}$ ) and BCN ( $[B]_0 = 1167 \mu\text{M}$ ).  
 $k(\text{obs}) = 0.001427 \text{ s}^{-1}$

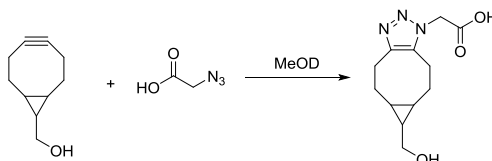


Linear plot of the reaction between BCN and tetrazine,  $k = 1.20 \text{ M}^{-1} \text{ s}^{-1}$ .

The second order rate constant was calculated to be  $1.20 \text{ M}^{-1} \text{ s}^{-1}$ .

### Kinetics measurement by NMR

The reaction between BCN and azide was monitored by NMR.



$^1\text{H}$ -NMR monitoring of BCN and azide was performed by rapid mixing ( $t=0$ ) of stock solutions A and B (0.25 mL each) in an NMR tube and immediate insertion into a 500 MHz NMR spectrometer. NMR spectra were measured at preset time-intervals.

Kinetics was determined by integration of  $\text{CH}_2$  group of azide compound in starting material and

product. The sum of these two integrals was taken as internal standard. Conversion was determined by the relative increase of CH<sub>2</sub> signals of product, compared to the sum of both signals.

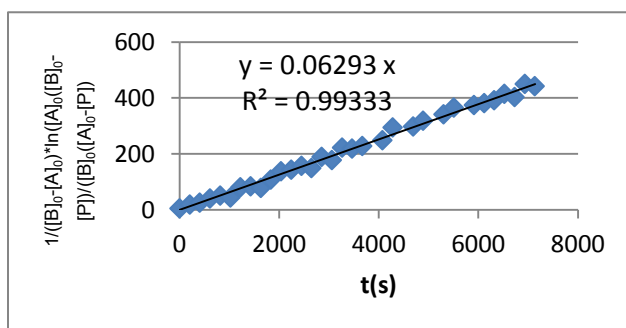
From the conversion plots thus obtained, the second order rate plots were calculated according to equation (3).

$$kt = \frac{1}{[B]_0 - [A]_0} \times \ln \frac{[A]_0([B]_0 - [P])}{([A]_0 - [P])[B]_0} \quad (3)$$

With  $k$  = 2<sup>nd</sup> order rate constant (M<sup>-1</sup>s<sup>-1</sup>),  $t$  = reaction time (s),  $[A]_0$  = the initial concentration of substrate A (mmol/mL),  $[B]_0$  = the initial concentration of substrate B (mmol/mL) and  $[P]$  = the concentration of product (mmol/mL).

Stock solution A (30mM): azide (1.9 mg, 0.0188 mmol) was dissolved in 0.627mL MeOD to give a 30 mM solution.

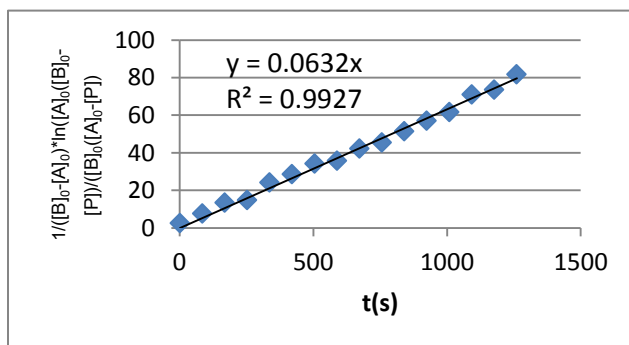
Stock solution B (36 mM): BCN (1.5 mg, 0.010 mmol) was dissolved in 0.278 mL MeOD to give a 36 mM solution.



Logarithmic plot of the reaction between azide ( $[A]_0=15$  mM) and BCN ( $[B]_0=18$  mM)  
 $k=0.063$  M<sup>-1</sup>s<sup>-1</sup>

Stock solution A (24mM): BCN (1.0 mg, 0.00666 mmol) was dissolved in 0.278mL MeOD to give a 24 mM solution.

Stock solution B (30 mM): azide (1.4 mg, 0.01386 mmol) was dissolved in 0.462 mL MeOD to give a 30 mM solution.



Logarithmic plot of the reaction between azide ( $[B]_0=15$  mM) and BCN ( $[A]_0=12$  mM)  
 $k=0.063 \text{ M}^{-1}\text{s}^{-1}$

The average second order rate constant was calculated to be  $0.063 \text{ M}^{-1}\text{s}^{-1}$ .

## Reference

- (1) Prescher, J. A.; Dube, D. H.; Bertozzi, C. R. *Nature* **2004**, *430*, 873.
- (2) Prescher, J. A.; Bertozzi, C. R. *Nature chemical biology* **2005**, *1*, 13.
- (3) Kho, Y.; Kim, S. C.; Jiang, C.; Barma, D.; Kwon, S. W.; Cheng, J.; Jaunbergs, J.; Weinbaum, C.; Tamanoi, F.; Falck, J.; Zhao, Y. *Proc Natl Acad Sci U S A* **2004**, *101*, 12479.
- (4) Link, A. J.; Vink, M. K.; Tirrell, D. A. *J Am Chem Soc* **2004**, *126*, 10598.
- (5) Saxon, E.; Luchansky, S. J.; Hang, H. C.; Yu, C.; Lee, S. C.; Bertozzi, C. R. *J Am Chem Soc* **2002**, *124*, 14893.
- (6) Kayser, H.; Zeitler, R.; Kannicht, C.; Grunow, D.; Nuck, R.; Reutter, W. *J Biol Chem* **1992**, *267*, 16934.
- (7) Mahal, L. K.; Yarema, K. J.; Bertozzi, C. R. *Science* **1997**, *276*, 1125.
- (8) Lee, S.; Koo, H.; Na, J. H.; Han, S. J.; Min, H. S.; Lee, S. J.; Kim, S. H.; Yun, S. H.; Jeong, S. Y.; Kwon, I. C.; Choi, K.; Kim, K. *ACS nano* **2014**, *8*, 2048.
- (9) Xie, R.; Dong, L.; Huang, R.; Hong, S.; Lei, R.; Chen, X. *Angewandte Chemie* **2014**, *53*, 14082.
- (10) Breidenbach, M. A.; Gallagher, J. E.; King, D. S.; Smart, B. P.; Wu, P.; Bertozzi, C. R. *Proc Natl Acad Sci U S A* **2010**, *107*, 3988.
- (11) Wang, H.; Wang, R.; Cai, K.; He, H.; Liu, Y.; Yen, J.; Wang, Z.; Xu, M.; Sun, Y.; Zhou, X.; Yin, Q.; Tang, L.; Dobrucki, I. T.; Dobrucki, L. W.; Chaney, E. J.; Boppart, S. A.; Fan, T. M.; Lezmi, S.; Chen, X.; Yin, L.; Cheng, J. *Nature chemical biology* **2017**, *13*, 415.

- (12) Mbua, N. E.; Li, X. R.; Flanagan-Steet, H. R.; Meng, L.; Aoki, K.; Moremen, K. W.; Wolfert, M. A.; Steet, R.; Boons, G. J. *Angew Chem Int Edit* **2013**, *52*, 13012.
- (13) Sun, T. T.; Yu, S. H.; Zhao, P.; Meng, L.; Moremen, K. W.; Wells, L.; Steet, R.; Boons, G. J. *J Am Chem Soc* **2016**, *138*, 11575.
- (14) Blackman, M. L.; Royzen, M.; Fox, J. M. *J Am Chem Soc* **2008**, *130*, 13518.
- (15) Taylor, M. T.; Blackman, M. L.; Dmitrenko, O.; Fox, J. M. *J Am Chem Soc* **2011**, *133*, 9646.
- (16) Patterson, D. M.; Nazarova, L. A.; Prescher, J. A. *Acs Chem Biol* **2014**, *9*, 592.
- (17) Devaraj, N. K.; Hilderbrand, S.; Upadhyay, R.; Mazitschek, R.; Weissleder, R. *Angewandte Chemie* **2010**, *49*, 2869.
- (18) Versteegen, R. M.; Rossin, R.; ten Hoeve, W.; Janssen, H. M.; Robillard, M. S. *Angewandte Chemie* **2013**, *52*, 14112.
- (19) Rossin, R.; van Duijnhoven, S. M.; Ten Hoeve, W.; Janssen, H. M.; Kleijn, L. H.; Hoeben, F. J.; Versteegen, R. M.; Robillard, M. S. *Bioconjug Chem* **2016**, *27*, 1697.
- (20) Yu, H.; Yu, H.; Karpel, R.; Chen, X. *Bioorganic & medicinal chemistry* **2004**, *12*, 6427.
- (21) Rahim, M. K.; Kota, R.; Haun, J. B. *Bioconjug Chem* **2015**, *26*, 352.
- (22) Yang, J.; Karver, M. R.; Li, W. L.; Sahu, S.; Devaraj, N. K. *Angew Chem Int Edit* **2012**, *51*, 5222.
- (23) Liu, D. S.; Tangpeerachaikul, A.; Selvaraj, R.; Taylor, M. T.; Fox, J. M.; Ting, A. Y. *J Am Chem Soc* **2012**, *134*, 792.
- (24) Karver, M. R.; Weissleder, R.; Hilderbrand, S. A. *Bioconjug Chem* **2011**, *22*, 2263.



- (25)Chen, W.; Wang, D.; Dai, C.; Hamelberg, D.; Wang, B. *Chem Commun (Camb)* **2012**, 48, 1736.
- (26)Lang, K.; Davis, L.; Torres-Kolbus, J.; Chou, C.; Deiters, A.; Chin, J. W. *Nature chemistry* **2012**, 4, 298.
- (27)Beckmann, H. S.; Niederwieser, A.; Wiessler, M.; Wittmann, V. *Chemistry* **2012**, 18, 6548.
- (28)Kawamoto, K.; Grindy, S. C.; Liu, J.; Holten-Andersen, N.; Johnson, J. A. *Acs Macro Lett* **2015**, 4, 458.
- (29)Rossin, R.; van den Bosch, S. M.; Ten Hoeve, W.; Carvelli, M.; Versteegen, R. M.; Lub, J.; Robillard, M. S. *Bioconjug Chem* **2013**, 24, 1210.
- (30)Karver, M. R.; Weissleder, R.; Hilderbrand, S. A. *Angewandte Chemie* **2012**, 51, 920.
- (31) Ford, K. L.; Zeng, W.; Heazlewood, J. L.; Bacic, A. *Frontiers in plant science* **2015**, 6.
- (32)Desaire, H. *Molecular & cellular proteomics : MCP* **2013**, 12, 893.

## CHAPTER 4

### PREPARATION OF WELL-DEFINED ANTIBODY–DRUG CONJUGATES (ADCS) THROUGH INVERSE ELECTRON DEMAND DIELS-ALDER REACTION (DARINV) AND STRAIN-PROMOTED ALKYNE-NITRONE CYCLOADDITION (SPANC)

Sun, T.; Li, X.; Hudlikar, M. S.; Liu, L.; Boons, G. J. To be submitted to *Bioconjugate Chemistry*.

## **Abstract**

ADCs have attracted much attention in recent decades and have become one of the fastest growing classes in the field of anticancer immunotherapy, which combine the selectivity of monoclonal antibodies and cytotoxicity of potent drugs. Homogeneous ADCs with the desired and prespecified DAR (drug-antibody ratio) has many advantages in treating cancers compared to heterogeneous mixtures. We prepared well-defined anti-CD22 ADCs through DARinv and SPANC by using tetrazine and nitron modified CMP-sialic acid derivatives. The fast kinetics of DARinv and SPANC guaranteed the efficient formation of ADC, and the formed ADCs showed dose-dependent cytotoxicity. Furthermore, DARinv and SPANC are orthogonal, which can be used together on the same mAb to deliver two different drugs to increase ADC efficacy and reduce toxicity of normal tissues at the same time.

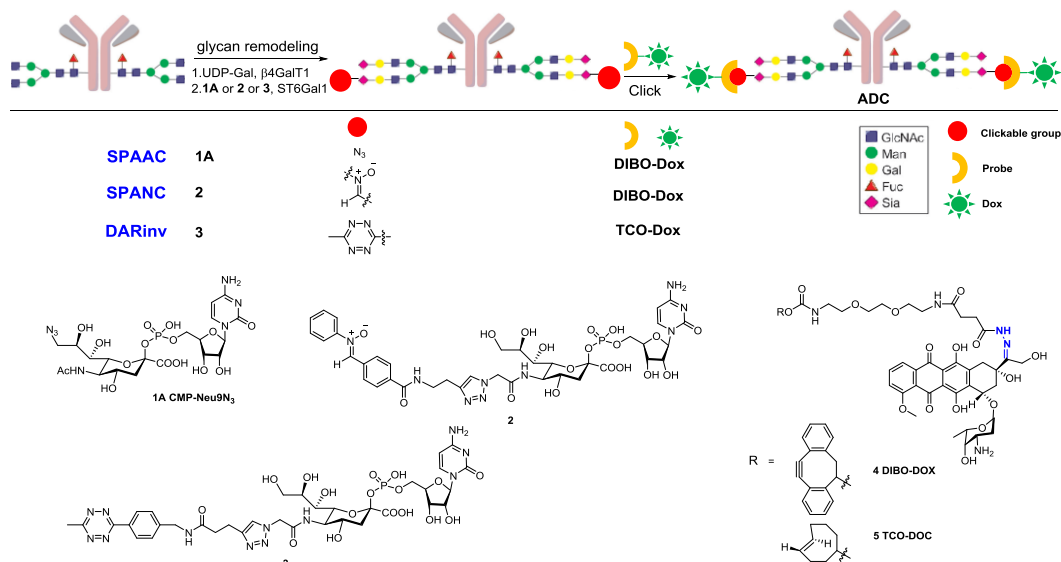
## Introduction

Antibody-drug conjugates (ADCs) are a promising class of anticancer agents, which intend to pursue the monoclonal antibodies (mAbs) as the potent source of delivering highly cytotoxic drugs selectively to the antigen expressing tumor cells. Many mAbs, such as avastin, rituximab, and cetuximab, are well known as standard treatments for solid tumors and hematological cancers.<sup>1</sup> On the other hand, pristine chemodrugs, such as vinblastine, doxorubicin, and paclitaxel, have limited use for cancer treatment because of their nonspecific toxicity.<sup>2-4</sup> The combination of cytotoxic drugs with mAbs would provide the best of both worlds, resulting in improved potency, reduced systemic toxicity, and preferable pharmacokinetics and biodistribution compared to traditional chemotherapy.<sup>5</sup> The approvals of brentuximab vedotin (Adcetris) and ado-trastuzumab emtansine (Kadcyla)<sup>6</sup> plus emerging data for many molecules in clinical trials highlight the potential for ADCs to offer new therapeutic options for patients.

A successful design of ADCs for cancer therapy requires selection of an appropriate target, a monoclonal antibody against the target, potent cytotoxic drug, and an appropriate linker that can conjugate the drug to the antibody. In the past decades, the fast development in protein engineering, bioorthogonal chemistry, and analytical methods have contributed to the development of site-specific conjugation methodologies for constructing homogeneous ADCs.<sup>7-12</sup> Site-specific conjugation, has been an important step in ADC development, enabled the production of homogeneous ADCs with the desired and prespecified drug-antibody ratio (DAR), giving more stable ADCs in vivo.<sup>13-15</sup> Since too few drug molecules attached on the

antibodies will lead to decreased efficacy and too many drug molecules will make the ADC unstable with altered pharmacokinetic properties, increased plasma clearance, reduced half-life and increased systemic toxicity.<sup>16</sup> As a result, more commonly the ADCs aim to attain a DAR close to 4.<sup>17</sup>

In 2014, our group prepared well-defined ADCs through glycan remodeling and strain-promoted alkyne-azide cycloaddition (SPAAC).<sup>18</sup> This is based on the fact that each heavy chain of an immunoglobulin G (IgG) antibody is modified at Asn297 with a complex biantennary *N*-linked oligosaccharide, which does not affect antigen binding but influences effector functions.<sup>19</sup> Moreover, it was observed that glycosyltransferases often tolerate chemical modifications in their sugar nucleotide substrates,<sup>20-23</sup> such as CMP-Neu5Ac.<sup>24</sup> Hence, enzymatic remodeling of this oligosaccharide would make it possible to introduce reactive groups that can be exploited for the site-specific attachment of cytotoxic drugs. CMP-Neu9N<sub>3</sub> (Scheme 4.1, compound **1A**) which has an azide at C9 position of sialic acid moiety was synthesized. They remodeled the oligosaccharides of an anti-CD22 monoclonal antibody and a control polyclonal antibody by using CMP-Neu9N<sub>3</sub>, the azido moieties of the glycans of the resulting antibodies can then react with DIBO attached doxorubicin (DOX) via SPAAC (Scheme 4.1, SPAAC with compound **1A**). DOX was conjugated to the antibody via an acid sensitive linker–hydrozone bond, which can be cleaved by acid-mediated hydrolysis in the lysosomal compartment after the ADCs enter the cell. In the cell culture studies, the formed ADC showed dose-dependent cytotoxicity.



**Scheme 4.1** Preparation of well-defined ADCs through glycan remodeling and click chemistry.

SPAAC, which does not require a toxic metal, has been widely used in labeling glycans in proteins and lipids of living cells. However, the scope of the approach has been limited because of relatively slow reaction kinetics ( $k_2 = 0.057 \text{ M}^{-1} \text{ s}^{-1}$  in MeOH with DIBO).<sup>25</sup> In many cases, sensitivity is the most important parameter. Defined as the number of azides that are reacted in a given time period, sensitivity depends on the intrinsic kinetics of the reaction and the concentrations of reactive reagents. In practice, the concentration of azides is determined by the abundance of target molecule and the efficiency of azide labeling. The concentration of the secondary tagging reagent (i.e., alkyne or DIBO) is typically limited by solubility and, in live cell or animal experiments, toxicity. Given these constraints, the improvement of reaction kinetics is critical to optimize a labeling strategy. We explored whether ADCs can be prepared by more effective bioorthogonal click reactions which may lead to better loading and less concentration of drugs.

Inverse electron demand Diels–Alder reaction (DARinv) does not employ toxic metal

catalysts, and the reaction between tetrazine and TCO was reported as the fastest bioorthogonal reactions to date ( $k_2 = 10^3$  and  $10^6 \text{ M}^{-1}\text{s}^{-1}$  compared to  $\text{N}_3 + \text{DIBO}$ ,  $k_2 = 0.057 \text{ M}^{-1}\text{s}^{-1}$  in MeOH)),<sup>26,27</sup> which we have discussed in details in the last chapter. Besides DARinv, another promising fast bioorthogonal reaction is Strain-promoted alkyne-nitrone cycloaddition (SPANC). SPANC is a cycloaddition between a nitrone and a cyclooctyne forming *N*-alkylated isoxazolines. Compared to SPAAC, it uses nitrones as the 1, 3-dipole rather than azides. The reaction kinetics ranges from 1 to  $32 \text{ M}^{-1}\text{s}^{-1}$ , depending on the substitution of the nitrone, which is 25-50 times faster than analogous reactions involving azides.<sup>28</sup> Although the reaction is extremely fast, it is difficult to incorporate nitrone into biomolecules through metabolic labeling. Labeling has only been achieved through post-translational peptide modification.<sup>29</sup>

We successfully prepared well-defined anti-CD22 ADCs through DARinv and SPANC by using tetrazine and nitrone modified CMP-sialic acid derivatives **2** and **3** (Scheme 4.1), with much shorter click reaction time compared to SPAAC. And the formed ADCs showed comparable dose-dependent cytotoxicity.

We explored the orthogonality and kinetics of three type click reactions (SPAAC, SPANC and DARinv). As we know, DIBO will not react with disubstituted tetrazine due to the steric hindrance.<sup>30</sup> And no cycloaddition reaction was observed between TCO and nitrone over a period of 2 hours at r.t. in MeOH. As a result, the DARinv (TCO + tetrazine) and SPANC (DIBO + nitrone) are orthogonal, which can be used together on the same mAb to deliver two different drugs and decrease drug resistance, which will dramatically increase ADC efficacy and reduce toxicity of normal tissues at the same time.<sup>31</sup>

## Results and discussion

### Synthesis of Modified Sugar Nucleotides.

Different from substrates of SPAAC, 1, 3-dipolar nitrones in SPANC reactions can bear up to three reactivity modulating R-groups and it was reported that nitrones bearing electron-withdrawing groups at the  $\alpha$ -C position reacted faster than the un-substituted parent nitron, or those bearing electron-donating groups.<sup>32</sup> Literature also has indicated that replacement of an *N*-methyl with a phenyl group led to a faster reaction.<sup>33</sup> So, we intended to synthesize CMP-sialic acid derivative **2** with a nitron at C5 position of sialic acid moiety through CuAAC (Figure 4.1). This molecule will be enzymatically tagged to the *N*-linked oligosaccharide of antibody, followed by strain-promoted cycloaddition with DIBO tagged drugs.

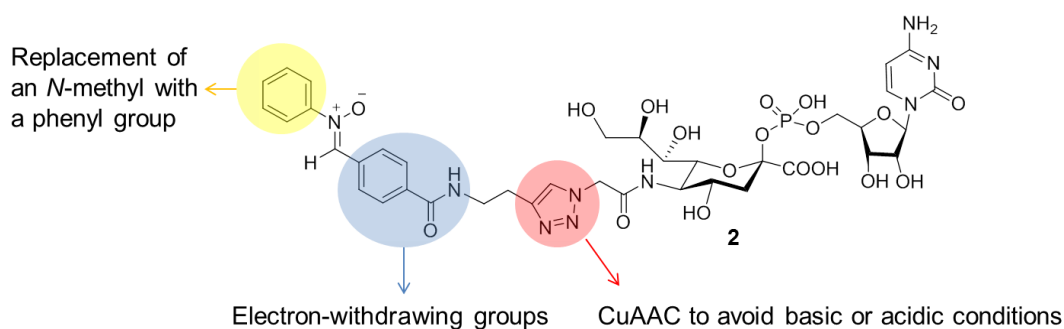


Figure 4.1 Structure of nitron modified CMP-sialic acid **2**.

The synthesis did not give too much trouble. Commercially available 4-formyl-benzoic acid was firstly coupled with 1-amino-3 butyne to give compound **6** in good yield. For the nitron formation reaction with *N*-hydroxy-benzenamine, traditional method using  $\text{NaHCO}_3$  in  $\text{Et}_2\text{O}/\text{H}_2\text{O}$  did not give the product. We searched literature, found that simply mixing of the two



starting materials in EtOH in a high concentration (500mM) resulted in nitron **7** in a high yield.<sup>34</sup> CuAAC of **7** with CMP-Neu5N<sub>3</sub> (**1B**) gave the final product **2**. And nitron at 5 position of CMP-sialic acid could also be tolerated by ST6Gal1, as proved by its successful transfer to LacNAc (Figure 4.2).

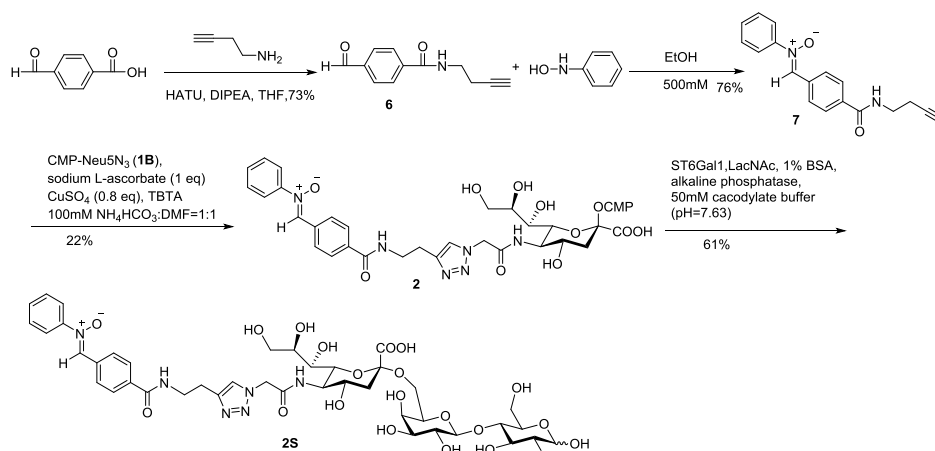


Figure 4.2 Synthesis of nitron modified CMP-sialic acid **2** and its successful transfer to LacNAc.

Tetrazine modified CMP-sialic acid derivative **3** was synthesized as described in Chapter

3:

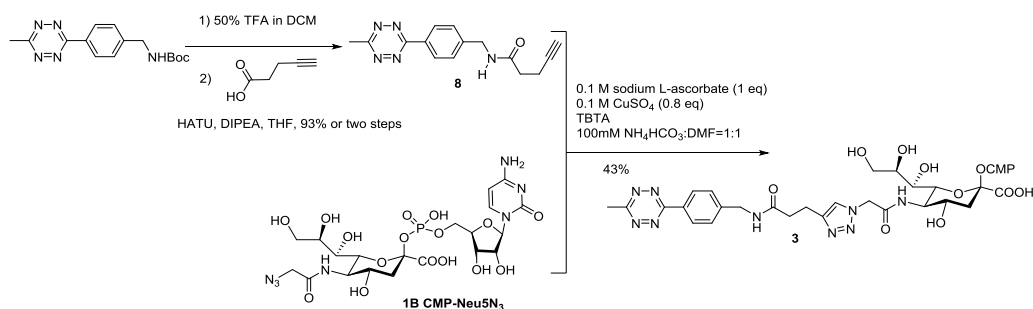


Figure 4.3 Synthesis of Tetrazine modified CMP-sialic acid derivative **3**.

### Kinetics study

With the nitron and tetrazine modified sialic acid derivatives in hand, we began to measure their reaction rates with corresponding ligands. To compare their kinetics with SPAAC

(DIBO + Azide reaction:  $k_2 = 0.057 \text{ M}^{-1} \text{ s}^{-1}$  in methanol), we measured the reaction constants in MeOH or MeOD by UV spectroscopy or  $^1\text{H}$  NMR at  $25^\circ\text{C}$ :  $k = 2.50 \text{ M}^{-1} \text{ s}^{-1}$ .

The kinetics between Tetrazine and TCO/BCN had been described in Chapter 3. And as we know, BCN can not only react with tetrazine through DARinv, but can also react with azide and nitron through 1, 3-dipolar cycloaddition (SPAAC and SPANC). So kinetics of three click-type reactions were compared as shown below (Figure 16).

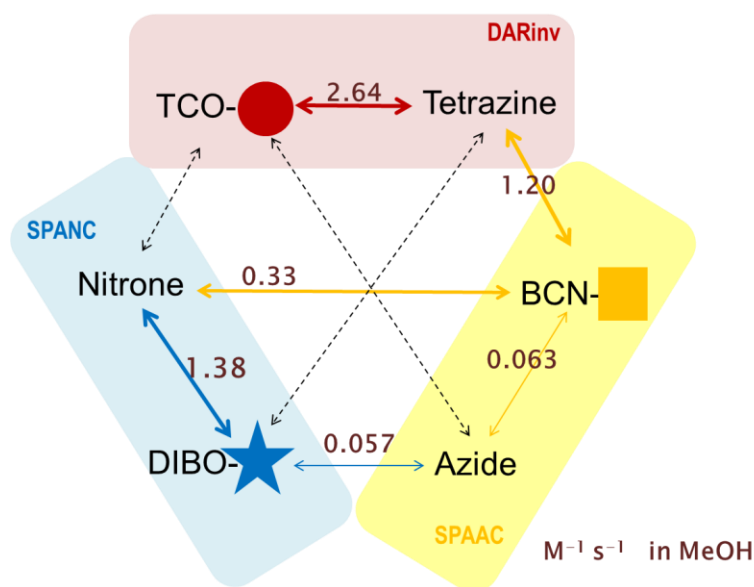


Figure 4.4 Comparison of three click-type reactions. The thickness of arrows correlates with reaction rate. Dashed lines highlight reactants that do not react with each other under tested conditions.

The TCO-Tetrazine pair gave the fastest kinetics, which is 50 times faster than DIBO-Azide pair. The Nitron-DIBO pair also has a high reaction rate, with  $k_2 = 1.38 \text{ M}^{-1} \text{ s}^{-1}$ .

#### Synthesis of DIBO or TCO modified Dox

DIBO and TCO modified DOX were synthesized through an acid-sensitive hydrazine linker.

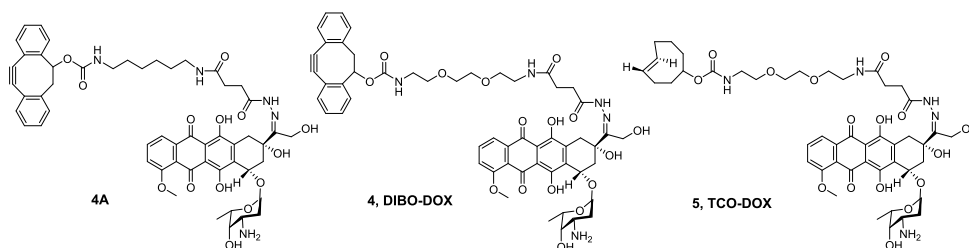


Figure 4.5 Structures of modified doxorubicins

Previously, compound **4A** (Figure 4.5), was synthesized by condensation of DIBO modified by a hydrazine linker with the ketone moiety of Dox through an alkyl linker. However, this compound has a relatively poor aqueous solubility, resulting in bad behavior (precipitation) in conjugation on antibody. Herein, compound **4** and **5**, which have a short PEG linker, were going to be synthesized using a similar synthetic route as **4A** (Figure 4.6).

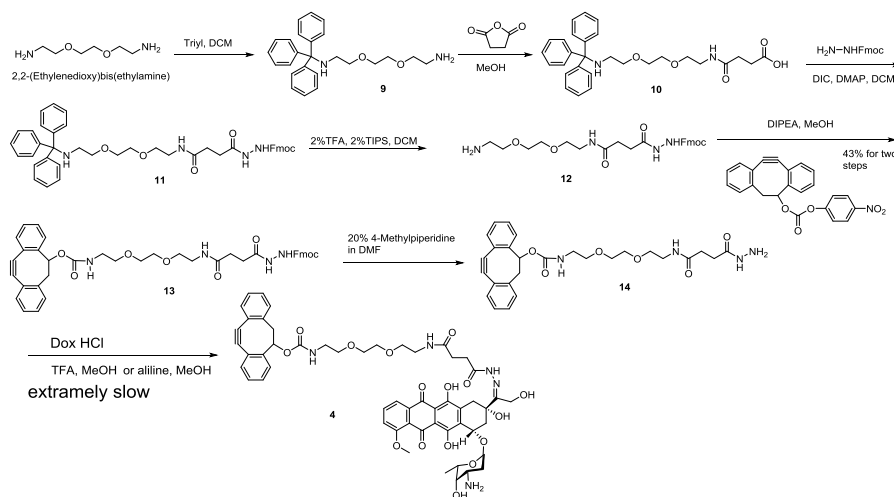


Figure 4.6 Old method to synthesize DIBO attached DOX.

From commercially available 2, 2'-(Ethylenedioxy)bis(ethylamine), one free amine was selectively protected by trityl group, followed by coupling with succinic anhydride, giving compound **10** with a carboxylic acid group. Condensation between **10** and 9-fluorenylmethyl carbamate was then carried out to give compound **11**. After removal of trityl group under acidic condition, coupling **12** with DIBO gave compound **13**, followed by basic deprotection of Fmoc,

compound **14** was obtained. However, the hydrazone formation step was extremely slow (Figure 4.6) even catalysts TFA or aniline was used. We suspected that the unique dipolar property of compound **14** would make this molecule aggregate to form a micelle, hiding the coupling position.

Based on this hypothesis, hydrazone formation step was carried out without DIBO (Figure 4.7). After removal of trityl group, Fmoc was also removed to give compound **15**. The reaction between **15** and Dox.HCl was very efficient, giving compound **16** with a yield of 58% for three steps, confirming our assumption. Next step with DIBO coupling performed smoothly, giving final product **4**.

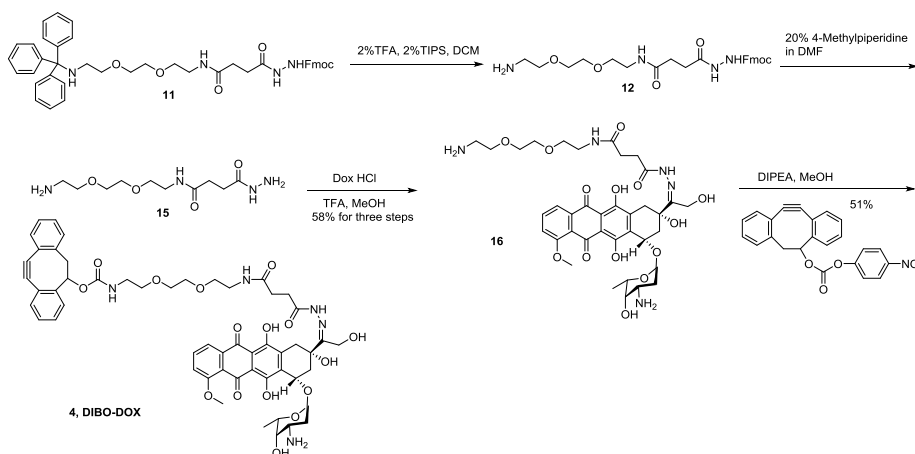


Figure 4.7 New method to synthesize DIBO attached DOX.

Compound **5** was also prepared with a similar strategy by coupling intermediate **16** with activated TCO (Figure 4.8).

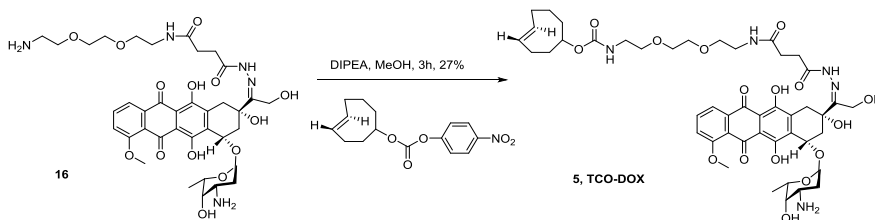


Figure 4.8 Synthesis of TCO attached DOX

### Fluorescence quenching by FRET

To establish the conjugation efficiency of SPANC, FITC (Ex/Em=490/525, Green) and TMR (Ex/Em= 555/572 , Orange) attached DIBO were synthesized by coupling of DIBO-PEG-NH<sub>2</sub> with activated fluorophores. However, After SPANC with nitron 7, we found that the fluorescence of FITC and TMR was quenched partly.

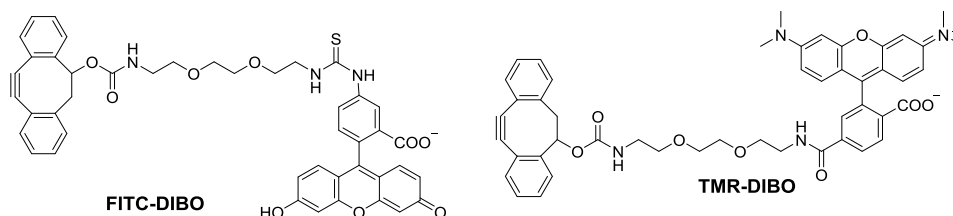


Figure 4.9 Structures of FITC-DIBO and TMR-DIBO.

We suspected that the quenching was caused by Fluorescence Resonance Energy Transfer (FRET). FRET is a physical phenomenon described the interaction between the electronic excited states of two molecules in which excitation is transferred from a donor molecule to an acceptor molecule through long-range dipole-dipole coupling.<sup>35,36</sup> This mechanism is dependent on the dipole orientations of both molecules and the distance between the two molecules (10 to 100 Å). The third requirement is the donor molecule's fluorescence emission spectrum must overlap the acceptor molecule's absorption spectrum. If the acceptor molecule is a fluorophore, the transferred energy will be emitted as fluorescence. If the acceptor molecule is not fluorescent, the absorbed energy is lost as heat, and no fluorescent light is emitted from the complex.<sup>35</sup>



Figure 4.10 Fluorescence resonance energy transfer (FRET).

To address this problem, a series of DIBO attached Fluorophores were synthesized. The chosen fluorophores (BODIPY, AF488, AF647) covered a wide range of emission wavelength, had different structures and colors (from green to far-red):

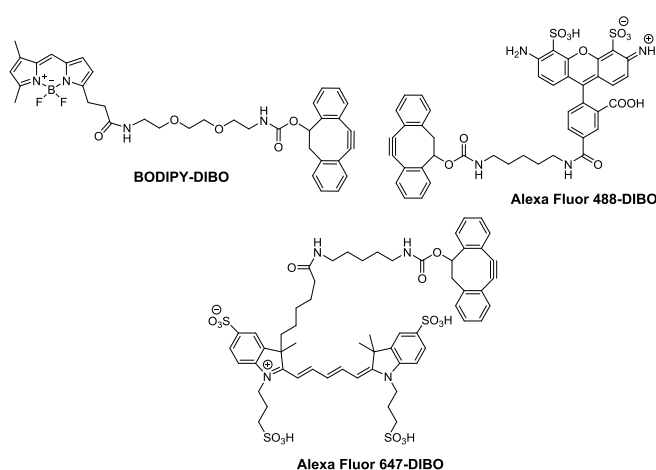
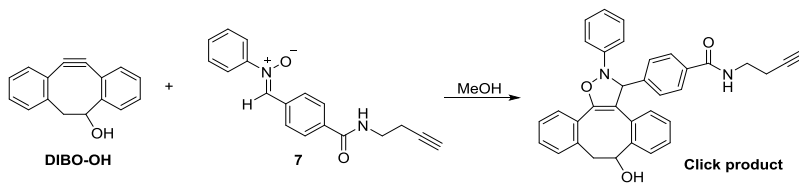
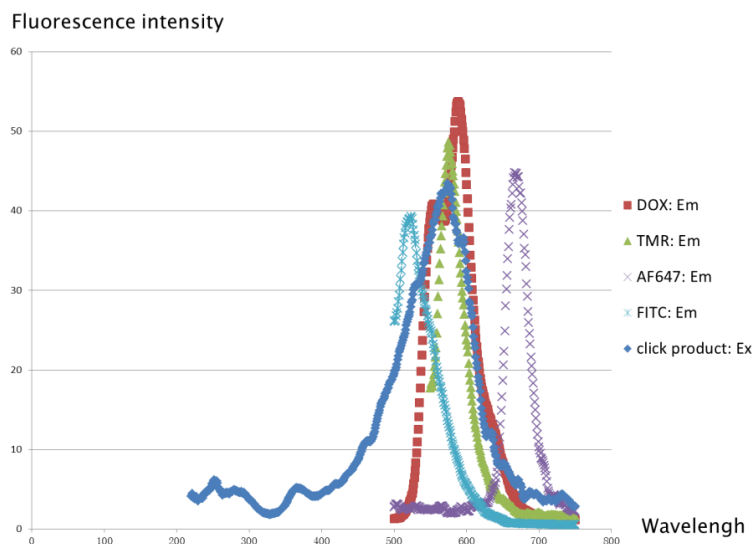


Figure 4.11 Structures of DIBO attached Fluorophores.

Together with FITC-DIBO, TMR-DIBO and DOX-DIBO, we measured their fluorescence emission spectrum, compared to the fluorescence absorption spectrum of click product of DIBO-OH with nitron **7**. As shown in scheme 4.2, the emission spectrums of all fluorophores had a big overlap with the absorption spectrum of the click product except AF647.





Scheme 4.2 Comparison of fluorescence absorption spectrum of click product and fluorescence emission spectrum of fluorophores (DOX, TMR, AF647, FITC).

Indeed, only AF647-DIBO did not lose its fluorescence intensity after click reaction with nitrene **7** (Table 4.1). As a result, AF647-DIBO will be used to determine the conjugation efficiency.

Table 4.1 Properties and fluorescence quenching results of AF488, FITC, TMR, DOX, AF647.

Name	Ex/Em	Color	Fluorescence
Alexa Fluor 488	494/517	Green	Quenched
FITC	490/525	Green	Quenched
TMR	555/572	Orange	Quenched
DOX	480/560-590	red	Quenched
Alexa Fluor 647	651/672	Far-red	<b>No</b>

Similarly, to establish the conjugation efficiency of DAR<sub>inv</sub>, AF488 attached TCO was synthesized (Figure 4.12). NHS activated AF488 was firstly reacted with 10 eq 2,2'-(Ethylenedioxy)bis(ethylamine) to give **17**. After biogel fine P-2 column purification to

remove the unreacted diamine, **17** was reacted with PNP activated TCO to give final product AF488-TCO.

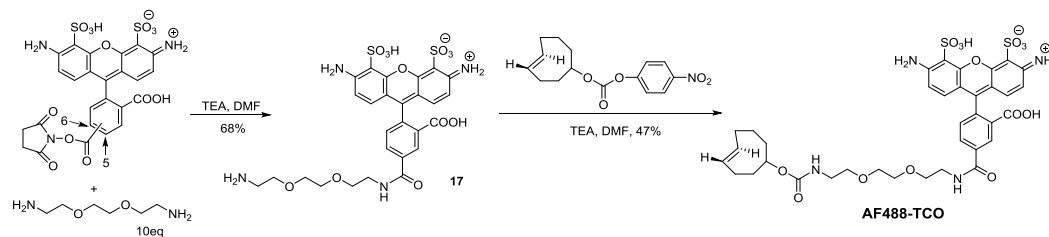
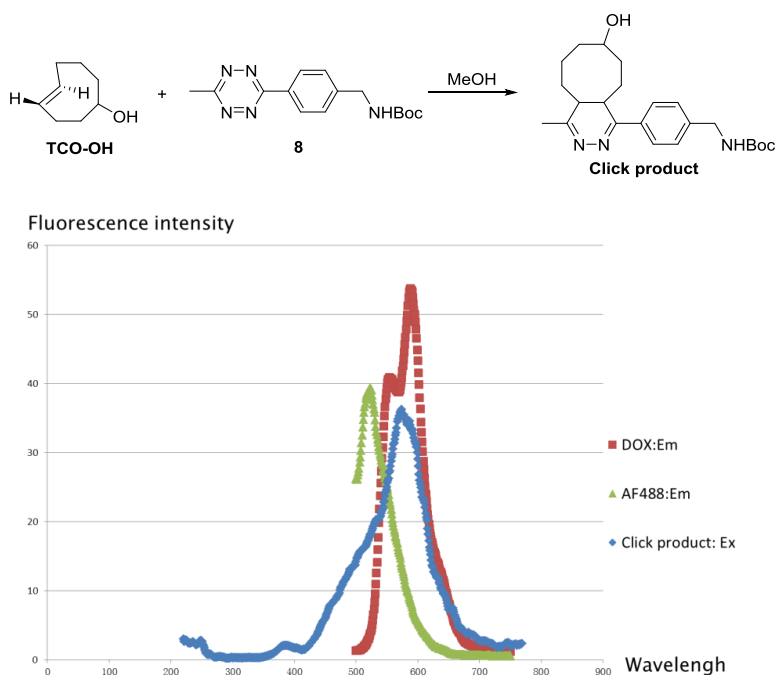


Figure 4.12 Synthesis of AF488-TCO

Together with DOX-TCO, we also measured their fluorescence emission spectrum, compared to the fluorescence absorption spectrum of click product of TCO-OH with tetrazine **8** as shown in scheme 4.3. The emission spectrum of DOX completely overlapped with the absorption spectrum of click product, while the emission spectrum of AF488 partly overlapped with the absorption spectrum of click product.



Scheme 4.3 Comparison of fluorescence absorption spectrum of click product and fluorescence emission spectrum of fluorophores (DOX, AF488).



After fluorescence intensity measurement before and after click reaction of DOX-TCO and AF488-TCO with tetrazine **8**, we found that the fluorescence of DOX was partly quenched by DARinv, while the fluorescence of AF488 was barely quenched.

Table 4.2 Properties and fluorescence quenching results of AF488 and DOX.

Name	Ex/Em	Color	Fluorescence
Alexa Fluor 488	494/517	Green	<b>NO</b>
DOX	480/560-590	red	quenched

#### Modification of control IgG with CMP-sialic acid derivatives

IgG Monoclonal antibodies are a very important class of therapeutic proteins used for treating cancer, infectious disease and other diseases. We used IgG as a control to study the conjugation efficiency and quantification. As we know, The Fc domain of IgG is a homodimer bearing two *N*-glycans at the conserved *N*-glycosylation sites (N297). The attached oligosaccharides exhibit considerable structural heterogeneity, in which the heptasaccharide core can be decorated with core fucose, bisecting *N*-acetylglucosamine, terminal galactose, and terminal sialic acid (Figure 4.13).<sup>37,38</sup>

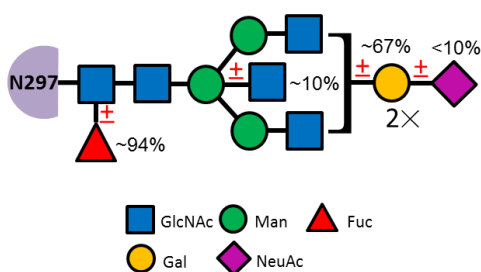
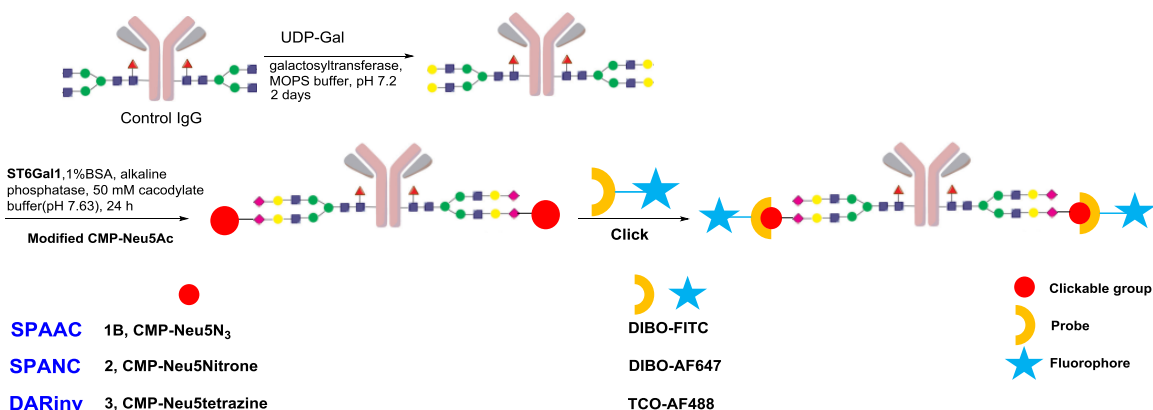


Figure 4.13 Typical Fc-linked glycans present in serum IgG heavy chains.

Since the *N*-linked heptasaccharide core is moderately galactosylated, but barely sialylated, IgG was first treated with UDP-Gal and bovine  $\beta$ -1,4-galactosyl transferase in MOPS buffer (pH 7.4) for two days to saturate IgG with galactose, followed by treatment with synthesized CMP-sialic acid derivatives (**1B**, **2** and **3**) in the presence of ST6Gal1 for 24 hours, giving chemical reporters modified IgGs on the bottom arms of the oligosaccharides according to our previous studies.<sup>18</sup> The remodeled IgGs then clicked with corresponding dyes.



Scheme 4.4 Preparation of fluorophores modified control antibodies.

A native PAGE gel was used to confirm IgG labeling with CMP-sialic acid derivatives and dyes. As we can see in Figure 4.14a, all native gel electrophoresis gave a major band at 150 kDa, which correspond to the molecular weight of IgG. Moreover, only three bands exhibited fluorescence (Typhoon 9400 Imager, Amersham) which were remodeled with ST6GalI, CMP-sialic acid derivatives (1B, 2, and 3) and exposed to fluorophore modified probes. This experiment demonstrated that the click procedures are efficient and selective.

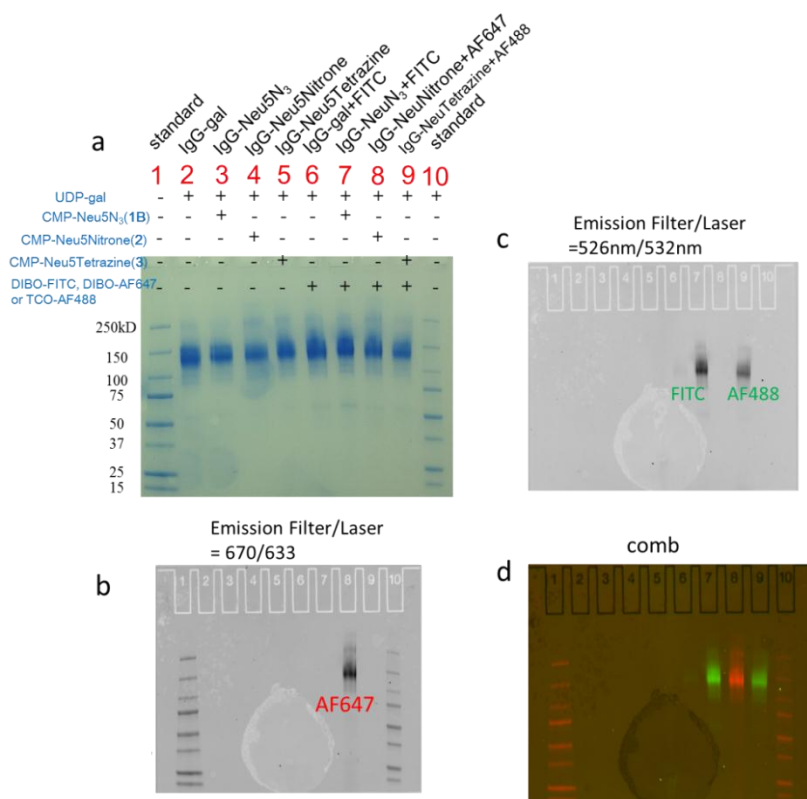


Figure 4.14 Native PAGE gel analysis of modified control IgGs using SPAAC, SPANC and DARinv.  
a) Coomassie blue staining of total protein; b) fluorescent scanning with Emission Filter/Laser=670/633;  
c) fluorescence scanning with Emission Filter/Laser=526/532; d) combination of b and c.

### Kinetics study on control antibodies

Kinetics study on control antibodies was carried out by reacting the azide, nitron and tetrazine modified antibodies with 2 eq DIBO-FITC, DIBO-AF647 and TCO-AF488, respectively. The click reactions were stopped at time points 5 min, 15min, 30min, 1h, 3h, 6h, 10h and 24h by removing the unreacted fluorophores using 10 kDa cutoff spin filter (Millipore). And the fluorescence intensities of the antibodies were measured to determine the click reaction yields after calibration with standard curve of fluorophores which is shown below:

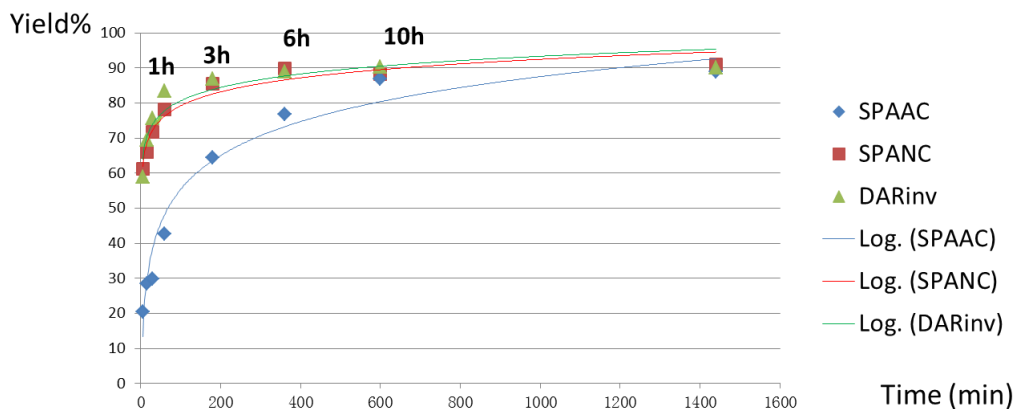
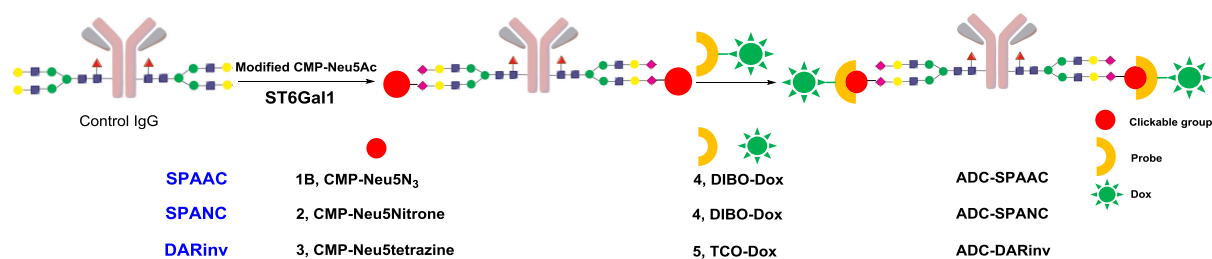


Figure 4.15 reaction rates on antibodies.

As we can see, construction of antibody-fluorophore conjugates through DARinv and SPANC gave much faster reaction rates, which were around 80% complete in 1 hour, while SPAAC only gave 40% completion in 1 hour, and 80% completion in 6 hours.

### Construction of control ADCs

Next, we prepared control antibody-DOX conjugates. Galactosylated antibodies were firstly transferred with modified sialic acid, the remodeled antibodies then clicked with DIBO-DOX/TCO-DOX (4 eq) to give the ADCs (Scheme 4.5).



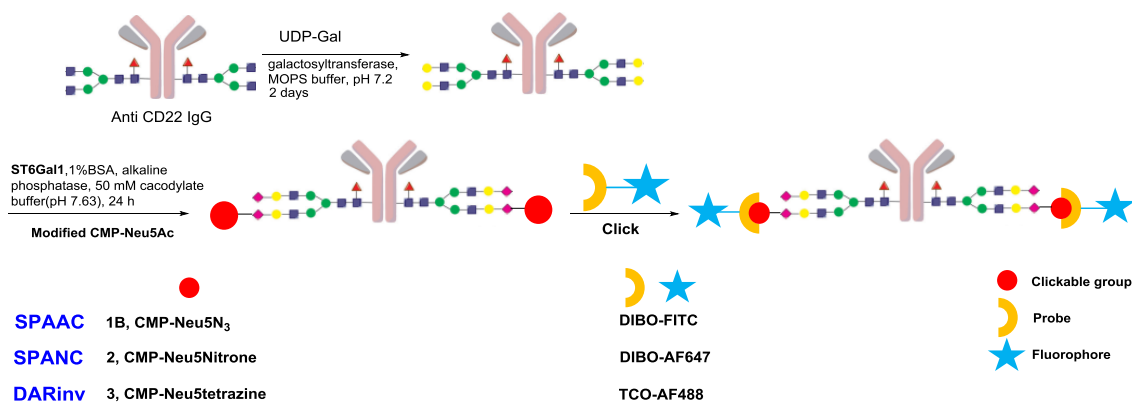
Scheme 4.5 Preparation of control antibody-DOX conjugates.

Quantification study of DOX was carried out by HPLC after acid cleavage of DOX from antibody. Control antibody samples were suspended in acetate buffer (pH 5.0) and stirred for 30

h. Next the solution was centrifuged (Milipore, centrifugation filters) to remove supernatant that contained released doxorubicin. This was further lyophilized and the amount of doxorubicin in given antibody preparations was quantified using HPLC with solvent gradient from 20 to 50% (0.01m TFA/acetonitrile) for 25 min per injection. The results demonstrated the presence of 2 DOX molecules per antibody for SPAAC, 2.3 DOX molecules per antibody for SPANC and 1.8 DOX molecules per antibody for DARinv, which is consistent with our previous finding.<sup>18</sup>

#### Modification of anti-CD22 IgG with CMP-sialic acid derivatives

The cell surface receptor CD22 undergoes constitutive endocytosis,<sup>39</sup> and is a clinically validated target for B-cell lymphoma, therefore it is a suitable target for the development of ADCs. As we have described for control IgG, anti-CD22 IgG was first treated with UDP-Gal and bovine  $\beta$ -1,4-galactosyl transferase in MOPS buffer (pH 7.4) for two days to saturate IgG with galactose, followed by treatment with synthesized CMP-sialic acid derivatives (**1B**, **2** and **3**) in the presence of ST6Gal1 for 24 hours, giving chemical reporters modified IgGs. The remodeled IgGs then clicked with corresponding dyes.



Scheme 4.6 Preparation of fluorophores modified anti CD22 antibodies.

A native PAGE gel was used to confirm IgG labeling with CMP-sialic acid derivatives and dyes. Similar as control IgGs, all native gel electrophoresis gave a major band at 150 kDa, which correspond to the molecular weight of IgG, and only three bands exhibited fluorescence (LI-COR<sup>®</sup> Odyssey CLx Imager and BIO-RAD Gel Doc<sup>TM</sup> EZ Imager) which were remodeled with ST6GalI, CMP-sialic acid derivatives (**1B**, **2**, and **3**) and exposed to fluorophore modified probes. This experiment demonstrated that the click procedures are also efficient and selective for anti CD22 IgGs.

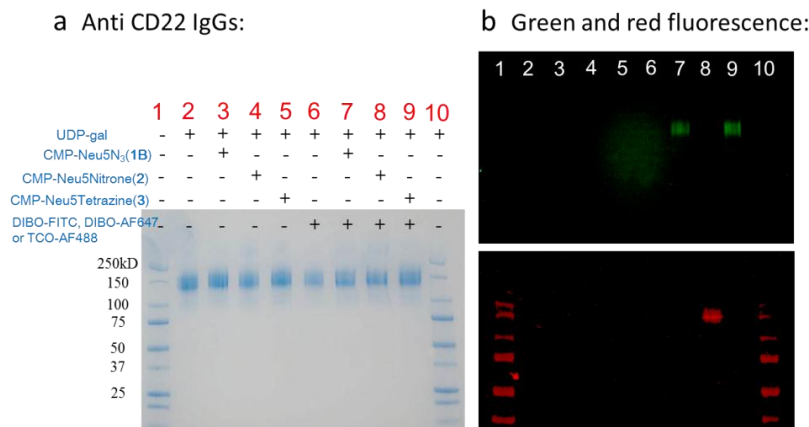
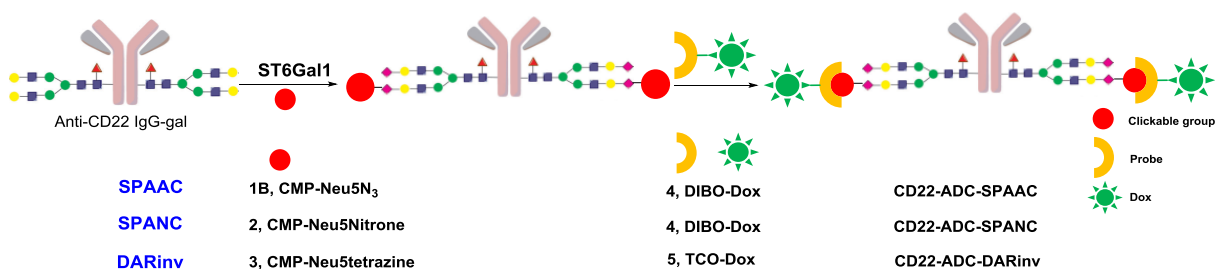


Figure 4.16 Native PAGE gel analysis of modified Anti CD22 IgGs using SPAAC, SPANC and DARinv.  
a) Coomassie blue staining of total protein; b) fluorescence scanning.

The quantification study of anti-CD22 IgGs were carried out by fluorescence intensity measurement by a POLARstar OPTIMA microplate reader (BMG LABTECH) using a 96-well fluorescence-based microplate. After construction of antibody-fluorophore conjugates, the fluorescence intensity measurements demonstrated the presence of 2.91 fluorophore molecules per antibody for SPAAC, 2.76 fluorophore molecules per antibody for SPANC and 2.72 fluorophore molecules per antibody for DARinv, which are slightly higher than control antibodies.

### Construction of anti-CD22 ADCs

The anti-CD22 ADCs were finally prepared. Galactose saturated anti-CD22 antibodies were further modified by CMP-sialic acid derivatives (**1B**, **2**, and **3**) in the presence of ST6Gal1, followed by click reaction with DIBO-DOX (**4**) or TCO-DOX (**5**) to give the functional ADCs.



Scheme 4.7 Preparation of anti-CD22 ADCs.

### Cytotoxicity study

Control or anti-CD22 ADCs (ADC-SPANC, ADC-DARinv, CD22-ADC-SPAAC, CD22-ADC-SPANC, CD22-ADC-DARinv) incubated with CD22 positive Daudi Burkett lymphoma cells. And cell viability was measured by MTT assay to access their potential of anticancer activity.

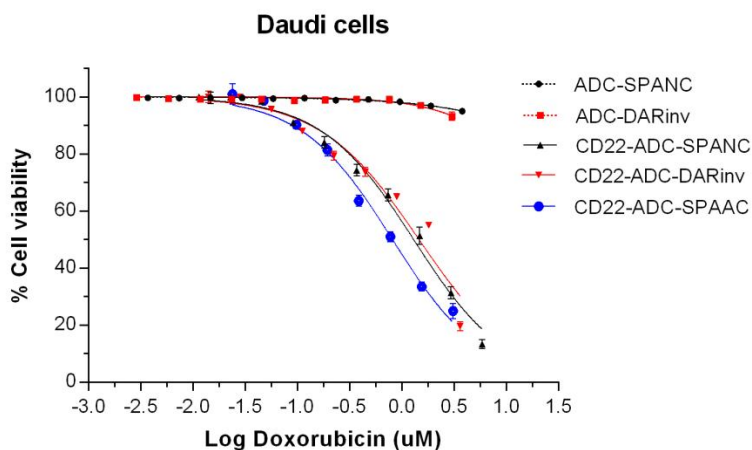


Figure 4.17 Cytotoxicity of the anti-CD22 antibody conjugated to Dox. Daudi B cells were incubated with various concentrations of control or anti CD22 IgGs for 48 h at 37°C. Cell viability was assessed by MTT assay. Data were fitted with Prism nonlinear regression software.

Table 4.3 The EC<sub>50</sub> values for CD22-ADC-SPANC, CD22-ADC-DARinv and CD22-ADC-SPAAC.

Compound	EC <sub>50</sub> in $\mu\text{M}$
CD22-ADC-SPANC	1.35
CD22-ADC-DARinv	1.47
CD22-ADC-SPAAC	1.2

As we can see in Table 4.3, anti CD22 ADCs constructed by SPANC and DARinv have comparable EC<sub>50</sub> values with anti CD22 ADCs constructed by SPAAC, which means the new construction methods worked efficiently as we expected.

## Conclusion

ADCs have generated intense interest for decades, and will eventually fulfill the promise of specific delivery of cytotoxic drugs to tumor cells. Future effort will be also addressed on site-specific conjugation modalities and optimization of linkers with balanced stability. Here, we



successfully generated ADC through SPANC and DARinv. With this new method, we can use more potent cytotoxic drugs in a much less concentration. Moreover, orthogonal SPANC and DARinv click reactions, can be used together on the same mAb to deliver two different drugs and decrease drug resistance, which will dramatically increase ADC efficacy and reduce toxicity of normal tissues at the same time.<sup>31</sup>

## **Experimental section**

### General methods and materials:

NeuAc and D-mannosamine HCl were purchased from Carbosynth LLC. Other reagents were obtained from commercial sources and used as purchased. Dichloromethane (DCM) was freshly distilled using standard procedures. Other organic solvents were purchased anhydrous and used without further purification. Unless otherwise noted, all reactions were carried out at room temperature (RT) in glassware with magnetic stirring. Organic solutions were concentrated under reduced pressure with bath temperatures < 30 °C. Flash column chromatography was carried out on silica gel G60 (Silicycle, 60-200 µm, 60 Å). Thin-layer chromatography (TLC) was carried out on Silica gel 60 F<sub>254</sub> (EMD Chemicals Inc.) with detection by UV absorption (254 nm) where applicable, by spraying with 20% sulfuric acid in ethanol followed by charring at ~150 °C or by spraying with a solution of (NH<sub>4</sub>)<sub>6</sub>Mo<sub>7</sub>O<sub>24</sub>·H<sub>2</sub>O (25 g/L) in 10% sulfuric acid in ethanol followed by charring at ~150°C. <sup>1</sup>H and <sup>13</sup>C NMR spectra were recorded on a Varian Inova-300 (300/75 MHz), a Varian Inova-500 (500 MHz) and a Varian Inova-600 (600/150 MHz) spectrometer equipped with sun workstations. Multiplicities are quoted as singlet (s), doublet (d), doublet of

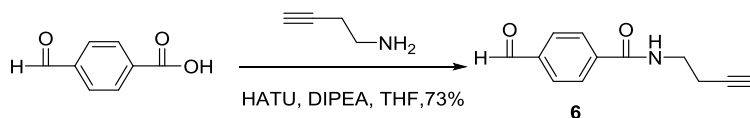
doublets (dd), triplet (t) or multiplet (m). All NMR signals were assigned on the basis of  $^1\text{H}$  NMR,  $^{13}\text{C}$  NMR, gCOSY and gHSQC experiments. All chemical shifts are quoted on the  $\delta$ -scale in parts per million (ppm). Residual solvent signals were used as an internal reference. Mass spectra were recorded on an Applied Biosystems 5800 MALDI-TOF or Shimadzu LCMS-IT-TOF mass spectrometer. The matrix used was 2,5-dihydroxy-benzoic acid (DHB). Reverse-Phase HPLC was performed on an Agilent 1200 series system equipped with an auto-sampler, fraction-collector, UV-detector and eclipse XDB-C18 column (5  $\mu\text{m}$ , 4.6  $\times$  250 mm or 9.4  $\times$  250 mm).

#### Biochemical reagents.

The control immunoglobulin G (IgG) was obtained from Athens Research and Technology, Athens, GA. CD22 antibody (HD239) was purchased from Santa Cruz. Biotechnology, Inc. Recombinant rat  $\alpha$ -(2,6)-sialyltransferase (ST6Gal I) were prepared by reported procedures.<sup>40</sup>

#### Chemical synthesis.

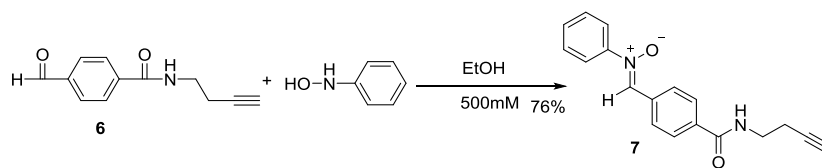
##### ***N*-(but-3-yn-1-yl)-4-formylbenzamide (6)**



4-formylbenzoic acid (600 mg, 4 mmol) and 1-amino-3-butyne (393  $\mu\text{L}$ , 4.8 mmol) were dissolved in dry THF (20 mL), the solution was cooled to 0  $^{\circ}\text{C}$ . 1-[Bis(dimethylamino)methylene]-1H-1,2,3-triazolo[4,5-b]pyridinium 3-oxid

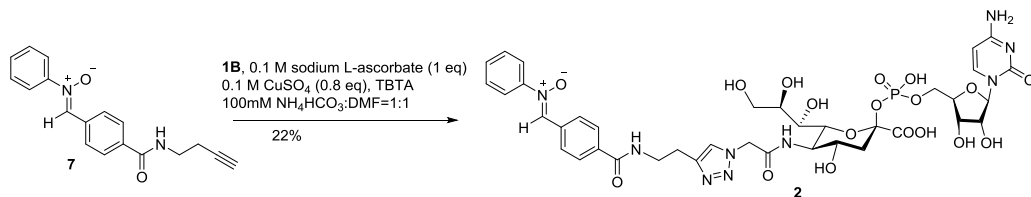
hexafluorophosphate (HATU, 2.28 g, 6 mmol) and *N,N*-Diisopropylethylamine (2.79 mL, 16 mmol) were added. The reaction mixture was then warmed to room temperature and stirred for 18 hours before it was concentrated under reduced pressure. The residue was diluted with ethyl acetate (30 mL), the solution was washed with 1 M HCl (30 mL \*2), brine, dried over MgSO<sub>4</sub> and the solvent was removed under reduced pressure. The residue was purified by silica gel column chromatography using a gradient of ethyl acetate in hexane (20% →25%) to give **6** (587 mg, 73%) as a white solid. <sup>1</sup>H NMR (300 MHz, cdcl<sub>3</sub>) δ 10.08 (s, 1H, HC=O), 8.03 – 7.86 (m, 4H, PhH), 6.54 (d, *J* = 8.6 Hz, 1H, NH), 3.64 (q, *J* = 6.2 Hz, 2H, NHCH<sub>2</sub>), 2.55 (td, *J* = 6.3, 2.6 Hz, 2H, CH<sub>2</sub>C≡C), 2.07 (t, *J* = 2.7 Hz, 1H, C≡CH).

**(Z)-1-(4-(but-3-yn-1-ylcarbamoyl)phenyl)-*N*-phenylmethanimine oxide (7)**



*N*-phenylhydroxylamine (12 mg, 0.11mmol) was added to a solution of **6** (20 mg, 0.1 mmol) in dry ethanol (0.2 mL). The reaction mixture was stirred at room temperature for 18 hours and then diluted with hexane (5 mL) while white precipitate was formed. The supernatant was removed by centrifugation, and the residue was washed with hexane twice and purified by silica gel column chromatography using a gradient of DCM in acetone (5% →10%) to give **7** (22 mg, 76%) as a white solid. <sup>1</sup>H NMR (300 MHz, cdcl<sub>3</sub>) δ 8.55 – 8.37 (m, 2H, PhH), 7.98 (s, 1H, N=CH), 7.94 – 7.85 (m, 2H, PhH), 7.82 – 7.72 (m, 2H, PhH), 7.54 – 7.44 (m, 3H, PhH), 6.64 (s, 1H, NH), 3.63 (q, *J* = 6.3 Hz, 2H, NHCH<sub>2</sub>), 2.54 (td, *J* = 6.4, 2.7 Hz, 2H, CH<sub>2</sub>C≡C), 2.07 (t, *J* = 2.6 Hz, 1H, C≡CH). <sup>13</sup>C NMR (75 MHz, cdcl<sub>3</sub>) δ 133.5, 129.8, 129.7, 128.9, 127.2, 121.7, 38.4, 19.6.

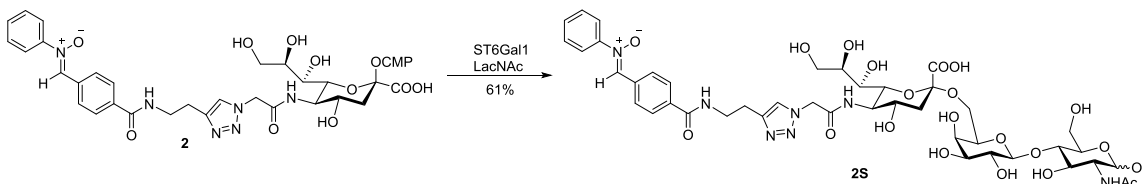
## Nitrone-CMP-Neu5N<sub>3</sub> (**2**)



A solution of **7** (14.0 mg, 0.048 mmol) in DMF (3 mL) was added to the solution of CMP-Neu5N<sub>3</sub> (**1B**, 21 mg, 0.032 mmol) in Tris-HCl buffer (100 mM, pH 7.5, 3 mL). To this mixture was added CuSO<sub>4</sub> (100 mM, 256  $\mu$ L), sodium L-ascorbate (100 mM, 320  $\mu$ L) and TBTA (3.4 mg, 0.0064 mmol). After stirring for 2 hours at ambient temperature, the reaction mixture was lyophilized to provide a residue that was applied to a C18 column, which was eluted with a gradient of methanol in 0.1 M NH<sub>4</sub>HCO<sub>3</sub> buffer (5%  $\rightarrow$ 25%). Fractions containing product were concentrated under reduced pressure, and the residue was redissolved in 1 mL water and lyophilized to provide **2** (6.5 mg, 22%) as a slightly yellow solid. <sup>1</sup>H NMR (600 MHz, d<sub>2</sub>O)  $\delta$  8.28 (d,  $J$  = 6.1 Hz, 2H, PhH), 7.94 – 7.90 (m, 1H, H-6, cyt), 7.88 (s, 1H, CH=C, triazole), 7.77 (d,  $J$  = 5.0 Hz, 1H, N=CH, nitrone), 7.71 – 7.65 (m, 2H, PhH), 7.63 – 7.57 (m, 2H, PhH), 7.47 – 7.41 (m, 3H, PhH), 6.06 (s, 1H, H-5, cyt), 5.81 (dd,  $J$  = 16.2, 3.7 Hz, 1H, H-1, rib), 5.14 (d,  $J$  = 3.3 Hz, 2H, triazole-CH<sub>2</sub>-C=O), 4.19 – 4.04 (m, 6H, H-2,3,4,5 rib, H-6 Neu), 4.01 – 3.94 (m, 1H, H-4), 3.84 (t,  $J$  = 10.3 Hz, 1H, H-5), 3.77 (t,  $J$  = 8.1 Hz, 1H, H-8), 3.70 (dd,  $J$  = 11.9, 2.3 Hz, 1H, H-9a), 3.57 (q,  $J$  = 6.1 Hz, 2H, NH<sub>2</sub>-CH<sub>2</sub>-CH<sub>2</sub>-triazole), 3.49 – 3.41 (m, 1H, H-9b), 3.30 (t,  $J$  = 11.5 Hz, 1H, H-7), 2.93 (d,  $J$  = 6.0 Hz, 2H, NH<sub>2</sub>-CH<sub>2</sub>-CH<sub>2</sub>-triazole), 2.34 (dd,  $J$  = 13.3, 4.7 Hz, 1H, H-3eq), 1.49 (td,  $J$  = 12.4, 5.5 Hz, 1H, H-3ax). <sup>13</sup>C NMR (151 MHz, d<sub>2</sub>O)  $\delta$  142.8, 131.1, 130.4, 130.2, 129.5, 127.4, 125.2, 121.6, 89.1, 83.1, 74.3, 71.4, 69.7, 69.2, 68.7, 66.5, 64.7,

63.0, 62.8, 52.1, 52.0, 41.1, 40.9, 39.5, 24.7. HRMS (ESI):  $m/z$  calcd for  $C_{38}H_{45}N_9O_{18}P$   $[M-H]^-$ : 946.2626; found  $m/z$ : 946.1999.

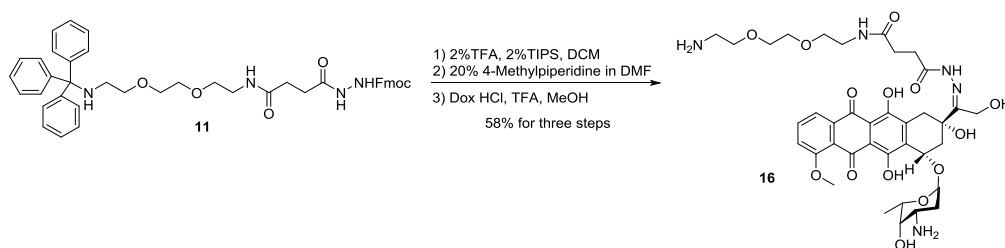
**Nitronyl Neu5Ac $\alpha$ (2,6)Gal $\beta$ (1,4)GlcNAc (2S):**



Recombinant  $\alpha$ -(2,6)-sialyltransferase (ST6Gal I) [GenBank P13721] (0.63 mg/mL, 25  $\mu$ L) and calf intestine alkaline phosphatase (10000 U/mL, 2.5  $\mu$ L) were added to a mixture of LacNAc (0.61 mg, 1.6  $\mu$ mol) in cacodylate buffer (50 mM, pH 7.63, 96  $\mu$ L) containing 0.1% BSA and **2** (1.5 mg, 1.6  $\mu$ mol) in an Eppendorf tube. The tube was incubated at 37  $^{\circ}$ C, and progress of the reaction was monitored by TLC (EtOAc : CH<sub>3</sub>OH : H<sub>2</sub>O : AcOH = 4:2:1:0.5, v:v:v:v), which after 5 hour indicated completion of the reaction. CH<sub>3</sub>OH (1  $\mu$ L) was added and the mixture was lyophilization to provide a residue that was applied to a C18 column, which was eluted with a gradient of methanol in water (5%  $\rightarrow$ 30%). Fractions containing product were concentrated under reduced pressure, and the residue was redissolved in 1 mL water and lyophilized to give **2S** (1.0 mg, 61%) as a slightly yellow solid. <sup>1</sup>H NMR (600 MHz, d<sub>2</sub>o)  $\delta$  8.31 – 8.25 (m, 2H, PhH), 7.90 – 7.84 (m, 1H, N=CH, nitrone), 7.76 (d,  $J$  = 15.4 Hz, 1H, CH=C, triazole), 7.71 – 7.64 (m, 2H, PhH), 7.60 (d,  $J$  = 7.7 Hz, 2H, PhH), 7.49 – 7.44 (m, 3H, PhH), 5.10 (d,  $J$  = 2.5 Hz, 2H, triazole-CH<sub>2</sub>-C=O), 5.03 – 4.97 (m, 1H, H-1'), 4.28 (t,  $J$  = 7.7 Hz, 1H, H-1''), 3.88 – 3.61 (m, 11H), 3.61 – 3.34 (m, 11H), 2.93 (t,  $J$  = 6.1 Hz, 2H, NH<sub>2</sub>-CH<sub>2</sub>-CH<sub>2</sub>-triazole), 2.51 (dd,  $J$  = 12.5, 4.7 Hz, 1H, H-3eq), 1.83 – 1.75 (m, 3H, Ac), 1.56 (t,  $J$  = 12.2 Hz, 1H, H-3ax). <sup>13</sup>C NMR (151

MHz, d<sub>2</sub>O)  $\delta$ 130.9, 130.4, 130.1, 129.5, 128.1, 125.1, 121.7, 103.4, 90.6, 80.8, 73.6, 72.3, 72.2, 71.6, 70.6, 69.8, 69.8, 69.2, 68.3, 68.3, 68.1, 63.3, 63.3, 62.5, 62.5, 60.1, 55.9, 53.3, 52.1, 51.9, 40.3, 40.0, 39.7, 25.1, 22.1. HRMS (ESI):  $m/z$  calcd for C<sub>41</sub>H<sub>63</sub>N<sub>11</sub>O<sub>21</sub>PS [M-H]<sup>-</sup>: 1006.3535; found  $m/z$ : 1006.2840.

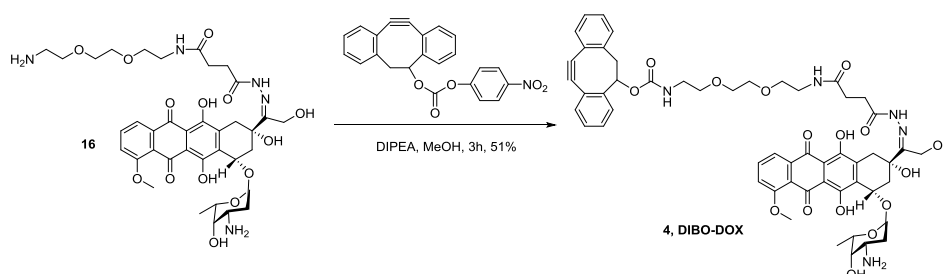
### NH<sub>2</sub>-PEG<sub>3</sub>-DOX (16)



To a mixture of trifluoroacetic acid (TFA, 3%) and triisopropylsilane (TIPS, 3%) in DCM (0.8 mL) was added Trt-PEG<sub>3</sub>-NHNHFmoc (**11**, 10 mg, 0.0138 mmol), the reaction mixture was stirred for 2 hours at room temperature, before it was quenched by adding 30  $\mu$ L *N,N*-Diisopropylethylamine. The solvent was removed under reduced pressure and the residue was dried under high vacuum for 1 hour. The residue was redissolved in dry DMF (1.5 mL), to the mixture was added 4-methylpiperidine (0.3 mL), and reaction mixture was stirred for 2 hours at room temperature, before the solvent was removed under reduced pressure and the residue was dried under high vacuum for another 1 hour. The residue was redissolved in dry MeOH (1.2 mL), to the mixture was added Doxorubicin hydrochloride (24 mg, 0.0414 mmol), trifluoroacetic acid (10  $\mu$ L), the reaction mixture was stirred overnight at room temperature, and applied to LH-20 column (1.5 m \*1.5 cm, eluted with DCM/MeOH=1/1) directly. The fractions containing the product were combined and concentrated under reduced pressure to give **16** (6.3 mg, 58%) as a red solid. <sup>1</sup>H NMR (500 MHz, cd<sub>3</sub>od)  $\delta$  8.01 (d,  $J$  = 7.4 Hz, 1H, PhH), 7.87 (t,  $J$  = 8.1 Hz, 1H,

PhH), 7.61 (d,  $J = 8.4$  Hz, 1H, PhH), 5.50 (d,  $J = 3.7$  Hz, 1H, H-1 sugar), 5.11 (t,  $J = 6.0$  Hz, 1H, CHO-sugar Dox), 4.68 – 4.54 (m, 2H, N=CCH<sub>2</sub>OH Dox), 4.24 (q,  $J = 6.7$  Hz, 1H, H-5 sugar), 4.05 (s, 3H, OCH<sub>3</sub>), 3.80 – 3.47 (m, 12H, OCH<sub>2</sub>CH<sub>2</sub>O, OCH<sub>2</sub>CH<sub>2</sub>N \*2, OCH<sub>2</sub>CH<sub>2</sub>NH, H-3 sugar, H-4 sugar), 3.39 (d,  $J = 4.3$  Hz, 1H, PH-CHH-C), 3.26 (t,  $J = 5.6$  Hz, 1H, PH-CHH-C), 3.17 – 3.09 (m, 2H, OCH<sub>2</sub>CH<sub>2</sub>NH), 2.82 – 2.31 (m, 6H, C=OCH<sub>2</sub>CH<sub>2</sub>C=O, CCH<sub>2</sub>CHO-sugar Dox), 2.12 – 1.88 (m, 2H, C-2 sugar), 1.35 – 1.29 (m, 3H, CH<sub>3</sub> sugar). <sup>13</sup>C NMR (126 MHz, cd<sub>3</sub>od) δ 135.8, 119.1, 118.9, 99.6, 72.4, 70.0, 69.6, 69.2, 69.2, 66.6, 66.6, 66.5, 57.5, 57.4, 55.7, 47.2, 39.6, 39.3, 39.1, 39.1, 38.8, 29.5, 29.2, 28.1, 28.1, 27.0, 27.0, 15.7. HRMS (ESI):  $m/z$  calcd for C<sub>41</sub>H<sub>63</sub>N<sub>11</sub>O<sub>21</sub>PS [M+Na]<sup>+</sup>: 810.3174; found  $m/z$ : 810.1628.

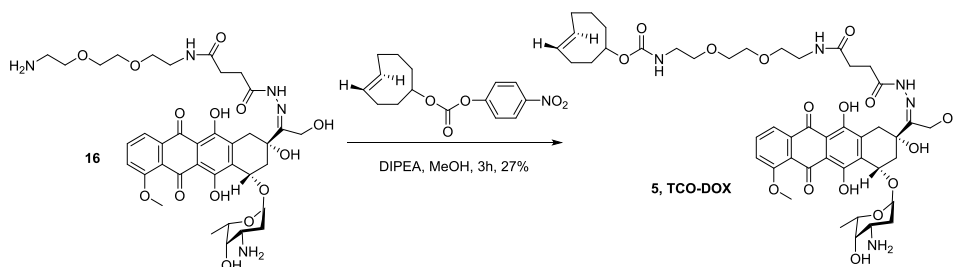
#### DIBO-PEG<sub>3</sub>-DOX (4)



**16** (5 mg, 0.00635 mmol) and DIBO-PNP (3.7 mg, 0.0096 mmol) were dissolved in MeOH (1 mL), DIPEA (2.2 μL, 0.0126 mmol) was added. The reaction mixture was stirred for 2 hours at room temperature, before it was concentrated under reduced pressure and the residue was purified by iatrobeads column chromatography using a gradient of methanol in CH<sub>2</sub>Cl<sub>2</sub> (10% → 30%) to give **4** (3.3 mg, 51%) as a red solid. <sup>1</sup>H NMR (500 MHz, cd<sub>3</sub>od) δ 8.03 – 7.89 (m, 1H, PhH Dox), 7.89 – 7.77 (m, 1H, PhH Dox), 7.60 – 7.47 (m, 2H, PhH Dox and DIBO), 7.41 – 7.16 (m, 7H, PhH DIBO), 5.50 – 5.39 (m, 1H, H-1 sugar), 5.33 (dt,  $J = 6.8, 2.5$  Hz, 1H, CHO DIBO),

5.13 – 5.01 (m, 1H, CHO-sugar Dox), 4.69 – 4.56 (m, 2H, N=CCH<sub>2</sub>OH Dox), 4.19 (dq, *J* = 20.5, 7.0 Hz, 1H, H-5 sugar), 4.03 (t, *J* = 7.1 Hz, 3H, OCH<sub>3</sub> DOX), 3.70 – 3.59 (m, 4H), 3.54 (ddd, *J* = 22.2, 8.5, 5.4 Hz, 5H), 3.40 – 3.34 (m, 2H), 3.30 (s, 5H), 3.28 – 3.24 (m, 1H), 3.20 – 3.13 (m, 1H), 3.12 – 3.04 (m, 1H), 2.95 (dd, *J* = 17.7, 6.0 Hz, 1H), 2.89 – 2.67 (m, 2H), 2.66 – 2.53 (m, 1H), 2.49 – 2.43 (m, 2H), 2.43 – 2.12 (m, 2H), 1.89 – 1.56 (m, 2H), 1.31 (s, 3H, CH<sub>3</sub> sugar). <sup>13</sup>C NMR (126 MHz, cd<sub>3</sub>od) δ 135.7, 129.6, 129.6, 127.9, 127.8, 126.8, 125.8, 125.4, 123.5, 119.1, 118.7, 100.5, 76.5, 71.9, 69.9, 69.9, 69.2, 67.2, 67.1, 58.0, 55.7, 54.8, 46.6, 45.7, 45.7, 40.4, 39.4, 39.0, 39.0, 39.0, 38.8, 33.7, 33.6, 33.1, 31.0, 30.2, 29.5, 29.3, 27.3, 15.9.

#### TCO-PEG<sub>3</sub>-DOX (5)



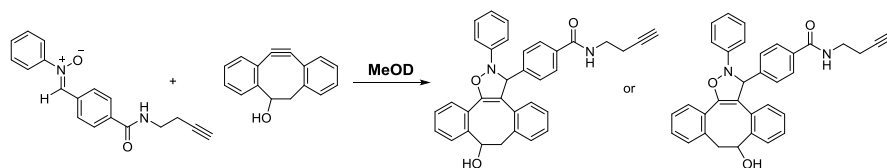
**16** (2.8 mg, 0.00356 mmol) and TCO-PNP (2.3 mg, 0.0078 mmol) were dissolved in MeOH (1 mL), DIPEA (2.2 μL, 0.0126 mmol) was added. The reaction mixture was stirred for 4 hours at room temperature, before it was concentrated under reduced pressure and the residue was purified by iatrobeads column chromatography using a gradient of methanol in CH<sub>2</sub>Cl<sub>2</sub> (10% → 50%) to give **5** (0.9 mg, 27%) as a red solid. <sup>1</sup>H NMR (600 MHz, cd<sub>3</sub>od) δ 7.98 (s, 1H, PhH), 7.81 (s, 1H, PhH), 7.53 (d, *J* = 8.4 Hz, 1H, PhH), 5.64 (q, *J* = 8.9 Hz, 1H, CH=CH TCO), 5.57 (dt, *J* = 19.1, 8.4 Hz, 1H, CH=CH TCO), 5.42 (q, *J* = 7.9, 7.0 Hz, 1H, H-1 sugar), 5.10 (s, 1H, CHO-sugar Dox), 4.61 (dd, *J* = 30.5, 15.5 Hz, 3H, N=CCH<sub>2</sub>OH Dox, CHO TCO), 4.20 (d, *J* =



82.4 Hz, 1H, H-5 sugar), 4.02 (s, 3H, OCH<sub>3</sub>, Dox), 3.69 – 3.43 (m, 11H), 3.37 – 3.30 (m, 2H), 3.27 – 3.20 (m, 3H), 2.85 – 2.00 (m, 11H), 1.99 – 1.45 (m, 7H), 1.27 (s, 3H, CH<sub>3</sub> sugar). <sup>13</sup>C NMR (151 MHz, cd<sub>3</sub>od) δ135.7, 129.3, 129.3, 119.2, 118.7, 100.5, 80.4, 75.8, 71.8, 69.9, 69.7, 69.3, 69.2, 57.6, 55.9, 55.1, 40.8, 40.2, 39.0, 38.9, 38.7, 38.7, 38.3, 38.2, 33.8, 33.8, 33.8, 33.8, 33.8, 33.6, 33.6, 32.1, 30.7, 30.7, 30.3, 29.8, 29.5, 27.3, 27.3, 25.2, 24.6, 24.6, 21.9, 21.9, 16.1.

### Kinetics measurement by NMR

The reaction between DIBO and Nitron was monitored by NMR.



Determination by UV spectroscopy was not possible owing to overlapping absorptions of DIBO and Nitron, <sup>1</sup>H-NMR monitoring was performed by rapid mixing (t=0) of stock solution A and B (0.3 mL each, [A]<sub>0</sub>= [B]<sub>0</sub>) in an NMR tube and immediate insertion into a 500 MHz NMR spectrometer. NMR spectra were measured at preset time-intervals (in general every 54 seconds) Kinetics was determined by measuring the decrease of the integral of the signal caused by the proton on nitron sp<sup>2</sup> carbon. A starting value of the integral of the proton signal was estimated, due to the fact that cycloaddition had already proceeded by the time of the first measurement. The conversion was determined by dividing the integral of the proton by the estimated starting value.

The second order rate was calculated according to equation (1):

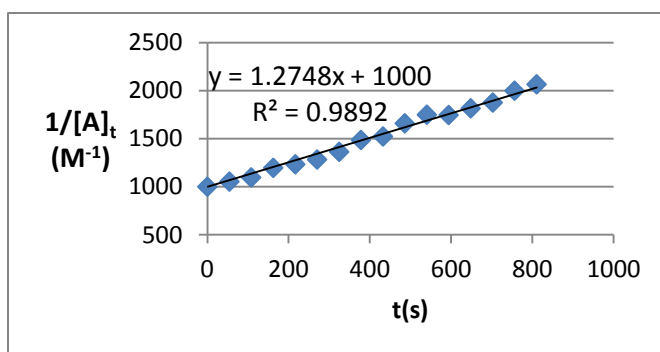
$$\frac{1}{[A]_t} = kt + \frac{1}{[A]_0} \quad (1)$$

With  $k = 2^{\text{nd}}$  order rate constant ( $\text{M}^{-1}\text{s}^{-1}$ ),  $t =$  reaction time (s),  $[A]_0 =$  the initial concentration of substrate A (mmol/mL).

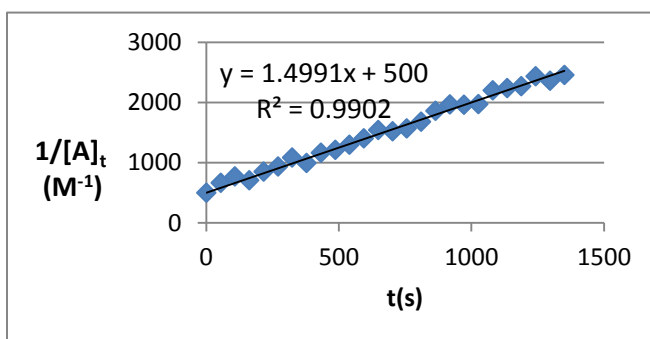
The kinetics was measured in triplicate with different concentrations of reactants A and B.

Stock solution A (5 mM, 4 mM and 2 mM): Nitron (4.2 mg, 0.0144 mmol) was dissolved in 2.875 mL MeOD to give a 5 mM solution. And this 5 mM solution was then diluted with MeOD to give 4 mM and 2 mM solutions.

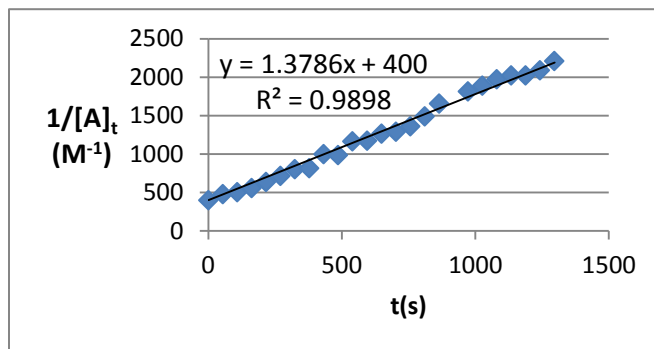
Stock solution B (5 mM, 4 mM and 2 mM): DIBO (2.6 mg, 0.0118 mmol) was dissolved in 2.363 mL MeOD to give a 5 mM solution. And this 5 mM solution was then diluted with MeOD to give 4 mM and 2 mM solutions.



Linear plot of the reaction between Nitron ( $[A]_0 = 1 \text{ mM}$ ) and DIBO ( $[B]_0 = 1 \text{ mM}$ )  
 $k = 1.27 \text{ M}^{-1}\text{s}^{-1}$



Linear plot of the reaction between Nitron ( $[A]_0 = 2 \text{ mM}$ ) and DIBO ( $[B]_0 = 2 \text{ mM}$ )  
 $k = 1.50 \text{ M}^{-1}\text{s}^{-1}$



Linear plot of the reaction between Nitron ( $[A]_0=2.5$  mM) and DIBO ( $[B]_0=2.5$  mM)  
 $k=1.38 \text{ M}^{-1}\text{s}^{-1}$

The average second order rate constant was calculated to be  $(1.27 + 1.50 + 1.38) / 3 = 1.38 \text{ M}^{-1}\text{s}^{-1}$ .

#### Kinetics measurement by UV

The reaction between BCN and Nitron was monitored by UV-Vis spectroscopy using a ten-fold (or more than ten-fold) excess of reactant B (BCN). The reaction was conducted at  $25^\circ\text{C}$  ( $\pm 0.5^\circ\text{C}$ ) in a 1-mL UV cuvette. Prepared solution A (500  $\mu\text{L}$ ) and B (500  $\mu\text{L}$ ) was rapidly mixed ( $t=0$ ) and immediately inserted into a 1 mL UV cuvette. Next, UV-absorption was measured at preset time intervals (in general every 15 seconds). The graphs obtained showed a decrease of the absorption over time.

The kinetics was measured in triplicate, with different concentration of reactant B.

The pseudo-first order rates were calculated according to equation (2):

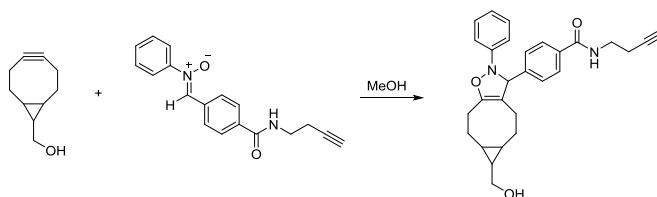
$$[A]_t = [A]_0 e^{-k(\text{obs})t} \quad (2)$$

With  $k(\text{obs})$  = pseudo-first order rate constant ( $\text{s}^{-1}$ ),  $t$  = reaction time (s),  $[A]_0$  = the initial concentration of substrate A (mmol/mL).

The second order rates were calculated according to equation (3):

$$k = k(\text{obs})/[B]_0 \quad (3)$$

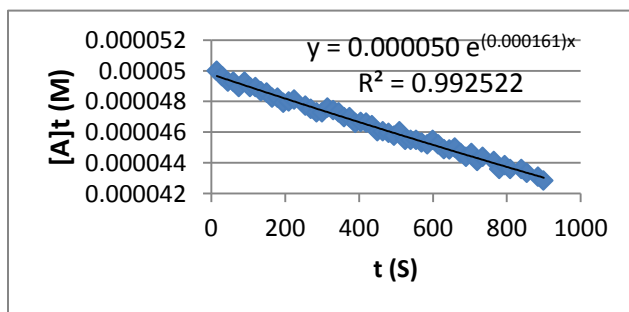
With  $k$  = 2nd order rate constant ( $M^{-1}s^{-1}$ ),  $[B]_0$  = the initial concentration of substrate B (mmol/mL).



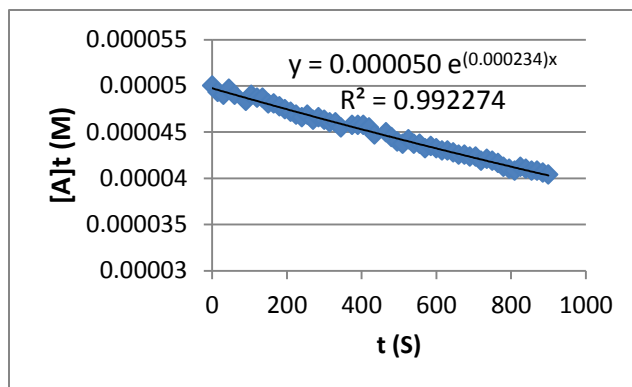
The reaction rates were measured by UV-Vis spectroscopy at 322 nm.

Stock solution A (100  $\mu M$ ): Nitrone (1.1 mg, 0.00377 mmol) was dissolved in 3.77 mL MeOH to give a 1 mM solution. And this 1 mM solution was diluted with MeOH to give a 100  $\mu M$  solution.

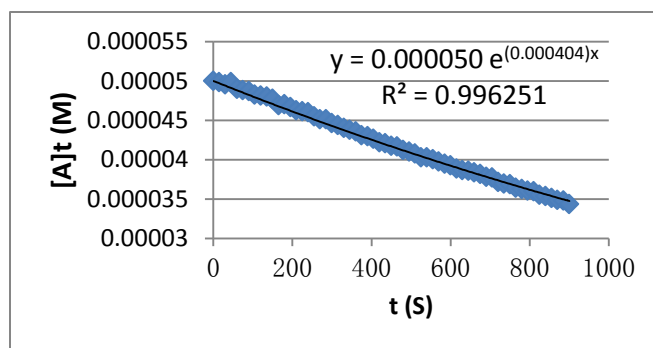
Stock solution B (1 mM, 1.5 mM and 2.333 mM): BCN-OH (1.2 mg, 0.008 mmol) was dissolved in 2.665 mL MeOH to give a 3 mM solution, and this 3 mM solution was diluted with MeOH to give 1 mM, 1.5 mM and 2.333 mM solutions.



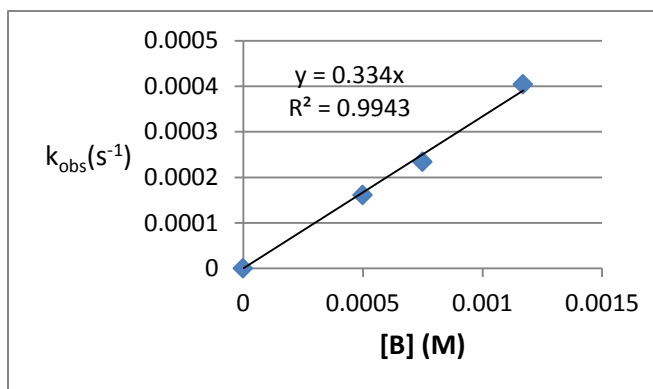
Exponential plot of the reaction between Nitrone ( $[A]_0 = 50 \mu M$ ) and BCN ( $[B]_0 = 500 \mu M$ ).  
 $k(\text{obs}) = 0.000161 s^{-1}$



Exponential plot of the reaction between Nitron ( $[A]_0 = 50 \mu\text{M}$ ) and BCN ( $[B]_0 = 750 \mu\text{M}$ ).  
 $k(\text{obs}) = 0.000234 \text{ s}^{-1}$



Exponential plot of the reaction between Nitron ( $[A]_0 = 50 \mu\text{M}$ ) and BCN ( $[B]_0 = 1167 \mu\text{M}$ ).  
 $k(\text{obs}) = 0.000404 \text{ s}^{-1}$



Linear plot of the reaction between Nitron and BCN,  $k = 0.33 \text{ M}^{-1} \text{ s}^{-1}$ .

The second order rate constant was calculated to be  $0.33 \text{ M}^{-1} \text{ s}^{-1}$ .

## Fluorescence quenching by FRET

The fluorescence intensity was measured by a fluorescence spectroscopy.

Solution S (1 mL): Fluorophore-DIBO or Fluorophore-TCO was prepared in a specific concentration.

Solution A (1 mL): 500  $\mu$ L solution S mixed with 500  $\mu$ L MeOH.

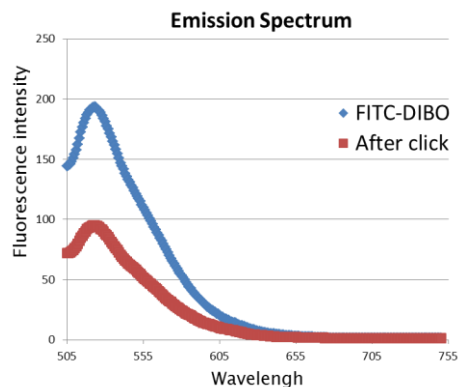
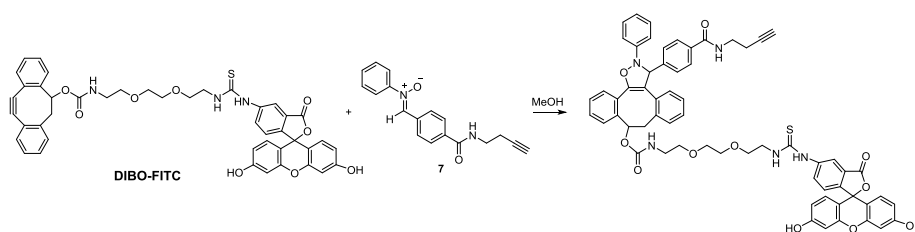
Solution B (1 mL): 500  $\mu$ L solution S mixed with 500  $\mu$ L nitrone **7** or tetrazine **8** (10 eq), 3 h at r.t.

Solution A (before click) and Solution B (after click) were inserted into a 1 mL UV cuvette in sequence and their fluorescence intensity of emission spectrum were measured.

### **FITC-DIBO + nitrone 7:**

Solution A: 500  $\mu$ L 90  $\mu$ M FITC-DIBO mixed with 500  $\mu$ L MeOH.

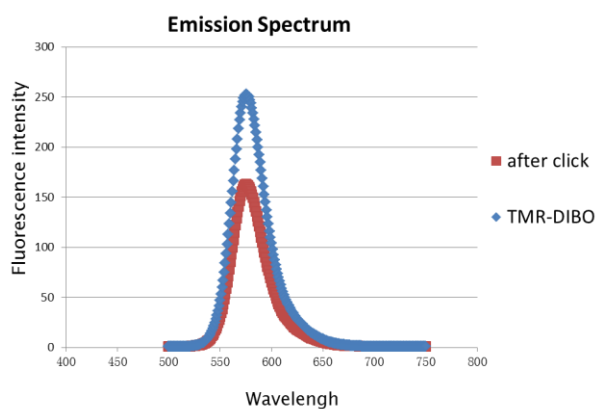
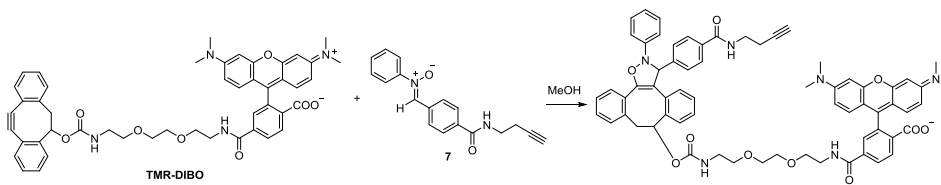
Solution B: 500  $\mu$ L 90  $\mu$ M FITC-DIBO mixed with 500  $\mu$ L 0.9 mM nitrone **7** (10 eq).



### TMR-DIBO + nitrone **7**:

Solution A: 500  $\mu\text{L}$  5  $\mu\text{M}$  TMR-DIBO mixed with 500  $\mu\text{L}$  MeOH.

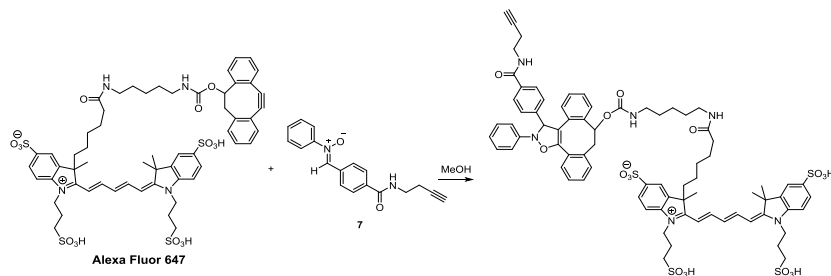
Solution B: 500  $\mu\text{L}$  5  $\mu\text{M}$  TMR-DIBO mixed with 500  $\mu\text{L}$  50  $\mu\text{M}$  nitrone **7** (10 eq).

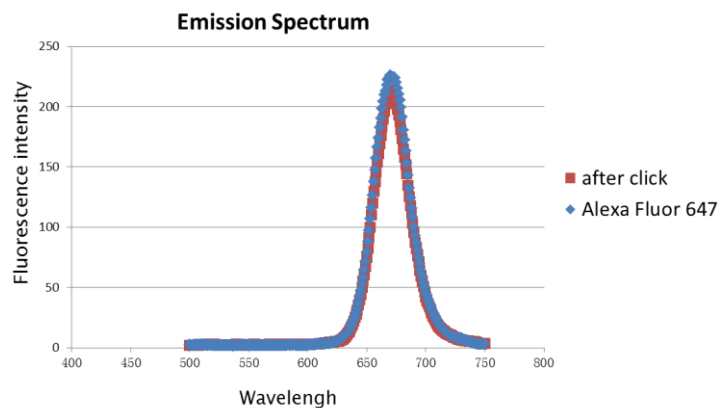


### AF647-DIBO + nitrone **7**:

Solution A: 500  $\mu\text{L}$  10  $\mu\text{M}$  TMR-DIBO mixed with 500  $\mu\text{L}$  MeOH.

Solution B: 500  $\mu\text{L}$  10  $\mu\text{M}$  TMR-DIBO mixed with 500  $\mu\text{L}$  100  $\mu\text{M}$  nitrone **7** (10 eq).

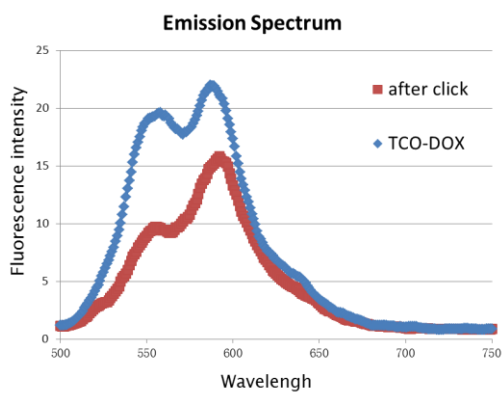
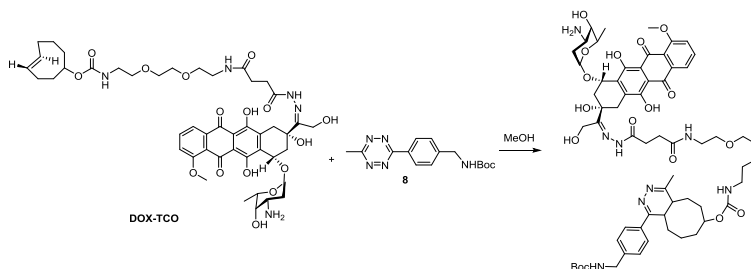




### DOX-TCO + tetrazine **8**:

Solution A: 500  $\mu$ L 10  $\mu$ M DOX-TCO mixed with 500  $\mu$ L MeOH.

Solution B: 500  $\mu$ L 10  $\mu$ M DOX-TCO mixed with 500  $\mu$ L 100  $\mu$ M tetrazine **8** (10 eq).

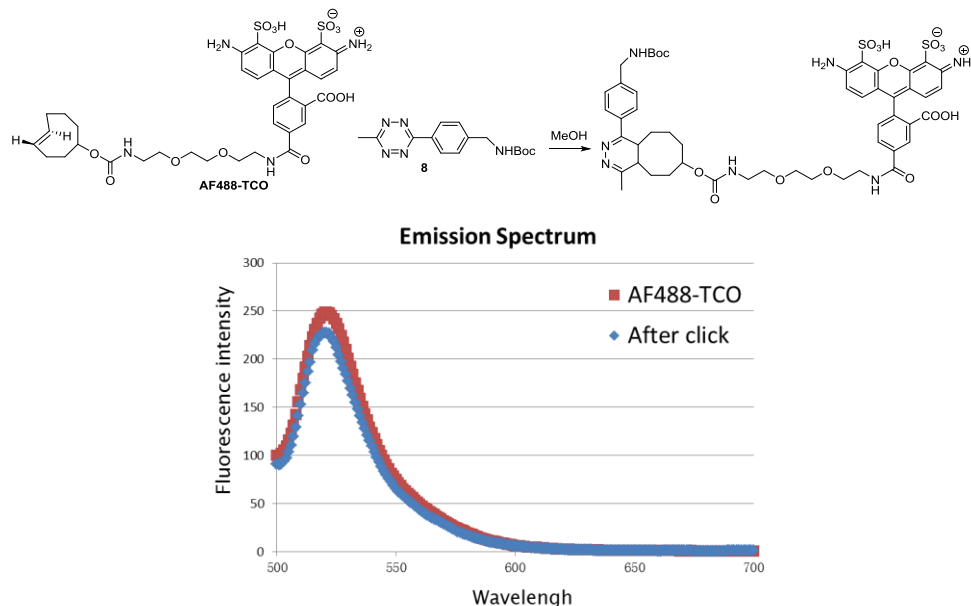


### AF488-TCO + tetrazine **8**:

Solution A: 500  $\mu$ L 0.4  $\mu$ M DOX-TCO mixed with 500  $\mu$ L MeOH.

Solution B: 500  $\mu$ L 0.4  $\mu$ M DOX-TCO mixed with 500  $\mu$ L 4  $\mu$ M tetrazine **8** (10 eq).





Remodeling of the glycans of the control- and anti-CD22 IgG antibodies. Adapted from reference [18]<sup>18</sup>

The control immunoglobulin G (IgG) was dialyzed for 24 h against water and then lyophilized. The antibody was resuspended in MOPS buffer (50 mM, pH 7.4) containing  $\text{MnCl}_2$  (20 mM). The galactosylation of the oligosaccharide was performed using UDP-galactose (10 mM), BSA ( $80 \mu\text{g mL}^{-1}$ ), calf intestine alkaline phosphatase ( $125 \text{ U mL}^{-1}$ ) and bovine  $\beta$ -1,4-galactosyl transferase ( $\beta 4\text{GalT1}$ ,  $100 \text{ mU mL}^{-1}$ ) at a final concentration of  $30 \text{ mg mL}^{-1}$  IgG. The resulting reaction mixture was incubated at  $37^\circ\text{C}$  for 24 h. Additional same amount of UDP-galactose and galactosyl transferase were added to ensure complete galactosylation, and the reaction mixture was incubated for an additional 24 h at  $37^\circ\text{C}$ . Galactosylated IgG was purified using a Protein A Sepharose Column (GE Healthcare) using a Tri-HCl buffer (50 mM, pH 7.05) for capture and washing, and a glycine buffer (100 mM, pH 3.0) for release. The antibody-containing fraction was

exchanged to cacodylate buffer (50 mM, pH 7.6) using an Amicon 10 kDa cutoff spin concentrator (Millipore). The sialylation of the galactosylated IgG antibody (final concentration of 11 mg mL<sup>-1</sup>) was conducted in cacodylate buffer (50 mM, pH 7.6), CMP-sialic acid derivatives (**1B**, **2**, or **3**, 5 mM), BSA (80 µg mL<sup>-1</sup>), calf intestine alkaline phosphatase (125 U mL<sup>-1</sup>) and GFP-ST6Gal I (0.35 mg mL<sup>-1</sup>) at 37 °C for 24 h. The sialylated IgG was purified by Protein A Sepharose column (GE Healthcare) as described above.

The anti-CD22 IgG antibodies was remodeled employing the same procedure.

#### Conjugation of remodeled control- and anti-CD22 IgG antibodies with fluorophores, or DIBO/TCO-DOX (**4** or **5**).

Fluorophores (DIBO-FITC or DIBO-AF647 or TCO-AF488) or DIBO/TCO-DOX (**4** or **5**) (final concentration, 67 µM) was added to the remodeled control or anti-CD22 IgG antibody (final concentration, 1 mg mL<sup>-1</sup>) in cacodylate buffer (50 mM, pH 7.63). The reaction mixture was placed in a shaker for 5 h at RT. The excess of reagent was removed by washing with cacodylate buffer (50 mM, pH 7.6) or PBS buffer using a 10 kDa cutoff spin filter (Millipore). The IgG conjugates were dissolved in cacodylate or PBS buffer for the cytotoxicity assay.

The fluorescent intensity of the conjugates and a series of standards were measured using a microplate reader (BMG Labtech). The concentration of protein was determined by the bicinchoninic acid assay (BCA, Pierce Biotechnology).

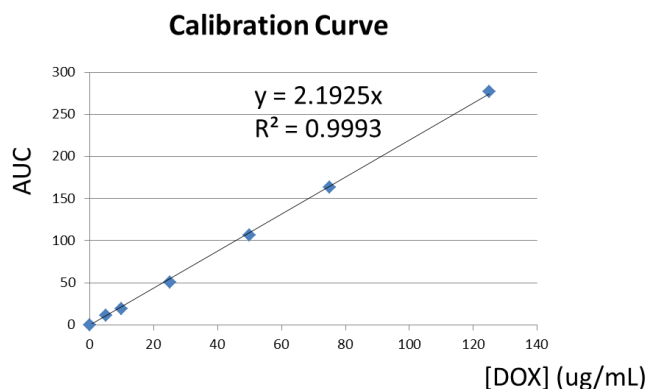
#### Detection of fluorophores-labeled antibodies.

The IgG antibody samples (~10 µg of protein) were resolved on Native gels (4-15%, Bio-Rad).

The gel was imaged using Typhoon 9410 Variable mode imager (Amersham Biosciences) for detection of fluorescent-labeled glycoproteins. Coomassie G-250 staining (GelCode Blue Stain Reagent, Thermo Scientific) was employed to detect proteins.

#### Quantification of doxorubicin on control IgGs by reverse phase HPLC.

Amount of doxorubicin loaded on control antibodies was estimated using Agilent 1100 series reverse phase HPLC (Eclipse XDBC18 column, 5  $\mu\text{m}$ , 4.6\*250 mm). Solvent system: Gradient from 20 to 50% (0.01 M TFA:acetonitrile) was used for 25 min/injection. Sample preparation: 3.333 mg mL<sup>-1</sup> of IgGs and doxorubicin standards were incubated with pH 5.0 acetate buffer for 30 h at room temperature. The solution was centrifuged (10k Milipore, centrifugation filters) to remove supernatant that contained the released doxorubicin. This was further lyophilized and prepared at given concentrations. Doxorubicin content in the antibodies was determined based on the calibration curves of the free doxorubicin standards (5, 10, 25, 50, 75, 100, 125, 150  $\mu\text{g}$  mL<sup>-1</sup>).

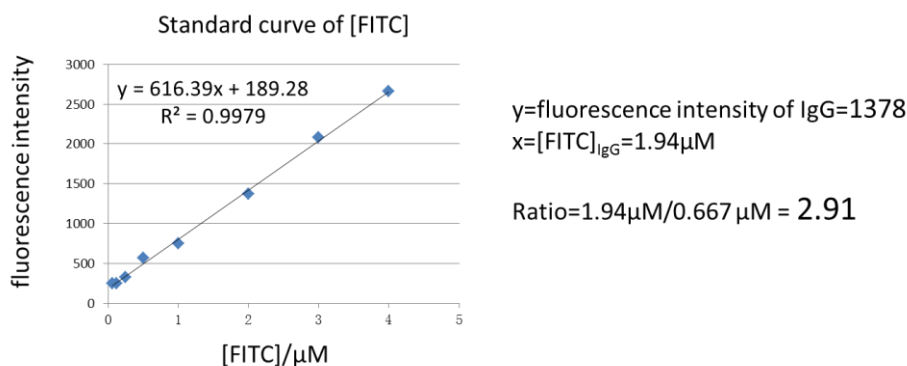


	AUC	[DOX] (ug/mL)	[IgG] (mg/mL)	Ratio (DOX/IgG)
SPAAC	51.7	23.58	3.333	2.0
SPANC	60.5	27.59	3.333	2.3
DARinv	47	21.44	3.333	1.8

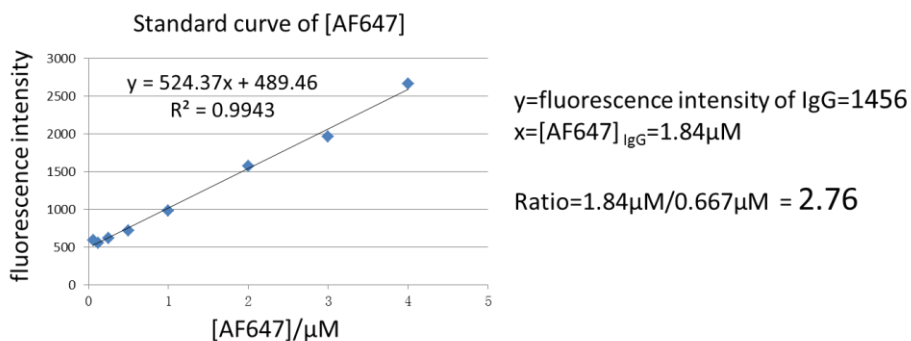
### Quantification study on anti-CD22 IgG by fluorescence intensity measurement.

The fluorescence intensity of fluorophores modified anti-CD22 IgGs (100 µg/mL or 0.667 µM) were measured by a POLARstar OPTIMA microplate reader (BMG LABTECH) using a 96-well fluorescence-based microplate. Fluorophores content in the antibodies was determined based on the calibration curves of the fluorophore standards (0.0625, 0.125, 0.25, 0.5, 1, 2, 3, 4 µM).

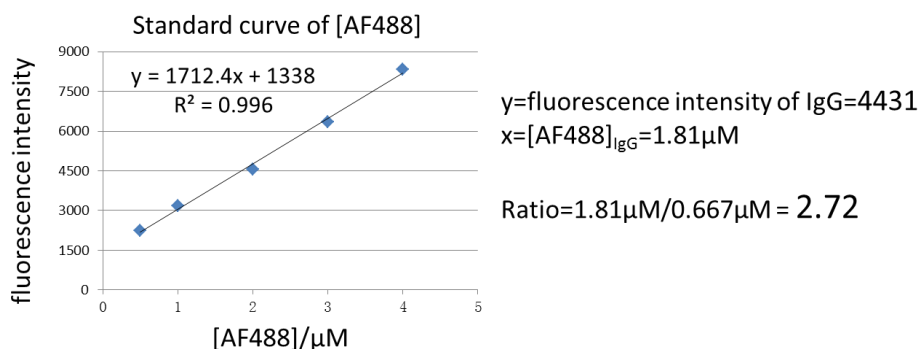
#### **SPAAC:**



#### **SPANC:**



## DARinv



### Cell lines and culture.

Human B lymphoblast cell, Daudi cells (CCL-213, ATCC) were cultured in ATCC-formulated RPMI-1640 medium with L-glutamine (2 mM), sodium bicarbonate (1.5 g L<sup>-1</sup>), glucose (4.5 g L<sup>-1</sup>), HEPES (10 mM) and sodium pyruvate (1.0 mM). The media was supplemented with penicillin (100 ug mL<sup>-1</sup>) and streptomycin (100  $\mu\text{g mL}^{-1}$ , Mediatech) and fetal bovine serum (FBS, 10%, BenchMark). Cells were maintained in a humid 5% CO<sub>2</sub> atmosphere at 37 °C and subcultured every 2-3 days.

### Cytotoxicity assay. Adapted from reference [18]

Cytotoxicity of CD22 positive Daudi Burkett lymphoma cells was determined by MTT uptake assay. On the day of exposure, exponentially growing cells were plated as 50,000 cells/well in 180  $\mu\text{L}$  in 96-well tissue culture plates (Nunc). Cells were then incubated with fresh medium (control), IgG-DOX (from SPAAC, SPANC, DARinv), anti-CD22 IgG-DOX (from SPAAC, SPANC, DARinv), DOX, DIBO-DOX (4) or TCO-DOX (5) (20  $\mu\text{L}$ , 10X in cell culture medium from PBS buffer for 48 h to give a final volume of 200  $\mu\text{L}$ /well. The viability was measured by quantifying

the cellular ability to reduce the water-soluble tetrazolium dye 3-(4,5-dimethylthiazole-2,5-diphenyl) tetrazolium bromide (MTT) to its insoluble formazan salt as follows. At 44 h, MTT ( $5 \text{ mg mL}^{-1}$  in PBS,  $10 \text{ }\mu\text{L/well}$ ) was added to the wells and the cells were further incubated for 4 h. At 48 h the supernatant was carefully removed and the water-insoluble formazan salt was dissolved in DMSO ( $120 \text{ }\mu\text{L/well}$ ). The absorbance was measured at 560 nm using a microplate reader (BMG Labtech). Data points were collected in triplicate and expressed as normalized values for untreated control cells (100%).

## Reference

- (1) Scott, A. M.; Wolchok, J. D.; Old, L. J. *Nature reviews. Cancer* **2012**, *12*, 278.
- (2) Chabner, B. A.; Roberts, T. G., Jr. *Nature reviews. Cancer* **2005**, *5*, 65.
- (3) Ducry, L.; Stump, B. *Bioconjugate Chemistry* **2010**, *21*, 5.
- (4) Iyer, U.; Kadambi, V. J. *J Pharmacol Tox Met* **2011**, *64*, 207.
- (5) Lambert, J. M. *Therapeutic delivery* **2016**, *7*, 279.
- (6) Zolot, R. S.; Basu, S.; Million, R. P. *Nat Rev Drug Discov* **2013**, *12*, 259.
- (7) Jeffrey, S. C.; Burke, P. J.; Lyon, R. P.; Meyer, D. W.; Sussman, D.; Anderson, M.; Hunter, J. H.; Leiske, C. I.; Miyamoto, J. B.; Nicholas, N. D.; Okeley, N. M.; Sanderson, R. J.; Stone, I. J.; Zeng, W.; Gregson, S. J.; Masterson, L.; Tiberghien, A. C.; Howard, P. W.; Thurston, D. E.; Law, C. L.; Senter, P. D. *Bioconjug Chem* **2013**, *24*, 1256.
- (8) Shinmi, D.; Taguchi, E.; Iwano, J.; Yamaguchi, T.; Masuda, K.; Enokizono, J.; Shiraishi, Y. *Bioconjug Chem* **2016**, *27*, 1324.
- (9) Dimasi, N.; Fleming, R.; Zhong, H.; Bezabeh, B.; Kinneer, K.; Christie, R. J.; Fazenbaker, C.; Wu, H.; Gao, C. *Molecular pharmaceutics* **2017**, *14*, 1501.
- (10) Mao, H.; Hart, S. A.; Schink, A.; Pollok, B. A. *J Am Chem Soc* **2004**, *126*, 2670.
- (11) Paterson, B. M.; Alt, K.; Jeffery, C. M.; Price, R. I.; Jagdale, S.; Rigby, S.; Williams, C. C.; Peter, K.; Hagemeyer, C. E.; Donnelly, P. S. *Angewandte Chemie* **2014**, *53*, 6115.
- (12) Zuberbuhler, K.; Casi, G.; Bernardes, G. J.; Neri, D. *Chem Commun (Camb)* **2012**, *48*, 7100.

(13)Junutula, J. R.; Raab, H.; Clark, S.; Bhakta, S.; Leipold, D. D.; Weir, S.; Chen, Y.; Simpson, M.; Tsai, S. P.; Dennis, M. S.; Lu, Y.; Meng, Y. G.; Ng, C.; Yang, J.; Lee, C. C.; Duenas, E.; Gorrell, J.; Katta, V.; Kim, A.; McDorman, K.; Flagella, K.; Venook, R.; Ross, S.; Spencer, S. D.; Lee Wong, W.; Lowman, H. B.; Vandlen, R.; Sliwkowski, M. X.; Scheller, R. H.; Polakis, P.; Mallet, W. *Nature biotechnology* **2008**, *26*, 925.

(14)Thompson, P.; Fleming, R.; Bezabeh, B.; Huang, F.; Mao, S.; Chen, C.; Harper, J.; Zhong, H.; Gao, X.; Yu, X. Q.; Hinrichs, M. J.; Reed, M.; Kamal, A.; Strout, P.; Cho, S.; Woods, R.; Hollingsworth, R. E.; Dixit, R.; Wu, H.; Gao, C.; Dimasi, N. *Journal of controlled release : official journal of the Controlled Release Society* **2016**, *236*, 100.

(15)Shen, B. Q.; Xu, K.; Liu, L.; Raab, H.; Bhakta, S.; Kenrick, M.; Parsons-Reponte, K. L.; Tien, J.; Yu, S. F.; Mai, E.; Li, D.; Tibbitts, J.; Baudys, J.; Saad, O. M.; Scales, S. J.; McDonald, P. J.; Hass, P. E.; Eigenbrot, C.; Nguyen, T.; Solis, W. A.; Fuji, R. N.; Flagella, K. M.; Patel, D.; Spencer, S. D.; Khawli, L. A.; Ebens, A.; Wong, W. L.; Vandlen, R.; Kaur, S.; Sliwkowski, M. X.; Scheller, R. H.; Polakis, P.; Junutula, J. R. *Nature biotechnology* **2012**, *30*, 184.

(16)Perez, H. L.; Cardarelli, P. M.; Deshpande, S.; Gangwar, S.; Schroeder, G. M.; Vite, G. D.; Borzilleri, R. M. *Drug Discov Today* **2014**, *19*, 869.

(17)Teicher, B. A.; Chari, R. V. *Clinical cancer research : an official journal of the American Association for Cancer Research* **2011**, *17*, 6389.

(18)Li, X. R.; Fang, T.; Boons, G. J. *Angew Chem Int Edit* **2014**, *53*, 7179.

(19)Jefferis, R. *Nat Rev Drug Discov* **2009**, *8*, 226.

(20)Schmaltz, R. M.; Hanson, S. R.; Wong, C. H. *Chemical reviews* **2011**, *111*, 4259.



- (21)Gross, H. J.; Brossmer, R. *European journal of biochemistry* **1988**, *177*, 583.
- (22)Mercer, N.; Ramakrishnan, B.; Boeggeman, E.; Verdi, L.; Qasba, P. K. *Bioconjug Chem* **2013**, *24*, 144.
- (23)Li, Q.; Li, Z.; Duan, X.; Yi, W. *J Am Chem Soc* **2014**, *136*, 12536.
- (24)Gross, H. J.; Brossmer, R. *Glycoconjugate journal* **1995**, *12*, 739.
- (25)Agard, N. J.; Baskin, J. M.; Prescher, J. A.; Lo, A.; Bertozzi, C. R. *Acs Chem Biol* **2006**, *1*, 644.
- (26)Blackman, M. L.; Royzen, M.; Fox, J. M. *J Am Chem Soc* **2008**, *130*, 13518.
- (27)Taylor, M. T.; Blackman, M. L.; Dmitrenko, O.; Fox, J. M. *J Am Chem Soc* **2011**, *133*, 9646.
- (28)McKay, C. S.; Blake, J. A.; Cheng, J.; Danielson, D. C.; Pezacki, J. P. *Chem Commun* **2011**, *47*, 10040.
- (29)Ning, X. H.; Temming, R. P.; Dommerholt, J.; Guo, J.; Ania, D. B.; Debets, M. F.; Wolfert, M. A.; Boons, G. J.; van Delft, F. L. *Angew Chem Int Edit* **2010**, *49*, 3065.
- (30)Karver, M. R.; Weissleder, R.; Hilderbrand, S. A. *Angewandte Chemie* **2012**, *51*, 920.
- (31)Perez, H. L.; Cardarelli, P. M.; Deshpande, S.; Gangwar, S.; Schroeder, G. M.; Vite, G. D.; Borzilleri, R. M. *Drug Discov Today* **2014**, *19*, 869.
- (32)McKay, C. S.; Moran, J.; Pezacki, J. P. *Chem Commun* **2010**, *46*, 931.
- (33)Ning, X.; Temming, R. P.; Dommerholt, J.; Guo, J.; Ania, D. B.; Debets, M. F.; Wolfert, M. A.; Boons, G. J.; van Delft, F. L. *Angewandte Chemie* **2010**, *49*, 3065.
- (34)Shintani, R.; Park, S.; Duan, W. L.; Hayashi, T. *Angewandte Chemie* **2007**, *46*, 5901.

- (35) Broussard, J. A.; Rappaz, B.; Webb, D. J.; Brown, C. M. *Nat Protoc* **2013**, 8, 265.
- (36) Varghese, S. S.; Zhu, Y. G.; Davis, T. J.; Trowell, S. C. *Lab on a chip* **2010**, 10, 1355.
- (37) Jefferis, R. *Biotechnology progress* **2005**, 21, 11.
- (38) Bondt, A.; Rombouts, Y.; Selman, M. H.; Hensbergen, P. J.; Reiding, K. R.; Hazes, J. M.; Dolhain, R. J.; Wuhler, M. *Molecular & cellular proteomics : MCP* **2014**, 13, 3029.
- (39) Molina, A. *Annual review of medicine* **2008**, 59, 237.
- (40) Mbua, N. E.; Li, X.; Flanagan-Steet, H. R.; Meng, L.; Aoki, K.; Moremen, K. W.; Wolfert, M. A.; Steet, R.; Boons, G. J. *Angewandte Chemie* **2013**, 52, 13012.

## CHAPTER 5

### CONCLUSION

We have explored different functionalized CMP-sialic acid for efficient cell surface glycoprotein labeling and construction of antibody-drug conjugates (ADCs), taking advantage of recombinant glycosyltransferases and various click reactions.

We developed one-step SEEL methodology, by employing a biotin modified CMP-sialic acid derivative. We found that this approach has exceptional efficiency compared to two-step SEEL or metabolic labeling, which greatly improved the ability to enrich and identify large numbers of tagged glycoproteins by LC-MS/MS. The one-step approach offers exciting possibilities to study the trafficking and identification of subsets of cell surface glycoconjugates with unprecedented sensitivity in whole cells. The transfer of the CMP-sialic acid derivatives on the cell surface requires galactosyl acceptors, which *in situ* can be generated by employing a bacterial neuraminidase that can remove the natural sialic acids but not the biotin-bearing sialic acids. As a result, co-neuraminidase treatment also decreases the total labeling time compared to traditional methods which makes it suitable for SEEL on cell types that may be sensitive to the conditions needed for this type of labeling. Furthermore, this methodology is highly selective for cell surface proteins because the employed enzymes and reagents will not cross the cell membrane. Moreover, the procedure is technically simple and can readily be expanded to the labeling of specific classes of glycoproteins by employing alternative glycosyltransferases.

Next, we explored a new two-step SEEL, which takes advantage of a sugar nucleotide functionalized by tetrazine, and fast bioorthogonal reaction-DARinv (Inverse electron demand Diels–Alder reaction). DARinv does not employ toxic metal catalysts, and the reaction between tetrazine and TCO was reported as the fastest bioorthogonal reactions to date. This new two-step approach has comparable efficiency with one-step SEEL benefit by the fast click reaction, but has broader applications. The tetrazine modified sialic acid is also not removed by neuraminidase, allowing labeling to be carried out in the presence of the neuraminidase. Two-step SEEL with TCO-PEG5K followed by western blot analysis with protein-specific antibodies could easily analyze protein by protein glycosylation status (*N*- vs. *O*-linked glycans) using different sialyltransferases (ST3Gal1, ST6Gal1, ST6GalNAc1 *et al*) in different cell types. Furthermore, the diversity of TCO attached compounds provides many possibilities that can be used to analyze subsets of cell surface glycoconjugates in details. For example, two-step SEEL with TCO-fluorophore could be employed to study the trafficking of cell surface glycoconjugates, and two-step SEEL with TCO-glycan, for example, TCO-HS (heparan sulfate) could easily engineer the cell surface and mimic the natural HS polymer, and thus modulate cellular functions such as cell differentiation and proliferation, cell-cell adhesion and communication. We believe this new technology will find numerous applications in other areas of biology and biomedicine.

We also prepared well-defined anti-CD22 ADCs by employing tetrazine and nitron modified CMP-sialic acid derivatives through DARinv and SPANC, and the formed ADCs showed comparable dose-dependent cytotoxicity with the one through SPAAC using CMP-Neu9Az. With this new method, we can use more potent cytotoxic drugs in a much less

concentration. Furthermore, DAR<sub>inv</sub> and SPANC are orthogonal, which can be used together on the same mAb to deliver two different drugs to increase ADC efficacy and reduce toxicity of normal tissues at the same time. ADCs have generated intense interest for decades, and will eventually fulfill the promise of specific delivery of cytotoxic drugs to tumor cells. Future effort will be also addressed on site-specific conjugation modalities and optimization of linkers with balanced stability.